2018

Effects of Increased Temperature and Copper Excess on the Physiology, Biochemistry and Gene Expression of Ectocarpus Siliculosus (Dillwyn) Lyngbye

Santillan-Sarmiento, Alex Renato

UNIVERSITY OF
PLYMOUTH

EFFECTS OF INCREASED TEMPERATURE AND COPPER EXCESS ON THE PHYSIOLOGY, BIOCHEMISTRY AND GENE EXPRESSION OF *Ectocarpus siliculosus* (DILLWYN) LYNGBYE

by

ALEX RENATO SANTILLÁN-SARMIENTO

A thesis submitted to the University of Plymouth
in partial fulfilment for the degree of

DOCTOR OF PHILOSOPHY

School of Biological and Marine Sciences

2018

Acknowledgements

Firstly, I would like to thank my family: María, Vicente, Verónica and Gabriella for their constant support during this journey. The culmination of my programme would not have been possible without your help and love.

I would like to express my sincere appreciation to all those who contributed in many ways to the completion of this work. I am greatly indebted to my director of studies Dr. Murray T. Brown for the continuous support throughout this work, for his patience and valuable knowledge. Under his guidance, I successfully overcame many difficulties and learned a lot about research and writing a thesis. I also would like to thank the rest of my supervisory team, Dr. John Moody for his guidance and advice, which significantly contributed to improve my research and make the most of our findings. 'Muchas Gracias' to Dr. Claudio Saez who has been a mentor, motivating me to pursue a career in phycology and kindly hosted me in his laboratory at Univerity of Playa Ancha in Chile to perform a great part of the research.

I would like to extend my appreciation to Dr. Alejandra Moenne and Dr. Francisco Cubillos and their respective groups for receiving me at University of Santiago the Chile to perform biochemical and molecular analysis. Especially, I would like to thank Dr. Alberto Gonzáles, Melisa Gómez and Fabiola Moenne for their assistance in biochemical techniques, Valentina Abarca for her support in extracting nucleic acids and Dr. Carlos Villarroel for his support in bioinformatics analysis. I thank Dr. Maria Greco and Dr. Mark Rawling for their help and advice in gene expression analysis. Many thanks to the technical support provided by all the technicians at Plymouth University, especially Angela Harrop and Roger Haslam. I gratefully aknowledge the friendship and support of Dr. Paula Celis-Plá for teching me about photo-physiology of algae.

I aknowledge the financial support of the Ecuadorean Government and Secretaria Nacional de Ciencia y Tecnologia (SENESCYT) for granting me a scholarship under the programme ‘Convocatoria abierta 2012 segunda fase’ which covered most of the cost of my research, maintenance and University fees. I also thank Santander Universities and Plymouth University for awarding me a ‘Santander Undergraduate, postgraduate & staff Mobility Support Scholarship 2014-15’ that allowed me to travel to Chile to establish collaboration with University of Santiago and University of Playa Ancha.

Finally, I would like to thank all the good people that I met during my stay in Plymouth, especially my ‘familia latina’ Karina, Paula, Mariana, Gustavo, Tasos, Luca, Cecilia, Marco, Mattia, Felipe y ‘mi parce’ Hugo Alexander. Also, thanks to all the ‘aliens’ and my geographers and geologists fellows, all of you made life enjoyable even during though times.

AUTHOR'S DECLARATION

At no time during the registration for the degree of Doctor of Philosophy has the author been registered for any other University award without prior agreement of the Doctoral College Quality Sub-Committee. Work submitted for this research degree at the University of Plymouth has not formed part of any other degree either at the University of Plymouth or at another establishment.

This study was financed with the aid of a studentship from Secretaria Nacional de Ciencia y Tecnologia (SENESCYT, Ecuador). The research was carried out in collaboration with the Universidad de Playa Ancha, Universidad de Santiago de Chile and The Francis Crick Institute.

Publications:

- A. Santillán-Sarmiento, P. S.M. Celis-Plá, C. A. Sáez, A. J. Moody, M. T. Brown. Combination of elevated copper and temperature in *Ectocarpus siliculosus* differentially affects photosynthesis, growth and accumulation (*In prep*.).

- A. Santillán-Sarmiento, C. Villaroel, F. A. Cubillos, A. Moenne, C. A. Sáez, A. J. Moody, M. T. Brown. Interactions between temperature and Cu stress involve regulation of photosynthesis and oxidative response in brown seaweed *Ectocarpus siliculosus* (*In prep*.).

Conferences:

- A. Santillán-Sarmiento, C. Villaroel, F. A. Cubillos, A. Moenne, C. A. Sáez, A. J. Moody and M. T. Brown. Increased seawater temperature offsets the deleterious effects of Cu in the model brown seaweed *Ectocarpus siliculosus*. SETAC Europe 28th Annual Meeting in Rome, Italy (May 2018). Poster presentation by A. Santillán-Sarmiento.

- A. Santillán-Sarmiento, A. J. Moody, A. González, A. Moenne, F. Moenne, C. A. Sáez and M. T. Brown. Interaction between increased temperature and Cu excess induces differential antioxidant enzymes responses in the brown macroalga *Ectocarpus siliculosus.* SETAC Europe 27th Annual Meeting in Brussels, Belgium (May 2017). Poster presentation by A. Santillán-Sarmiento.

- A. Santillán-Sarmiento, P. Celis-Plá, M. T. Brown. Increased temperature enhances photosynthesis and inhibits copper uptake in *Ectocarpus siliculosus*. 18th International Conference on Heavy Metals in the Environment, Ghent, Belgium (September 2016). Oral presentation by A. Santillán-Sarmiento.

Word count of main body of thesis: 38,488

Signed:……

Alex Renato Santillán Sarmiento

Effects of increased temperature and copper excess on the physiology, biochemistry and gene expression of *Ectocarpus siliculosus* (Dillwyn) Lyngbye

by Alex Renato Santillán-Sarmiento

Abstract

Brown algae are an important group of organisms inhabiting coastal ecosystems worldwide. Because of their sessile nature, they are exposed to natural abiotic stresses such as high and low irradiances, desiccation, thermal fluctuations and mechanical stress, as well as anthropogenic-derived stresses such as chemical pollution. While the impacts of metal pollution affect brown algae on a local scale, there is growing concern on the potential interactions between pollutants and abiotic pressures resulting from global climate change. The main objective of this study was to determine the nature of the interactions (synergistic, additive or antagonistic) of different concentrations of copper in combination with increased temperatures in controlled laboratory experiments using the model brown alga *Ectocarpus siliculosus* as a proxy for brown seaweeds, which are globally important primary producers and bioengineers of near-shore waters. The responses in *E. siliculosus* were evaluated at different levels of biological organisation. At the whole organism level Cu or temperature affected growth but no interactions occurred. Antagonistic interactions occurred between stressors in the photosynthetic efficiency response (measured as chlorophyll *a* fluorescence), being less affected by Cu at higher temperatures. The bioaccumulation of Cu ions showed and antagonistic response to temperature as less Cu ions were accumulated at elevated temperature. The concentrations of H_2O_2 and lipid peroxides (TBARS), which are indicators of oxidative stress, were synergistically affected by interactions of stressors. In contrast, the concentrations of antioxidants ascorbate and glutathione reflected both additive and antagonistic interactions respectively. This also occurred in the activity of antioxidant

enzymes (superoxide dismutase, ascorbate peroxidase, catalase and glutathione reductase) and the expression of related genes. Finally, the results of the biochemical and physiological tests were integrated with the whole transcriptome response to temperature and Cu stress. These results showed that interactions between temperatures and Cu stress could be highly complex, but also lead to the discovery of potential stress markers such as light harvesting complex proteins and several transporters. This research provides new insights into the responses of brown macroalgae to metal and thermal stress. Those responses indicate that synergistic or antagonistic interactions can occur at different levels of organisation, being the regulation of antioxidant metabolism, photosynthetic physiology and related gene expression, the most important mechanisms involved. This information will aid to understand potential effects of climate change on the toxicity of metals for macroalgae in estuaries and coasts affected by pollution.

Table of Contents

List of Tables

List of Figures

List of Abbreviations

Abbreviation	Meaning
SST	Sea surface temperature
NSW	Natural seawater
RGR	Relative growth rate
PAR	Photosynthetically active radiation
RLC	Rapid light curve
F_v/F_m	maximum photochemical quantum yield of PSII
ETR_{max}	maximum electron transport rate
α	quantum efficiency of photosynthesis
E_k	minimum saturating irradiance
NPQ_{max}	maximum non-photochemical quenching
ROS	Reactive oxygen species
ROM	Reactive oxygen metabolism
CAT	Catalase
APX	Ascorbate peroxidase
SOD	Superoxide dismutase
GR	Glutathione reductase
TBARS	Thiobarbituric acid reactive substances
GSH	Reduced glutathione
GSSG	Glutathione disulphide
ASC	Ascorbate
DHA	Dehydroascorbate
MDHAR	Monodehydroascorbate reductase
GS	Glutathione synthase
MET	Metallothionein
GO	Gene Ontology

Chapter I

Literature review: Metal pollution and temperature in marine algae

1.1. Metal pollution in the marine environment

Metals, such as copper, lead, zinc or cadmium, are a well-known group of persistent pollutants. Despite their natural occurrence at low concentrations in aquatic ecosystems, human activity is largely responsible for their abnormal release and accumulation in the environment (Costa *et al.*, 2011). A clear example of this is the use of leaded petrol in North America until the end of 1970s. This caused up to fifty-fold increases of Pb in the surface waters of North Atlantic and Pacific Oceans due to atmospheric input (Patterson, 1965; Patterson *et al*., 1976; Veron *et al*., 1993; Véron *et al*., 1998). Successive studies have demonstrated that concentrations in surface waters decreased by 30 to 40% since 1979, in response to a corresponding decline of the tropospheric deposition due to a replacement of leaded petrol (Véron *et al.*, 1993). Other than air deposition, anthropogenic metal loads enter the sea via outfalls along major rivers and estuaries from industrial and mining activities (Ridgway *et al.*, 2003). A recent study has shown that despite it being 100 years since mining activities declined in south-west England, the concentrations of metals, such Ag, Cu, Pb and Zn, in sediments and deposit-feeders remain atypically high in five estuaries, which is probably due to the poor wave action in many sheltered creeks (Rainbow *et al.*, 2011). Regarding the problem of metal pollution, the member countries of the Oslo/Paris convention for the Protection of the Marine Environment of the North-East Atlantic (OSPAR) have already taken action to reduce pollution impacts. The Quality Status Report 2010 (see http://www.ospar.org) shows that decreases in levels of emissions of Hg, Cd and Pb occurred in the 1990s in some member countries because of technological and regulatory advances (OSPAR, 2010). However, further declines in emissions have been more difficult to achieve due to economic and technical problems. Besides, concentrations of the above mentioned metals in fish and shellfish exceeded the EU food standards in some industrialised sites of

Denmark, UK, Germany, Spain and Norway (OSPAR, 2010), which indicates that metals still prevail in the most impacted sites representing a threat for marine and human life.

In seawater, metals can exist in complexes with suspended particles, which eventually are deposited in sediments, or with organic and inorganic ligands that are in a dissolved state (Bryan & Langston, 1992), but also in their free dissolved form as cations (Gledhill *et al.*, 1997). Many metals can cycle between different oxidation and complexation states (Byrne *et al*., 1988; Byrne, 2002), which affect their behaviour in aquatic systems because of the differences in the reactivity, kinetic lability, solubility or volatility (in the case of Hg) of different oxidation states. The variety of chemical species and complexes that metals can form in marine environments strongly influence their availability to the biota exposed to them (Sunda & Huntsman, 1998). For example, only the dissolved fraction of metals can be internalised in the cells of macroalgal thalli (Phillips, 1977), whereas other organisms, such as the deposit feeders *Nereis diversicolor* and *Scrobicularia plana*, can also accumulate metals bound to sediments (Rainbow *et al.*, 2011). Thus not all metal species are (bio) available for uptake by living organisms. Iron, for example, occurs primarily in the thermodynamically stable Fe^{3+} state, which is barely soluble. Reduction of Fe^{3+} to Fe^{2+} by photochemical or biological means, results in increases of the biological availability of iron since the resulting Fe^{2+} is much more soluble, has much more rapid ligand exchange kinetics, and forms much weaker complexes, allowing it to reoxidize rapidly to Fe^{3+}. This redox cycle increases the concentrations of biologically available dissolved Fe^{2+} and Fe^{3+} inorganic species, thus increasing the algal uptake of iron (Hudson & Morel, 1990; Miller *et al.*, 1995; Sunda & Huntsman, 1998).

Some metals, such as Fe, Zn, Mn, Cu, Co, Mo and Ni, are essential micronutrients acting as components of the active sites of protein complexes or as cofactors in enzymatic

reactions (Theophanides, 1984; Connan and Stengel, 2011a; Brown *et al*., 2012). Other metals have no known biological role, which is the case for Hg, Ag, Pb, and Sn (Sunda & Huntsman, 1998). However, beyond certain thresholds, both essential and non-essential metals can accumulate within marine biota, becoming toxic to the organisms exposed. For example, Küpper *et al*. (2002) found that substitution of Mg^{2+} by Cu^{2+} in chlorophyll molecules was one of the main mechanisms responsible for metal toxicity in green (*Scenedesmus quadricauda*), red (*Anthithamnion plumula*) and brown (*Ectocarpus siliculosus*) algae at elevated total Cu concentrations. Metals accumulated in primary producers such as phytoplankton and macroalgae may eventually reach high levels in trophic chains in a process called biomagnification (Connell, 1989). Biomagnification is defined as the increase of metal concentration, in the tissues of organisms at higher levels in a food chain (Croteau *et al.*, 2005), ultimately representing a hazard for humans that rely on seafood (Gray, 2002; Van Oostdam *et al.*, 2005).

Marine macroalgae (seaweeds) are important primary producers occurring along coasts and estuaries worldwide. They are key habitat structuring agents, harbouring a high biodiversity and functioning as ecological bioengineers (Graham, 2004; Christie *et al*., 2009). Such characteristics link them culturally and economically to humans through the provision of ecosystem goods and services ranging from food to medicine to storm protection (Rönnbäck *et al.*, 2007). Numerous species of macroalgae thrive in the intertidal and subtidal zone where they are normally exposed to a broad range of natural environmental stressful conditions, including desiccation, changes in salinity, UV radiation and temperature fluctuations, as well as anthropogenic-derived stressors such as pollution by metals (Contreras *et al*., 2009). In the next sections the effects of metals and temperature fluctuations in marine algae and the potential interactions between these stressors are reviewed with emphasis on brown seaweeds, however, examples from other groups will be used when required.

1.2. Metals in marine algae

1.2.1. Metal uptake

Marine algae possess mechanisms for metal uptake because most of them are essential nutrients for their metabolism. Iron, for example, is one of the most important trace elements for algal growth, and it is essential for several biochemical processes such as photosynthetic and respiratory electron transport (Sugie *et al.*, 2010). In photosynthetic stramenopiles (e.g. diatoms and brown seaweeds), iron plays a key role in cytochrome c_6 as the catalyst for electron transfer from the cytochrome b_6f complex to the P700 chlorophyll in photosystem I (Raven, 2013). However, the mechanisms used by organisms for nutrient acquisition can be the gateway for 'non-nutritive' toxic metals (Sunda & Huntsman, 1998). In proximity of the algal cell surface, metals will first encounter the cell wall. This porous external layer constitutes a hydrophilic matrix of negatively charged sites due to the presence of a variety of functional groups including carboxyl (-COOH), hydroxyl (-OH), and sulfhydryl (-SH) that are associated with different components of the cell wall, such as polysaccharides, peptidoglycan and proteins (Bermúdez *et al.*, 2011). These functional groups readily bind metal cations and their complexes, which migrate eventually reaching the plasma membrane. This membrane is a hydrophobic phospholipidic barrier characterised by the existence of transport proteins and/or ion channels that facilitate the movement of ions across it (Campbell *et al.*, 2002). However, active transport is not the only mechanism for metal uptake; some neutrally charged, non-polar complexes, such as $HgCl_2$, and CH_3HgCl, can diffuse directly across bilayer membranes due to their lipid solubility (Gutknecht, 1981). Although both mechanism of transport, passive and active, are important to the intracellular uptake and detoxification of metal ions, beyond some threshold

concentrations, especially in metal-polluted zones, those mechanisms are insufficient to avoid intracellular excess of toxic and essential metals (Pinto *et al.*, 2003).

1.2.2. Metal toxicity

In algae, the general order of toxicity is considered to be: Hg >Cu >Cd > Ag > Pb > Zn (Lobban and Harrison, 1994; Gaur and Rai, 2001).Studies on the concentration of metals in a wide range of marine organisms have demonstrated that toxic threshold concentrations vary between organisms and elements (Rainbow & Luoma, 2011). This level of variability is due to a combination of exclusion and detoxification strategies which are species specific and determine the resistance of organisms to metals (Decho and Luoma, 1994; Chapman *et al*., 1996; Brown *et al*., 2012). For example, in the brown seaweed *E. siliculosus*, different biochemical strategies were observed between individuals isolated from locations with different Cu-pollution history (Roncarati *et al*., 2015; Sáez *et al*., 2015). Similar results were observed in other seaweed groups (Ratkevicius *et al*., 2003; Brown *et al*., 2012).

The toxic effects of metals are apparent at different levels of biological organization including molecular, cellular and whole-organism. For instance, inhibition of growth at concentrations of 50 μg L^{-1} of mercury was observed in the cosmopolitan green algae *Ulva latuca* (Costa *et al*., 2011). Other effects of mercury, the most toxic metal for algae, include inhibition of photosynthesis, reduction of chlorophyll content and increased cell permeability (Rai *et al.*, 1981). Copper appears as one of the most toxic metals for algae (Gaur & Rai, 2001; Han & Choi, 2005). In fact, it has been used as algicide or antifouling agent in paints for ship hulls and due to its efficiency in inhibiting algal growth (Thomas *et al*., 1977; Strömgren, 1980; Andersson and Kautsky, 1996; Tsai, 2016). It is of particular interest that beyond certain threshold concentrations Cu is more toxic than other metals despite the fact it is an important micronutrient. The particular

toxicity of Cu can be attributed to the relative stability of metal ion complexes described by the Irving-Williams series (Irving and Williams, 1953). They observed that stability of bivalent ions of the first transition series increased across the period, being maximum for Cu. Thus, when present in excess, more stable Cu complexes can displace other metals, such as zinc, from their cognate ligands in metalloproteins altering protein structures or inhibiting enzymatic activities (Festa and Thiele, 2011). Cu has also widespread targets at cellular level, which eventually lead to reductions in growth and mortality. For instance, Nielsen *et al*. (2003) found that elevated concentrations of Cu inhibited the fixation of the polar axis in *Fucus serratus* zygotes. Another key cellular process affected by copper is photosynthesis (Reed and Moffat, 1983; Rijstenbil *et al*., 1994; Küpper *et al*., 2002).

1.2.2.1. Metals and reactive oxygen metabolism

The toxic effects of Cu and other metals have also been associated with the production of reactive oxygen species (ROS) inside cells (Collén & Davison, 1999a; Pinto *et al.*, 2003; Ratkevicius *et al.*, 2003). The term 'reactive oxygen species' refers to reduced forms of oxygen that are more reactive than molecular oxygen and thus capable to cause oxidative damage to proteins, DNA and lipids (Desikan *et al.*, 2005). Those species include the superoxide anion ($\bullet O_2^-$), hydrogen peroxide (H_2O_2), singlet oxygen ($^1O_2$) and hydroxyl radical ($\bullet OH$) (Dring, 2005). ROS are unavoidably produced in mitochondria, chloroplast and peroxisomes of unstressed cells as by-products of aerobic metabolic processes such as respiration and photosynthesis (Apel & Hirt, 2004). For example, O_2 is photoreduced in photosystem I (PSI) of chloroplasts generating $\bullet O_2^-$ as the primary product (Asada, 1999). At low concentrations, ROS are signalling molecules coordinating key cellular processes such as gene expression (op den Camp *et al*., 2003; Foyer and Noctor, 2011). However, under a wide range of abiotic and biotic

environmental stresses, the accumulation of ROS can lead to oxidative stress in algae and plants (Collén and Davison, 1999; Pinto *et al*., 2003; Dring, 2005). Oxidative stress in algae can be manifested as membrane damage, increase of antioxidant-enzymes activities and transcripts of genes coding for enzymes involved in the ROS metabolism as observed in Cu-exposed green alga *Ulva compressa* (Contreras-Porcia *et al.*, 2011).

Metals can directly participate in reactive oxygen metabolism (ROM) of algae acting as cofactors in several enzymes. For example Fe, Mn, Cu and Zn are cofactors of the several isoforms of the enzyme superoxide dismutase (SOD), which constitutes the first line of defence against ROS and are located in different cellular compartments (Alscher *et al.*, 2002). Metals such as Cu^{2+} and Fe^{3+} may also contribute to the production of hydroxyl radical (•OH) participating in the Haber-Weiss and Fenton reactions (Kehrer, 2000; Pinto *et al*., 2003; Dring, 2005). Also, it has been proposed that oxidative stress induced by metal ions in algae is due to the disruption of photosynthetic electron transport chains in chloroplasts and mitochondria, leading to the formation of $\bullet O_2^-$, and $^1O_2$ (Okamoto *et al*., 2001; Dring, 2005). Gene expression regulation of ROM related genes has been observed in algae undergoing stress by metals . For example, Wu *et al*. (2009) found that the expression of genes involved in ROM in the green seaweed *Ulva fasciata*, such as methionine sulfoxide reductase A (*UfMsrA*), thioredoxin (*UfTrx*), cyclophilin (*UfCyp*), and ferritin (*UfFer*), was increased mainly by short-term exposure (0 – 12 h) to Cu (0 – 50 µM). However, the level of expression of other set of genes associated to antioxidant defence, including superoxide dismutase (*UfMnsod* and *UfFesod*), ascorbate peroxidase (*UfApx*), glutathione reductase (*UfGr*) and catalase (*UfCat*), was only higher after 4 days exposure to excess Cu. These results were to some extent supported later by a microarray analysis in the brown seaweed *E. siliculosus*, where an overlap in the transcriptome responses to Cu and H_2O_2 stress was observed (Ritter *et al.*, 2014), confirming thus, the link between Cu stress and ROM.

In order to mantain redox homeostasis inside the cell, algae and plants evolved complex arrays of non-enzymatic and enzymatic detoxification mechanisms of defence against the cytotoxic properties of ROS (Apel & Hirt, 2004). The main non-enzymatic cellular defences against ROS are secondary metabolites including reduced glutathione (GSH), ascorbate (ASC), isoprenoids and phenolic compounds. Such compounds act in concert with antioxidant enzymes such as superoxide dismutase (SOD), ascorbate peroxidase (APX), glutathione reductase (GR), glutathione peroxidase (GPx) and catalase (CAT) to keep the intracellular redox equilibrium (Dietz, 2005; Feierabend, 2005; Foyer *et al*., 2005; Grace, 2005; Mittler and Poulos, 2005; Smirnoff, 2005; Foyer and Noctor, 2011b; Noctor *et al*., 2012). Ascorbate and glutathione are two efficient scavengers of ROS acting principally in chloroplasts in a cycle known as the "Halliwell-Asada-Foyer" or "ascorbate–glutathione" pathway (Asada, 1999; Foyer & Noctor, 2011). In this pathway ascorbate readily donates an electron to reduce H_2O_2 to form H_2O and monodehydroascorbate (MDHA) or dehydroascorbate (DHA), in a reaction catalysed by ascorbate peroxidase (APX) (Smirnoff, 2005). The ascorbate pool is regenerated from MDHA and DHA by the enzyme dehydroascorbate reductase (DHAR) using reduced glutathione (GSH) as the reductant (Alscher *et al.*, 1997). The resulting oxidised glutathione (GSSG) is in turn reduced by the enzyme glutathione reductase (GR) using NADPH (Foyer & Noctor, 2011). In the cytosol and peroxisomes, catalase (CAT) will break down H_2O_2 in H_2O and O_2 (Asada & Takahashi, 1987; Collén & Davison, 1999a). The above-mentioned enzymes involved in the ascorbate/glutathione pathway in addition with SOD, which catalyzes the disproportionation of $\bullet O_2^-$ to O_2 and H_2O_2, and CAT that converts H_2O_2 to H_2O and O_2, are referred as 'antioxidant enzymes' (Dring, 2005; Feierabend, 2005). The activity of those enzymes has also been related to the removal of ROS and the tolerance to oxidative stress in seaweeds exposed to excess of metals (Ratkevicius *et al*., 2003; Contreras *et al*., 2005, 2009; Sáez *et al*., 2015; Moenne *et al*.,

2016). For example, the low tolerance of *Fucus distichus* to oxidative stress was related to the reduced activities of CAT, APX and SOD compared with activities of same enzymes in *F. spiralis* and *F. evanescens* (Collén & Davison, 1999a). Other secondary metabolites proposed to have a role as antioxidants are isoprenoid compounds, which also have photoprotective characteristics and are commonly found in photosynthetic membranes. For example, carotenoids (e.g. fucoxanthin in algae) are able to quench $^1O_2$ and react with lipid radicals generated by ROS (Smirnoff, 2005). Other important aromatic metabolites are the phenolic compounds, such as hydroxy-cinnamic acids (HCAs), flavonoids, anthocyanins, α-tocopherol (vitamin E), tocotrienols and tannins. Those compounds are excellent antioxidants due to the electron donating capacity of their one or more 'acidic' phenolic hydroxyl group (Grace, 2005), which can be oxidised to phenoxyl radicals that are less reactive than ROS (Bors *et al.*, 1994; Pedrielli *et al.*, 2001). However, their efficacy as antioxidants in algae remains to be proven as higher levels of phenolics were observed in *Fucus distichus*, a species susceptible to oxidative stress (Collén & Davison, 1999a). In contrast, a recent study found that higher levels of phenolic compounds were associated to higher antioxidant power in copper-tolerant strains of *E. siliculosus* (Sáez *et al.*, 2015c).

1.2.3. Metal resistance

Marine algae have extracellular, cell surface-bound and intracellular mechanisms to detoxify or reduce the toxic effects of metals. Extracellular and cell surface-bound mechanisms are identified as exclusion mechanisms and include exudation of compounds that bind metal in the surrounding media (Gledhill *et al.*, 1999) and chelation of cations by polysaccharides (alginates and fucoidan) in the cell wall (Davis *et al.*, 2003). The cell wall polysaccharide composition varies across the different groups of marine macroalgae, sometimes being used as a taxonomic trait (Bold, 1985). The alginic acid or alginate of

brown algae is considered the most important macromolecule involved in metal complexation. It is a linear molecule formed by mannuronic (M) and guluronic (G) acid residues irregularly arranged (Lee, 2008). The mannuronic acid to guluronic acid ratios (M:G) of alginates vary greatly between different species, populations and tissues within the more complex brown algae (Venegas *et al.*, 1993). This ratio appears to be a determining factor in the metal binding capacity of the cell wall (Haug, 1961; Davis *et al*., 2003). Specifically, Haug (1961) found that the affinity of alginates for divalent cations increased with the guluronic acid content. Phenolics (also referred as polyphenols) represent one of the most important organic compounds exudates in algae; other than their role as antioxidants, they have been examined as metal chelators (Connan & Stengel, 2011b). Thus, likely the release of phenolics in the proximate environment alters metal speciation and thereby reduces their bioavailability. Exudation of phenolic compounds from algae represents an important source of organic matter to the seas (Sieburth, 1969). Other than metal chelators they have been proposed as antigrazing agents and in photoprotective roles (Ragan and Jensen, 1978; Swanson and Druehl, 2002; Shibata *et al*., 2006, 2014).

The intracellular mechanisms of metal detoxification involve the production of peptide metal chelators, such as phytochelatins and metallothioneins, and/or polyphenols (e.g. phlorotannins) (Cobbett and Goldsbrough, 2002; Pawlik-Skowrońska *et al*., 2007; Connan and Stengel, 2011b). The enzymatically synthesized short-chain peptides called phytochelatins (PCs) and the gene-encoded cysteine-rich proteins called metallothioneins (MTs) are important intracellular chelators of metals (Cobbett, 2000; Cobbett and Goldsbrough, 2002). The general structure of PCs is $(\gamma\text{-Glu-Cys})_n\text{-Gly}$, where chain length "n" varies between 2 and 11 units (Grill *et al*., 1989; Rauser, 1995; Perales-Vela *et al*., 2006). Although they were first described in plants, they have been found in other organisms such as worms (Liebeke *et al.*, 2013) and algae exposed to metals (Gaur and

Rai, 2001; Perales-Vela *et al*., 2006; Pawlik-Skowrońska *et al*., 2007; Roncarati *et al*., 2015). The thiol groups of the Cys provide their metal binding capacity (Rauser, 1995). Besides its role in antioxidant defences, glutathione (GSH) is the precursor for the synthesis of PCs catalysed by the enzyme phytochelatin synthase (PCS) (Gaur & Rai, 2001). Pawlik-Skowrońska *et al*. (2007) have demonstrated that production of PCs can be induced in natural assemblages of seaweeds belonging to distinct phylogenetic groups. The longest PC chain length was found in *Fucus* spp. and correlated with the most polluted site of collection. It appears that a combination of thiol peptides of GSH and PCs are involved in the detoxification and tolerance of some species of seaweeds, but such resistance varies between species occurring in the same environments. Similar results were recently obtained in different strains of the model brown algae *E. siliculosus*. Roncarati *et al*. (2015) found that not only the concentrations of PCs but also the expression of genes related in the PC and GSH biosynthetic pathway was increased in response to 0.8 μM of total Cu. In this case, intraspecific variations in the response were observed between two strains of *E. siliculosus* isolated from a Cu-polluted and a pristine site.

MTs are small cysteine-rich proteins found in a wide range of organisms from unicellular to humans (Kay *et al.*, 1991). The amino acidic sequence of MTs include conserved motifs of Cys-Cys Cys-X-Cys, Cys-X-Y-Cys, where the thiol groups of Cys residues account for the metal binding capacity of MTs (Merrifield *et al.*, 2004). Their occurrence and role in macroalgae has been studied in few species such as *Cladophora* spp. (Cao *et al.*, 2015), *Ulva compessa* (Contreras-Porcia *et al.*, 2011) and *Fucus vesciculosus* (Morris *et al*., 1999; Merrifield *et al*., 2004, 2006). The only gene for MTs identified in *F. vesciculosus* was predicted to code for a 67-amino-acid protein containing 16 Cys residues (24%) (Morris *et al.*, 1999). As part of the same study, MT of *F. vesciculosus* (fMT) was expressed in *E. coli* and the resulting protein was able to bind Cd

and Cu. Additionally, exposure to elevated Cu induced the expression of the MT gene. The ability of the fMT-recombinant protein to bind arsenic (Merrifield *et al.*, 2004; Singh *et al.*, 2008) and Cd (Merrifield *et al.*, 2006) was also tested as a bioremediation tool.

As reviewed above, phenolics are related in different ways to metal stress tolerance. In addition to their role as antioxidants, they have been proposed as extra and intracellular metal chelators (Ragan *et al*., 1979; Pedersen, 1984; Connan and Stengel, 2011b; Roncarati *et al*., 2015). In brown algae, phenolics are stored within cellular vacuoles called physodes (Swanson & Druehl, 2002). Some authors suggested that intracellular phenolic compounds produced by brown seaweeds are able to bind metals and transport them outside the cell (Gledhill *et al.*, 1999).

1.2.4. Eco-physiological significance

The interplay between the above-mentioned stress mechanisms and detoxifying strategies allows seaweeds to tolerate metal-polluted environments. This and other characteristics, such as their abundance in coasts and estuaries, sessile nature and high concentration factors for metals, have contributed to the use of these organisms as indicators of pollution by trace metals (Phillips, 1977). In addition, seaweeds can integrate temporal fluctuations of only the dissolved bioavailable fraction of metals in marine ecosystems (Rainbow, 1995). Many species of seaweeds have already been tested as bioindicators of metal pollution. For example, apical parts of *Ascophyllum nodosum* (Fucales, Phaeophyta) were suggested as sensitive biological indicators for copper but not for iron (Stengel & Dring, 2000; Villares *et al.*, 2005). Another seaweed considered as good bioindicator for a range of metals is *Fucus vesciculosus* (Forsberg *et al.*, 1988; Cairrão *et al.*, 2007). However, not all the populations or species of algae show the same levels of resistance to metals. For instance, five distinct populations of the red seaweed *Gracilariopsis longissima* showed the same levels of resistance and accumulation of Cu

(Brown *et al.*, 2012). In contrast, interpopulation differences in the response to Cu have been identified in *Fucus serratus* and *E. siliculosus* in the laboratory (Nielsen *et al.*, 2003b; Roncarati *et al.*, 2015; Sáez *et al.*, 2015c), where higher resistance to Cu was observed in individuals sampled at metal polluted sites. Comprehensive understanding of intraspecific and interspecific variation in the response of seaweeds to metals would allow their validation as biomonitors (Brown *et al.*, 2012). Furthermore, such knowledge is becoming crucial in current times as unpredictable interactions with metal pollution could arise from other anthropogenically-derived stress factors, such as ocean warming.

1.3. Temperature variations and marine algae responses

Temperature is critical abiotic factor playing a central role in most of marine life inhabiting oceans, reefs and estuaries (Hutchins, 1947; Somero, 2002; Somero, 2011; Bartsch *et al*., 2012; Eggert, 2012; Takao *et al*., 2015). The relative easiness to measure and control temperature has allowed scientist to determine experimentally the response of particular species to changes in temperature. Thus, upper and lower limits at which some organisms can grow, reproduce or complete the life cycle have been estimated (Kempner, 1963; Brock, 1967; Doemel and Brock, 1970; Brock, 1985; Eggert *et al*., 2003; Rosa *et al*., 2012; Clarke *et al*., 2013). However, the optimal temperatures for most of the marine life is usually related to the prevailing regimes in their natural habitats (Somero, 2002). Beyond the maximal upper and lower limits, temperature may be lethal for aquatic organisms. Thus, individual, species and populations have a tolerance zone determined by an interaction of developmental, genetic and environmental stimuli (Cairns *et al*., 1975; Heugens *et al*., 2001). Such interactions will determine the eurythermal or stenothermal nature of a particular species, being eurythermal the organisms able to thrive in environments with larger seawater temperature fluctuations, while stenothermal organisms only occur in regions with narrow temperature variations (Eggert, 2012). In

this context, three kinds of responses to temperature can be distinguished for sessile organisms such as seaweeds: “short-term physiological regulation” (seconds to minutes), “phenotypic acclimation” to variable environmental conditions (hours to days) and “evolutionary genetic adaptation” to prevailing local conditions (millions of years) (Eggert, 2012). Extensive thermal physiology studies in marine animals, such as mussels and crabs, had looked at different levels of biological organisation (e.g. cellular and molecular) (see Somero, 2002, 2011). In contrast, available information on macroalgae responses to temperature mainly focuses on the effects on growth, photosynthetic performance or survival.

Past studies had intended to determine the eurythermal or stenothermal nature of marine algae by assessing performance traits such as growth, photosynthesis and reproduction (Wiencke *et al*., 1994; Eggert and Wiencke, 2000; Eggert *et al*. , 2003). A high inter- and intraspecfic variation was observed in the responses, but the optimum ranges were correlated to the prevailing temperature regimes at the collection site or origin of the isolates (Bolton, 1983; Bischoff-Bäsmann *et al*., 1997; Graiff *et al*., 2015). For example, Bolton (1983) described the brown filamentous alga *Ectocarpus siliculosus* as eurythermal from laboratory assays. However, its optimal temperature ranges for growth and long-term survival were related to the collection site, even when such isolates had been acclimated for many years to 20 °C in laboratory conditions. The latter indicates the presence of genetic adaptations to gradual variation of ambient temperature also known as an “ecocline”. There is evidence indicating that species of macroalgae endemic to environments with low seasonal temperature variation, such as the tropics and Antarctica, are stenothermal compared to eurythermal species occurring in temperate regions, where seasonal fluctuations in temperature are more evident (Bischoff-Bäsmann and Wiencke, 1996; Bischoff-Bäsmann *et al*., 1997). For instance, great interspecific variations in temperature tolerance has been observed in 53 species of benthic algae from

the “cold-temperate” North Sea (Lüning, 1984). However, all the species but one (*Monostroma undulatum*) were able to photosynthesise in a range of 0 to 20 °C. Among the brown algae, *Fucus* spp. and *Cladostephus spongiosus* were the most tolerant, surviving at 28 °C, and *Chorda tomentosa* and *Laminaria* spp. the more sensitive, surviving only up to 18 and 20 °C, respectively. In contrast, the Antarctic endemic red seaweeds *Gigartina skottsbergii* and *Ballia callitricha* were able to growth only in the narrow range of 0 to 5 °C (Eggert & Wiencke, 2000).

Although alterations in growth reflect the effects of temperature on the overall metabolism, this does not necessarily correspond to the responses of specific physiological processes such as photosynthesis (Davison, 1987; Kübler and Davison, 1993; Graiff *et al*., 2015). Eggert and Wiencke (2000) for instance, observed that the temperature optima for photosynthesis were above the temperature optima for growth, in both eurythermal and stenothermal Antarctic species. Similar results were observed in two species of the genus *Lomentaria* (Kübler *et al.*, 1991), where growth inhibition occurred at lower temperature than photosynthesis inhibition (30 and 35 °C, respectively) for *L. baileyana*, a “temperate-subtropical” species, compared to *L. orcadensis* (20 and 30 °C), a “boreal-temperate” species. Despite the mismatch between growth and photosynthesis optima, the responses of both traits reflected local adaptations to the seaweed’s habitat, the tropical species being able to tolerate higher temperatures compared to the boreal-temperate species.

Besides genetic adaptations to prevailing temperatures regimes, phenotypic acclimation to changes in temperature also play an important role in seasonal responses to ambient temperature. For example, Kübler and Davison (1993) showed in laboratory experiments that the red seaweed *Chondrus crispus* presents different degrees of photoinhibition when exposed to thermal stress. However, this species is able to

acclimatise to growth temperatures up to 20 °C. Individuals acclimated at 20 °C tolerated brief exposure to extremely high temperatures better than individuals acclimated to 5 °C. The enhanced resistance to high temperature was associated with a reduced degree of photoinhibition of the 20 °C-grown plants. This study suggests that acclimation may play an important role in the success of intertidal species under changing environments even over short time scales. However, an often-ignored aspect of temperature response experiments in seaweeds is the life stage of the individuals tested. Species with heteromorphic life stories (e.g. Laminariales) may show different temperature tolerances for each life stage (tom Dieck (Bartsch), 1993). Also, in *Fucus vesciculosus*, germination success is reduced by 90% at 25 °C compared to 15 °C, which indicates differences in susceptibility to temperature of different developmental stages in seaweeds (Wahl *et al.*, 2011). A more comprehensive understanding of the responses of different life stages and levels of biological organisation in seaweeds is needed to fully understand the effects of temperature in these organisms.

Temperature is responsible for alterations in chemical reaction rates. Thus, the sum of chemical reactions that determine metabolic pathways are affected by temperature (Denman *et al*., 1996; Hochachka and Somero, 2002). Enzymes in living systems catalyse most of metabolic reactions and each enzyme-catalysed reaction shows an optimum temperature that also depends on pH (Lobban and Harrison, 1994; Hochachka and Somero, 2002). Davison and Davison (1987) studied the activities of several key enzymes of carbon and nitrogen metabolism under different growth temperatures in *Saccharina latissima* (*Laminaria saccharina*). The enzymes analysed performed differently; for example, the activities (measured at 20 °C) of glyceraldehyde-3-phosphate dehydrogenase and Rubisco, both involved in the Calvin-cycle, were inversely proportional to the growth temperature (ranging from 0–20 °C). However, the activities of the enzymes involved in respiration: malate dehydrogenase (MDH), mannitol-1-

phosphate dehydrogenase (M-1-PDH) and phosphoenol-pyruvate carboxykinase (PEP-CK) were unaffected by changes in growth temperature. The variation observed at the biochemical level suggest that different strategies, such as reduction of the Krebs cycle enzymes activities, may be involved in phenotypic adaptation to seasonal variation of seawater temperatures.

Photosynthesis and respiration are complex ensembles of single chemical reactions whose overall optimum rates can be affected differentially by temperature ultimately determining the growth optimum for a species (Davison, 1991). The potential for acclimation of photosynthesis to sub- and supra-optimal temperatures was tested in seven isolates of the tropical to warm-temperate green alga *Valonia utricularis* (Eggert *et al.*, 2006). In the mentioned study, it was demonstrated that Mediterranean/Atlantic isolates of *V. utricularis* are able to acclimatise the relative photosynthetic electron transport rate (rETR) to suboptimal temperatures in contrast to Indo/west Pacific isolates. However, at supra-optimal temperature (30°C) the same isolates showed signs of photoinhibition (measured as a reduction of maximal quantum yield: F_v/F_m) and reductions in pigment content, while the Indo/west Pacific isolates did not differ from each other. In a similar way, populations of *Asparagopsis taxiformis* from Hawaii and California were tested for their photosynthetic capacity of short term and seasonal acclimation to the natural variability in temperature in their environment (Padilla-Gamiño & Carpenter, 2007). The populations from California showed different trends in maximum net photosynthesis ($Pnet_{max}$) and maximum rETR between seasons, while the population from Hawaii did not. Besides, there is some evidence that species occurring in the intertidal may respond faster to changes in temperature compared to individuals occurring in the subtidal measured as expression of heat shock proteins (Henkel *et al.*, 2009). Thus, the examples above suggest that populations occurring in environments with greater temperature fluctuations have also a greater acclimation potential, allowing them

to acclimate to seasonal and short-term variations in temperature compared to individuals living in less variable environments such as the tropics or sublittoral zones.

When temperature surpasses the capacity of seaweeds to acclimate heat and cold stress, it can disrupt cellular processes. The extent of the damage will depend on the time scale of the exposure. After short-term exposure (hours) species may recover depending on their tolerance range. However, long term exposure to disruptive temperatures may impair cellular processes such us photosynthesis and enzymatic activity (Allakhverdiev *et al.*, 2008; Eggert, 2012). The main temperature-sensitive sites in the photosynthetic apparatus are suggested to be: photosystem II (PSII) and the oxygen evolving complex, ATP synthase and enzymes in the Calvin cycle (Allakhverdiev *et al.*, 2008). Other effects at the cellular level are alterations to chloroplast ultrastructure under cold stress and induction of the expression of chaperones also known as heat shock proteins (Sørensen *et al*., 2003; Collén *et al*., 2007; Henkel *et al*., 2009; Eggert, 2012). It has been proposed that alterations to the fluidity of membranes may act as a sensor for changes in temperature (Los & Murata, 2004). Thus, this hypothesis was tested by using mutants of the cyanobacterium *Synechocystis* knocked out for genes coding for fatty acid desaturases (Inaba *et al.*, 2003). The authors of this study concluded that a decrease in membrane fluidity after exposure to cold stress and the subsequent transduction of this signal led to the regulation of gene expression as highlighted using microarray technique. In contrast, the response to heat stress was not related to a signal resulting from rigidification of membranes. Another study also used microarrays to assess the whole transcriptome response of the red alga *Chondrus crispus* to thermal and other natural stresses (Collén *et al.*, 2007). Forty-six genes, including two polyubiquitins, peroxinectin, helicase, HSP-16, -60, and -70, metalloproteinase, glyoxalase, thioredoxin and others, were proposed as markers of thermal stress.

Although much effort has been made in evaluating the responses of seaweeds to temperature in different habitats, the basis for thermal tolerance and acclimation remain unknown for the different groups of seaweeds. Recent studies have demonstrated the importance of thermal studies in seaweeds as some data suggest that local declines in marine macrophytes such as *Saccharina latissima* and *Fucus* spp. are in part due to increase of sea-surface temperatures (Andersen *et al*., 2013; Graiff *et al*., 2015; Takao *et al*., 2015; Wernberg *et al*., 2016). However, there is some evidence that a combination of high pCO_2 and elevated temperatures might be beneficial for some species such as *Cystoseira tamariscifolia* (Phaeophyceae) (Celis-Plá *et al.*, 2017). The advent of new techniques such as next-generation sequencing and the other omics technologies will aid the study of the molecular basis of thermal responses, an issue that is becoming more relevant in the face of climate change scenarios. Additionally, considerations for interactions with other local stressors (Al-Janabi *et al.*, 2016) such as nutrient availability or pollutants are becoming a necessity to understand the real impacts of human activities on seaweeds assemblages.

1.4. Interactions between metal pollution and temperature

Marine ecosystems are of vital importance for the planet in terms of ecology and economy; for example, coastal habitats are estimated to provide between 30 and 40% of the average global value of annual ecosystem goods and services (e.g. nutrient cycling, food production, raw materials, etc.) (Costanza *et al*., 1997, 2014; de Groot *et al*., 2012). Coastal zones are the home of one third of world's human population, relying mainly on services provided by these ecosystems (Barbier, 2012). A seemingly inexorable growth in the population, which is predicted to increase to 9.7 billion by the year 2050 and 11.2 billion by 2100, according to the current predictions of the United Nations organisation (http://www.un.org/en/development/desa/news/population/2015-report.html), is giving

rise to increases in direct and indirect pressures on nearshore ecosystems globally. One such direct pressure is input of chemical contaminants, which can lead to pollution and decline in water quality (Clark *et al.*, 1997). Most organic and inorganic contaminants, such as, aliphatic and aromatic compounds, radionuclides and metals (Chakraborty *et al.*, 2014; Jepson & Law, 2016; Lodenius, 2016) can be persistent in the ocean ecosystems and are, therefore, regarded as serious threats to the well-being of marine biota (Kamala-Kannan *et al.*, 2008). The rise in world population not only generates impacts, such as pollution, at local scales, anthropogenic-derived emissions of CO_2 from e.g. fossil fuels combustion, are a major cause of observed changes in the global climate including warming of the atmosphere and oceans due to the greenhouse effect (IPCC, 2014). While pollution is threatening marine life on a local-immediate scale, long-term rises of sea temperatures will most likely have wider effects on entire populations causing shifts in distribution of organisms and on global biogeochemical cycles (Harley *et al*., 2006; Doney, 2010; Doney *et al*., 2012). Thus, organisms such as marine macroalgae (seaweeds) that inhabit coastal and estuarine environments, are exposed to dynamic multiple environmental stressors (Figure 1).

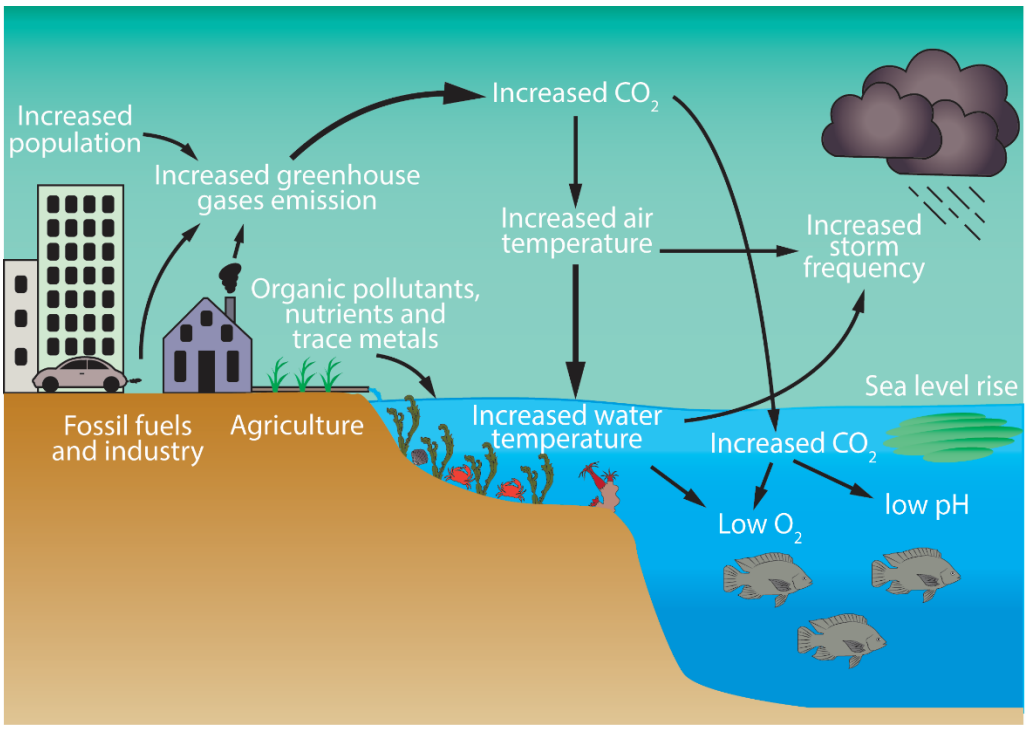

Figure 1.1. Different sources of environmental stressors for nearshore ecosystems

Despite the great advances in understanding the effects of metal stress in marine macroalgae, studies considering these pollutants acting in interaction with other abiotic stressors such as temperature, pH, UV radiation or other pollutants are still scarce. Temperature increase is probably the most evident consequence of global climate change. In the last fifty years the heat content of the upper oceans has increased substantially with a mean global sea-surface temperature (SST) increase of approximately 0.4°C (Levitus *et al*., 2009) and the warming trend is expected to accelerate in the next 50–100 years (Harley *et al.*, 2006). Mackenzie and Schiedek (2007) analysed an SST data set for North and Baltic seas since 1861 and 1880 respectively. These authors found that since 1985 summer SSTs increased at nearly triple the global warming rate partly as a consequence of increased frequency of extremely warm years. An evident sign of global warming is the decline of sea ice extent in the Arctic and along the western Antarctic Peninsula (Stroeve *et al*., 2007; Stammerjohn *et al*., 2008). On a broader scale, warming may also increase water-column vertical stratification, affecting ocean currents, mixing and

ventilation (Doney *et al*., 2012). As not all aspects of stress generated by climate change can be covered here, this section will emphasize the effects of temperatures and its potential interaction with metal stress in macroalgae.

Although much of the information about the effects of temperature and trace metals in marine macroalgae has been generated independently for each type of stress (as reviewed above), there is a lack of empirical data about the combined effects of these factors. Just few publications reviewed the effects of interactive stressors including metal and temperature (Cairns *et al*., 1975; Heugens *et al*., 2001; Sokolova and Lannig, 2008; Holmstrup *et al*., 2010). Moreover, the information provided in these papers mainly addressed the interactions in invertebrate or fish species. When a combination of two or more stressors is affecting an organism, the interactions may be of three types: synergistic, antagonistic or additive (Cairns *et al*., 1975; Darling and Côté, 2008; Todgham and Stillman, 2013). A synergistic interaction occurs when the effect of a combination of stressors is larger than the sum of the individual effects (Folt *et al.*, 1999). On the other hand, an antagonistic interaction occurs when the combined effect of stressors is smaller than the sum of the single effects (Darling & Côté, 2008). If the combined effect matches the sum of the individual effects, then the interaction of stressors is considered additive (Halpern *et al.*, 2008). Most of the studies looking at interactions between metals and temperature have found synergistic interactions (Holmstrup *et al.*, 2010). For example, erratic heart rate was observed in the common shore crab *Carcinus maenas* exposed to sublethal copper concentrations at higher (25°C) and lower (5°C) temperatures than the collection site (17°C) indicating, to some extent, synergistic effects of temperature extremes in Cu toxicity (Camus *et al*., 2004). In another animal example, Jacobson *et al*. (1997) found increased copper sensitivity of larvae of the freshwater mussel *Actinomaias pectorosa* at elevated temperature. In addition, a rise in temperature from 10 to 25°C resulted in a decrease of LC_{50} – 24h (the Cu concentration at which 50% of the larvae

died in a period of 24 hours) from 132 to 42 μg L^{-1} copper. Other examples of interactive effects come from terrestrial plants. Cadmium interacted synergistically with elevated temperatures inhibiting growth of shoot and root in seedlings of two varieties of wheat (*Triticum aestivum*). In contrast, exposure of the seedlings to Pb did not show any effect on the same parameters (Öncel *et al.*, 2000).

Temperature may affect metal toxicity in macroalgae in both indirect and direct ways usually complex to evaluate in nature. For example, changes in temperature and pH may affect the speciation of metal species in seawater (Byrne *et al.*, 1988), which in turn may affect the availability of metals for uptake by algal cells. Temperature may also affect the polysaccharides that constitute the cell wall (Aksu, 2002) affecting the binding capacity and thus an important metal-tolerance mechanism. The properties of biological membranes properties may also be affected allowing increased permeability for metal ions and other toxicants (Cairns *et al.*, 1975; Maheswari *et al.*, 1999). Thus, temperature may affect toxicant diffusion rates resulting in higher toxicant uptake rates, but elimination and detoxification mechanisms, such as production of intra and extracellular metal chelators, may counteract the thermal effect on uptake rate, as the rates of these processes may increase as well (Hochachka and Somero, 2002; Holmstrup *et al*., 2010; Hurd *et al*., 2014). The reported increase in toxicity as temperatures increase suggest that the effect on uptake rates is more important than the effect on detoxification rate (Heugens *et al.*, 2001). As reviewed in previous sections, temperature and metals have been shown to inhibit photosynthesis in seaweeds *in vitro* when assessed independently. Therefore, it is tempting to suggest that a combination of both stresses would act synergistically to affect photosynthetic performance of macroalgae. However, this assumption remains speculative due to insufficiency of empirical data about such interactions in macroalgae. Nevertheless, some data have been generated in two species belonging the freshwater green algae genus *Chlorella*. In the species *C. vulgaris* an increase of temperature, from

24 to 31°C, induced higher alterations to PSII quantum yield (F_v/F_m) and a greater decrease of total photosynthetic performance compared to copper effect alone (Oukarroum *et al.*, 2012). A thermophilic strain of *C. pyrenoidosa* grown at an optimal temperature of 35°C showed enhanced inactivation of PSII, measured as a decrease in F_v/F_m, when exposed to lower temperatures (30, 25, 20 and 15°C) and concentrations of Cu up to 0.4 μM. However, this effect was observed only when algae were cultured under light (Vavilin *et al.*, 1995). More recently, a study examined the effects of a combination of Cu and different temperatures in adults and juvenile *Fucus serratus* (Nielsen *et al.*, 2014). The authors found that both temperature and Cu do not affect photosynthetic parameters, such as rETR or F_v/F_m, in adult individuals, while the opposite occurred in germlings. Thus, early stages of development were suggested to be more sensitive to the combination of stressors. These studies support the idea that deviations from the optimal temperature for growth may enhance the toxic effects of metals in the photosynthetic apparatus. Still other factors such as irradiance may take part in the modulation of the responses.

Other intracellular effects of temperature on metal toxicity were examined by Wang and Wang (2008) in the marine diatom *Thalassiosira nordenskioeldii*. They showed that either high accumulation of Cd at 24°C or poor detoxification capacity at 30.5°C was responsible of the higher concentrations of Cd in the metal-sensitive fraction (MSF, organelles plus heat-denatured proteins) resulting in higher sensitivity to this metal at increased temperatures. Other mechanisms acting in this diatom such as N deficiency and GSH depletion explained partially the increased sensitivity at 30.5°C. Although Cd^{2+} induced the production of phytochelatins, the ratio between intracellular Cd and PCs did not explain the temperature-dependent metal tolerance or toxicity. Changes in temperature may lead the production of ROS in plant cells (Prasad, 1996; Dummermuth *et al.*, 2003). As high temperatures inactivate the translation of most proteins in plants,

with the exception of specific heat-shock proteins (Feierabend, 2005), translation of antioxidant enzymes such as catalase may be inhibited at high temperatures (Hertwig *et al.*, 1992). However, the role of temperature in the ROM of macroalgae under metal stress remains largely unknown, although some data have been generated by Collén *et al*. (2007) as reviewed in the previous section.

A widespread intracellular response to stress observed is the enhanced synthesis of stress proteins or heat shock proteins (HSP) (Schlesinger, 1990). These ubiquitous proteins are highly conserved and expressed at constitutive levels under normal conditions (Torres *et al.*, 2008). Metals and other environmental factors such as temperature elicit changes in transcription of HSP genes (Guo & Ki, 2012). Major families of HSP include HSP110, HSP100, HSP90, HSP70, HSP60, HSP40, HSP10 and small HSP families (16–24 kDa), which are distinguished based on their sequence homology and molecular weight (Feder & Hofmann, 1999). However, not all of these families are stress-inducible. For example, Kammenga *et al*. (1998) found that HSP60 and HSP70 were induced under heat stress and HSP60 was also induced under Cu and Cd stress in the nematode *Plectus acuminatus*. In the green algae *Enteromorpha (Ulva) intestinalis* HSP70 was also induced with thermal stress, but this family of proteins was not sensitive to Cu stress at environmentally relevant concentrations (Lewis *et al.*, 2001). In *Fucus serratus* and *Lemna minor* exposed to Cd, the production of HSP70 increased to a maximum and subsequently decreased as the stressor levels increased (Ireland *et al.*, 2004). The peak observed may be due to the fact that energy cost of HSP expression would offset their protection capacity (Torres *et al.*, 2008).

The study of interactions between stressors in marine macrophytes is becoming an urgent necessity as the world has started to see seaweeds as a sustainable alternative for biomass production. Wahl *et al*. (2011) reviewed several types of interactions in the

genus *Fucus*. Those studies revealed high levels of complexity when a combination of stresses was evaluated. As changes in environmental temperature are a direct consequence of climate change, it should be a priority to evaluate the combination of temperature and other abiotic and human-derived stressors that may act at local scales (Schiedek *et al.*, 2007; Harley *et al.*, 2012; Nikinmaa, 2013). In this respect, the use of model organisms can provide new insights into the basal molecular responses of organisms under stress. Recently, *Ectocarpus siliculosus* has emerged as a model organism for the study of genetic and genomics in the brown algae (Peters *et al.*, 2004; Coelho *et al.*, 2012a). The application of molecular tools, such as quantitative Polymerase Chain Reaction (qPCR) and Next Generation Sequencing (NGS), in this model organism will allow a better understanding of responses to abiotic stresses caused by pollution or global change, ultimately allowing the creation of 'fingerprints' or 'signatures' for specific and general responses to stress.

1.5. *Ectocarpus siliculosus* as a model for the study of abiotic stresses

The brown algae (Phaeophyceae) are a class of marine organisms of global ecological and economic importance. They belong to the division Heterokonta (Stramenopiles) which are distantly related to other groups of algae and green plants (Charrier *et al*., 2008; Fig. 1.2a). Their evolutionary history is of much interest because this group evolved novel metabolic, physiological, cellular and ecological characteristics including unusual biomolecules such as polysaccharides that have a wide range of applications in industry (Peters *et al.*, 2004). However, this evolutionary distance from other more studied groups represent a problem for the study of these algae because other well developed model organisms for plants and animals are of limited relevance to brown seaweeds (Charrier *et al.*, 2008). The above-mentioned reasons encouraged the development of *Ectocarpus siliculosus* (Dillwyn) Lyngbye (Ectocarpales, Phaeophyceae)

as a model organism for the brown algae (Coelho *et al.*, 2012a). *Ectocarpus siliculosus* (Figure 1.2c) is a filamentous brown alga belonging to the order Ectocarpales (see phylogeny in Figure 1.2a,b). This species has a worldwide distribution in temperate regions, but does not occur in the tropics and south of the Antarctic convergence (Charrier *et al.*, 2008). Members of the Ectocarpales order are closely related to the more differentiated and complex Laminariales (kelps), which are major components of the marine flora (Villegas *et al.*, 2008; Sáez *et al.*, 2012). *Ectocarpus* spp. can be found in a wide range of habitats, from marine to low-salinity including a record from freshwater in Australia (West & Kraft, 1996). This seaweed is able to grow on different substrata including submersed man-made structures such as wharfs, buoys and ship hulls (Charrier *et al.*, 2008), as well as growing on rocks and epiphytically on other marine organisms (Russell, 1983).

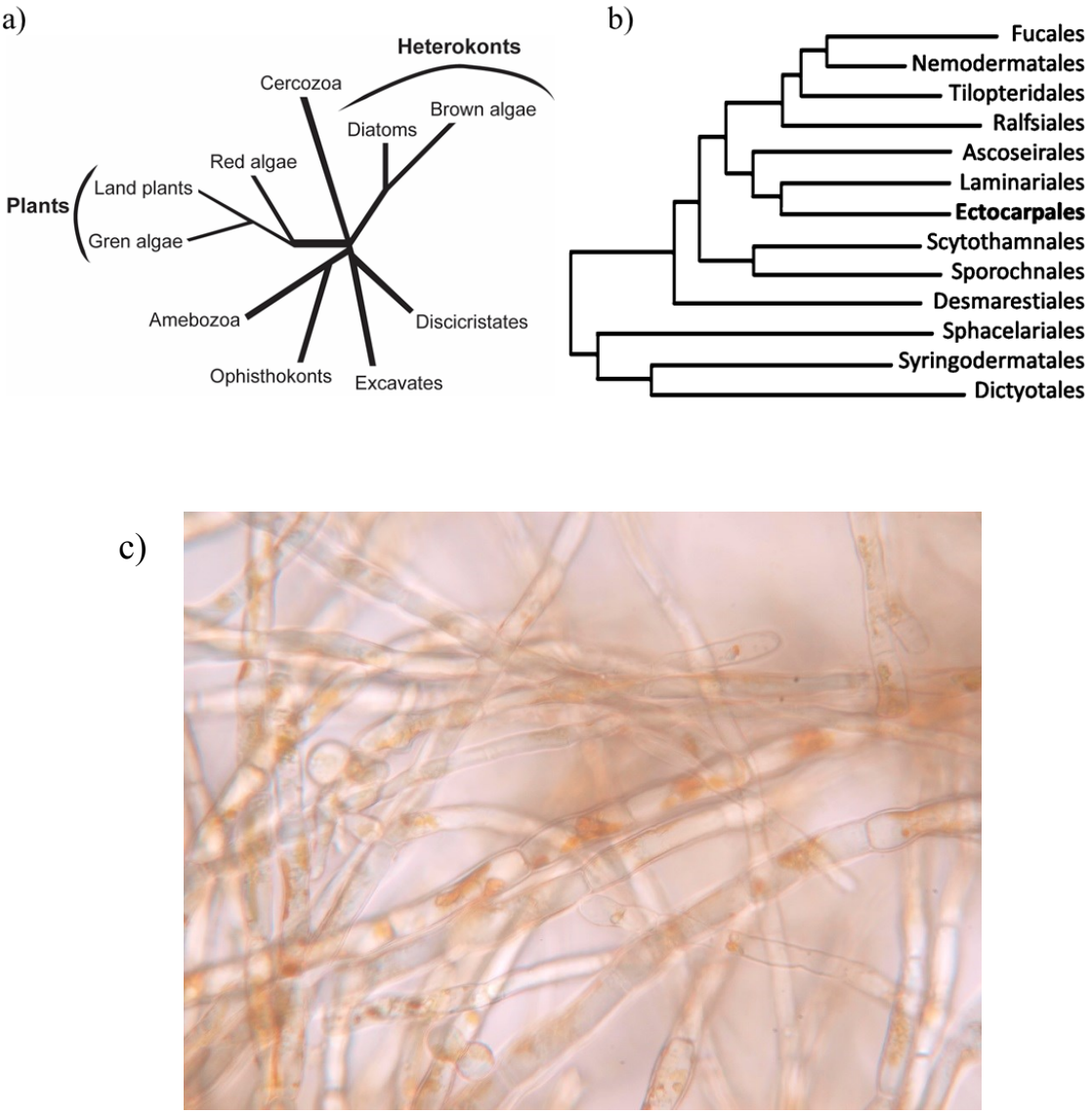

Figure 1.2. a) Phylogeny of brown algae within eukaryotes (adapted from Charrier *et al*., 2008). b) Order Ectocarpales within the brown algae (adapted from Silberfeld *et al*., 2010). c) *E. siliculosus* filaments

In nature, the filamentous thallus of *E. siliculosus* can grow to ca. 30 cm, but in laboratory culture filaments may become fertile whith only 3 cm (Charrier *et al.*, 2008). The life cycle comprises of two independently growing macroscopic phases: a diploid (2n) sporophyte, which produces few lateral filaments and develops from a prostrate base, and a morphologically different haploid (n) gametophyte that is richly branched and devoid of a prostrate base (Peters *et al.*, 2008). After the germination of the zygote,

subsequent mitoses leads to the development of a uniseriate linear filament composed of round and elongated cells. Fifteen days after germination filaments emerge from this basal structure developing a young prostrate sporophyte (comparable in function to a holdfast of other brown algae) within ca. 20 days (Le Bail *et al.*, 2008a). Under favourable conditions erect filaments or "upright filaments" emerge contributing to the formation of an adult filamentous sporophyte structure (Charrier *et al.*, 2008). Sporophytes produce two types of reproductive organs: plurilocular and unilocular sporangia, both mainly localised in the upright filaments (Müller, 1964). The former are cone-shaped and contain a number of locules generated by successive mitosis. Biflagellated mitospores can swim shortly after release and ultimately initiate a new generation of sporophytes. In unilocular sporangia, a single meiosis is followed by several mitoses to produce about 100 meiospores (50% male and 50% female). These meiospores germinate to produce the haploid gametophyte generation. Gametophytes are dioecious and generate either male or female gametes exclusively in plurilocular gametangia (Charrier *et al.*, 2008). Gametes, which resemble mitospores in terms of motility, fuse to produce diploid zygotes, which develop into a new sporophyte generation (Coelho *et al.*, 2012a). Further complex features of the life cycle have been described in Charrier *et al*. (2008) and Bothwell *et al*. (2010).

One reason that led to the proposal of *E. siliculosus* as a genetic and genomic model organisms for the brown algae was its long history of research (Coelho *et al.*, 2012a). Other important features are its small size, ability to complete the life cycle in Petri dishes in just three months, high fertility and the ease to perform genetic crosses. Additionally, its genome (214 Mbp) is relatively small compared with other morphologically more complex brown algae, such as *Laminaria digitata* and *Fucus serratus* (Peters *et al.*, 2004; Charrier *et al.*, 2008; Cock *et al.*, 2010). The publication of the *E. siliculosus* genome by Cock *et al*. (2010) represented a milestone for the study of

novel aspects of the biology of this species and, more generally, the evolution of brown algae. Following the assembly of the genome sequence, additional tools have been developed including expressed sequence tag (EST) collection, whole genome tiling arrays, EST-based expression microarrays (Dittami *et al*., 2009; Ritter *et al*., 2014), a genetic map (Heesch *et al.*, 2010), proteomics (Ritter *et al.*, 2010), metabolomics (Prigent *et al.*, 2014) and genetic crossing protocols (Coelho *et al.*, 2012b). Some of the above-mentioned approaches have already shown high intra-specific genomic variability between ecotypes of this species, supporting the concept of *E. siliculosus* as a complex of cryptic species (Dittami *et al.*, 2011b).

Despite the fact that *Ectocarpus* occurs in relatively stressful coastal environments, exposed to continuous variations in temperature, salinity, irradiance and pollution, little is known about its ecophysiology (Charrier *et al.*, 2008). Regarding temperature tolerance, *E. siliculosus* appears to be eurythermic based on data obtained from strains collected in the whole range of distribution from the Arctic to warm habitats (Bolton, 1983). That study demonstrated that growth temperature optima for different strains are correlated to the temperature of the collection site. For example, a strain collected in Port Aransas, TX (USA) showed a growth temperature range of 5–26°C, an optimum temperature at 20°C and the highest upper survival temperature (UST) of 33°C. In contrast, other strains collected in more temperate regions such as Norway showed values of 5–23, 20 and 23°C for the same parameters (Bolton, 1983; Wiencke *et al.*, 1994). The data suggest the wide ecological and geographic range of the species has been achieved at least in part due to evolution of genetic variation in temperature tolerance between populations. These authors also found that gametophyte generation is less tolerant that the sporophyte with respect to temperature tolerance. Recently, Peters *et al*. (2010) explained partially the differentiation between generations by observation of *E. crouaniorum* phenology. They found that sporophytes occur all year round while

gametophytes are ephemeral, occurring only in spring. Therefore, the sporophyte generation might be expected to be more resistant to extreme conditions. Other stressful conditions (e.g. hypo and hyper-salinity, oxidative stress) were recently assessed in a global gene expression analysis of *E. siliculosus* (Dittami *et al.*, 2009). This study found that almost 70% of the expressed genes were regulated in response to at least one of the stressors, which represents an extensive reprogramming of the transcriptome during the acclimation to mild abiotic stress. Understanding mechanisms of stress at cellular and molecular levels may allow the early detection of stress cause by toxicity of contaminants or climate change.

Toxic effects generated by exposure to metal pollution and the mechanisms of tolerance in brown algae are other interesting topics to explore using the new "omics" platforms available for *E. siliculosus*. A proteomic study in two strains of *E. siliculosus*, Es32 from a non-polluted site in Peru and Es524 from a Cu-polluted site in Chile, revealed local genetic adaptation related to the contamination history of the strains (Ritter *et al.*, 2010). Similarly, Sáez *et al*. (2015b) examined the antioxidant responses of three strains of *E. siliculosus* with different Cu-pollution histories. All strains showed different detoxification strategies with Es524 (Cu-polluted origin, Chile) being the most tolerant to Cu compared with LIA08-4 (pristine origin, Scotland) the most sensitive, and EcREP10-11 (Cu-polluted origin, England) having an intermediate response. An additional study with the strains Es524 and LIA08-4, reported differences in levels of expression of genes involved in the phytochelatin (PCs) biosynthetic pathway (Roncarati *et al.*, 2015). The increased sensitivity to Cu of LIA08-4 was attributed in part to the decreased production of PCs. Recent transcriptomic and metabolomic analyses further demonstrated Cu-induced oxidative stress in *E. siliculosus*, showing the activation of oxylipin and repression of inositol signalling pathways in addition to other conserved processes for Cu and H_2O_2 stress (Ritter *et al.*, 2014).

1.6. Problem and aim of the project

Although most of the knowledge about the mechanisms of stress in marine macroalgae has been obtained from carefully controlled single-factor experiments, the non-linear interactions observed in multifactorial studies has raised concerns about the misleading interpretations that could arise from such studies. Marine habitats are multivariate environments where abiotic and biotic interactions take place in a complex manner. Besides the necessity of understanding the interplay of different naturally occurring factors of stress affecting marine biota, the alarming rates at which climate change is taking place have raised many questions about the magnitude of the consequences of anthropogenic pressures in the marine environment. This indicates that actions should be taken to fill gaps in current knowledge about potential effects of altered climate cycles at different scales. The Intergovernmental Panel on Climate Change (IPCC) has maintained an up-to-date view of the current state of scientific knowledge relevant to climate change through regular publications of assessment reports since 1988. The information compiled in these reports has raised concerns about impacts, in the mid and long-term, of increased atmospheric and oceanic temperatures on all living organisms. Other threats such as ocean acidification, altered storm patterns and increased solar radiation have all been identified as a consequence of human greenhouse emissions.

In a similar way, classic ecotoxicology studies have focussed on the effects of exposure to single toxicants under laboratory conditions. Most of those studies have used environmentally irrelevant concentrations of toxicants. For example, Connan and Stengel, 2011a and b, used up to 70 μM in exposure experiments. However, copper concentrations in pristine environments and offshore range from 1 to 10 nm (Brown & Newman, 2003), while in metal polluted ecosystems do not surpass 4 μM (Correa *et al*., 1996; Correa *et al*., 1999; Bonanno and Orlando-Bonaca, 2018). Additionally, chemical persistent

pollutants such as metals occur simultaneously with other abiotic stress factors, and so research on combinations of such factors is required to achieve accurate extrapolations from the laboratory tests to the natural environment. The importance of such information spans many disciplines from management of the marine resources, policy making, biomonitoring and biotechnology. Also, it will improve the predictions of the real impacts of pollutants such as metals in a climate change context. Metals are a well-studied group of persistent pollutants affecting marine ecosystems. Ecotoxicological studies on metals have found different degrees of impact in a broad range of organisms, including marine macroalgae (seaweeds). However, the underlying mechanisms of metal stress and tolerance in seaweeds remain unclear.

The main aim of this study was to determine the nature of the interactions (synergistic, additive or antagonistic) of different concentrations of copper in combination with increased temperatures in the model brown alga *Ectocarpus siliculosus*. The responses in *E. siliculosus* were evaluated at different levels of biological organisation, which were divided into three specific objectives tested in the experimental chapters of this thesis:

- The first objective was to assess the responses to a combination of both stressors at the organismal level (measured as growth rate), photosynthetic physiology (measured as chlorophyll *a* fluorescence and changes in photosynthetic pigments) and bioaccumulation of Cu ions (Chapter III).

- The second objective was to evaluate the responses at the biochemical level by measuring parameters related to the reactive oxygen metabolism, namely, concentrations of H_2O_2 and lipid peroxides (TBARS), which are indicators of oxidative stress. Additionally, the concentration of antioxidants molecules (glutathione, ascorbate and phenolic compounds) and the activity of antioxidant enzymes (superoxide dismutase,

ascorbate peroxidase, catalase and glutathione reductase) was estimated. The results of the biochemical test were linked to the gene expression of related genes assessed by RT-qPCR (Chapter IV).

- The third objective was to study the whole transcriptome response to temperature and Cu stress (by RNA-seq technology) and integrate the results in the light of the previous two Chapters findings (Chapter V).

- Finally, in chapter VI we provided a general discussion on the relevance of the study of interactions between different stressors, the limitations and advantages of laboratory assays and the new perspectives for future work arisen from the findings of this work.

Chapter II

General Materials and Methods

2.1. Experimental design

All algal biomass used in laboratory assays was produced as described in section 2.2. When enough biomass was attained, it was transferred to individual polycarbonate flasks following the experimental design specific for each chapter. In chapter III, algal biomass was transferred to flasks containing four Cu concentrations: 0 (no Cu added), 0.8, 1.6 and 3.2 μM of total Cu (Cu_T) and flasks were divided into two controlled environment chambers (Sanyo, MLR 350T) at different temperatures: 15 °C (control) and 25 °C (elevated) for a total of n = 3 replicates per treatment (Figure 2.1.a). Endpoints were measured after 6 days of exposure based on the results of previous trials showing that 3.9 μM of Cu decreased the maximum quantum yield of photosystem II (F_v/ F_m) after 6 days of exposure at 15 °C. Elevated temperature of 25 °C was chosen as 2-4 degrees above the maximum temperatures recorded in the site of collection of the *E. siliculosus* strain used (see section 2.2.). This was in agreement with sea warming predictions until the end of the century (IPCC, 2014; Laffoley & Baxter, 2016).

In Chapters IV and V, a different experimental design was applied due to budget limitations. Samples were exposed to only to two Cu concentrations: 0 (no Cu added) and 2.4 μM of Cu_T and flasks were divided into two controlled environment chambers (Sanyo, MLR 350T) at different temperatures: 15 °C (control) and 19 °C (elevated) for a total of n = 3 replicates per treatment (Figure 2.1.b). In this case, Cu concentrations and duration of exposure (10 days) were chosen to allow comparison with similar studies (Roncarati *et al*., 2015; Sáez *et al*., 2015c). Elevated temperature treatment was chosen as 4 degrees above the mean temperature at which algal cultures have been kept for long-term storage after collection.

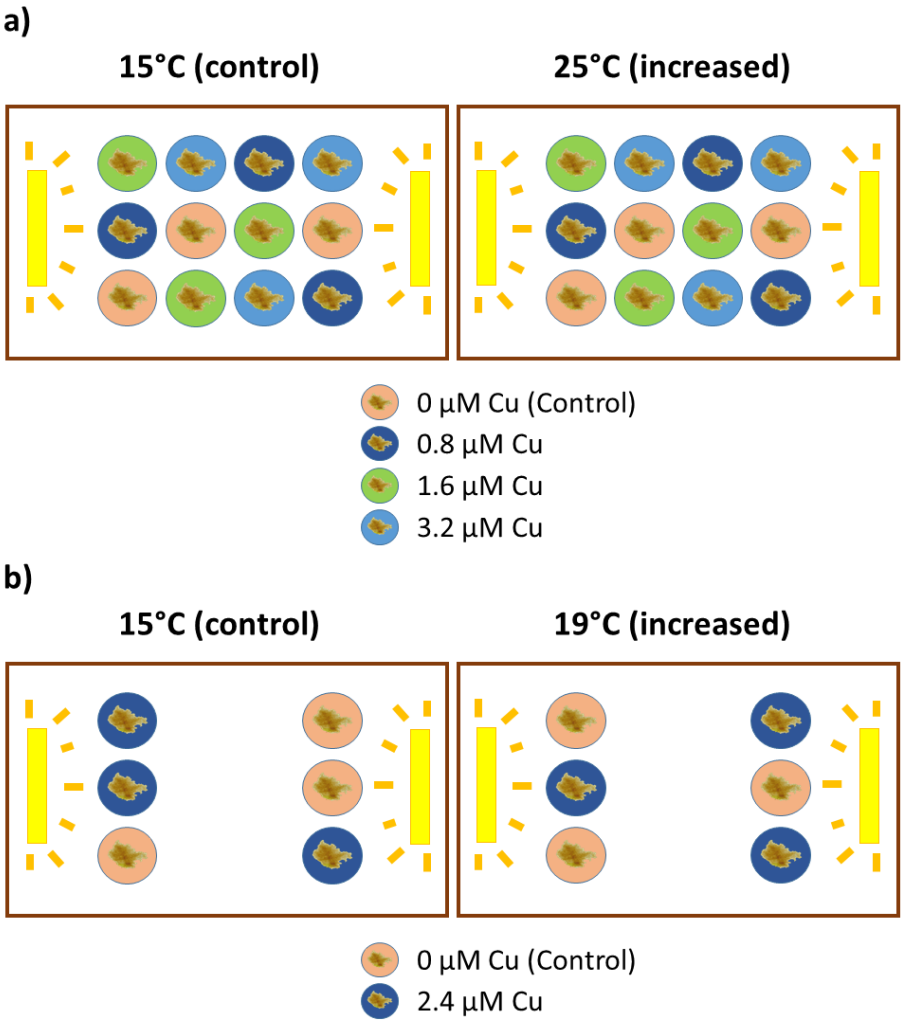

Figure 2.1. a) Experimental design used in Chapter III and b) Experimental design used in Chapters IV and V.

2.2. Algal cultures

All experiments were performed with the *Ectocarpus siliculosus* strain Es524 isolated from Caleta Palito (Chañaral, Chile), a coastal site known to be impacted by high levels of Cu pollution resulting from mining activities (Roncarati *et al.*, 2015). The sea surface temperature in the region varies between 15 and 22 °C for the summer months, with a mean of 18.3 °C for the year 2016 (http://www.shoa.cl), and 13 and 15 °C for the winter months, with a mean of 14.1 °C for the same year. Stock cultures of the strain

Es524 are maintained in the collection of Plymouth University and in the Culture Collection of Algae and Protozoa (CCAP) with the accession number: CCAP 1310/333.

To ensure reproducibility of experiments and optimal biomass yield, all algae biomass was obtained from axenic cultures. Preparation of cultures are described below.

2.2.1. Material sterilization

All glassware and plastic-ware used in algal culturing were washed thoroughly, soaked in 5% HCl for 24 h, in order to remove any remaining metal ions, and then rinsed in deionised water and dried before autoclaving.

Ten litre volume autoclavable polycarbonate carboys (Clearboy 2251-0020, Thermo Scientific Nalgene) were used to maintain the stock cultures, along with autoclavable closure vents (2162-0831, Thermo Scientific Nalgene) to provide aeration to cultures.

All materials and consumables used in culturing were disposed of in autoclavable plastic bags, including any biological remains.

2.2.2. Preparation of laminar flow cabinet

The preparation, manipulation of cultures or preparation of non-hazardous solutions were performed in a laminar flow cabinet (Heraguard Eco, Thermo Scientific). The cabinet was left running for 10 minutes prior to use and then cleaned with 70% ethanol and adsorbent paper. All essential materials such as bottles with medium, tweezers, pipettes, scissors, etc. were cleaned with 70% ethanol and retained inside the cabinet to avoid contamination. Tweezers used to manipulate biological tissues were soaked regularly with ethanol (99%) and allowed to dry to reduce risk of biological

contamination. In the same way, gloves were soaked in 70% ethanol regularly and replaced whenever working outside the hood to avoid further contamination.

2.2.3. Media preparation

2.2.3.1. Provasoli enriched seawater

Algal cultures were maintained in Provasoli enriched seawater (PES) growth media (Provasoli & Carlucci, 1974), comprising a nutrient solution (Table 2.1) added to sterile natural seawater (NSW) according to Coelho *et al*., (2012). Stocks solutions (1, 3, 4 and 5) were prepared separately, autoclaved at 122 °C for at least 15 min, and later stored at 4 °C in amber-coloured glass bottles. "Solution 2" was sterilised by filtration using a syringe sterile filter unit (pore size 0.22 μm; Millex®, Merck Millipore, Ireland) to avoid degradation of vitamins.

Table 2.1. Stock solutions for preparation of Provasoli solution.

Solution 1 (10×)		
Reagent	*Quantity (for 1 L)*	*Final concentration*
H_3BO_3 (MW = 61.8)	1.9 g	30.7 mM
$FeCl_3$ (MW = 162.2)	0.05 g	0.3 mM
$MnSO_4 \cdot H_2O$ (MW = 169)	0.273 g	1.6 mM
$ZnSO_4 \cdot 7H_2O$ (MW = 287.5)	0.0367 g	0.127 mM
$CoSO_4 \cdot 7H_2O$ (MW = 281.1)	0.008 g	28 μM
EDTA (0.5 M, pH 8)	11.4 mL	5.7 mM

Solution 2 (10×)		
Reagent	*Quantity (for 500 L)*	*Final concentration*
Vitamin B_{12} (cyanocobalamin) (MW = 1356.4)	3.35 mg	4.9 μM
Thiamine hydrochloride (vitamin B_1) (MW = 337.3)	165 mg	978 μM
Biotin $C_{10}H_{16}N_2O_3S$ (MW = 244.3)	1.65 mg	13.5 μM
Tris (Trizma base) $C_4H_{11}NO_3$ (MW = 121.1)	166.5 mg	2.7 mM

Solution 3 (10×)		
Reagent	*Quantity (for 1 L)*	*Final concentration*
$(NH_4)_2Fe(SO_4)_2 \cdot 6H_2O$ (MW = 392.1)	1.17 g	3 mM
EDTA (0.5 M, pH 8)	6.8 mL	3.4 mM

Solution 4 (10×)		
Reagent	*Quantity (for 1L)*	*Final concentration*
$NaNO_3$ (MW = 84.99)	23 g	270 mM

Solution 5 (10×)		
Reagent	*Quantity (for 1L)*	*Final concentration*
$C_3H_7Na_2O_6P \cdot 5H_2O$ "Glycerol phosphate disodium salt hydrate isomeric mixture" (MW = 216.04)	3.33 g	15.4 mM

Provasoli medium was prepared by combining the five solutions described above. One hundred millilitres of Solutions 1, 3, 4 and 5 plus 10 mL of Solution 2 were added to Milli-Q water to prepare one litre solution. The pH was adjusted to 7.8 with 0.1 M HCl solution. Provasoli medium was aliquoted into small glass bottles (20, 50, 100 or 200 mL) autoclaved and stored at 4 °C.

To prepare 1 L of PES, 20 mL of Provasoli medium were added to 1 L of natural seawater. The seawater was filtered using 0.45 μm nitrocellulose membrane filters (Millipore, Ireland) and poured into Nalgene polycarbonate bottles to be autoclaved as described above. Provasoli and seawater were autoclaved separately to avoid precipitation. Addition of Provasoli to NSW was performed in a laminar flow cabinet (Heraguard Eco, Thermo Scientific). PES was stored at 15°C.

2.2.3.2. Cu-enriched natural seawater

A stock solution of 3mM $CuSO_4$ was prepared and stored in polyethylene and polycarbonate bottles, which adsorb low concentrations of metal ions. Stocks were kept in the dark at 4°C for up to three months. The stock solution was used to prepare Cu-enriched natural seawater medium. Seawater was filtered and autoclaved in polycarbonate bottles as described above, and then kept at 15°C in the growth chambers used for experiments. Copper concentrations for experiments were prepared by diluting the stock solution with sterile seawater 24 h before the beginning of experiments to allow the stabilization of metal ions in the medium and temperature.

2.2.4. Production of algal biomass for experiments

Natural seawater was filtered and autoclaved (see previous section) in 10 L carboys (Nalgene) and, after cooling, Provasoli solution was added at a ratio of 20 mL per 1 L of NSW. The medium was kept at 15 °C for 24 h before inoculation with algal

material. Medium was replaced every three weeks to stimulate growth. All procedures were performed in a horizontal laminar flow cabinet following the steps described in Section 2.2.2. Carboys containing algal cultures were maintained in controlled conditions with a constant temperature of 15 °C and a light/dark cycle of 14/10 hours at irradiance 40-50 μmol photons m^{-2} s^{-1}. Clean air was pumped into the medium by using a sterile filter unit (pore size 0.22 μm; Millex®, Merck Millipore, Ireland) to maintain algal material in suspension.

2.3. Methodologies to assess whole organism and physiological responses

2.3.1. Growth rates

Relative growth rates (RGR) were estimated volumetrically using a modified version of the method described by Dring (1967). *Ectocarpus siliculosus* has an irregularly branching filamentous morphology, which does not allow reliable measuring of wet biomass or length. Thus, measurement of the compacted volume of the filaments can be estimated using blood sedimentation (Wintrobe) tubes. These are thick-walled tubes, 11 cm long and graduated in mm^3. Volume (V) was recorded at time of inoculation (t_0) and at the end of the experiments (t_1). Relative growth rates were estimated using the formula:

$[(Vt_1/Vt_0)^{1/t} -1] \times 100$ (% d^{-1}) (adapted from Yong *et al*. (2013)).

After placing small quantities of biomass (*ca*. 30 mg) into Wintrobe tubes, they were centrifuged (Hettich, Germany) for 5 min at low speed (4,226 g_{av}) to stack the filaments at the bottom of the tube. After centrifugation the initial volume of biomass (mm^3) was recorded. The biomass was then placed in a flask containing experimental medium. The same procedure was used to determine the volume at the end of the experimental period.

2.3.2. Photosynthetic physiology

To assess photosynthetic performance, the non-invasive technique of chlorophyll *a* fluorescence was applied to small amounts (*ca*. 30 mg) of algal filaments. A protocol was adapted from that of Celis-Plá *et al*. (2014a), to be used with a 'MINI-PAM Photosynthesis Yield Analyzer' (Walz, Germany), which allows for the measurement of several fluorescence parameters in samples exposed to metal and thermal stress. Since their introduction in 1986, pulse-amplitude-modulation (PAM) fluorometers have become the main instrument for eco-physiological studies in algae and plants (Schreiber, 1986, 2004). New and compact instruments such as the MINI-PAM allow highly accurate estimations of overall quantum yield (Y) of photochemical energy conversion, as well as dynamic measurements and induction of photosynthesis (Ralph & Gademann, 2005). The MINI-PAM fluorometer emits a weak beam of red modulated light (measuring light) in short pulses (3 μs) through a fibre optic directed towards the sample. Thus, the detector of the instrument can selectively identify and amplify only the chlorophyll fluorescence generated by the modulated measuring light and ignore all other background light (Beer *et al.*, 2014). The fluorescence measured by the PAM fluorometer is termed "F" and is expressed as relative fluorescence units. Chlorophyll *a* fluorescence is used as an indicator because is one of three competitive pathways of chlorophyll de-excitation in the reaction centres and antenna. The other two pathways are photochemical energy conversion at the photosystem II (PSII) (photochemistry) and non-photochemical loss of excitation at the antenna and reaction centres (heat dissipation). Both processes are able to quench fluorescence yield and so they are referred as photochemical and non-photochemical quenching (Cosgrove & Borowitzka, 2010). Thus, fluorescence yield can reach its maximum when photochemical and non-photochemical quenching are at their minimum. The contribution of these two mechanisms is essential for interpretation of changes in fluorescence. Therefore, by measuring the fluorescence yield by PAM

fluorometry it is possible to identify changes in the photochemistry efficiency and heat dissipation. To achieve this, the PAM instruments allows to apply the so-called saturation pulse (SP) method (Schreiber, 2004). This method consist of a strong pulse of white light applied to a sample in order to close all the PSII reaction centres, photochemical quenching thus becomes zero and remaining quenching must be non-photochemical (Cosgrove & Borowitzka, 2010). The saturation pulse method can be applied in dark-adapted (e.g. before dawn) or light-adapted samples (e.g. samples exposed to day light or artificial light able to drive photosynthesis, also called actinic). Adaptation of samples to a period of darkness allows the opening (oxidation) of PSII reaction centres and electron transport chain, the relaxation of photoprotective mechanisms (xanthophyll cycle) and the depletion of *trans*-thylakoid (ΔpH) gradient (Ralph & Gademann, 2005). Consequently, when a SP is applied to a dark-adapted sample, photochemical quenching becomes zero, non-photochemical quenching will be negligible and fluorescence yield can reach its maximum. On the other hand, when a SP is applied to light-adapted (illuminated) samples, photochemical quenching and non-photochemical quenching will act to quench the fluorescence yield and therefore the maximum value will be lower (Cosgrove & Borowitzka, 2010).

Fluorescence yield resulting only from the weak measuring light of the MINI-PAM (< 0.5 μmol photons m^{-2} s^{-1}) oriented to a photosynthetic organism is called minimum fluorescence (F_o in dark-adapted and F in light-adapted samples). By applying a subsequent SP of white light (> 10 000 μmol photons m^{-2} s^{-1}) for a short period (< 1 s) the reaction centres become transiently reduced (closed). Therefore, fluorescence yield resulting from the measuring light will be maximum (F_m for dark-adapted and F_m' in light-adapted samples). The difference between maximum and minimum fluorescence yield is called variable fluorescence (F_v for dark-adapted and ΔF for light-adapted samples) and represents the degree of photochemical quenching (Beer *et al.*, 2014). From the minimum

and maximum fluorescence, the quantum yields of energy conversion in PSII can be calculated (see Schreiber, 2004, for demonstration), i.e. 'maximum quantum yield' (or F_v/F_m) for dark-adapted samples and 'effective quantum yield' (or $\Delta F/F_m'$ or simply Y) for light-adapted samples (also known as the Genty parameter) (Genty *et al.*, 1989). The maximum quantum yield is calculated with the formula: $F_v/F_m = (F_m - F_o)/F_m$ and the effective quantum yield as: $\Delta F/F_m' = (F_m' - F)/F_m'$ (Ralph and Gademann, 2005; Beer *et al*., 2014). These quotients are an indication of the fraction of absorbed quanta used for PSII photochemistry (quantum yield or Y). Any change in these parameters, in response to particular stimuli, indicates changes at the PSII level (Klughammer & Schreiber, 2008), and hence are useful indicators of an environmental stress affecting photosystem II. Assuming that a short SP is not able to change non-photochemical quenching, the lowering in F_m, determined after a SP in light adapted samples, is a measure of non-photochemical quenching (NPQ; Schreiber, 2004). NPQ in the MINI-PAM is calculated with the Stern-Volmer equation: $NPQ = (F_m - F_m')/F_m'$. This parameter describes the ability of a tissue to dissipate the energy absorbed in excess as heat within the antennae matrix (Enríquez & Borowitzka, 2010).

Besides the photochemical and non-photochemical pathways of de-excitation energy, the PAM also allows to estimate the rates of linear electron transfer between photosystems, which have been proven to be comparable to O_2 evolution rates under low light conditions (Beer *et al.*, 2000). With the knowledge of quantum yield (Y), defined as electrons transported per photons absorbed by pigments in PSII, it is possible to estimate the electron transport rate (ETR) by multiplying Y by the absorbed irradiance (E_a) of that photosystem (i.e. $E_a \times 0.5$, assuming the percentage of absorbed photons by each photosystem is equally distributed 50:50). The amount of incident irradiance (E_i) or photosynthetically active radiation (PAR) can be obtained with a suitable quantum sensor. Also, E_a can be estimated by measuring the PAR (λ = 400-700 nm) reaching a quantum

sensor with and without the thallus covering it (Beer *et al*., 1998; Beer *et al*., 2000). So, an absorption factor or absorptance (A) can be calculated as A = 1 – T (assuming reflectance = 0), where T is the transmittance (calculated as $T = E_t / E_i$, being E_t the transmitted irradiance through the thallus measured by a PAR sensor; Figueroa *et al*., 2014). Thus, the E_a for photosystem II can be expressed as $E_a = E_i \times A \times 0.5$. Therefore, ETR can be calculated with formula: ETR (µmol electrons m^{-2} s^{-1}) = $Y \times E_i \times A \times 0.5$ (Schreiber, 2004; Figueroa *et al*., 2009; Enríquez and Borowitzka, 2010; Beer *et al*., 2014). However, while it is generally assumed that the percentage of absorbed photons is evenly distributed between photosystem in plants, this may not be always the case in other photosynthetic organisms such as marine algae (Grzymski *et al*., 1997; Figueroa *et al*., 2003). Thus, in brown algae the value of 0.8 is preferred instead of 0.5, and the formula to calculate ETR becomes: ETR = $Y \times E_i \times A \times 0.8$ (Figueroa *et al*., 2014; Celis-Plá *et al*., 2014a).

The MINI-PAM instrument also allows for evaluating dynamics changes of PSII physiology by applying the Rapid Light Curve (RLC) automatic function (White and Critchley, 1999; Ralph and Gademann, 2005). Besides the saturation pulse, the halogen lamp of the MINI-PAM is also able to irradiate the sample with up to 12 different PAR intensities for short periods. This allows the calculation of quantum yields and consequently the ETR at different irradiance levels. RLCs are similar to a traditional photosynthesis vs. irradiance curve (*P-E* or *P-I*) (Falkowski & Raven, 2007), which are commonly used to describe photosynthetic rates by using O_2 or CO_2 gas exchange measurements under different light conditions. The RLC uses the ETR (instead of O_2 or CO_2) as a function of irradiance. After calculating the ETR, with the formula stated above, the plot ETR vs. irradiance (measured as PAR) resembles a traditional *P-E* curve (see Figure 2.2). However, the RLC is not equivalent to a *P-E* curve because it does not reach steady state conditions at each irradiance level. Nevertheless, RLC measurements under

controlled conditions may be useful for estimating the actual state of the photosynthesis, reflecting the immediate short-term light history of a sample, but not the optimal state as in traditional *P-E* curves (Ralph & Gademann, 2005). After fitting the ETR data to a mathematical model, e.g. the model presented by Eilers and Peeters, (1988), different components can be identified in a typical RLC (Figure 2.2). First, under low irradiance the initial rise of the curve (slope) (α), which is proportional to the efficiency of light capture. Then, at moderate irradiance, the rates of electron transport become saturated and the curve reaches a plateau as photosynthesis achieves its maximum capacity (ETR_{max}). With further increase of irradiance, the curve tends to decline as dynamic changes in the PSII occur (White & Critchley, 1999). The E_k parameter or minimum saturating irradiance is calculated from the intercept of the extended line of the initial slope (α) and the ETR_{max} (ETR_{max}/α; Sakshaug *et al*., 1997). E_k is related to quenching, thus, at irradiances less than E_k photochemical quenching dominates, while non-photochemical quenching dominates at irradiances above E_k (Ralph & Gademann, 2005).

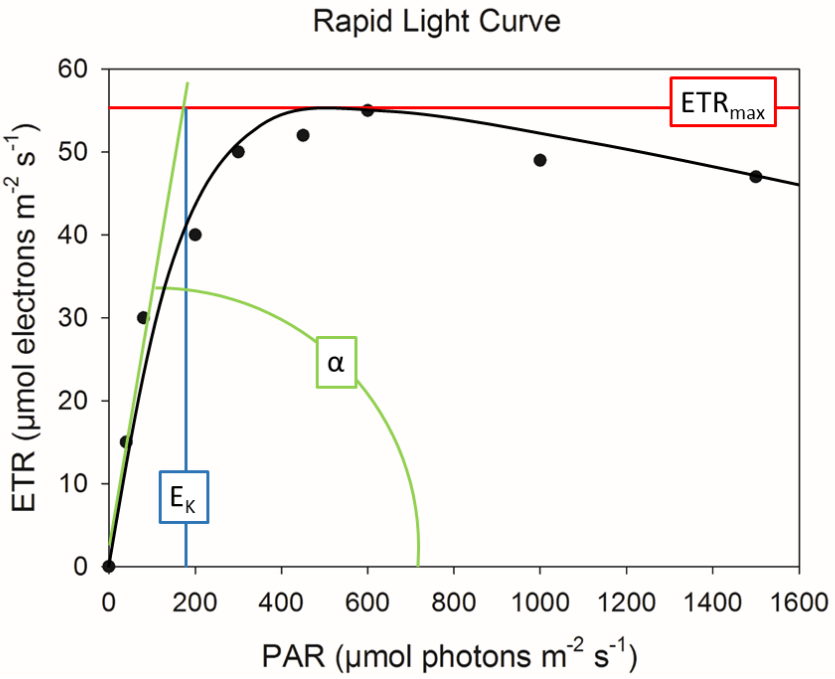

Figure 2.2. Schematic representation of a Rapid Light Curve and its components: maximum ETR (ETR_{max}), initial slope (α) and minimum saturating irradiance (E_K)(adapted from Pfündel, (2007).

In the present study, we standardised a protocol to assess the photosynthetic performance of *E. siliculosus* by applying the RLC method. Algae were grown for seven days in glass Petri dishes containing 50 mL of sterile NSW at a constant irradiance (PAR = 50 µmol photons m^{-2} s^{-1}) and 14:10h light/dark cycle. Medium was enriched with DCMU (3-(3,4-diclorofenil)-1,1-dimetilurea), an inhibitor of electron transfer from PSII (Popovic *et al.*, 2003), at concentrations of 0, 1, 10 and 50 µg L^{-1} in triplicates per each concentration. After the exposure period a small clump of filaments was dark-adapted for a standard period of 15 min (as reported in Celis-Plá *et al*. (2014b) for brown algae) using the dark leaf clip (DLC8, Walz) submerged in the experimental medium. Following the dark-adaptation period, F_o and F_m were determined with the first saturating light pulse (>10 000 µmol m^{-2} s^{-1} PAR) to obtain the maximum quantum yield (F_v/F_m). RLC was automatically started after the first saturation pulse and consisted of exposing samples to

8 steps of increasing irradiances (E_1 = 44, E_2 = 148, E_3 = 307, E_4 = 494, E_5 = 743, E_6 = 1029, E_7 = 1529, E_8 = 2059, μmol m^{-2} s^{-1}), each of 20 s duration (Celis-Plá *et al*., 2014b). Subsequent saturation pulses (>10 000 μmol m^{-2} s^{-1} PAR) were applied automatically at the end of each incubation step for each irradiance level to estimate $\Delta F/F_m'$ and ETR. The internal halogen lamp of the MINI-PAM (type Bellaphot, Osram) provided white light for incubation. The MINI-PAM was controlled via a PC and the software WinControl (Version 2.0, WALZ) was used to obtain RLCs.

With each saturation pulse, the relative ETR was calculated according to the formula stated previously in this section for brown algae. At each step of the RLC, the incident irradiance (E) provided by the halogen lamp of the MINI-PAM was measured with a PAR quantum sensor (Skye Instruments, Wales-UK). Absorptance (A = 1 – T) was estimated by measuring the amount of light transmitted (transmittance, $T = E_t/E_i$) through several clumps of algae and the mean was calculated. The same PAR quantum sensor and a white light lamp where used to estimate the transmittance as described earlier in this section. In order to compare all RLCs, they were fitted to a model developed by Eilers and Peeters (1988). The estimators of photosynthetic rate and efficiency: maximum ETR (ETR_{max}) and the initial slope (α) of the function ETR vs. irradiance were obtained from the tangential function reported by Eilers and Peeters (1988), according to Celis-Plá *et al*. (2014b). Finally, the minimum saturating irradiance (E_k) was calculated from the intercept between ETR_{max} and α.

Results from this trial are summarised in Figure 2.3. Data for the photosynthetic parameters F_v/F_m, ETR_{max}, α and E_k were analysed with one-way ANOVA. Significant differences between treatments were obtained by Tukey's *post hoc* test with a confidence level of 95%. As expected, the herbicide DCMU was able to inhibit the photosynthetic efficiency and rates as shown by the parameters F_v/F_m, ETR_{max} and α (Figure 2.3a, b, c).

Maximum quantum yield (F_v/F_m) and the efficiency of light capture for photosynthesis (α) were significantly reduced at 10 and 50 $\mu g\ L^{-1}$ ($P < 0.05$), indicating that these are the most sensitive parameters to the toxic effect of DCMU. However, the ETR_{max} showed a different pattern. At low DCMU concentrations (1 $\mu g\ L^{-1}$) ETR_{max} increased significantly compared to control conditions ($P < 0.05$); this may be related with processes of acclimation or upregulation of PSII or, alternatively, to regulation of PSI (Hosler & Yocum, 1987). Similarly, small increases in F_v/F_m and α were observed at 1 $\mu g\ L^{-1}$; but this was not statistically different from the control ($P = 0.234$; $P = 0.280$, respectively). A further ten-fold rise in DCMU concentration caused a decrease in the ETR_{max}, though, not statistically different from control conditions ($P = 0.257$). The highest concentration of DCMU (50 $\mu g\ L^{-1}$) caused a large reduction in electron transport rate ($P < 0.05$).

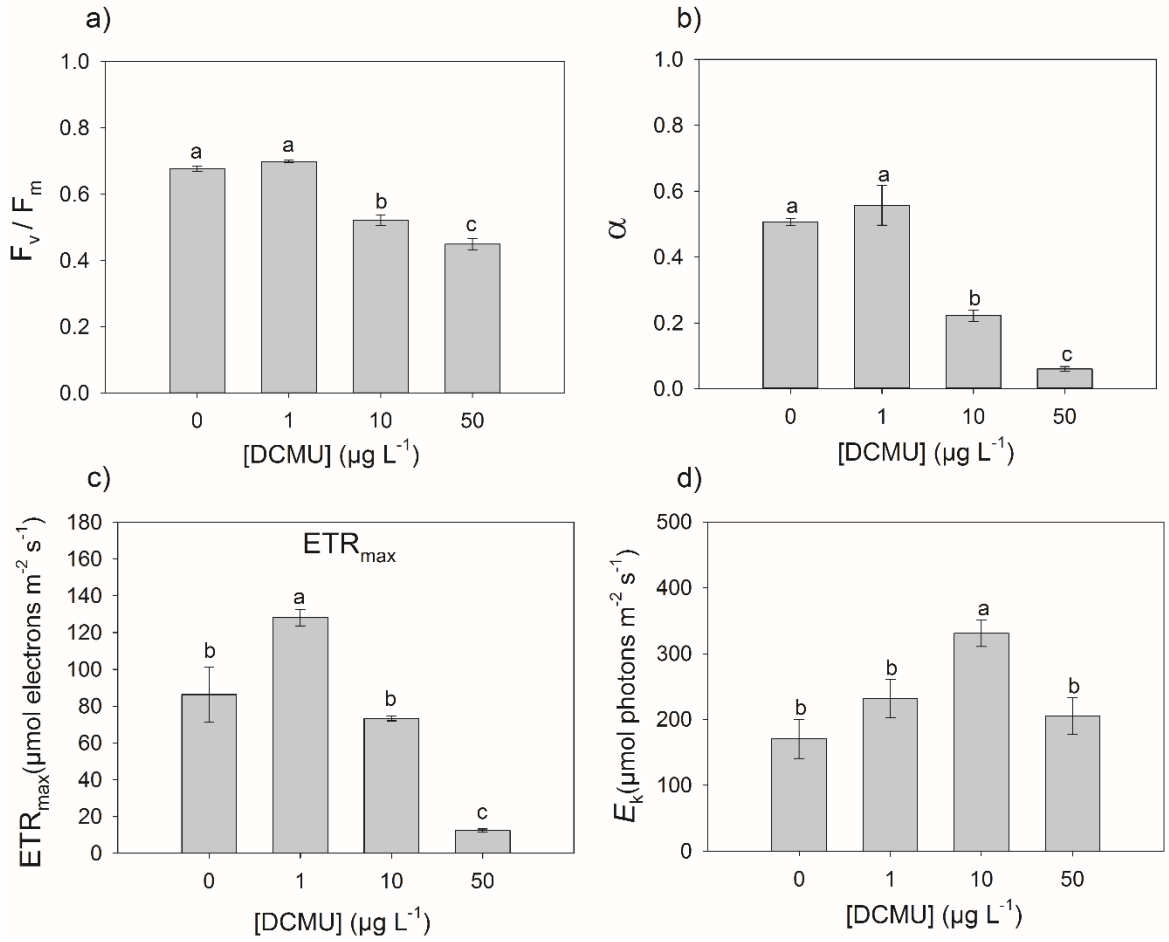

Figure 2.3. Chlorophyll *a* fluorescence parameters obtained by applying the saturation pulse and RLC methods using a MINI-PAM fluorimenter (Walz, Germany) in dark-adapted samples of *E. siliculosus* exposed to different concentrations of DCMU for 7 days. Different letters represent significant differences between treatments at the 95% confidence level ($P < 0.05$). Error bars represent ± 1 SD, $n = 3$. (a) F_v/F_m: maximum quantum yield, (b) α: photosynthetic efficiency, (c) $rETR_{max}$: maximum relative electron transport rate (d) E_k: minimum saturating irradiance.

Finally, there was a significant increase in minimum saturating irradiance (E_k) under 10 µg L^{-1} treatment ($P < 0.05$). This can be visualised from the shape of the fitted curves (Figure 2.4), where at low irradiances the photosynthetic rate in the 10 ug L^{-1} (blue dotted line) is lower than the control (purple dotted line). However, at higher irradiance the photosynthetic rates are similar in both treatments. This may indicate that disturbances

in light capture and electron transfer may cause impairment in energy use and dissipation processes. However, we must note that in this case a single value of absorptance was used in the calculations of ETR, which might have caused underestimation of the difference between treatments.

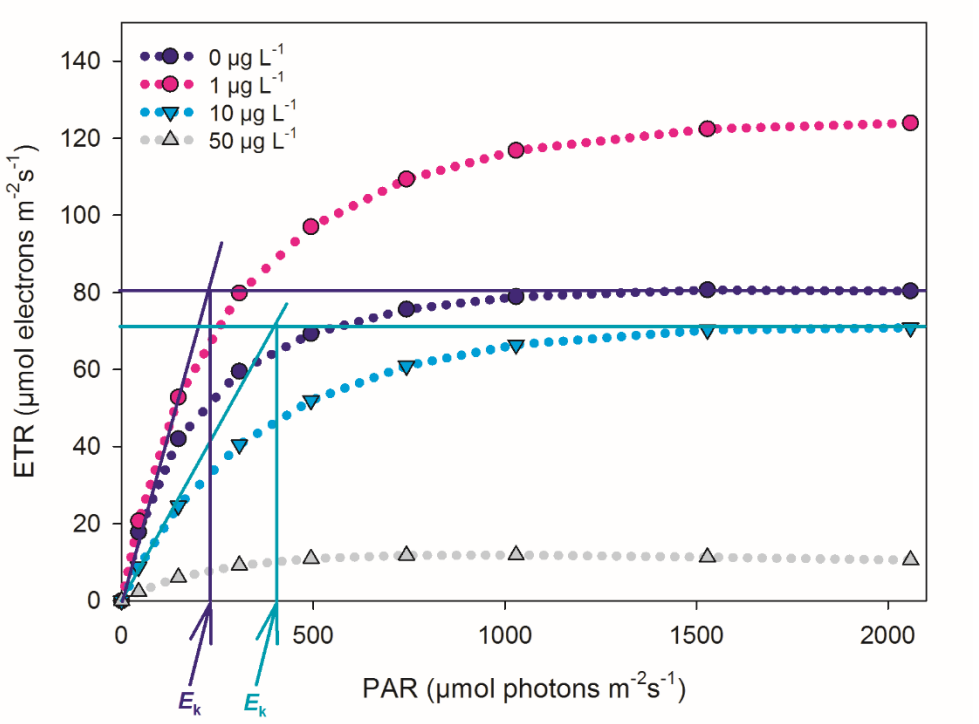

Figure 2.4. Rapid light curves in *E. siliculosus* samples exposed to different concentrations of the herbicide DCMU fitted to the Eilers and Peeters (1988) model. Dotted lines represent the average fit of three replicates (n = 3). Horizontal solid lines represent ETR_{max} and vertical solid lines represent the intercept between ETR_{max} and the initial slope (α).

In conclusion, this experiment showed that the physiological status of photosystem II in *E. siliculosus* could be assessed by measuring chlorophyll *a* fluorescence and RLCs under controlled conditions. Negative effects on photosynthesis observed above 1 µg L^{-1} DCMU are in agreement with other toxicity studies in different species of unicellular algae where the effective concentration (EC_{50}) values ranged from

2.4 to 95 μg L^{-1} (DeLorenzo & Fulton, 2012). We suggest to use individual values of absorptance for a better estimation of ETR.

2.4. Analytical, biochemical and molecular biology methods

Although growth rate and photo-physiological measurements were used throughout the thesis, most of the biochemical and molecular methods were specific to each chapter and are discussed in detail within them.

In Chapter III, we applied analytical and biochemical techniques to assess the responses of *E. siliculosus* to the stress applied at the whole organisms. To determine the pigments content of the samples we used the dimethyl sulfoxide (DMSO) method developed by Seely *et al*. (1972) and standardised by Sáez *et al*. (2015c). In order to distinguish between the cell wall-bond and the intracellular Cu accumulation, we washed samples in ethylenediaminetetraacetic acid (EDTA) according to Hassler *et al*. (2004) and then digested and measured as describe in Roncarati *et al*. (2015).

In Chapter IV, we used different biochemical and molecular tools to assess the effects of stressors at the molecular level. The concentrations of oxidative stress indicators (H_2O_2 and thiobarbituric acid reactive substances TBARS) and antioxidants (ascorbate and glutathione) were measured following the procedure described by Sáez *et al*. (2015c). To assess the activities of superoxide dismutase (SOD), ascorbate peroxidase (APX), glutathione reductase (GR) and catalase (CAT), protein extracts were obtained according to Ratkevicius *et al*. (2003) with small modifications. The concentrations of protein in extracts were estimated by the Bradford method (Bradford, 1976). Activities of CAT, APX and GR were measured according to Ratkevicius *et al*. (2003) and activity of SOD was measured according to Gonzalez *et al*. (2012). Concentrations of total phenolic compounds were obtained with the method described in Celis-Plá *et al*. (2014a) with

some modifications. Samples were extracted in pure methanol and mixed with Folin-Ciocalteu (Folin & Ciocalteu, 1927) reagent solution. Phloroglucinol (1,3,5-trihydroxybenzene, Sigma P3502) was used as standard. To characterise the methanol-soluble polyphenolic compounds, samples were extracted as for total phenolic compounds; then, filtered (0.22 μm) and analysed in by high performance liquid chromatography (HPLC). Phenolic compounds were identified by using the absorption spectra of several commercial standards representing the main groups of phenolic compounds (hydroxycinnamic acids (HCAs), flavonoids and tannins). Also, the release of phenolic compounds into the experimental media was estimated by the method described in Celis-Plá *et al*. (2014a). Finally, the expression of genes related to metal-induced oxidative stress and thermal stress was assessed by real time qPCR. Our colleague Dr. Maria Greco extracted nucleic acids according to Greco *et al*. (2014), carried out primer design and performed qPCRs according to Roncarati *et al*. (2015).

In Chapter V, methods described previously in this chapter were used to assess photosynthetic performance and growth. Experiments were performed in the laboratory of Dr. Alejandra Moenne during my visit at University of Santiago de Chile (USACH). Transcriptomic analysis was performed in collaboration with the group of Dr. Francisco Cubillos from USACH. Extracted RNA was sent to Beijing Genomics Institute (BGI) for RNA sequencing. Dr. Carlos Villaroel from USACH performed bioinformatics analyses.

Chapter III

The combined effects of copper excess and elevated temperature on growth, photosynthetic performance and Cu accumulation in *E. siliculosus*

3.1. Introduction

Copper (Cu) is a highly toxic and persistent (not biodegradable) pollutant in marine environments affected by human activities such as mining (Nor, 1987; Correa *et al*., 1999). Brown seaweeds (Paeophyceae) can readily accumulate Cu ions that, beyond certain thresholds, are known to inhibit growth and photosynthesis (Gledhill *et al*., 1997; Küpper *et al*., 2002; Nielsen *et al*., 2003; Nielsen and Nielsen, 2010; Connan and Stengel, 2011a). Besides exposure to chemical stressors such as Cu, brown seaweeds are exposed simultaneously to multiple other environmental factors, such as shifts in temperature, pH and irradiance, because of the highly dynamic nature of the coastal environments they inhabit (Wahl *et al*., 2011; Todgham and Stillman, 2013). Observed increases in ocean temperature due to climate change has raised concerns of the direct and indirect implications of warming to marine life (Laffoley & Baxter, 2016). In this context, understanding the potential interactions between a global stress factor (e.g. warming) and a local stressor (e.g. Cu pollution) on the (eco-) physiology of seaweeds has become a necessity in order to improve predictions about the ecological consequences of environmental change on natural populations of seaweeds.

Copper is an effective inhibitor of seaweed growth, which is the rationale for its use as an additive in antifouling paints (Omae, 2003). Reductions in growth rate have been used to assess the differential sensitivity or resistance of red (Brown and Newman, 2003; Brown *et al*., 2012), green (Moenne *et al.*, 2016) and brown (Nielsen *et al.*, 2003b; Nielsen & Nielsen, 2010) seaweeds species to Cu ions. For example, reductions in growth were observed at lower concentrations for the brown algae *Pelvetia canaliculata* and *Fucus spiralis* (12 µg L^{-1}) compared to other brown seaweeds such as *F. serratus* (25 µg L^{-1}) and *F. vesiculosus* (50 µg L^{-1}) (Strömgren, 1980). However, differences in growth can also occur between populations of the same species or life stages (Nielsen *et al*., 2003;

Brown *et al*., 2012; Roncarati *et al*., 2015). For instance, relative growth rates of strains of *Ectocarpus siliculosus* isolated from pristine sites were significantly more reduced than isolates from Cu-polluted sites (Roncarati *et al.*, 2015). While Cu is an essential metal for photosynthetic functions (Yruela, 2013), in excess it can impair photosynthetic physiology (Rai *et al*., 1981; Fernandes and Henriques, 1991; Küpper *et al*., 2002; Joshi and Mohanty, 2004). For example, Cu, and zinc are able to substitute the central atom of magnesium in chlorophyll molecules (Küpper *et al.*, 1996), forming non-functional chlorophyll molecules which are not adapted to light harvesting (Küpper *et al*., 1998, 1996, 2002). Also, production of non-functional chlorophylls was suggested to be the reason for decreases in basal (F_o) and maximal (F_m) chlorophyll *a* fluorescence in non-tolerant populations of *F. serratus* exposed to Cu as high as to 2 µM (Nielsen *et al.*, 2003b).

Temperature is also able to inhibit algal growth and it is a key determinant for the rates of chemical reactions of metabolic processes within the cell (Davison, 1987, 1991). For example, Davison (1987) found that temperature could influence enzymes related with the primary metabolism of *Saccharina latissima*, where Q_{10} values were lower in sporophytes grown at 0 to 5 °C compared to sporophytes grown at 10 to 20 °C. However, the effects of temperature are not uniform and, as with responses to Cu exposure, they can vary between and within species. The Antarctic brown algae *Ascoseira mirabilis* Skottsberg for instance, exhibited upper survival temperatures (UST's) between 15 and 18°C, while those of cold-temperate species, such as *Adenocystis utricularis* and *Scytothamnus fasciculatus*, were between 21 and 25 °C (Wiencke *et al.*, 1994). Conversely, different isolates of the filamentous brown alga *Ectocarpus siliculosus* (Dillwyn) Lyngbye have been shown to be eurythermal (Bolton, 1983) although, growth and range of survival temperatures were correlated with the temperature regimens at the collection sites (Bolton, 1983). This was recently confirmed by experiments in *E.*

siliculosus aimed to find quantitative trait loci (QTL) related to thermal stress (Avia *et al.*, 2017). In those experiments, the parental strains used came from locations with different temperature regimes, which might have conferred the offspring with an improved capacity to withstand temperatures up to 26 °C. Temperature is also responsible for alterations in the photosynthetic status of seaweeds. Like growth, the effects of temperature on photosynthesis in seaweeds vary across species and populations. For example, in isolates of the green seaweed *Valonia utricularis* from the Mediterranean Sea the maximum quantum yield of photosynthesis (F_v/F_m) decreased at 30 °C while isolates from the Indo/west Pacific were not affected (Eggert *et al.*, 2006). In contrast, it was observed that F_v/F_m was greater in embryos of *F. evanescens* growing at 20 °C compared to those growing at 5 °C (Major and Davison, 1998).

Although there is literature available on the interactions between temperatures and other stressors such as excess UV radiation in other seaweeds species (Altamirano *et al*., 2003; Cruces *et al*., 2013; Rautenberger *et al*., 2015), studies assessing interactions of metals and other environmental stressors are rare. Different studies in two species of the green microalgae *Chlorella* sp. have demonstrated that Cu and temperature can interact modulating the photosynthetic physiology of these micro-algae (Vavilin *et al*., 1995; Oukarroum *et al*., 2012); however, the results were contradictory. Vavilin *et al*. (1995) observed that photoinhibition caused by Cu was greater at lower temperatures while in the study of Oukarroum *et al*. (2012) the opposite occurred. A recent study has shown that negative effects of Cu on survival of *Fucus serratus* germlings were exacerbated when exposed to a combination of temperature (22 °C) and Cu (1 µM) compared to individuals growing at 6 and 12 °C and the same Cu concentration (Nielsen *et al.*, 2014). This was in contrast to adults, which were mostly unaffected. Those studies confirm that temperature can indeed affect the toxicity of Cu in green microalgae and seaweeds, but the mechanism and the extent of such modulation remain to be clarified. Seaweeds readily

accumulate Cu in their cell walls and intracellularly; however, this distinction is rarely studied. There is evidence that in non-polluted sites most of the Cu accumulates intracellularly (Ryan *et al.*, 2012), whereas, in seaweeds from Cu impacted sites more is accumulated extracellularly (Roncarati *et al.*, 2015). This exclusion mechanism may account for the resistance capacity of some species to heavily polluted environments. Additionally, there is a strong relationship between the changes in temperature and bioavailability of Cu species to algae (Byrne *et al*., 1988; Gledhill *et al*., 1997). Thus, increased temperature due to climate change might modulated the metal uptake capacity of seaweeds by either altering the biochemical processes behind exclusion mechanisms or by reducing availability due to altered speciation.

In the present study, we examined the potential interactions between Cu excess and increased temperature in the filamentous brown seaweed *Ectocarpus siliculosus* (Dillwyn) Lyngbye. *E. siliculosus* has arisen as a model for the study of brown algae due to its ease of cultivation in the laboratory and the availability of its genome sequence (Cock *et al.*, 2010). These characteristics make *E. siliculosus* an organism of choice to assess more in deep the different aspects of seaweeds' ecotoxicology. The effects of different levels of copper and increased temperature were evaluated by measuring the relative growth rate, photosynthetic physiology (measured by chlorophyll *a* fluorescence), pigment composition and Cu accumulation capacity.

3.2. Materials and methods

3.2.1. Culture conditions and experimental design

Ectocarpus siliculosus strain Es524 (CCAP 1310/333) was grown in 10L polycarbonate bottles containing sterile natural seawater (NSW), enriched with Provasoli medium (Provasoli & Carlucci, 1974) to promote growth (see chapter 2). Cultures were

grown for 3 weeks in a controlled environment chamber (Sanyo, MLR 350T) at 15 °C, an irradiance of 45-50 μmol photons m^{-2} s^{-1} (supplied by cool white, Sylvania *luxline plus* fluorescent tubes), 14:10h light/dark cycle, and aeration to provide movement and to avoid nutrient gradients around filaments. Once sufficient biomass was obtained for experimentation, approximately 500 mg of fresh tissue (FW) were transferred, in triplicate, into individual polycarbonate flasks containing 100 mL of NSW for a period of acclimation of 6 days.

After the acclimation period, material was exposed to one of eight treatments comprising a combination of temperature: 15 °C (control) and 25 °C (elevated) and Cu concentration: 0, 0.8, 1.6, and 3.2 μM of total Cu (Cu_T), for an additional 6 days for photosynthetic measurements, pigment and metal analysis, and for 14 days for growth measurements. The increased temperature was chosen as 2 - 4 degrees above the maximum temperature recorded in the north region of Chile (Pizarro a *et al.*, 1994), from where strain Es524 was collected. Media were renewed every 2 days to avoid Cu depletion due to complexation of ligands released by algal cells (Gledhill *et al.*, 1999).

3.2.2. Growth rate

To assess growth rates, clumps of ca. 30 mg FW biomass were exposed in similar polycarbonate flasks for 14 days to combinations of temperature and Cu according to the treatments described above. This amount of time was chosen to facilitate growth measurements. Relative growth rates (RGR) were estimated volumetrically by using the method described by Dring (1967) (see section 2.3.1 for details). Variations in volume (V) were recorded at time of inoculation (t_0) and after 14 days of exposure (t_1) with the aid of blood sedimentation (Wintrobe) tubes. RGR were calculated using the formula: $[(Vt_1/Vt_0)^{1/t} -1] \times 100$ (% d^{-1}) (Yong *et al.*, 2013).

3.2.3. Photosynthetic physiology

Chlorophyll *a* fluorescence was measured, using the Rapid Light Curve (RLC) method (White and Critchley, 1999; Ralph and Gademann, 2005; Figueroa *et al*., 2014), with a MINI-PAM Photosynthesis Yield Analyzer (Walz, Germany; see section 2.3.2 for details). About 30 mg FW biomass were used to determine the parameters: maximum photochemical quantum yield of PSII (F_v/F_m), efficiency of light capture for photosynthesis (α), maximum electron transport rate (ETR_{max}), minimum saturating irradiance (E_k) and maximum non-photochemical quenching (NPQ_{max}). To ensure the same dark adaptation of all samples, pre-dawn measurements were performed by transferring each sample to the 'dark leaf' clip (DLC8, Walz) 5 minutes before measuring. The maximum quantum yield (F_v/F_m), where $F_v = F_m - F_o$ (Schreiber *et al*., 1995), was calculated from basal fluorescence (F_o) and maximal fluorescence (F_m) in the dark-adapted samples obtained from the first saturating light pulse (SP; >10000 μmol photons m^{-2} s^{-1}), which is the first step of the RLC. Following the first SP, the instrument runs automatically eight light incubations steps (20 seconds each) at increasing irradiances (E_1 = 25, E_2 = 76, E_3 = 157, E_4 = 249, E_5 = 375, E_6 = 508, E_7 = 748, E_8 = 1028 μmol photons m^{-2} s^{-1}). A SP was applied at the end of 20 seconds at each irradiance level to measure basal (F) and maximal fluorescence (F_m') in the light-adapted state, which were used for the calculation of Y (ΔF/Fm′) (See section 2.3.2). The MINI-PAM was operated remotely with the WinControl (Version 2.0, WALZ) software supplied by the manufacturer.

Electron transport rate (ETR) at each irradiance level of RLC was calculated according to the formula: $ETR = Y \times E_i \times A \times 0.8$ (Figueroa *et al*., 2014; Celis-Plá *et al*., 2014; Beer *et al*., 2014). where Y is the effective quantum yield in the light-adapted state, E_i is the incident irradiance (μmol photons m^{-2} s^{-1}), A is the absorptance of the sampled

algae (Figueroa *et al.*, 2014) and 0.8 is the fraction of photons absorbed by PSII in brown algae (Celis-Plá *et al.*, 2014a). The RLCs resulting from the ETR vs. incident irradiance (PAR) were fitted to a mathematical model (Eilers & Peeters, 1988) and α and ETR_{max} were obtained from the tangential function as an estimator of photosynthetic efficiency. Minimum saturating irradiance (E_k) was calculated from the intercept between ETR_{max} and α (Celis-Plá *et al.*, 2014; Ralph and Gademann, 2005). Finally, NPQ at each irradiance level was calculated as $NPQ = (F_m - F_m')/F_m'$. Similarly, the curve resulting from the plot NPQ vs PAR was fitted to the same model to calculate the maximum non-photochemical quenching (NPQ_{max}) as an estimator of heat dissipation processes.

3.2.4. Pigments content

The concentrations of the photosynthetic pigments chlorophyll *a* (Chl*a*), *c* (Chl*c*) and fucoxanthin (Fx) were estimated according to the method developed by Seely *et al.* (1972). This method is based in the ability of the solvent dimethyl sulfoxide (DMSO) to alter the lipid bilayer of biological membranes (Yu & Quinn, 1998) and denature proteins (Jackson & Mantsch, 1991), which allows the extraction of the pigments from cells. At the end of experiments, fresh biomass (FW) of *E. siliculosus* was rinsed with distilled water and then blotted dry with absorbent paper. Then, about 200 mg FW were placed in a 1.5 mL centrifuge tube containing 800 µL of DMSO and after 5 min of incubation at room temperature, samples were centrifuged at 21,000 $g_{av.}$ for 1 min (Hawk 15/05, Sanyo) to separate the biomass from the extract. The supernatant was diluted using a ratio 4:1 of DMSO:distilled-water and the absorbance measured with a spectrophotometer (JENWAY 7315, Cole-Parmer, UK) at λ = 665, 631, 582 and 480 nm. Pigment content was calculated using the equations:

$[Chla] = A_{665}/72.5$

$$[\text{Chl}c] = (A_{631} + A_{582} - 0.297A_{665})/61.8$$

$$[\text{Fx}] = (A_{480} - 0.722(A_{631} + A_{582} - 0.297A_{665}) - 0.049A_{665})/130$$

Pigments concentrations expressed in g L^{-1} were corrected for extraction volume, transformed to molarity and reported on a dry weight basis.

3.2.5. Metal analysis

Inductively coupled plasma mass spectrometry (ICP-MS) was used to determine the metal accumulation by algal tissues. The ICP source consists of a plasma torch, which is formed by three coaxially aligned quartz tubes inserted in a high radio frequency (HF; typically 27 MHz) coil. Gas argon is passed through the torch tubes and HF energy is applied to the coil. When a spark is added to the highly energized Ar atoms, electrons are stripped and the plasma is formed and fed by the coil by coupling electric energy into the gas, ensuring a continuously flowing plasma (Hill, 2006; Gross, 2017). The Ar ions and free electrons are agitated by the HF field to reach temperatures of approximately 5,000-10,000 Kelvin within the plasma. The sample is introduced in liquid form, meaning biomass has to be dissolved in an aqueous solution, usually concentrated nitric acid, prior to analysis. The liquid is converted to an aerosol using a nebulizer and is then sprayed into the centre of the plasma. Rapidly the particles within the aerosol are dried, atomized, ionized, excited and relaxed (Hill, 2006; Olesik, 1991). Ions are then pumped into the mass analyser. The mass spectrometer (MS) sorts the ions generated in the plasma based on their mass to charge ratio (m/z) so that only ions with a specific m/z reach the detection system. The signal intensity for a given ion is proportional to its concentration in the solution presented to the instrument (Hill, 2006).

After Cu exposure experiments, samples of algal biomass were treated to determine the proportion of Cu that was adsorbed by cell walls and intracellular

concentrations. For intracellular Cu content, samples were soaked in autoclaved NSW containing 10 mM ethylenediaminetetraacetic acid (EDTA), which is known to chelate metals ions associated to the cell wall (Hassler *et al.*, 2004). For total Cu content samples were not treated before acid-digestion. Both EDTA-treated and untreated samples were freeze-dried for 24 h (Super Modulyo, Edwards). Dried algal samples were weighed and then acid-digested with 2 mL of 70% (w/w) HNO_3 in a microwave oven (MARSXpress, CEM corporation, UK) using three heating cycles of 120°C (7 min), 155°C (7 min) and 170°C (20 min). After acid-digestion, samples were diluted to 5 mL with milli-Q water and copper concentrations were determined by ICP-MS (Thermo Scientific, Hemel Hempstead, UK). A calibration curve was prepared with pure Cu standards in 4% HNO_3 (SCP science, Canada) at concentrations ranging from 0.05 ppm to 0.5 ppm diluted in milli-Q water. In order to validate the method, equal amounts of certified reference material (dried seaweed powder of *Fucus* spp., IAEA-140/TM) (Coquery *et al.*, 1997) were acid-digested and analysed in the same way as *E. siliculosus* experimental biomass. A Cu standard of know concentration was re-measured at intervals of 10 samples in order to control the calibration of the instrument. Cu concentrations were transformed to molarity and are reported on a dry weight basis.

3.2.6. Statistical analysis

The effects of the treatments on the measured parameters were assessed using analysis of variance (two-way ANOVA) for factors: Temperature (2 levels) and copper treatment (4 levels) and their interaction, followed by Tukey's *post-hoc* tests. Shapiro-Wilk and Levene's tests were used on datasets to assess the normality and homogeneity of variance respectively. When assumptions of normality or homogeneous variance were not met, data were transformed using the square root function. The statistical package used was SPSS version 23 (IBM, Corp.).

3.3. Results

3.3.1. Growth

No significant interaction was observed between Cu treatment and temperature ($P = 0.252$; Table 3.1a). There was no significant difference in the response to Cu at either temperature ($P = 0.199$). However, there were significant decreases in RGR between 15 and 25 °C at the two highest Cu concentrations ($P < 0.05$; Figure 3.1).

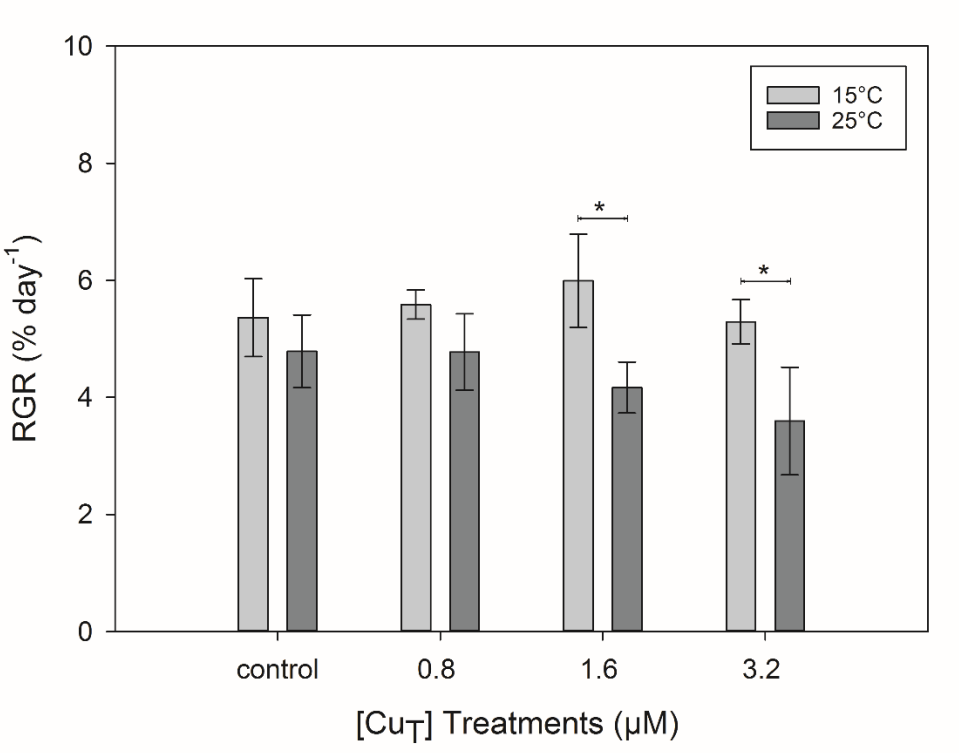

Figure 3.1. Relative growth rates (RGR) of *Ectocarpus siliculosus* exposed to four Cu concentrations (0, 0.8, 1.6, 3.2 µM Cu_T) and two temperatures (15 °C and 25 °C) for 14 days. Asterisks indicate significant differences ($P < 0.05$) found after Tukey's test for factor 'temperature' within Cu concentration, and crosses for factor 'copper' within temperature. Error bars represent ± 1 SD, $n = 3$.

Table 3.1. ANOVA results showing the effects (significance level α = 0.05) of increased temperature and Cu excess on: a) relative growth rate, b) photosynthetic parameters, c) pigments content, d) copper accumulation and of *Ectocarpus siliculosus*. F_v /F_m: maximum quantum yield, α: efficiency of light capture for photosynthetic, ETR_{max}: maximum electron transport rate, E_k: minimum saturating irradiance, NPQ_{max}: maximal non-photochemical quenching, Chl*a*: Chlorophyll *a*, Chl*c*: Chlorophyll *c*, Fx: Fucoxanthin, RGR: relative growth rate.

	Source of variation	df	MS	*F*	*P*		Source of variation	df	MS	*F*	*P*
a)											
RGR	Cu	3	0.68	1.74	0.199						
	Temperature	1	9.05	**23.13**	**<0.001**						
	Cu × Temperature	3	0.59	1.50	0.252						
	Residual	16	0.39	0.39							
b)											
F_v/F_m	Cu	3	0.00048	2.43	0.103	**α**	Cu	3	0.0027	1.08	0.384
	Temperature	1	0.00197	**10.06**	**0.006**		Temperature	1	0.0273	**10.82**	**0.005**
	Cu × Temperature	3	0.00034	1.731	0.201		Cu × Temperature	3	0.0133	**5.26**	**0.010**
	Residual	16	0.0002				Residual	16	0.0025		
ETR_{max}	Cu	3	18.51	2.50	0.097	**E_k**	Cu	3	203.67	2.85	0.070
	Temperature	1	112.0	**15.11**	**0.001**		Temperature	1	1466.4	**20.53**	**<0.001**
	Cu × Temperature	3	49.78	**6.72**	**0.004**		Cu × Temperature	3	454.81	**6.37**	**0.005**
	Residual	16	7.41				Residual	16	71.44		
NPQ_{max}	Cu	3	0.059	0.97	0.430						
	Temperature	1	1.191	**19.66**	**<0.001**						
	Cu × Temperature	3	0.013	0.212	0.886						
	Residual	16	0.061								
c)											
Chl a	Cu	3	50.43	0.75	0.537	**Chl c**	Cu	3	406.8	0.63	0.607
	Temperature	1	35.19	0.52	0.479		Temperature	1	102.9	0.16	0.695
	Cu × Temperature	3	152.63	2.28	0.119		Cu × Temperature	3	1185.4	1.83	0.182
	Residual	16	66.99				Residual	16	647.3		
Fx	Cu	7	5150.77	**3.43**	**0.042**						
	Temperature	1	26730.7	**17.80**	**<0.001**						
	Cu × Temperature	7	4045.47	2.69	0.081						
	Residual	32	1501.59								
d)											
Accum. Internal	Cu	3	4.136	**113.7**	**<0.001**	**Total**	Cu	3	14.38	**206.8**	**<0.001**
	Temperature	1	0.663	**18.23**	**<0.001**		Temperature	1	0.384	**5.52**	**0.032**
	Cu × Temperature	3	0.342	**9.41**	**<0.001**		Cu × Temperature	3	0.426	**6.12**	**0.006**
	Residual	16	0.036				Residual	16	0.07		

3.3.2. Photosynthetic physiology

Significant interactions between stressors were observed for all the photosynthetic parameters derived from the rapid light curves ETR vs. PAR (α, ETR_{max} and E_k; $P < 0.05$) but not for F_v/F_m and NPQ (Table 3.1b). For Maximum quantum yield (F_v/F_m), significantly decreased at 15 °C treatments compared to 25 °C in the 1.6 and 3.2 µM Cu_T treatments but not at other Cu concentrations (Figure 3.2 a). Although the factor Cu did not show significant differences for α (light capture efficiency), there was a significant interaction between Cu and temperature, with decreases at 15 °C in 1.6 and 3.2 µM Cu_T compared to 25 °C ($P < 0.05$) (Figure 3.2 b). The maximum electron transport rate (ETR_{max}) was greater at 15 °C in 0.8 and 3.2 µM compared to 25 °C under the same Cu treatments. At 15 °C, ETR_{max} was significantly greater at 3.2 µM Cu_T compared to 0 and 1.6 µM Cu_T ($P < 0.05$) (Figure 3.2 c). The minimum saturating irradiance (E_k) was higher at 15 °C in 1.6 and 3.2 µM Cu_T compared to 25 °C at the same Cu concentrations. At 15 °C, E_k was significantly higher at 3.2 µM Cu_T than 0 and 0.8 µM Cu_T ($P < 0.05$) (Figure 3.2 d). For NPQ_{max} (heat dissipation estimator), the only significant differences were between 25 °C and 15°C in 1.6 and 3.2 µM Cu_T ($P < 0.05$) (Figure 3.2 e).

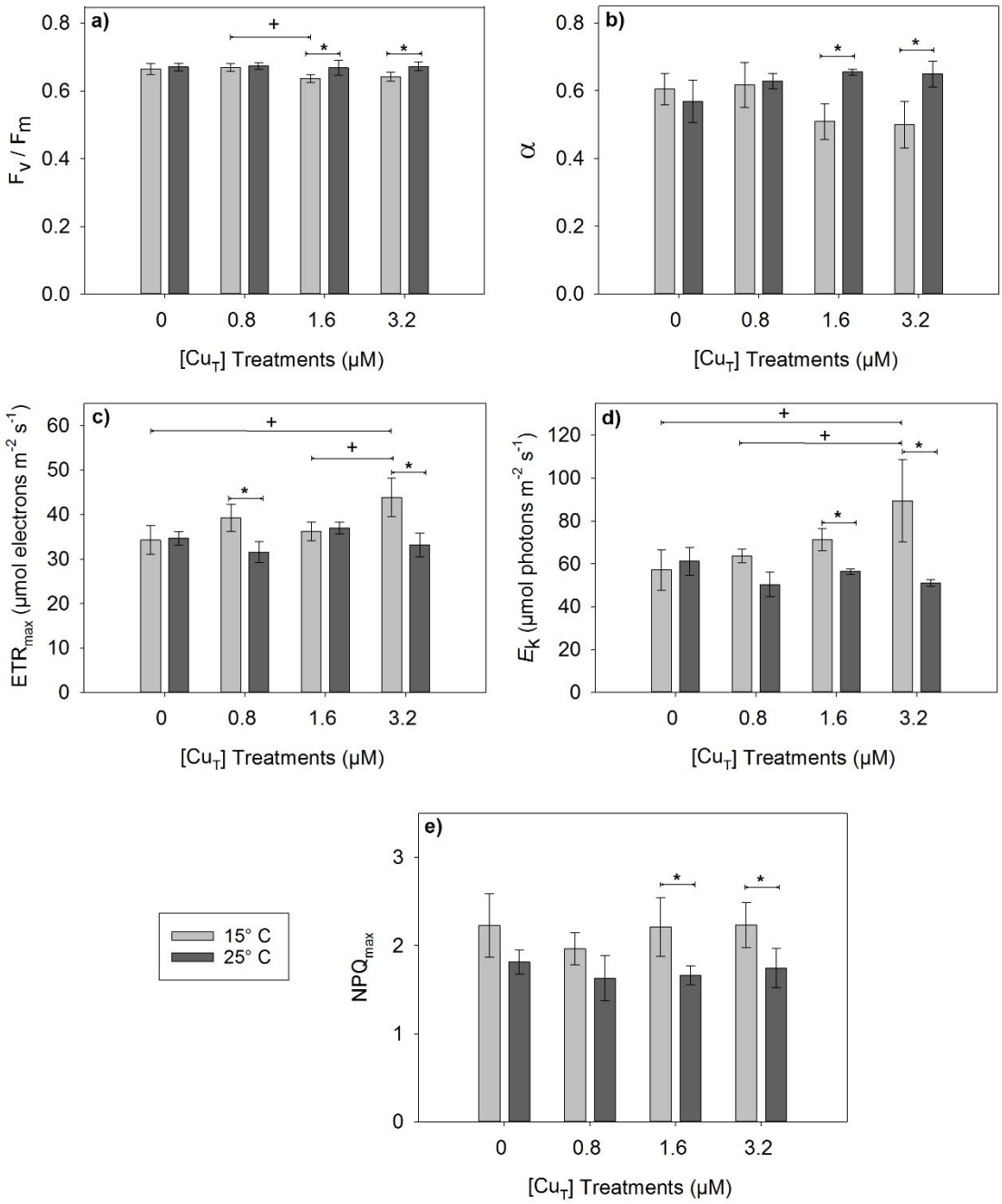

Figure 3.2. Photosynthetic parameters in *Ectocarpus siliculosus* exposed to four Cu concentrations (0, 0.8, 1.6, 3.2 µM) and two temperatures (15 °C and 25 °C) for 6 days. Asterisks indicate significant differences ($P < 0.05$) found after Tukey's test for factor 'temperature' within Cu concentration, and crosses for factor 'copper' within temperature. Error bars indicate ± 1 SD, $n = 3$. (a) F_v/F_m: maximum quantum yield, (b) α: light harvesting efficiency, (c) ETR_{max}: maximum electron transport rate, (d) E_k: minimum saturating irradiance, (e) NPQ_{max}: maximal non-photochemical quenching.

3.3.3. Pigments content

There were no statistical differences in the concentrations of chlorophyll *a* and chlorophyll *c* (Figure 3.3) between any treatments following 6 days of exposure (Table 3.1 c). In contrast, concentrations of the accessory pigment fucoxanthin (Fx) were significantly reduced at 15 °C in 0.8, 1.6 and 3.2 µM Cu_T treatments ($P < 0.05$), while no difference was observed at 25 °C between Cu treatments. No statistical significant interaction was observed between factors for Fx.

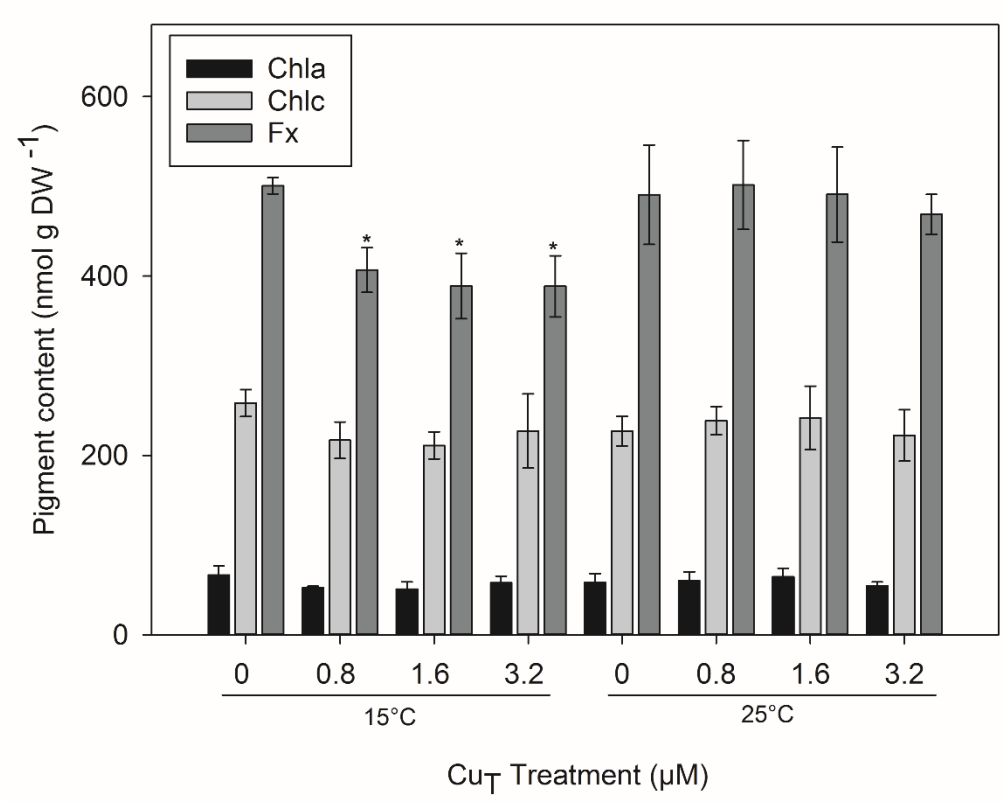

Figure 3.3. Concentrations of (a) chlorophyll a, (b) chlorophyll c, and (c) fucoxanthin in *Ectocarpus siliculosus* exposed to four Cu concentrations (0, 0.8, 1.6, 3.2 µM) and two temperatures (15 °C and 25 °C) for 6 days. Asterisks indicate significant differences ($P < 0.05$) found after Tukey's test for factor 'temperature' within Cu concentration, and crosses for factor 'copper' within temperature. Error bars indicate ± 1 SD, $n = 3$.

3.3.4. Cu accumulation

Total accumulation (intracellular + extracellularly bound) increased with Cu treatments at both temperatures (Figure 3.4. a). However, when exposed to 3.2 µM Cu_T significantly less accumulated at 25 °C ($P < 0.05$). This was reflected in a significant interaction term ($P < 0.05$) (Table 3.1 d). In general, intracellular Cu concentration significantly increased ($P < 0.05$) with Cu treatments at both temperatures, except between 0.8 and 1.6 µM at 25 °C, where no difference was observed (Figure 3.4. b). When analysing temperature within Cu, intracellular accumulation was significantly reduced at 25 °C compared to 15 °C at 1.6 and 3.2 µM Cu_T treatment ($P < 0.05$). A significant interaction term ($P < 0.05$) was observed as intracellular Cu was dependent of the temperature and not only the Cu treatment. When comparing the percentage of intracellular and extracellularly bound Cu, it appears that at 25 °C about half of Cu ions (50.05 %) is accumulated extracellularly and the other half (49.95 %) intracellularly at the 1.6 µM Cu_T treatment and similarly for the 3.2 µM Cu_T treatment (Table 3.2). In contrast, at 15 °C proportionally more Cu is bound intracellularly at 1.6 and 3.2 Cu_T treatment.

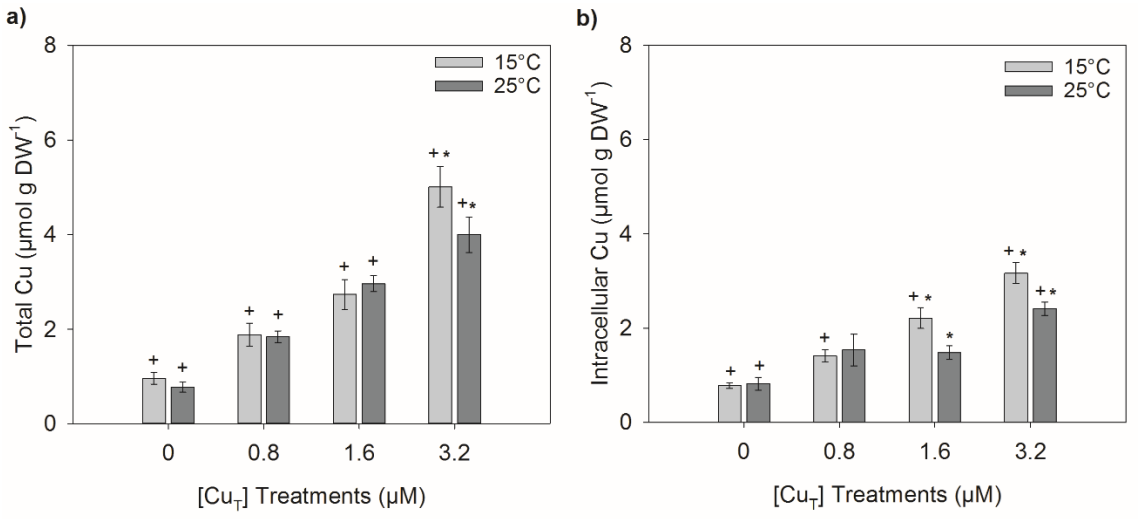

Figure 3.4. Total (a) and intracellular (b) copper accumulation in *Ectocarpus siliculosus* exposed to four Cu concentrations (0, 0.8, 1.6, 3.2 µM) at two temperatures: 15 °C and 25 °C for 6 days. Asterisks indicate significant differences ($P < 0.05$) found after Tukey's test for factor 'temperature' within Cu concentration, and crosses for factor 'copper' within temperature. Error bars indicate ± 1 SD, $n = 3$

Table 3.2. Percentage (means) of intracellular and extracellularly bound Cu ions in *E. siliculosus* after 10 days of exposure to four Cu concentrations (0, 0.8, 1.6, 3.2 µM Cu_T) and two temperatures: 15 °C and 25 °C for 6 days. Standard deviations are shown in parenthesis.

	Cu accumulation (%)			
Cu treatment	**15 °C**		**25 °C**	
	intracellular	*extracellular*	*intracellular*	*extracellular*
Control	82.18 (6.9)	17.82 (6.9)	93.12 (14.6)	6.88 (14.6)
0.8 µM	73.47 (10.0)	26.53 (10.0)	83.28 (14.2)	16.72 (14.2)
1.6 µM	81.42 (9.9)	18.58 (9.9)	50.11 (6.2)	49.89 (6.2)
3.2 µM	63.36 (1.7)	36.64 (1.7)	58.12 (5.2)	41.88 (5.2)

3.4. Discussion

The results presented in this chapter provide evidence that the effects of a combination of different Cu concentrations and increased temperature can interact differentially in the growth, photosynthetic physiology and Cu accumulation responses of *Ectocarpus siliculosus*. Interactions between both factors of stress were absent for growth, maximum quantum yield of PSII (F_v/F_m), maximum non-photochemical quenching (NPQ_{max}) and pigments (Table 3.1 a, b, c). In contrast, interactions between Cu and temperature were observed in all photosynthetic parameters derived from rapid light curves (RLC; α, ETR_{max} and E_k) and for accumulation of Cu ions (Table 3.1 c).

As previously reported temperature plays a key role in the growth and physiology of marine macroalgae (Eggert, 2012). Our results of relative growth rates indicate that temperature is an important factor for algal growth as significant reductions in growth

rate were observed at supra-optimal temperature of 25 °C regardless of the Cu concentration in the growth medium (Figure 3.1) (Table 3.1 a). These findings are contrary to some other studies. For example, Major and Davison (1998) observed that embryos of the brown seaweed *F. evanescens* were larger when growing at 20 °C compared to 5 °C. However, such interspecific differences in the response to temperature may be correlated to the optimal temperature range for growth of the specific species. This was shown to be the case in different isolates of *E. siliculosus*, where different optimal growth temperatures were related to the original collection site (Bolton, 1983). Also, different susceptibilities to temperature have been observed in other brown algal species such as *Ecklonia radiata, Scytothalia dorycarpa* and *Sargassum fallax* that correspond to latitudinal and temperature gradients (Wernberg *et al.*, 2016). In contrast, there was no significant change in RGR over the range of Cu concentrations used in this study (Table 3.1. a). These results confirm those obtained by Saez *et al*. (2015a) and indicate that this strain of *E. siliculosus* is able to thrive in highly Cu-polluted environments.

Similarly, temperature stress caused significant reductions in F_v/F_m, but in contrast to RGR, these occurred at 15 °C rather than 25 °C on exposure to the two highest Cu treatments of 1.6 and 3.2 µM Cu_T (Figure 3.2. a). Thus, a 10 °C increase in temperature did not negatively affect the photosynthetic efficiency, even at high copper concentrations. This phenomenon has also been reported in a similar study for both germling and adult stages of the brown alga *Fucus serratus* (Nielsen *et al.*, 2014). In that study, F_v/F_m was unaffected in adults and increased in germlings exposed to 1 µM Cu_T at 22°C compared to individuals grown at 12 °C. Also, in the green microalga *Chlorella pyrenoidosa* F_v/F_m was notably reduced at 15 °C even at very low copper concentrations (< 0,4 µM Cu_T) compared to algae incubated at 20, 25, 30 and 35 °C (Vavilin *et al.*, 1995). Light capture efficiency (α) was also reduced at 15 °C compared to 25 °C, at the two

highest Cu concentrations (1.6 and 3.2 μM). This strongly indicates that light harvesting is, at least, partially responsible for the decrease in maximum quantum yields and is dependent on the level of Cu exposure as there was a significant interaction between temperature and Cu for α (Figure 3.2. b, Table 3.1. b). Machalek *et al*. (1996) noted that in *Laminaria saccharina* (*Saccharina latissima*), α was affected by temperature, which was dependent on the light adaptation status of the samples prior to taking measurements. The latter indicates that interactions of different types of stress may affect the light capture efficiency of brown algae. Cu-induced reductions in α at 15 °C and high external Cu concentrations may indicate an uncoupling in energy transfer between the antenna and the reaction centres, probably due to an impairment of the light harvesting capacities of PSII, caused by the substitution of Cu^{2+} for Mg^{2+} in the chlorophyll molecules as suggested by Küpper *et al*., (1996, 1998, 2002). However, the absence of damage under Cu exposure at 25 °C indicates that acclimation or repair mechanisms are activated to deal with exposure to multiple stressors (Nielsen *et al.*, 2014). In the current study, interactions between the two environmental variables also occurred for minimum saturating irradiance (E_k) and maximum electron transport rate (ETR_{max}). Both parameters increased at 15 °C but the extent of the increase was dependent on the level of Cu exposure. For example, samples exposed to the highest Cu concentration (3.2 μM) showed higher levels of ETR_{max} at 15 compared to 25 °C, which helps explain the maintenance of the RGR at 15 °C. However, the increase in E_k may imply that higher irradiances are necessary to maintain the primary metabolism under Cu stress. This is supported by studies on the enzymatic activity of enzymes related to primary metabolism such as RUBISCO in *S. latissima* (Davison, 1987; Davison and Davison, 1987), where this enzyme was found to maintain higher activities at lower temperatures. The high activity of this enzyme was related to the tolerance of the algae to low temperatures, allowing it to maintain growth and high photosynthetic rates. Thus, an elevated E_k may

be indicative of increased primary metabolic reactions in response to stress. Alternatively, the increase in E_k and ETR_{max} may imply a temperature-mediated regulation of photosynthesis, allowing faster electron flow along the electron transport chain and thus avoiding possible photoinhibition. This is supported by the discovery of marked changes in lipid compositions in response to changes in temperature in the Antarctic rhodophyte *Palmaria decipiens* (Becker *et al.*, 2010), which are thought to facilitate a dynamic turnover of proteins associated to photosynthetic membranes such as D1. The NPQ_{max} (heat dissipation indicator) was lower at 25 compared to 15 °C at 1.6 and 3.2 μM Cu_T (Figure 3.2. e). These results match other results in *Fucus vesciculosus*, where reductions of NPQ_{max} were also observed at increased temperatures (Al-Janabi *et al.*, 2016). The higher levels of NPQ_{max} at 15 °C indicate an enhanced heat dissipation as more light is being adsorbed (as observed from increased E_k) and/or not being used effectively, consequently, the energy probably has to be dissipated as heat via mechanisms such as the xanthophyll's cycle (Latowski *et al.*, 2011).

The concentrations of chlorophyll (Chl *a* and *c*) were neither affected by Cu nor temperature (Table 3.1. c, Figure 3.3.). In contrast, the concentrations of fucoxanthin (Fx) were increased at 25 °C (Figure 3.3.) at all Cu treatments, which can be related to alterations in light harvesting as discussed above. Temperature can affect pigment concentrations; for example, *S. latissima* grown at 20 °C compared with 0-5 °C had higher concentrations of Chl *a*, Chl *c* and fucoxanthin, which was associated with increased light harvesting efficiency (Davison, 1987). Also, in embryos of *Fucus evanescens* (Major & Davison, 1998), Fx content was significantly higher at 20 °C compared with 5 °C, due to an increase in PSII reaction centre densities. These findings agree with our results for Fx and light harvesting efficiency (α), both of which increased at 25°C. Such response seems to be the result of acclimation to temperature. However, the effect of temperature acclimation was not part of this study and will require further investigation.

Ectocarpus siliculosus accumulated Cu at both the temperatures assessed. However, increasing the temperature to 25 °C affected the total accumulation of Cu (Figure 3.4. a), and particularly the intracellular fraction, which was lower at 25 °C than 15 °C in the 1.6 and 3.2 µM Cu treatments (Figure 3.4. b). This implies that transport and/or Cu exclusion mechanisms are regulated at elevated temperatures as about 50% of the total content is accumulated extracellularly at 25 °C compared with about 80% at 15°C in the 1.6 µM Cu treatments (See Table 3.2). Some studies suggest that resistance to excess copper in brown algae may be due to a combination of exclusion and intracellular mechanisms of detoxification (tolerance; Hall *et al*., 1979; Connan and Stengel, 2011; Roncarati *et al*., 2015). The strain used in this study was collected from a Cu polluted site and is considered Cu-resistant (Ritter *et al.*, 2010; Roncarati *et al.*, 2015; Sáez *et al.*, 2015c), therefore, we could hypothesise that the rates of detoxification mechanisms will be increased at higher temperatures (See Chapter IV). However, temperature itself can alter the stability and structure of cell membranes and thus contribute to a differential uptake of Cu ions due to alterations in high and low-affinity Cu transporters such as members of the Ctr family (Hope and Aschberger, 1970; Quinn, 1988; Puig and Thiele, 2002). Another possibility is that an increase in temperature promoted an enhanced synthesis of organic ligands, such as polyphenols, to detoxify intracellular excess of Cu by releasing the ligand-metal complexes extracellularly (Gledhill *et al*., 1999; Connan and Stengel, 2011). Additionally, both Cu and temperature have been reported to cause modifications in the cell wall of both algae and plants (Visviki and Rachlin, 1994; Sáez *et al*., 2015a). For instance, a recent cytophysiological study on *E. siliculosus* strain Es524 demonstrated that 2.4 µM Cu reduced the cell length and led to plasmolysis, and these changes were partially attributed to alterations in the cell wall structure (Sáez *et al*., 2015a). Lima *et al*. (2013) found that increased temperature changed the organization of cell-wall polysaccharides in coffee leafs, and disordered cell wall

microfibrils were observed in *Chara vulgaris* after exposure to cadmium and inorganic lead, which resulted in local wall protuberances (Heumann, 1987). Sharma and Azeez (1988) found that the accumulation of Cu and Co was increased at higher temperatures in the cyanobacteria *Anacystis nidulands* and *Spirulina platensis*; however, the temperatures used in that study (25-45 °C) were outside the range used in this one. In contrast, our results suggest that the interaction between stressors may be antagonistic for Cu accumulation, but further research is required to discriminate the mechanisms responsible for reduced accumulation at increased temperatures.

3.5. Conclusions

While there is limited empirical information on the interactions between environmental factors, such as temperature, and metal exposure toxicity, there is a growing concern that global warming will alter the responses of biota to metal pollution. Most findings so far suggest that increased temperature increases sensitivity to metals (Öncel *et al*., 2000; Wang and Wang, 2008; Oukarroum *et al*., 2012; Kimberly and Salice, 2014). However, there is some evidence that higher temperatures may increase Cu-resistance in bacteria (Boivin *et al*., 2005) and brown algae (Nielsen *et al*., 2014). The results presented here provide valuable information to better understand the interactive effects of increased temperature and excess Cu in the stress response of *E. siliculosus*. To some extent, the results of photosynthetic physiology and accumulation corroborate the hypothesis put forward by Nielsen *et al*. (2014), who suggested that increased temperature helps to offset the negative impacts of exposure to high Cu concentrations. However, more in-depth studies assessing different algae species and metals as well as responses at other levels of biological organisation would contribute to understand the effects of warming on metal metabolism.

Chapter IV

Oxidative damage and antioxidant response to a combination of excess copper and increased temperature in *E. siliculosus*

4.1. Introduction

The toxic effects of copper excess in seaweeds occur first at the biochemical level. One mechanism of Cu toxicity in macroalgae is the accumulation of reactive oxygen species (ROS), which may lead to oxidative stress and subsequent damage of cellular components (Collén *et al*., 2003; Nielsen *et al*., 2003; Contreras *et al*., 2009; Gonzalez *et al*., 2010; Sáez *et al*., 2015). Oxidative stress is characteristic of the cellular stress responses of any organism exposed to environmental stress. To counteract the effects of metal-induced oxidative stress, algae use a battery of intracellular detoxification strategies such as synthesis of low molecular weight antioxidant compounds, increased activities of antioxidant enzymes and enhanced expression of genes involved in metal detoxification (Pinto *et al*., 2003; Dring, 2005; Ritter *et al*., 2014; Moenne *et al*., 2016). Additionally, macroalgae can produce intra- and extracellular metal chelators (Ragan *et al*., 1979; Gledhill *et al*., 1999; Connan and Stengel, 2011). Increase in the concentrations of low molecular weight antioxidants such as ascorbate (ASC), glutathione (GSH) and phenolic compounds in response to Cu exposure have been reported in green and brown algae (Ratkevicius *et al*., 2003; Sáez *et al*., 2015c). Similarly, increases in the activity of enzymes superoxide dismutase (SOD), ascorbate peroxidase (APX), glutathione reductase (GR) and catalase (CAT) and the expression of their corresponding genes (*SOD*, *APX*, *GR* and *CAT*) were found after exposure to elevated Cu concentrations (Wu and Lee, 2008; Wu *et al*., 2009; Contreras-Porcia *et al*., 2011; Sáez *et al*., 2015b; see Section 1.2). However, those strategies seem to be species specific and are related to the history of Cu exposure of the individuals assessed (Moenne *et al.*, 2016). Although the aforementioned mechanisms have been observed in laboratory (Ratkevicius *et al.*, 2003) and field conditions (Sáez *et al.*, 2015a), little is known on the potential effect of additional environmental stressors such as increases in seawater temperature due to global warming.

Seaweeds are naturally exposed to variations in temperature and other abiotic factors such as salinity, high irradiance, desiccation, etc. It has been noted that the mechanisms involved in the response to those environmental stressors are at least partially mediated by reactive oxygen metabolim (ROM) (Collén & Davison, 1999a,b,c). Thus, the production and regulation of intracellular ROS is thought to be involved not only in stress tolerance but also in signalling and regulation of gene expression (Dring, 2005). Both increases and decreases of seawater temperature can trigger the production of ROS in algae (Collén and Davison, 1999a; Choo *et al*., 2004; Rautenberger and Bischof, 2006; Cruces *et al*., 2013). Similar to Cu stress, the ROM response to temperature is highly variable between and within species, and it is correlated to the prevailing temperature in the seaweeds' natural habitat. For example, oxidative damage (measured as malondialdehyde concentration) and SOD activity were higher in Antarctic algae at temperatures close to 0 °C than at 10 °C, while the opposite was found for sub-Antarctic species (Rautenberger & Bischof, 2006). Despite the rare information available on the biochemical responses to temperature in macroalgae, there is a growing interest to identify the mechanism(s) that drive algal responses to ongoing ocean warming (Celis-Plá *et al.*, 2017).

Brown algae are a group of marine photosynthetic organisms of great ecological and economic importance. While several studies have contributed to understanding the role of ROM in the response to increased levels of Cu and other metals (Pinto *et al*., 2003; Moenne *et al*., 2016), information on the combined effect of Cu and increased temperature in the brown seaweeds is rare. The emergence of the filamentous seaweed *Ectocarpus siliculosus* as a model for the study of brown algae and the sequencing of its genome, has allowed for the study of stress mechanisms at the biochemical and molecular levels (Dittami *et al*., 2009; Ritter *et al*., 2010; Coelho *et al*., 2012; Ritter *et al*., 2014; Sáez *et al*., 2015b). From those studies, overlap in the response to copper and oxidative

stresses has been demonstrated. However, the nature of interactions between different stressors may be complex. Some attempts to describe the interactive effects of several anthropogenic and natural factors of stress have been made in plants (see Alexieva and Ivanov, 2003). For example, often the combined action of several stressors increases their deleterious effect, surpassing the simple additive effect of their action alone (cross-synergism). In contrast, some plants exposed to a single stress factor can increase their resistance to subsequent adverse impacts (cross-adaptation). In the present study, we exposed *E. siliculosus* to a combination of increased temperature and Cu excess in order to evaluate the interactions between these stress factors. To assess the oxidative stress responses, concentrations of hydrogen peroxide (H_2O_2) and lipid peroxidation (as thiobarbituric acid reactive substances [TBARS]) were measured. Reactive oxygen metabolism (ROM) was assessed by measuring the concentration of water soluble antioxidants: ascorbate (ASC), glutathione (GSH) and phenolic compounds, the activity of antioxidant enzymes (SOD, APX, GR, CAT) and the expression of antioxidant enzyme genes: catalase (*CAT*), ascorbate peroxidase (*APX*), superoxide dismutase (*SOD*), glutathione reductase (*GR*) as well as metal and thermal stress-related genes: glutathione synthase (*GS*), monodehydroascorbate reductase (*MDHAR*), heat shock protein 70 (*HSP70*) and metallothionein (*MET*).

4.2. Materials and methods

4.2.1. Experimental design and culture conditions

Algal biomass was grown as described in Section 2.2. Once enough biomass was produced, 500 mg of fresh weight filaments were transferred to individual polycarbonate flasks containing 125 mL of sterile NSW. Samples were maintained for two days at 15 °C and irradiance 45-50 μmol photons m^{-2} s^{-1} (cool white, Sylvania luxline plus fluorescent tubes), 14:10h light/dark cycle. After this period, samples were exposed to

experimental treatments, which consisted of a combination of two factors: "Cu concentration" and "Temperature", with two levels each. The levels for Cu concentration were 0 (control) and 2.4 µM (increased) total copper (Cu_T) and the levels for temperature were 15 (control) and 19 °C (increased). Samples were exposed to the treatments for ten days to allow comparison with previous studies of chronic exposure to Cu in *E. siliculosus*. Experimental media were replaced every 2 days.

4.2.2. Oxidative stress indicators

To assess oxidative stress, the relative concentrations of hydrogen peroxide (H_2O_2) and lipid peroxides were measured. The method described by Velikova *et al.* (2000) for the determination of H_2O_2 was adapted for a plate reader. This method is based on the oxidation of potassium iodide (KI) by H_2O_2, which produce I_3^- resulting in the development of a yellowish solution (Junglee *et al.*, 2014). Frozen FW biomass (100 mg) was homogenised in 1 mL of 10% trichloroacetic acid (TCA) with the mechanical aid of acid-washed sand. The mortar was kept in ice during the homogenisation process. Homogenates were transferred to 1.5 mL tubes and centrifuged at 21,000 $g_{av.}$ for 10 minutes at 4 °C (Hawk 15/05, Sanyo). After centrifugation, 50 µL of supernatant were added to each well of a 96-well clear flat-bottom microtitre plate (Sterilin™, Thermofisher scientific). Then, 150 µL of 50 mM potassium phosphate and 100 µL of 1M potassium iodide were added to each well and the absorbance at λ = 390 nm was recorded in a plate reader (SpectraMax 190, Molecular Devices). Hydrogen peroxide was diluted from a 30% stock to prepare fresh standards at concentrations between 0 to 320 µM. Concentrations in samples were retrieved from a calibration standard curve obtained from standards.

Levels of lipid peroxidation were assessed by measuring the thiobarbituric acid reactive substances (TBARS). The protocol is a modification of the method described by

Heath and Packer (1968), to be used in a plate reader. Extractions were performed as described above for H_2O_2. After the centrifugation step, 400 µL of supernatant were mixed with 400 µL of 0.5% thiobarbituric acid (diluted in 0.3% NaOH) and the mixture was transferred to a water bath and incubated at 95 °C for 45 minutes. Following the incubation period, the mixture was cooled to room temperature. Finally, 200 µL of mixture were transferred to each well of a 96-well clear flat-bottom microtitre plate (Sterilin™, Thermofisher scientific) and absorbance was measured at 532 nm. A calibration standard curve was prepared with standards of 1,1,3,3 tetraethoxypropane diluted in 10% TCA, in a concentration range of 0 to 32 µM, which breaks down to malondialdehyde (MDA) under the assay conditions.

4.2.3. Concentrations of ascorbate (ASC) and dehydroascorbate (DHA)

Concentrations of ASC and DHA were estimated with a modification of the method described by Benzie and Strain (1996). The so called FRAP reagent develops an intense blue colour when the complex ferric-tripyridyltriazine (Fe^{3+}-TPTZ) is reduced to the ferrous form (Fe^{2+}), which has maximum absorption at 593 nm. This is achieved by a reductant, such as ascorbate, assuming it is the only antioxidant molecule in the sample. To extract ascorbate 300 mg FW biomass samples were ground to a fine powder in a mortar with the aid of liquid nitrogen (LN). Then, 1.2 mL of 0.1 M HCl were added and the mixture was transferred to a 1.5 µL centrifuge tube. Samples were centrifuged at 21,000 $g_{av.}$ for 10 minutes at 4 °C. To determine levels of ASC, 10 µL of supernatant were transferred to each well of a 96-well clear flat-bottom microtitre plate (Sterilin™, Thermofisher scientific). Then, 290 µL of FRAP reagent (acetate buffer pH 3.6 + 10 mM TPTZ + 20 mM $FeCl_3.6H_2O$; mixed in a ratio 10:1:1) were added to each well containing samples and the absorbance measured at 593 nm (SpectraMax 190, Molecular Devices). Total ASC levels were determined by incubating 500 µL of supernatant with 5 µL of 100

mM dithiothreitol at room temperature for 1 h. The reaction was stopped by addition of 5 μL of 5% N-ethylmaleimide. Spectrophotometric determination was performed as for ASC. Concentrations of ascorbate and total ascorbate were obtained with a calibration curve by using standards of L-ascorbic acid (Sigma-A7506) in a range of 0 to 500 μM. DHA concentrations were obtained from subtraction of ASC from total ascorbate values.

4.2.4. Concentrations of reduced (GSH) and oxidised (GSSG) glutathione

Glutathione (GSH) and glutathione disulphide (GSSG) concentrations were measured using a modification of the method described by Queval and Noctor (2007). This method depends on the reduction of 5,5'-dithiobis 2-nitro-benzoic acid (DTNB), also known as Ellman's reagent, catalysed by glutathione reductase. Extractions were performed as for ASC. After the centrifugation step, 300 µL of supernatant were neutralised with 5 µL of 5M K_2CO_3 to a pH between 6.0 – 7.0. Levels of total glutathione (GSH plus GSSG) were measured by adding 10 µL of neutralised supernatant to each well of a 96-well clear flat-bottom microtitre plate (Sterilin™, Thermofisher Scientific). The reaction was started by adding 290 µL of 100 mM sodium phosphate buffer, pH 7.5, containing 6 mM EDTA, 0.5 mM NADPH, 0.6 mM DTNB, and 1 unit of GR (Sigma Aldrich, G3664). After automatic mixing for 3 s, the increase in absorbance was monitored at 412 nm for 5 min. GSH at a concentration of 20 µM was used as a standard. To measure GSSG, 250 µL of neutralised supernatant were incubated with 5 µL of 2-vinylpyridine (VPD) for 30 min at room temperature. After incubation, the mixed solution was centrifuged for 5 min at 4 °C to reduce the excess of VPD. The reaction to determine GSSG was performed as for GSH using GSSG standards (5 µM). To calculate GSH and GSSG concentrations, the rates of increase in absorbance were calculated over the linear part (first 90 s) of the curve A_{412} vs time. All rates were corrected by subtracting the rates of the blank assays (no GSH or GSSG), then divided by the rate of standards and multiplied by the standards' concentrations.4.2.5. Antioxidant enzyme activities

Activities of four antioxidant enzymes, superoxide dismutase (SOD), ascorbate peroxidase (APX), glutathione reductase (GR) and catalase (CAT) were measured from the same protein extract. Proteins were extracted according to Ratkevicius *et al*. (2003). About 1.5 g of frozen biomass were ground to a fine powder in a mortar with liquid

nitrogen. A mixture of 100 mM potassium phosphate buffer (pH 7) with 1 mM dithiothreitol (DTT) were added at a rate of 3 mL per 1 g of biomass. Then, the homogenate was filtered through Miracloth filter tissue (Calbiochem) and centrifuged at 12,000 $g_{av.}$ for 20 min at 4 ºC. To precipitate proteins, the supernatant was transferred to a new tube and 0.5 g of ammonium sulphate was added per each millilitre of supernatant recovered. The mixture was then shaken for 2 h at 4 ºC and then centrifuged at 12,000 $g_{av.}$ for 40 min at 4 ºC. Finally, the resulting pellet was re-suspended in 100 mM potassium phosphate buffer (pH 7), containing 0.1mM Dithiothreitol (DTT) and 10% glycerol. Protein concentrations in the extracts were determined using the Bradford method with bovine serum albumin as standard (Bradford, 1976). Extracts were stored at -80 ºC for further analyses.

The activities of CAT, APX and GR were measured according to Ratkevicius *et al*. (2003). To assay CAT activity, 30 µg of protein extract were added to 1 mL of 50 mM potassium phosphate buffer (pH 7) containing 11 mM H_2O_2 and the decrease in absorbance at 240 nm was recorded for 5 min. Activity was calculated with the extinction coefficient (ε) of 40 M cm^{-1}. APX activity was determined by adding 30 µg of protein extract to 100 mM potassium phosphate buffer (pH 7) containing 11 mM H_2O_2 and 0.5 mM ascorbate. The decrease in absorbance at 290 nm was followed for 5 min and activity was calculated with ε = 2.8 mM cm^{-1}. GR activity was assayed by adding 30 µg of protein extract to 100 mM potassium phosphate buffer (pH 7) containing 0.5 mM GSSG and 0.15 mM NADPH. Change in absorbance was monitored at 340 nm for 5 min and activity calculated with ε = 6.27 mM cm^{-1}. Activity of SOD was measured according to Gonzalez *et al*. (2012) based on the principle of inhibition by SOD of nitroblue tetrazolium (NBT) photoreduction (Beauchamp & Fridovich, 1971). Between 40–50 µg of protein extract were added to 1 mL of a mixture comprising potassium phosphate buffer (pH 7), 0.1 mM EDTA, 1.3 mM L-methionine, 0.02 mM riboflavin and 0.6 mM NTB. The mixture was

incubated for 15 min under white light (> 100 µmol $m^{-2}s^{-1}$), including a control reaction without protein. A second control reaction was carried out in the dark and this used as the baseline for spectrophotometric determination of reduction in absorbance at 560 nm. One unit of SOD activity is defined as the necessary amount of enzyme to inhibit 50% of the photoreduction of NBT, considered to be 100% the absorbance of the non-protein control.

4.2.6. Total phenolic compounds level

Concentrations of total phenolic compounds were measured as described by Celis-Plá *et al*. (2014a) with modifications. Samples (250 mg FW biomass) were pulverised in a pre-cooled mortar with the aid of acid-washed sand and 250 mL of 99% methanol. Homogenate was gently agitated overnight in a platform mixer (RPM5, Ratek) at 4 °C in the dark and then centrifuged at 6,000 $g_{av.}$ for 30 min. The concentration of total phenolic compounds was obtained by mixing 100 µL of supernatant with 6 mL of dH_2O and 0.5 mL of Folin-Ciocalteu (Folin & Ciocalteu, 1927) reagent solution. After mixing vigorously, the solution was alkalinised with 1.5 mL of 20% Na_2CO_3 anhydrous and diluted to a final volume of 10 mL. After 2 hours in the dark at 4 °C, absorbance was measured at 760 nm in a spectrophotometer (Cary 8454, Agilent). Phloroglucinol (1,3,5-trihydroxybenzene, Sigma P3502) was used as standard at concentrations ranging 0 to 200 ug mL^{-1}. The release of polyphenols in the seawater media were measured as according to Celis-Plá *et al*. (2014a). Optical density of the NSW media used in the experiments was measured at 270 nm at the end of the experiments. Phloroglucinol dissolved in filtered and autoclaved NSW was used as standard in concentrations from 0 to 130 µg mL^{-1}.

4.2.7. Quantification of Methanol-Soluble Polyphenolic Compounds

For analysis of the composition of phenolic compounds, samples were extracted as described above for total polyphenols. The supernatant was filtered through a syringe PVDF filter (0.22 μm) and an aliquot of 20 μL of extract was then analysed by high performance liquid chromatography (HPLC; Agilent model 1260 Infinity, column Agilent Eclipse XDB-C18 [4.6 mm inner diameter, 150 mm length and 5 μm particle size]) coupled to a photodiode array detector. Samples were eluted by applying a gradient of 1% (v/v) phosphoric acid (A) and 100% acetonitrile (B) using the program: 90% A – 10% B for 0 to 5 min, 75% A – 25% B for 5 to 8 min, 65% A – 35% B for 8 to 15, 65% A – 35% B for 15 to 17 min and 90 % A – 10% B for 17 to 20 min. Flow rate was 1 mL min^{-1} at 25 °C. Peaks were detected at 254, 280, 314 and 340 nm and identified using the absorption spectra of pure commercial standards (Sigma-Aldrich) of *trans*-cinnamic acid, *p*-coumaric acid, benzoic acid, salicylic acid, caffeic acid, ferulic acic, chlorogenic acid, vanillic acid, gallic acid, sinapic acid, escopoletin, esculetin, kaempferol, apigenin, catechin, morin, rutin, luteolin, ellagic acid and phloroglucinol. Quantification was achieved by a calibration curve obtained with pure standards at concentrations ranging from 0 to 1 mg mL^{-1}.

4.2.8. Release of phenolic compounds

Samples of experimental media (NSW or Cu-enriched NSW) were collected after 10 d exposure experiments and filtered using a syringe sterile filter unit (pore size 0.22 μm; Millex®, Merck Millipore, Ireland). Determination of polyphenols in seawater was performed according to Celis-Plá *et al*., (2014a). Optical density was measured at 270 nm for each sample. A calibration curve was obtained with standards of phloroglucinol dissolved in filtered sterile NSW. Concentrations are expressed as mg g^{-1} DW.

4.2.9. Gene expression analysis

Gene expression analyses of genes involved in ROS and metal metabolism were performed on RNA extracts obtained by the method described by Greco *et al*. (2014), with some modifications. The protocol for extraction of nucleic acids consisted of 6 phases performed at 4 °C (unless specified). Phase one was cell lysis, inactivation of cellular nucleases and separation of nucleic acids from cell debris. This phase consisted of mechanical disruption of 100 mg frozen FW biomass in a high speed tissue homogeniser (Precellys24, Bertin Technologies) using specific tubes from a Precellys lysing kit (MK28-Hard tissue grinding, Bertin Technologies) in presence of extraction buffer (EB: 100 mM Tris-HCl, pH 9.5; 150 mM NaCl; 1.0% sarkosyl; 5 mM DTT). After homogenisation, tubes were centrifuged at 9,000 $g_{av.}$ for 45 s and supernatant transferred to a 15mL centrifuge tube. Phase two was removal of polysaccharides by adding a mixture of absolute ethanol (1/9 volume of supernatant) and 3 M potassium acetate pH 4.8 (1/4 volume of supernatant) and gentle mixing. Further precipitation of polysaccharides and proteins was achieved with the aid of a solution of 2 mL chloroform: isoamyl alcohol (24:1, v/v) and gentle shaking for 30 min and vortexing. Samples were centrifuged at 14,000 $g_{av.}$ for 20 min to allow separation of the aqueous and organic phases. After recovering the aqueous phase in a new tube, additional removal of proteins and polysaccharides was achieved by adding 0.2–0.3 volumes of absolute ethanol and 1 volume of chloroform, shaking and centrifugation as the previous step. Phase three was precipitation of nucleic acids by incubation of the resulting aqueous phase from the previous step, in a mixture of isopropanol, 3 M sodium acetate, (pH 5.2) and 1% of 2-mercaptoethanol at -80°C for 1 h. After incubation, samples were centrifuged at 12,000 $g_{av.}$ for 30 min to obtain a pellet of nucleic acids. Phase four was washing the pellet of nucleic acids twice in 75% ethanol and centrifugation at 12,000 $g_{av.}$ for 20 min. After centrifugation, all remaining ethanol was discarded and the pellet was allowed to air dry

at room temperature. Phase five was resuspending the dried DNA/RNA pellet in 40–50 µL of nuclease-free water. Phase six was treating nucleic acids with DNase I (10 U μL^{-1}) to obtain pure RNA. All samples were stored at -80 °C.

Reverse transcription was performed on 2 µg of total RNA from each sample with the High Capacity RNA-to-cDNA kit (Applied Biosystems) in a final volume of 20 µL, according to the kit instructions. Specific oligonucleotide primers were designed as described in Roncarati *et al*. (2015) using PRIMER3web software (version 4.1.0) (Untergasser *et al.*, 2012) and based on the most recent annotation version (V2) of the genome of *E. siliculosus*, which is available from the online resource for community annotation of eukaryotes ORCAE (Sterck *et al.*, 2012). Specificity was tested *in silico* using Primer-BLAST (Ye *et al.*, 2012). Each primer pair (Table 4.1.) used was designed to obtain a final PCR product of between 100- and 150-base pair in length. Primer pairs were tested for different parameters: i) robustness, successful amplification over a range of annealing temperatures, ii) specificity, the generation of a single peak in the significant peak in the melting curve, and iii) the consistency of highly reproducible C_T values within the reactions of a triplicate. The average efficiency of primer pairs used ranged between 0.95 and 1.0.

All genes were quantified on the same batch of cDNAs, to minimise experimental variation that could be due to cDNA synthesis. The quantitative RT-PCR reaction was performed with a QuantStudio 7 Flex Real-Time PCR System (Applied Biosystems) in a 20 µL total volume containing: 10 µL of PowerUp™ SYBR® Green Master Mix (Applied Biosystems), 400 nM of each primer and 75 ng of cDNA. Reactions were performed in triplicate using the following cycles: 95 °C for 10 min, 40 cycles of 95 °C for 15 s and 60 °C for 1 min. To test primer specificity, melting curve analysis (from 60 °C to 95 °C with an increased heating rate of 0.5 °C s^{-1}) was performed after

amplifications. The method described by Livak and Schmittgen (2001) was used to calculate relative levels of gene expression, according to the $2^{-\Delta\Delta C_T}$ method, where $\Delta\Delta C_T$ = [(C_T target gene – C_T reference gene) $_{\text{treated sample}}$ – (C_T target gene – C_T reference gene) $_{\text{control sample}}$], and the cycle threshold (C_T) value was obtained from quantitative RT-PCR. Gene expression data were normalised to the expression of ARP2 subunit of the actin-related protein complex ARP2/3. Stability of ARP2 expression is reported in Le Bail *et al*. (2008b). Normalised gene expression was reported in relation to control conditions i.e. 0 µM Cu_T at 15 °C.

Table 4.1. Detail of genes selected for qRT-PCR analysis. Gene IDs from ORCAE database (http://bioinformatics.psb.ugent.be/orcae/overview/EctsiV2). For CAT and HSP70 primers were designed in conserved regions of four and two loci respectively.

Gene Symbol	Function	Gene ID	Oligonucleotides (Forward-Reverse) 5′ – 3′	PCR product length (bp)
Fe/Mn SOD	Superoxide dismutase	Ec-25_000220.1	GTTTGGGAGCACGCCTACTA ACACGGGTGTACTCGGACTC	110
MDHAR	Monodehydroascorbate reductase	Ec-26_002470.1	CCTCCTCTGATTTCCCCTTC ATCAACGGAAACTGCCTGAC	116
APX	Ascorbate peroxidase	Ec-19_000230.1	ACGCACCAAGTAAGGGAAACC AGGCATTTGTCGGTTTCCAG	136
GR	Glutathione reductase	Ec-24_001330.1	ACGGAGACGCACCTATTCAT TTTTCCGTCGTCGAGTTCTT	128
CAT	Catalase	Ec-11_003410.1 Ec-26_000310.1 Ec-00_008240.1 Ec-00_010030.1	GAGAACACCTTCACGAGCGG GTCATCACCCAGTCGTACTCGA	104
GS	Glutathione synthase	Ec-18_004530.1	CTCCTACGAGCAAACCAAGG GGCCAGAACATCTTTCAGGA	106
HSP70	Heat-shock protein 70	Ec-05_005600.1 Ec-05_005600.2	TCGCCAAGACCGAAATACTC GTCGTGGGAGTCCATCATTT	140
MET	Metallothionein	Ec-20_001230.1	CGTGCGGATCCGTGAAGCAG TTCCTCCCGAGGTGCACTTGC	111

4.2.10. Statistical analysis

The effects of the treatments on the measured endpoints were assessed using analysis of variance (two-way ANOVA) for factors: Temperature (2 levels) and copper concentration (2 levels) followed by Tukey post-hoc tests. Shapiro-Wilk and Levene's tests were used on datasets to assess the normality and homogeneity of variance,

respectively. When assumptions were not met, $\log_{10}$ transformation was applied to data. The statistical package used was SPSS version 23 (IBM, Corp.). When a significant interaction between factors was determined after two-way ANOVA, the Abotts' formula (Teisseire *et al*., 1999; Chesworth *et al*., 2004) was used to determine synergism or antagonism between Cu and temperature. This formula compares expected and observed decreases or increases, where expected decreases or increases are expressed as percentage C_{exp} can be predicted as follows:

$$C_{exp} = A + B - \left(\frac{AB}{100}\right)$$

Where *A* and *B* are the decreases or increases caused when the factors of stress act alone. The ratio of inhibition (*RI*) was then calculated for the combined stressors as follows:

$$RI = \frac{observed\ increase\ or\ decrease}{C_{exp}}$$

Interactive effects were evaluated by comparing *RI* with 1. *RI* values > 1 indicated synergism and *RI* values < 1, antagonism. The mean and standard deviation of *RI* was calculated from three replicates for each treatment. Both synergism and antagonism were assumed only if the mean *RI* was greater than one standard deviation from 1. Additivity was assumed where a non-significant interaction term for factors Cu concentration and temperature was observed after two-way ANOVA.

4.3. Results

4.3.1. Oxidative stress indicators

A significant interaction was observed between Cu and temperature in the levels of H_2O_2 ($P < 0.05$). For temperature within Cu concentration, no differences were

observed between 15 and 19 °C for the control (0 µM Cu_T) treatment ($P = 0.052$) and a significant increase was observed at 19 °C for the 2.4 µM Cu_T treatment ($P < 0.05$) after Tukey's tests (Figure 4.1, left). For Cu concentration within temperature also significant increases were observed between at 2.4 µM Cu_T at both temperatures compared to controls (0 µM Cu_T) ($P < 0.05$). A similar pattern of response to the treatments was observed for lipid peroxidation levels (measured as TBARS concentrations) (Figure 4.1, right). However, a significant decrease was observed at 19 °C for temperature within control (0 µM Cu_T) treatment ($P < 0.05$). The interaction between Cu and temperature was synergistic for both H_2O_2 and TBARS accumulation (Table 4.2).

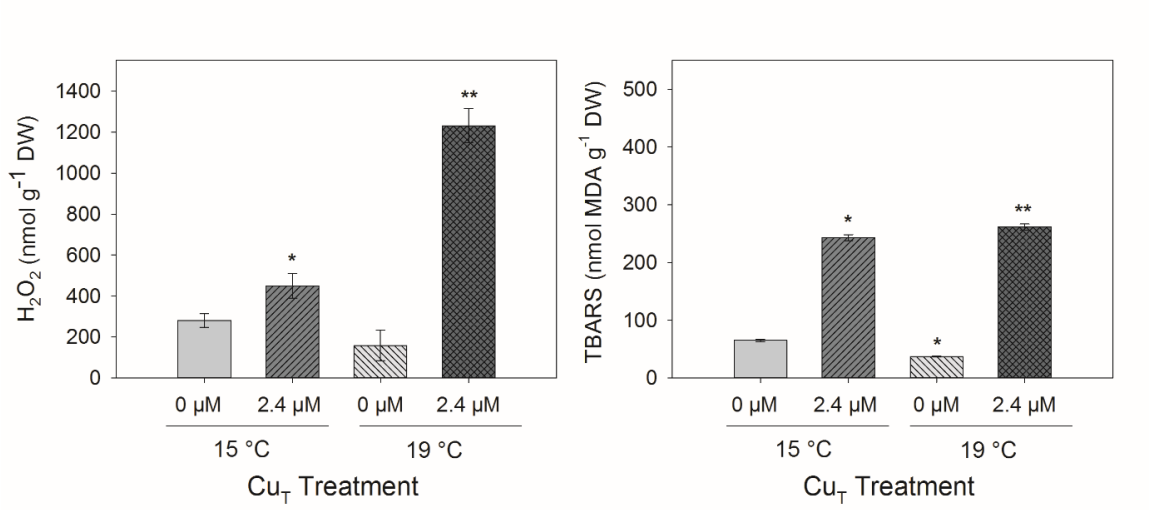

Figure 4.1. Oxidative stress parameters: hydrogen peroxide (left) and lipid peroxides (right) in *Ectocarpus siliculosus* exposed to a combination of Cu concentrations (0 and 2.4 µM Cu_T) and two temperatures (15 °C and 19 °C) for 10 days. Single asterisks indicate main significant differences ($P < 0.05$) found after Tukey's test. Double asterisks indicate a significant interaction between Cu and temperature. Error bars represent ± 1 SD, $n = 3$.

Table 4.2. The interactive effect of Cu treatment and increased temperature in *E. siliculosus* biochemical and molecular variables.

Combined treatment (Cu_T × Temperature)	Variable	Mean *RI* ± S.D.	Interactive effects
2.4 µM + 19 °C	H_2O_2	5.81 ± 1.18	> 1 Synergistic
	TBARS	2.71 ± 0.02	> 1 Synergistic
	GSH	0.65 ± 0.04	< 1 Antagonistic
	GSSG	0.62 ± 0.04	< 1 Antagonistic
	Total phenolics	0.47 ± 0.05	< 1 Antagonistic
	Catechin	0.83 ± 0.05	< 1 Antagonistic
	Phenolics release	0.54 ± 0.14	< 1 Antagonistic
	APX	0.51 ± 0.17	< 1 Antagonistic
	GR	0.52 ± 0.05	< 1 Antagonistic
	APX	0.26 ± 0.07	< 1 Antagonistic
	SOD	0.24 ± 0.09	< 1 Antagonistic
	MDHAR	0.69 ± 0.30	< 1 Antagonistic
	MET	0.07 ± 0.01	< 1 Antagonistic

4.3.2. Concentrations of antioxidant compounds

No significant interactions between Cu and temperature were observed for ASC ($P = 0.593$) and DHA ($P = 0.232$). However, significant increases of both were found for the 2.4 µM Cu_T treatment ($P < 0.05$) within each temperature, but there were no differences between 15 and 19 °C (Figure 4.2.). The increase in DHA at 2.4 µM Cu_T and 15°C (1.57 µmol) and 19 °C (1.25 µmol) was greater than that of ASC at 15 °C (0.39 µmol) and 19 °C (0.32 µmol) for the same Cu treatment.

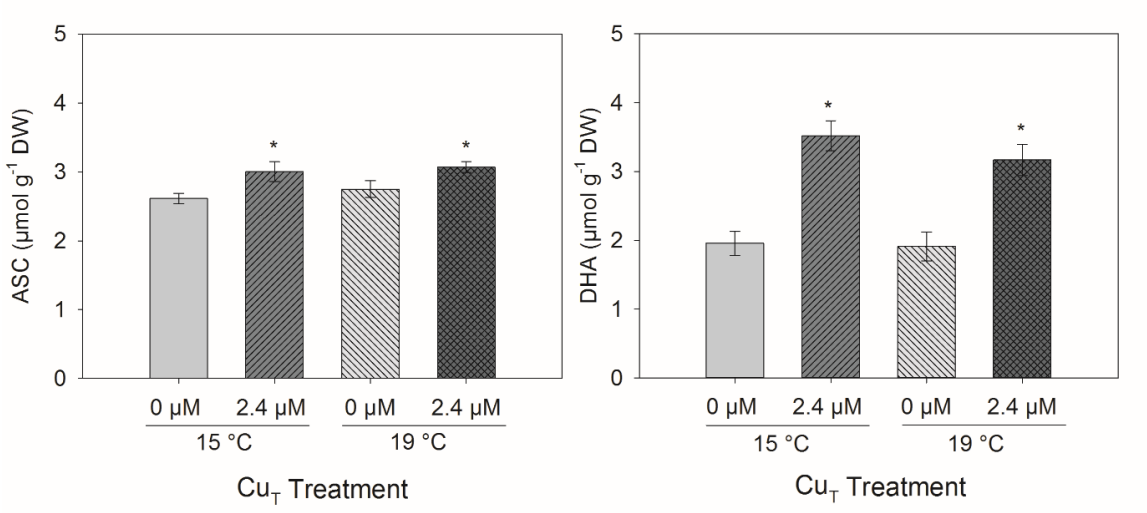

Figure 4.2. Concentrations of ascorbate (ASC) and dehydroascorbate (DHA) in *Ectocarpus siliculosus* exposed to a combination of two Cu concentrations (0 and 2.4 µM Cu_T) and two temperatures (15 °C and 19 °C) for 10 days. Single asterisks indicate main significant differences ($P < 0.05$) found after Tukey's test. Error bars represent ± 1 SD, $n = 3$.

In contrast, significant interactions were observed between Cu and temperature for GSH and GSSG ($P < 0.05$). For temperature within Cu concentrations, the response was different for GSH compared to GSSG. There was a significant reduction in GSH concentration at 19 °C compared to 15 °C at 0 µM Cu_T ($P < 0.05$), while GSSG concentrations increased significantly (Figure 4.3.) ($P < 0.05$). At 2.4 µM Cu_T, the response was the same for both GSH and GSSG concentration, i.e. there was a significant decrease at 19 °C, but the decrease (67.88 µmol GSH and 18.37 µmol GSSG) was smaller than the decrease at 15 °C (90.24 µmol GSH and 33.76 µmol GSSG). For Cu treatment within temperature there were significant reductions in GSH and GSSG ($P < 0.05$) under 2.4 µM Cu_T treatment at 15 and 19 °C. The ratio of inhibition (*RI)* values for these two variables were < 1, indicating an antagonistic interaction (Table 4.2.).

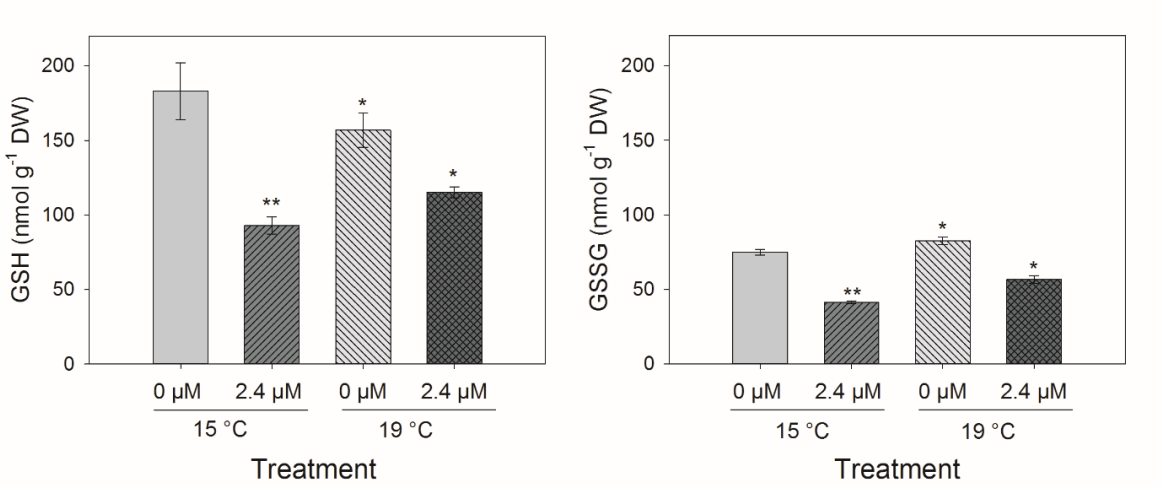

Figure 4.3. Concentrations of reduced (GSH) and oxidised (GSSG) glutathione in *Ectocarpus siliculosus* exposed to a combination of Cu concentrations (0 and 2.4 µM Cu_T) and temperatures (15 °C and 19 °C) for 10 days. Single asterisks indicate main significant differences ($P < 0.05$) found after Tukey's test. Double asterisks indicate a significant interaction between Cu and temperature. Error bars represent ± 1 SD, $n = 3$.

A significant interaction between Cu concentration and temperature was observed for concentrations of total intracellular phenolic compounds estimated with the Folin-Ciocalteu method ($P < 0.05$). For temperature within Cu controls a significant decrease was observed at 19 °C compared to 15 °C ($P < 0.05$), while no difference was observed between 15 and 19 °C under 2.4 µM Cu_T (Figure 4.4. a). For Cu within temperature a significant decrease was observed for 2.4 µM Cu_T at 15 °C ($P < 0.05$) and for 0 µM Cu_T at 19 °C ($P < 0.05$). Of all the individual methanol-soluble polyphenolic tested, only the flavonoid catechin could be identified. Both stress factors also affected the concentrations of catechin with significant differences for Cu, temperature and the interaction term ($P < 0.05$). For temperature within Cu concentration there was a significant decrease at 19 °C at both 0 and 2.4 µM Cu_T ($P < 0.05$) (Figure 4.4. b). Similarly, for Cu within temperature, concentrations of catechin were significantly lower than controls at 2.4 µM Cu_T in both temperatures. The concentrations of phenolic compounds released into the

experimental media were significantly higher at 2.4 μM Cu_T at both temperatures than under control conditions and there was a significant interaction between stress factors ($P < 0.05$). For temperature within Cu concentration, there was a significant increase at 19 °C compared to 15 °C for both 0 and 2.4 μM Cu_T ($P < 0.05$) (Figure 4.4. c). For Cu within temperature, there was a significant increase in phenolic release at 2.4 compared to 0 μM Cu_T at both 15 and 19 °C. The *RI* values were < 1 for intracellular and released phenolic compounds, indicating an antagonistic interaction between Cu and temperature (Table 4.2.). However, when total intracellular and released phenolic concentrations were analysed together a pattern similar to the production of TBARS was found (Figure 4.4 d), where a synergistic interaction between Cu and temperature ($P < 0.05$) could be observed.

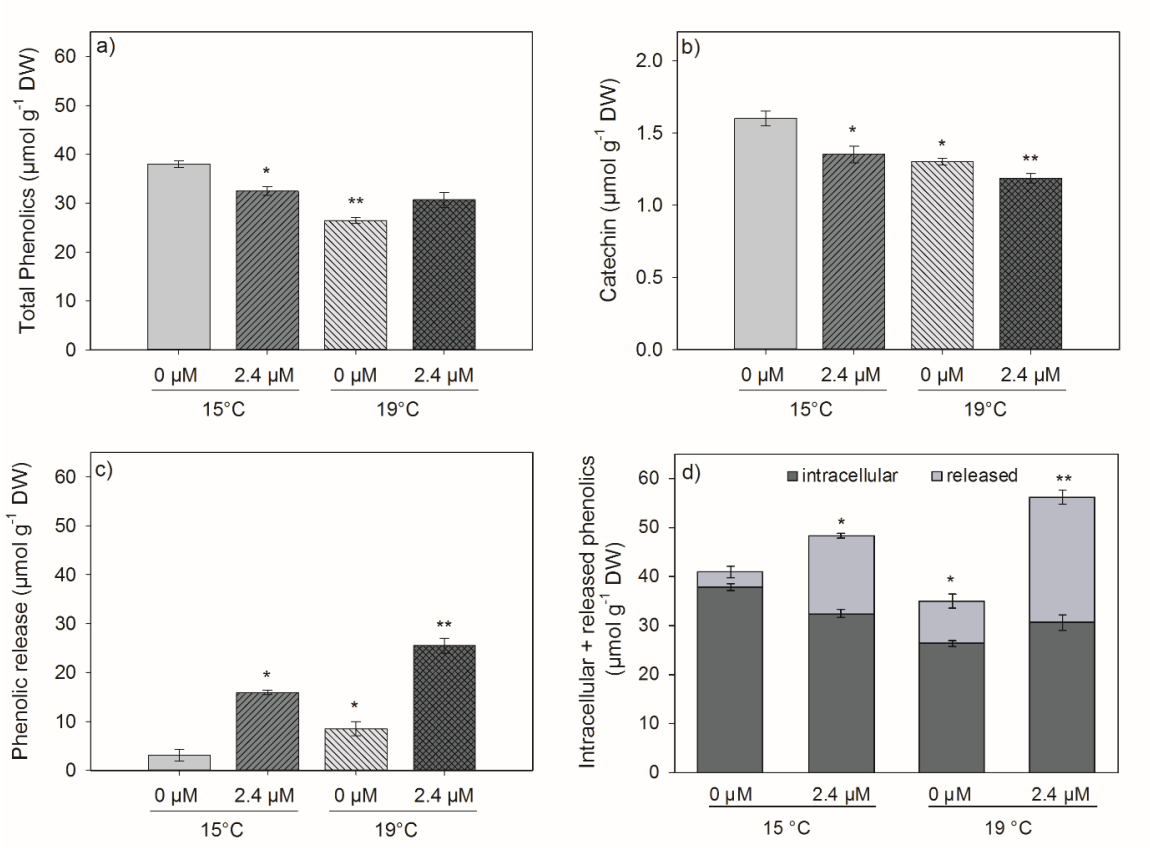

Figure 4.4. Concentrations of total intracellular (a) and released (c) phenolic compounds in *Ectocarpus siliculosus* exposed to a combination of Cu concentrations (0 and 2.4 µM Cu_T) and temperatures (15 °C and 19 °C) for 10 days. Concentrations of identified phenolic compounds: catechin (b) with the total concentration of intracellular + released phenolics (d) are also shown. Single asterisks indicate main significant differences ($P < 0.05$) found after Tukey's test. Double asterisks indicate a significant interaction between Cu and temperature. Error bars represent ± 1 SD, $n = 3$.

4.3.3. Antioxidant enzyme activities

For catalase (CAT) there were no significant differences for factors temperature ($P = 0.365$), Cu ($P = 0.146$) and interaction term ($P = 0.686$) (Figure 4.5. a). However, the activities of ascorbate peroxidase (APX), superoxide dismutase (SOD) and glutathione reductase (GR) were differentially affected by the applied treatments. Significant differences for Cu concentration, temperature and the interaction term were observed for APX activity ($P < 0.05$). APX activity significantly increased at 2.4 µM Cu_T at both temperatures ($P < 0.05$). However, the increase of APX activity at 19 °C was not as great as at 15 °C when exposed to Cu (Figure 4.5. b). No change in APX activity was observed under 0 µM Cu_T at both temperatures. The activity of SOD decreased significantly at the higher temperature (19°C) for controls and Cu exposure ($P < 0.05$), although no significant interaction with Cu was observed ($P = 0.346$) (Figure 4.5. c). On the other hand, a statistically significant interaction was observed in the activity of GR ($P < 0.05$). There was a decrease between 15 and 19 °C in the 0 µM Cu_T treatment to a level similar to that of 2.4 µM Cu_T at both temperatures (Figure 4.5. d). In fact, the *RI* values for APX and GR activity again were < 1 indicating antagonism between both stressors.

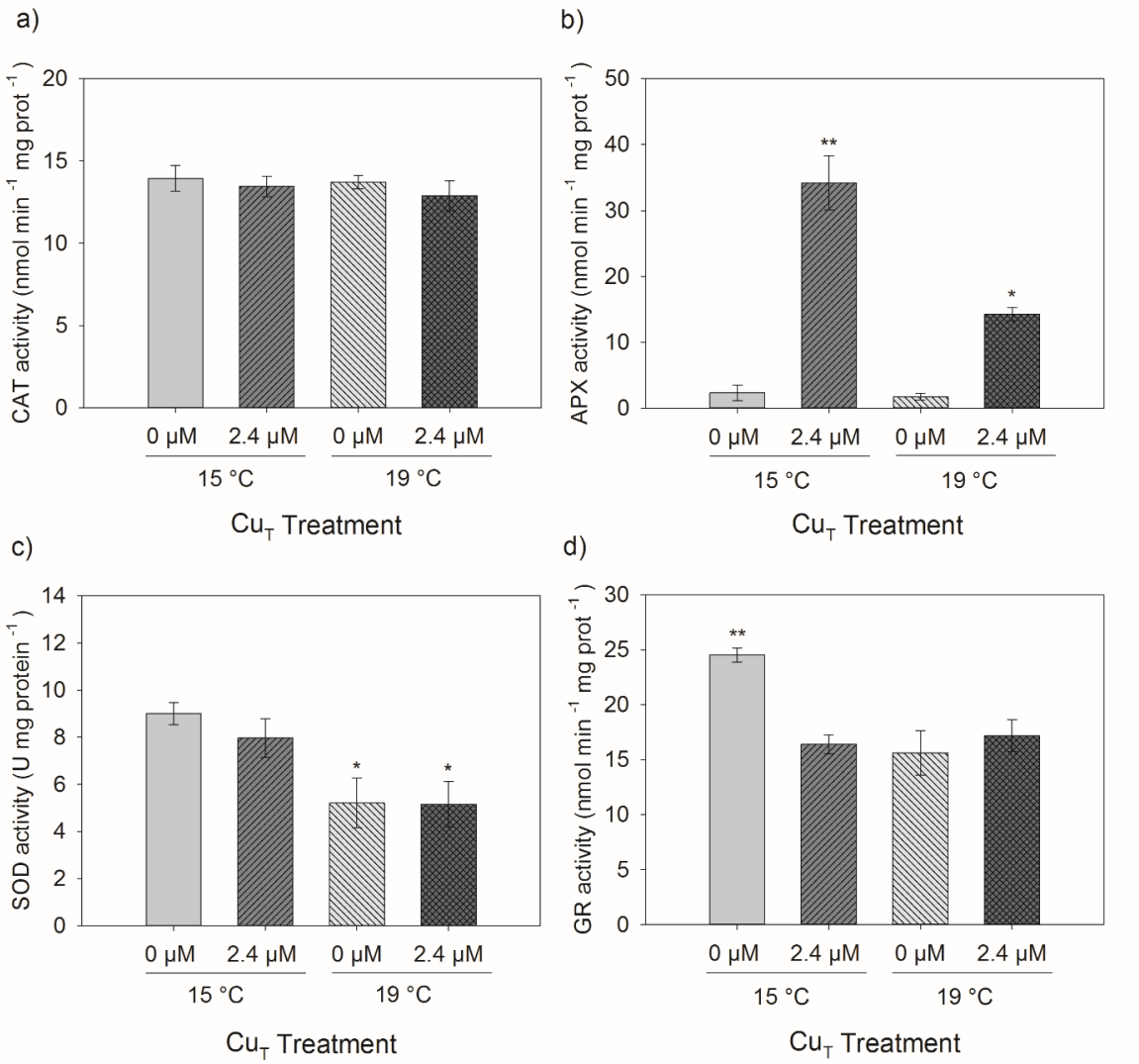

Figure 4.5. Activities of antioxidant enzymes in *Ectocarpus siliculosus* exposed to a combination of Cu concentrations (0 and 2.4 µM Cu_T) and temperatures (15 °C and 19 °C) for 10 days. a) catalase, b) ascorbate peroxidase, c) superoxide dismutase and d) glutathione reductase. Single asterisks indicate main significant differences ($P < 0.05$) found after Tukey's test. Double asterisks indicate a significant interaction between Cu and Temperature. Error bars represent ± 1 SD, $n = 3$.

4.3.4. Gene expression analysis by RT-qPCR

The expression of genes related to ROM in *E. siliculosus* was similar to the activity of the gene products (antioxidant enzymes). No differences were observed in the expression of catalase gene (*CAT*) for any treatment combination (Figure 4.6 a). However, significant interactions between factors Cu and temperature were observed for the expression of ascorbate peroxidase (*APX*), superoxide dismutase (*SOD*), monodehydroascorbate reductase (*MDHAR*) and metallothionein (*MET*) genes ($P < 0.05$). There was an increase in the expression of *APX* for 2.4 µM Cu_T at both temperatures ($P < 0.05$) (Figure 4.6 b). However, such increase was greater at 15 than 19 °C. No difference in expression was observed for Cu controls at both temperatures. A similar pattern was observed for *SOD*, but in this case there was also a significant decrease in expression at 19 °C for the 0 µM Cu_T treatment ($P < 0.05$) (Figure 4.6 c). The expression of *MDHAR* was significantly reduced at 2.4 µM Cu_T (15 °C) and also for Cu controls at 19 °C ($P < 0.05$). However, the reduced expression at 2.4 µM Cu_T and 19 °C was no greater than exposure to Cu at 15 °C or for controls at 19 °C (Figure 4.6 f). The expression of *MET* was significantly increased only for 2.4 µM Cu_T at 15 °C ($P < 0.05$) (Figure 4.6 h). No significant interaction between stress factors was observed in the expression of the genes for glutathione reductase (*GR*), glutathione synthase (*GS*) and heat shock protein 70 (*HSP70*). The expression of *GR* was significantly reduced by both increased Cu (2.4 µM Cu_T) and increased temperature (19 °C) ($P < 0.05$) (Figure 4.6 d). The reduction in expression under the combination of 2.4 µM Cu_T and 19 °C was not statistically different to that of exposure to 2.4 µM Cu_T at 15 °C. The response of *GS* showed a significant reduction in expression under 2.4 µM Cu_T at 15 °C compared to the other treatments ($P < 0.05$) (Figure 4.6 e). The expression of *HSP70* was significantly reduced only at 19 °C for both Cu treatments ($P < 0.05$) (Figure 4.6 g). Antagonism

between Cu and temperature in the expression of *APX*, *SOD, MDHAR* and *MET* was assumed as *IR* values were all < 1.

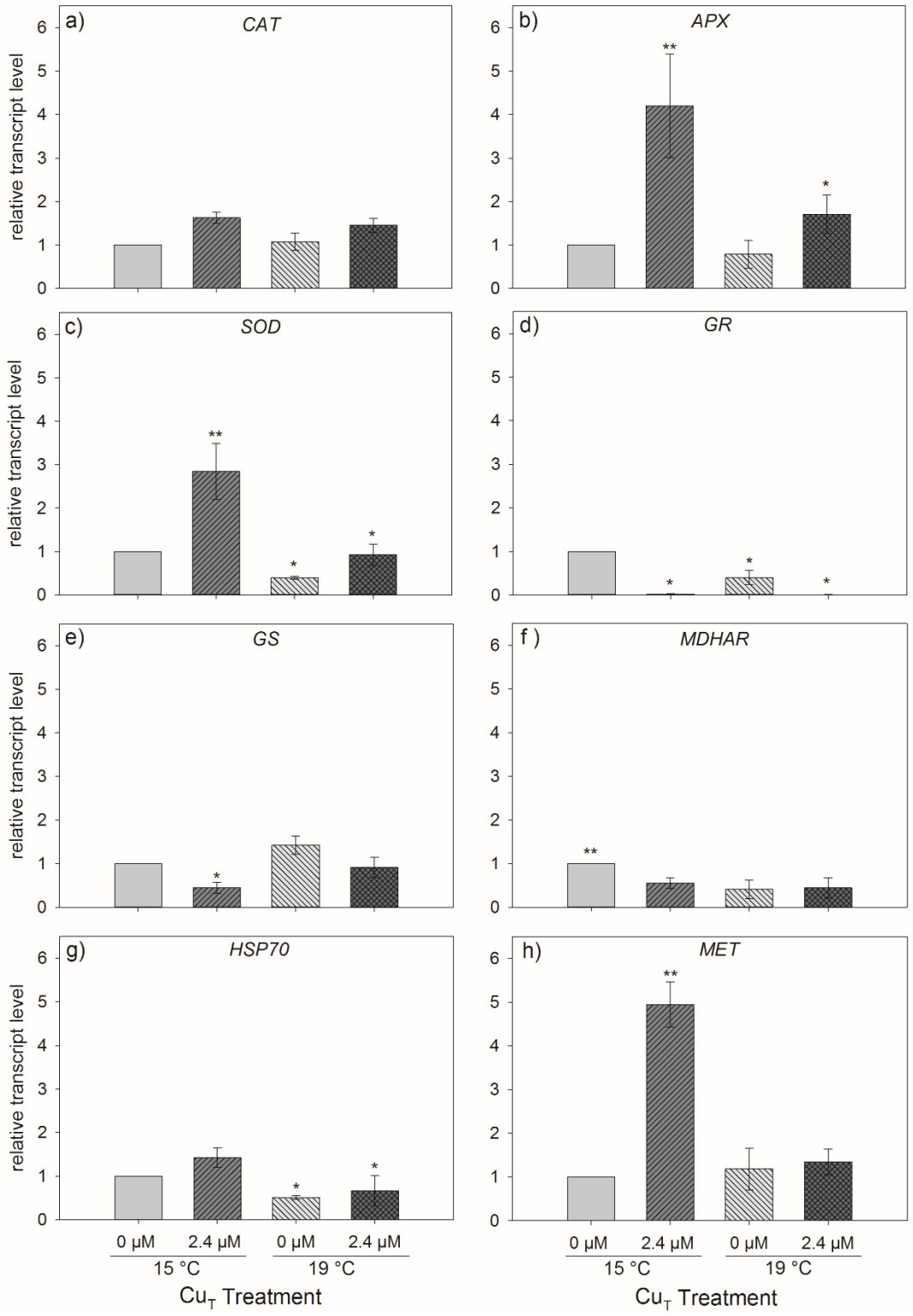

Figure 4.6. Pattern of expression of 8 genes: catalase (a), ascorbate peroxidase (b), superoxide dismutase (c), glutathione reductase (d) glutathione synthase (e), monodehydroascorbate reductase (f), heat shock protein 70 (g) and metallothionein (h) in *Ectocarpus siliculosus* exposed to a combination of Cu concentrations (0 and 2.4 µM Cu_T) and temperatures (15 °C and 19 °C) for 10 days. The expression was normalized to the expression of *ARP2* subunit of the actin-related protein complex ARP2/3, the housekeeping gene. Single asterisks indicate main significant differences ($P < 0.05$) found after Tukey's test. Double asterisks indicate a significant interaction between factor Cu and Temperature. Error bars represent ± 1 SD, $n = 3$.

4.4. Discussion

The results of this study demonstrate that Cu stress and elevated temperature do interact to affect the reactive oxygen metabolism (ROM) of the brown alga *E. siliculosus*. The increased concentrations of hydrogen peroxide and TBARS suggest that a combination of 2.4 µM of Cu_T and an increase of 4 °C can act synergistically to generate higher levels of ROS and consequently oxidative damage, e.g. lipid peroxidation (Figure 4.1). In contrast, an antagonistic interaction was observed for most parameters related to the antioxidant response and related gene expression (Table 4.1.). For example, the levels of the water-soluble antioxidant GSH were considerably lower under Cu compared to temperature treatment, but the reduction under the combined stress was not as low as expected from the sum of the individual stressors. This suggest that an increase of 4 degrees ameliorates the response of the algae to Cu stress. Three processes acting simultaneously could explain this: 1) temperature directly affects the enzymatic kinetics and exudation of chelating metabolites, 2) temperature directly alters the gene expression and translation of antioxidant and detoxifying enzymes, and 3) reactive oxygen species (ROS) generated by the combination of both stressors affect the gene expression and enzymatic activity.

In support of the first mechanism, our results show that algae exposed to 19 °C had a lower TBARS content (Figure 4.1, left) and lower total phenolic compounds (intracellular + released) (Figure 4.4 d); furthermore, no increase in H_2O_2 was observed. This suggest that an increase in 4 °C itself is does not induce and enhanced ROS production, but could increase the rates of several reactions such as membrane transport (Hochachka & Somero, 2002) and/or alter membrane fluidity (Los & Murata, 2004) and cell wall composition (Torres *et al*., 1991; Lima *et al*., 2013). This could directly affect metal uptake and resistance mechanism related to exclusion of Cu and chelation in the

cell wall and extracellularly (Gledhill *et al*., 1997; Connan and Stengel, 2011). The latter is in agreement with reduced intracellular and total Cu accumulation in algae exposed to both high temperatures and Cu concentrations observed in Chapter III. The increase in release of phenolic compounds from tissues into the media (at 19 °C) also lends support to this view (Figure 4.4 c). In contrast, the intracellular concentrations of phenolics were reduced under all stress treatments, which indicates an increased transport of compounds and exudation to the culture media. There is some evidence that the production of phenolics in algae is regulated by environmental factors including temperature (Connan *et al*., 2004; Kamiya *et al*., 2010; Rickert *et al*., 2016). For example, the phlorotannin concentrations of five perennial sargassacean species varied seasonally, showing a peak during July and August and gradually decreasing in the winter (Kamiya *et al.*, 2010). In addition, it has been observed that brown algae exposed to Cu are able to increase the phenolic content in cell walls, probably by mobilisation of storage vesicles called physodes (Schoenwaelder, 2002), and release them to the culture media (Connan & Stengel, 2011b). It was suggested that cell wall-bound and released phenolic compounds act as metal-chelating molecules playing a central role in metal tolerance of brown algae species. The results of the current study also show an increase in the released phenolic compounds in the 2.4 μM of Cu_T treatment (24.28 % ± 2.79 of the total: intracellular + released). Although temperature induced a decrease in the total production of phenolics (Figure 4.4 d), the concentrations were highest under the combination of Cu and temperature (45.4% ± 0.57 of the total), which indicates that exudation of phenolic compounds is an important mechanisms under Cu and temperature stress. Additionally the greater release of phenolics under a combination of temperature and Cu stress imply an active transport of Cu chelated intracellularly by phenolic compounds (Ragan *et al*., 1979; Gledhill *et al*., 1999). Thus, the antagonistic effect between temperature and Cu

could be explained with a higher exclusion and detoxification capacity of Cu ions due to and enhanced temperature- and Cu-induced phenolic production and release.

Temperature effects in organisms are universal, affecting every aspect from structure of macromolecules to biochemical reaction rates (Hochachka & Somero, 2002). Therefore, the second mechanism proposes that temperature affects several biochemical processes such as respiration, carbon fixation and ROM (Davison and Davison, 1987; Davison, 1987; Collén and Davison, 2001). In chloroplasts, the ascorbate-glutathione pathway is an important mechanism of ROS detoxification, which combines the reducing capacity of ascorbate and glutathione with the activity of several antioxidant enzymes (see Figure 4.7) (Asada, 1999; Foyer and Noctor, 2011). These enzymes have been observed to act differentially in algae exposed to Cu stress (Ratkevicius *et al*., 2003; Contreras *et al*., 2009; Sáez *et al*., 2015c; Moenne *et al*., 2016). For example, in *Ulva compressa* collected from Cu-polluted sites the activities of APX were increased compared to individuals collected from pristine sites (Ratkevicius *et al.*, 2003). However, the activities of catalase (CAT), glutathione peroxidase (GP), dehydroascorbate reductase (DHAR) and glutathione reductase (GR) did not increase and the latter even decreased in individuals collected from the Cu-polluted location Palito (north of Chile). These results are similar to those in the present study on *E. siliculosus* strain Es524, which was also isolated from Palito, where a significant increase in APX and a decrease in GR activities occurred in Cu-exposed samples (Figure 4.5, b and d). Similarly, CAT activity was not affected by exposure to Cu (Figure 4.5 a). In contrast, the results from a recent study on Es524 showed increased activities of CAT, APX and SOD under Cu stress (Sáez *et al.*, 2015c). A possible explanation for this difference is that in those studies a chemically defined artificial seawater medium (AQUIL) was used for the Cu exposure experiments. In the present study, the use of natural seawater could have affected the bioavailability of Cu as dissolved organic matter (DOM) is present in natural seawater and could have

complexed Cu ions (Gledhill *et al.*, 1997). Additionally, it is likely that changes in temperature and pH could have altered the speciation of dissolved Cu (Byrne *et al.*, 1988). While no increase of ROS was observed in the 19 °C treatment, the activities of SOD and GR were reduced. This also occurred in the brown seaweed *Fucus vesiculosus* grown in the laboratory at 20 °C compared to 0 °C and also in samples collected in summer and winter, where activities of antioxidant enzymes were lower at high temperatures and in summer (Collén & Davison, 2001). This indicates that the role of ROS is more important under cold than heat stress. However, this can also indicate that gene expression or translation processes are differentially affected by temperatures as some discrepancies were observed between enzymes. The combined effect of Cu and temperature showed an increase in APX activity; however, the increase was not as high as for exposure to Cu at 15 °C. This same pattern was observed in the expression of *APX* gene, indicating again an antagonistic interaction between Cu exposure and temperature. Antagonism in gene expression and in-vitro activity of enzymes is probably due to the apparent inhibitory effect of temperature on the gene expression of some antioxidant enzymes, which may be controlled by temperature-sensitive transcription factors. For example, Collén *et al*. (2007) found that some transcription factor genes such as a zinc-finger and helicases were regulated by high temperatures in *Chondrus crispus*. This may also explain the discrepancies between the gene expression patterns of *GR* and *SOD* with the in-vitro measurements of enzymatic activities.

The proposed third mechanism is the result of a combination of the first two. Beyond certain thresholds Cu can increase the production of ROS, antioxidants and activate antioxidant enzymes as can thermal stress (Collén and Davison, 1999a; Wu *et al*., 2009). Besides their role as highly toxic reactive oxidants, at low concentrations ROS act also as signalling molecules that can regulate gene expression through signal transduction cascades or modification of transcription factors (Apel and Hirt, 2004;

Desikan *et al*., 2005). Therefore, the accumulation of ROS by Cu exposure can be boosted by a suppression of antioxidant enzyme gene expression and activity due to temperature increase. This in turn can further regulate gene expression in unexpected ways. For example, in the present study the increased expression of *APX* and *SOD* under the combined action of Cu and temperature was not as great as the increase under Cu alone. Additionally, the expression levels of *SOD*, *GR*, *MDHAR* and *HSP70* were reduced at 19 °C. This could be an indication of a direct inhibitory effect of temperature on the expression of those genes. Thus, under a combination of Cu and temperature the effects of both stressors might tend to cancel (see results and discussion sections in Chapter V). Although a comparable effect on the photosynthetic response was observed (Nielsen *et al.*, 2014), this should be further tested by applying the thermal stress after acclimating the samples to Cu stress and *vice versa*. The greater accumulation of ROS and TBARS under the combination of stressors may also be the result of inactivation of detoxifying enzymes by H_2O_2 (Uchida and Kawakishi, 1994; Shibata *et al*., 2014). This could explain the reduction in concentrations of GSH. For example, in the ascorbate-glutathione pathway in the chloroplast (see Figure 4.7) the concentrations of GSH and GSSG are dependent of DHAR and GR activity (Foyer and Noctor, 2011; Noctor *et al*., 2012). Although the activity of DHAR was not evaluated, the activity of GR was reduced and also the *GR* gene expression. The concentrations of GSH and GSSG are not always in agreement with other components of the ascorbate-glutathione pathway (Collén and Davison, 2001; Contreras *et al*., 2009). This is probably due to the use of GSH use in other processes such as the production of phytochelatins in response to Cu stress (Cobbett and Goldsbrough, 2002; Roncarati *et al*., 2015); or due to the down-regulation of genes involved in the GHS synthesis pathway such as *glyoxalaseI* and *glyoxalaseII* (Yadav, 2010). However, the gene for glutathione synthase (*GS*) was not affected by the combined stress (Figure 4.6). On the other hand, the concentrations of ASC, and particularly of

DHA, were confirmed by our results to be effective indicators of Cu stress (Ratkevicius *et al.*, 2003) but not of thermal stress (Figure 4.2).

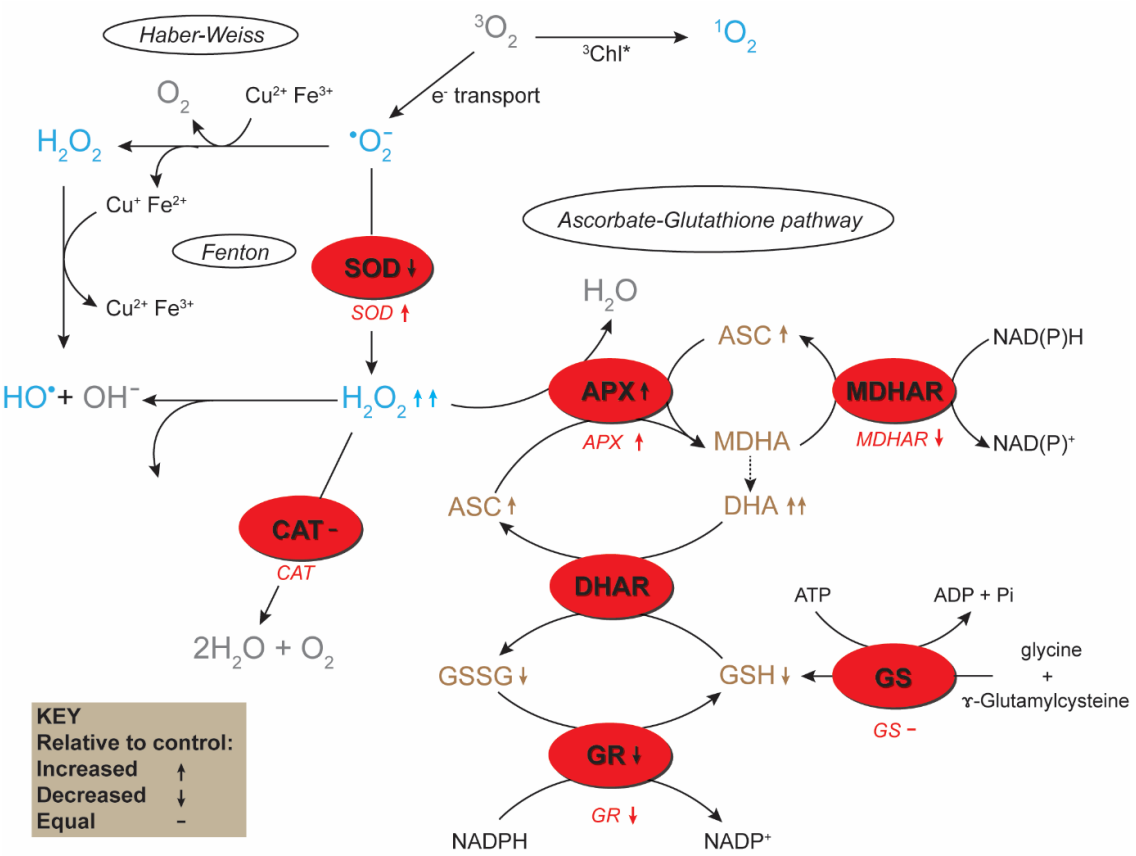

Figure 4.7. Schematic representation of the effects of a combination of 2.4 µM Cu_T and 19 °C in the ROM of *E. siliculosus* after 10 days of exposure.

Although the three mechanisms discussed above partially explain the observed interactions, other routes and processes could be involved. For example, the expression of *MET* would favour the first mechanism because it was only up-regulated by Cu exposure but not under the combination of Cu and thermal stress. This supports the idea of an enhanced exclusion mechanism under combined stress. However, accumulation of ROS suggests that photosynthetic and/or respiratory electron transfer chains continued to produce ROS under Cu stress, but temperature decreased expression of antioxidant enzymes genes (e.g. *MDHAR* and *GR*), which would impair the antioxidant scavenging system in chloroplasts (Figure 4.7). In other cellular compartments, other mechanisms

such as the Haber-Weiss and Fenton-like reactions may account for the accumulation of ROS due to increased Cu in chronic exposure experiments (Dring, 2005; Halliwell, 2006). Alternatively, the high presence of H_2O_2 could also be the result of diffusion from the culture media (Knauert & Knauer, 2008) due to exogenous production of ROS by Cu and other compounds released in the media. However, this hypothesis requires further testing.

4.5. Conclusions

The complex interactions between copper and thermal stress were confirmed by the results of the present study. As seen in Figure 4.7, activities of antioxidant enzymes occurring in different cellular compartments have a different behaviour when exposed to a combination of stressors. This is likely caused by the direct effect of temperature on enzymatic kinetics or alternatively by their inactivation due to the high levels of ROS. Additionally, discrepancies between gene expression and activities of enzymes, such as SOD, is indicative of uncoupling between transcription and translation. Also the concentrations of water soluble antioxidants were variable, with ascorbate being the only antioxidant that increased under Cu-only and the combined stress, but not under thermal stress. We conclude that some enzymes and antioxidants are perhaps more important than others in the response to metal stress (Collén and Davison, 2001; Contreras *et al*., 2009; Sáez *et al*., 2015c) and that interaction with thermal stress could create disturbances in the intracellular milieu having multiple effects on different levels. Additional research using new approaches and technologies are needed to untangle the complexity of interactions between multiple stressors.

Chapter V

A transcriptomic approach to evaluate interactions between Cu and thermal stress in *Ectocarpus siliculosus*

5.1. Introduction

Brown algae are an essential group of organisms inhabiting coastal ecosystems worldwide. Because of their sessile nature, they are exposed to natural abiotic stresses such as high and low irradiances, desiccation, thermal fluctuations and mechanical stress, as well as anthropogenic-derived stresses such as chemical pollution (Davison and Pearson, 1996; Dring, 2005; Dittami *et al*., 2011; Rautenberger *et al*., 2015). While the impacts of metal pollution affect brown algae on a local scale, there is a growing concern on the potential interactions between pollutants and abiotic pressures resulting from global climate change (Russell *et al*., 2009; Horta *et al*., 2012). Many ecophysiological studies have addressed the growth and photosynthetic responses of brown algae to abiotic factors such as temperature variation (Davison, 1987; Gómez *et al*., 2009; Andersen *et al*., 2013; Jueterbock *et al*., 2014; Graiff *et al*., 2015). On the other hand, some biochemical mechanisms, such as the production of intracellular metal chelators, reactive oxygen species and antioxidants, have been proposed to be involved in metal stress and tolerance response (Roncarati *et al*., 2015; Sáez *et al*., 2015). However, information on combinations of stressors and the response of brown algae at the transcriptomic level is still scarce.

With the sequencing of the relatively small genome of *Ectocarpus siliculosus* (200 Mbp), new genomic resources have been developed, allowing the in-depth study of mechanisms of stress and tolerance (Dittami *et al*., 2009; Cock *et al*., 2010). For example, global expression studies using microarrays in *E. siliculosus* have shown that abiotic stress such as hypo- and hypersalinity, and oxidative stress generate a wide reprogramming of the transcriptome (Dittami *et al.*, 2009). From a meta-analysis based on those expression experiments and Cu-stress transcriptomics, it was shown that there is an overlap between the responses of *E. siliculosus* exposed to acute Cu stress and

oxidative stress induced by addition of H_2O_2 to growth media (Ritter *et al.*, 2014). In addition, several putative genes for chlorophyll binding and light harvesting complex proteins, antioxidant enzymes and transporters were regulated by acute Cu and H_2O_2 stress (Dittami *et al.*, 2010). With the arrival of next-generation deep-sequencing technologies such as Illumina or Roche 454 pyrosequencing, a more precise method for both mapping and quantifying transcriptomes has been developed. This method is called RNA-seq (RNA sequencing) and provides several advantages over traditional technologies such as microarrays or SAGE (Wang *et al.*, 2009). Consequently, there is a growing number of RNA-seq studies on the responses of brown algae to environmental stressors (Wang *et al*., 2013; Liu *et al*., 2014a; Liu *et al*., 2015; Kumar *et al*., 2017). For example, RNA-seq data highlighted the complex response of kelp, *Saccharina japonica*, to thermal stress, and also the identification of several putative genes as potential markers of thermal stress, such as several heat-shock, antioxidant and transporter proteins among others (Liu *et al.*, 2014b).

Despite the advances in understanding whole-transcriptome responses to Cu stress and other abiotic factors independently, few such studies have assessed the interactions between metals and other environmental stressors in algae. Some information has been generated in the kelp *Saccharina latissima*, where interactions between light and temperature stress have been tested using microarrays (Heinrich *et al.*, 2012). A combination of high irradiance and high temperature induced a higher regulation of photosynthetic components and stress-related genes, suggesting that the interactive effects are harmful for the alga. In the present study, we investigated the effects of single and combined exposure of the model brown alga *E. siliculosus* to chronic copper excess and increased temperature. Previous studies in *E. siliculosus* have assessed the acute response of this species to Cu stress and other abiotic stresses, often using unrealistic levels of the stress factors. We used a strain (Es524) that has long-term laboratory

acclimation at 15 °C and exposed it to an increase of 4 °C in temperature, according to the predictions of ocean warming for the next 80 years (IPCC, 2014; Laffoley and Baxter, 2016). A sub-lethal Cu concentration of 2.4 μM Cu_T (or 150 μg L^{-1}), as previously determined (Roncarati *et al*., 2015; Sáez *et al*., 2015), was used as the increased Cu treatment. The growth, photosynthetic and transcriptomic responses to treatments were assessed at the end of a 10 day period of exposure.

5.2. Materials and methods

5.2.1. Experimental design and culture conditions

Filaments of *E. siliculosus* strain Es524 to be used in experiments were obtained from axenic cultures as described in Section 2.1.3. Once enough biomass was produced, 500 mg of fresh weight (FW) of filaments were transferred to individual polycarbonate flask containing 125 mL of sterile natural seawater (NSW) and maintained for two days at 15 °C under a light/dark cycle of 14/10 hours at an irradiance of 40-50 μmol photons m^{-2} s^{-1}. After this period, samples were exposed in triplicates to experimental treatments, which consisted of combinations of two Cu concentrations and two temperatures as follow: '0 μM Cu_T and 15 °C' (control), '2.4 μM Cu_T and 15 °C' (Cu-only), '0 μM Cu_T and 19'(temperature-only) and 2.4 μM Cu_T and 19 °C' (combined). Material was exposed to the treatments for 10 days to allow comparison with previous studies of chronic exposure to Cu in *E. siliculosus* (Roncarati *et al*., 2015; Sáez *et al*., 2015c). Experimental media were replaced every 2 days.

5.2.2. Growth rate

To assess growth rates, clumps of *ca*. 30 mg FW biomass were exposed for 10 days to combinations of temperature and Cu according to the treatments described above. Relative growth rates (RGR) were estimated volumetrically by using the method

described by (Dring, 1967; See Section 2.3.1 for details). Differences in RGR were analysed using two-way ANOVA for factors 'Cu concentration' (two levels: 0 and 2.4 µM Cu_T) and 'temperature' (two levels: 15 and 19 °C). Differences between treatments were detected using Tukey's *post-hoc* tests.

5.2.3. Photosynthetic physiology

Photosynthetic performance was estimated via clorophyll *a* fluorescence. The Rapid Light Curve (RLC) method (White and Critchley, 1999; Ralph and Gademann, 2005) described in Section 2.3.3 was used to measure and calculate several photosynthetic parameters with a MINI-PAM Photosynthesis Yield Analyzer (Walz, Germany). The algal filaments used to assess growth were used to generate the RLCs. To ensure the same dark adaptation of all samples, pre-dawn measurements were performed. Filaments were transferred to a 'dark leaf' clip (DLC8, Walz) 5 minutes before each measuring. The DLC8-clip permits to keep an equal distance (5 mm) between the fibre optics of the instrument and the sample. The MINI-PAM was operated remotely with the WinControl (Version 2.0, WALZ) software. The first saturating light pulse (SP; >10000 µmol photons m^{-2} s^{-1}) of the RLC was on dark-adapted samples, allowing the determination of basal (F_o) and maximal fluorescence (F_m). These parameters were then used to calculate the maximum quantum yield (F_v/F_m), where $F_v = F_m - F_o$ (Schreiber *et al.*, 1995). Following the first SP, the halogen lamp automatically turned on to incubate the samples for 20 s at the first (E_1) of eight increasing irradiances levels (E_1 = 25, E_2 = 76, E_3 = 157, E_4 = 260, E_5 = 385, E_6 = 532, E_7 = 790 and E_8 = 1076 µmol photons m^{-2} s^{-1}). A SP was applied after incubation at each irradiance level to determine the basal (F) and maximal fluorescence (F_m') in the light-adapted state. These parameters allowed for the calculation of the effective quantum yield (Y) of light adapted samples after incubation at each irradiance level with the formula: $Y= (F_m'- F)/F_m'$.

Electron transport rate (ETR) at each irradiance level of RLC was calculated according to the formula: $ETR = Y \times E_i \times A \times 0.8$ (Figueroa *et al*., 2014; Celis-Plá *et al*., 2014; Beer *et al*., 2014), where Y is the effective quantum yield in the light-adapted state, E_i is the incident irradiance (μmol photons m^{-2} s^{-1}), A is the absorptance of the sampled algae (Figueroa *et al.*, 2014) and 0.8 is the fraction of photons absorbed by PSII in brown algae (Celis-Plá *et al.*, 2014a). ETR data were plotted against incident irradiance and the resulting curve was fitted to the model described by Eilers and Peeters (1988). From fitted curves, the maximum electron transport rate (ETR_{max}) and the efficiency of light capture for photosynthesis (α) were obtained as estimators of photosynthetic efficiency. Minimum saturating irradiance (E_k) was calculated from the intercept between ETR_{max} and α (Ralph & Gademann, 2005). Non-photochemical quenching (NPQ) was calculated as $NPQ = (F_m - F_m')/F_m'$ after each irradiance level. Similar to ETR data, a curve of NPQ vs. irradiance was generated and fitted in order to obtain the maximum non-photochemical quenching (NPQ_{max}). Differences between photosynthetic parameters were analysed by two-way ANOVA for the same factors specified in for RGR and Tukey's post-hoc tests used to identify the differences between treatments.

5.2.4. RNA-seq analysis

To avoid degradation of RNA, all materials used in RNA extraction and purification were incubated overnight in diethylprocarbonate (DEPC) and then autoclaved. All plastic consumables were RNAse-free certified. Frozen biomass (300 mg) was pulverised with the aid of liquid nitrogen in a pre-cooled mortar to obtain a fine powder. The powder was mixed with the extraction buffer of an E.Z.N.A.® Total RNA Kit I (Omega Bio-Tek) and subsequent steps were followed according to the manufacturer's instructions. Between 5 and 15 μg of extracted RNA were treated with 10 U of DNase I (Promega) to remove DNA traces. Samples were cleaned using a GeneJET

RNA Cleanup and Concentration Micro Kit (Thermo Scientific). Confirmation on RNA integrity was done using a bioanalyser (Agilent 2100). Libraries for RNA-seq were constructed using a TRuSeq RNA Sample Prep Kit v2 (Illumina) in duplicate for each treatment. Total RNA (1 μg) was used for mRNA enrichment using mRNA purification magnetic beads. Enriched mRNA was eluted and fragmented at 94 °C for 5 min. RT-PCR was used to obtain double-stranded cDNA from the previously fragmented mRNA, followed by end repair, single A base addition and adapter index ligation. The ligation product was amplified by PCR, obtaining a final product size of *ca.* 260 bp. Paired end RNA sequencing with an average insert size of 145 bp was conducted on a HiSeq 4000 high-throughput sequencing system (Illumina) at Beijing Genomics Institute (BGI) in a single lane for all the treatments. Eight libraries were sequenced and read length was 100 bp.

Obtained RNA-seq reads without adaptors were assessed for quality using FastQC (Andrews, 2010) ran in standard mode, phred score 33+. High quality reads were determined as 'per base sequence quality' above Q30 but tails above Q20, no kmer overrepresenttion found, GC percentage distribution was as expected so no further processing was performed. Reads were aligned to the latest version (V2) of the *E. siliculosus* genome (https://bioinformatics.psb.ugent.be/gdb/ectocarpusV2/) using BBMap version 36.84 (Bushnell, 2014). Alignments were then processed and gene counts were obtained utilizing featureCounts version 1.5.0-p3 (Liao *et al*., 2014), command: "featureCounts" "-a" "all_gtf.gtf" (STANDARD SETTINGS) -requireBothEndsMapped -minFragLength 50 -minFragLength 600 using the latest annotation of the *E. siliculosus* genome (15/03/2017). Differential expression analysis was performed with DESeq2 *R* package version 1.14.1 using the Wald test (Love *et al.*, 2014). The gene expression levels of 'increased copper' (2.4 μM Cu_T), 'increased temperature' (19 °C) and the 'combined treatments' (2.4 μM Cu_T + 19 °C) were compared to the expression of the control

treatment (0 μM Cu_T at 15 °C) using the default generalised linear model for comparison between control and treated samples. *P*-values were adjusted utilizing the default Benjamin–Hochberg correction (Benjamini & Hochberg, 1995). Genes showing an adjusted *P*-value < 0.05 were assigned as differentially expressed.

5.2.5. GO enrichment analysis

A gene ontology (GO) list was obtained from the *E. siliculosus* genome project (https://bioinformatics.psb.ugent.be/gdb/ectocarpusV2/). GO enrichment analysis of the differentially expressed genes (DEGs) was implemented using the GOseq R package (Young *et al.*, 2010) and found which GO terms are over-represented (or under-represented) using annotations for that gene set. The criteria for the calculation of *P*-values for over- and under-represented GO terms is detailed in Young *et al*. (2010). The results were visualized using the REVIGO web tool (Supek *et al.*, 2011), which summarizes long lists of GO terms, removes redundant terms and visualizes them in semantic similarity-based scatterplots.

5.3. Results

5.3.1. Growth rate

Significant differences were found for Cu concentration ($P < 0.05$) but not for temperature ($P = 0.869$) and the interaction term ($P = 0.109$). A significant decrease in RGR at 2.4 µM Cu_T treatments was identified following application of the Tukey's *post-hoc* test ($P < 0.05$; Figure 5.1).

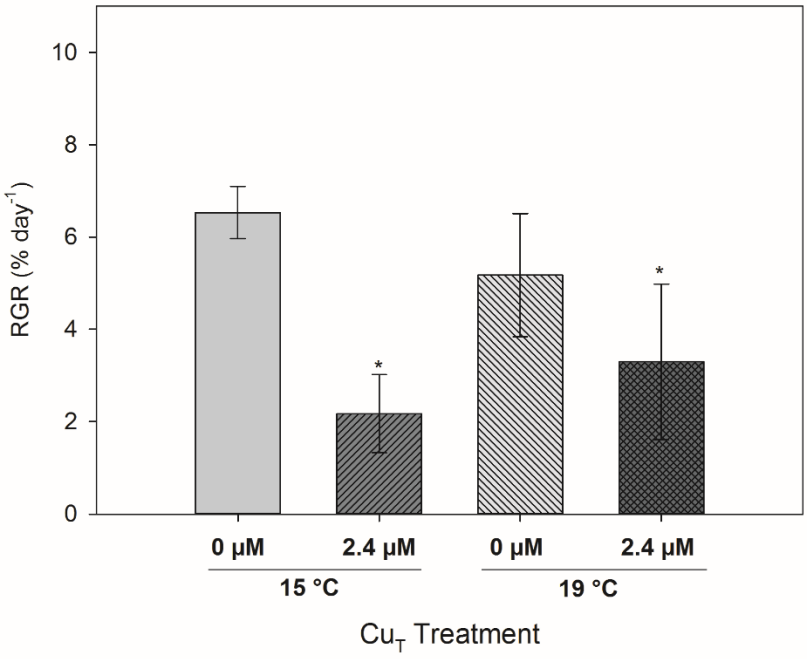

Figure 5.1. Relative growth rate of *Ectocarpus siliculosus* exposed to a combination of Cu concentrations (0 and 2.4 µM Cu_T) and two temperatures (15 °C and 19 °C) for 10 days. Asterisks indicate main significant differences ($P < 0.05$) found after Tukey's test. Error bars represent ± 1 SD, $n = 3$.

5.3.2. Photosynthetic parameters

As described in Section 2.3.2, chlorophyll *a* fluorescence is a powerful tool for the assessment of mechanisms of stress in photosynthetic organisms. There was a significant interaction between Cu and temperature for the maximum quantum yield of PSII (F_v/F_m) ($P < 0.05$). The treatment of 2.4 μM Cu_T caused a greater reduction in F_v/F_m at 15 °C than 19 °C and this reduction was also significantly different from control (0 μM Cu_T) at 15 °C ($P < 0.05$; Figure 5.2 a). Although the pattern of α was similar to that for F_v/F_m, there was no significant interaction between Cu concentration and temperature ($P = 0.103$). A significant reduction was only observed for temperature at 15 °C for treatment 2.4 μM Cu_T ($P < 0.05$; Figure 5.2 b). No significant differences were observed between treatments for the ETR_{max} and E_k parameters (Figure 5.2 c, d). NPQ_{max} showed significant reductions at 19 °C for both 0 and 2.4 μM Cu_T ($P < 0.05$; Figure 5.2 e), but there was no significant interaction between these stress factors.

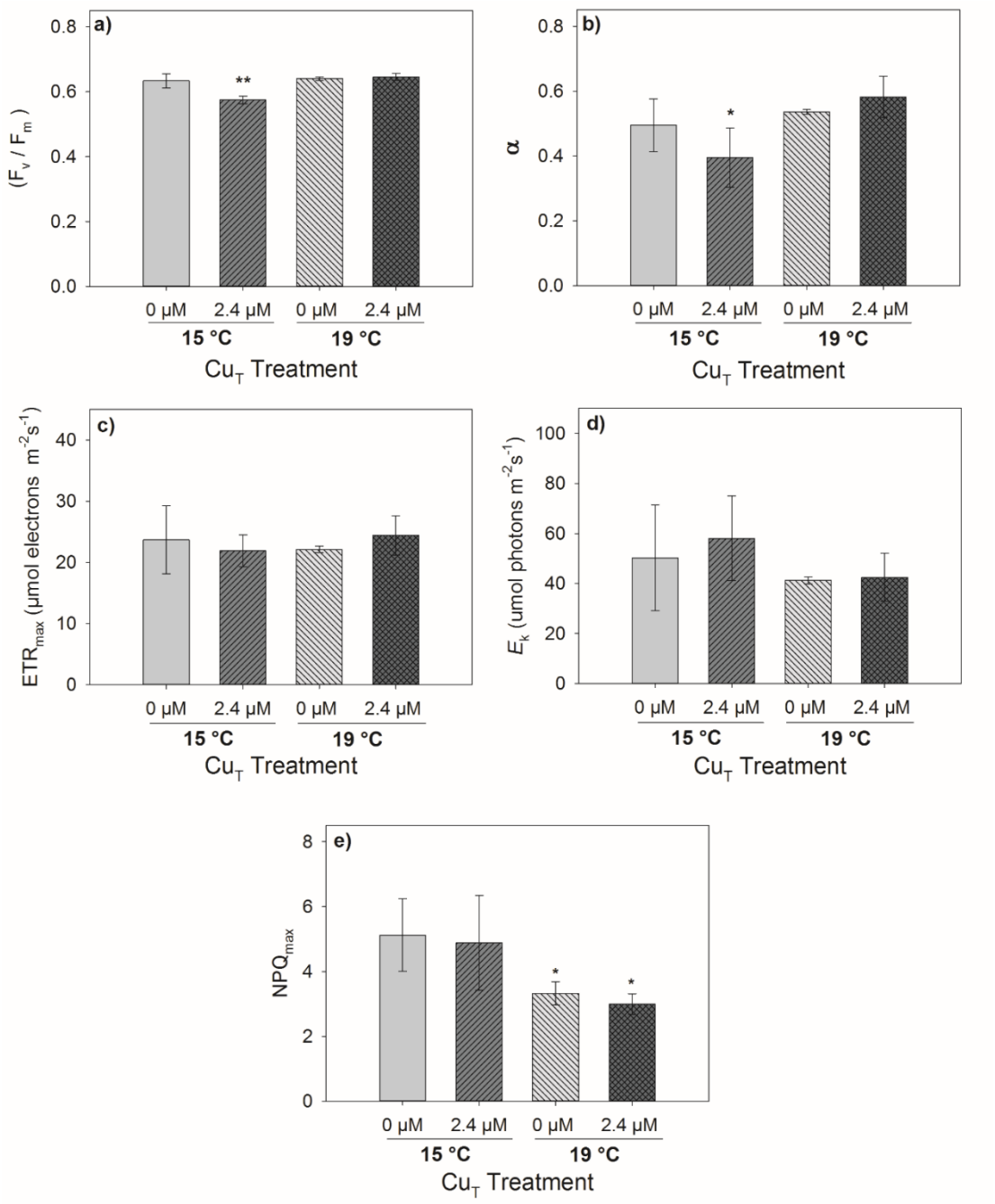

Figure 5.2. Photosynthetic parameters obtained with the rapid light curve method (RLC) in *Ectocarpus siliculosus* exposed to a combination of Cu concentrations (0 and 2.4 µM Cu_T) and two temperatures (15 °C and 19 °C) for 10 days. Asterisks indicate main significant differences ($P < 0.05$) found after Tukey test. Error bars indicate ± 1 SD, $n = 3$. (a) F_v/F_m: maximum quantum yield, (b) α: light capture efficiency, (c) ETR_{max}: maximum electron transport rate, (d) E_k: minimum saturating irradiance.

5.3.3. RNA-seq

The total number of reads obtained after high-throughput sequencing is reported in Table 5.1 for each sample. The percentage of mapped reads ranged from 79.9 to 88.5% and the percentage of quantified reads from 57 to 63.3%.

Table 5.1. Details of reads obtained and mapped per sample after pair-end HiSeq 4000 sequencing and FastQC quality control (Phred score 33+). All reads annotated and quantified were used for DE analysis (except genes showing 0 counts in all samples).

Sample	Total reads after QC	% of reads mapped with 'BBmap'	% of reads quantified by 'featureCounts' annotated to genome
0 μM Cu_T (15 °C)-1	45055490	85.6	63.3
0 μM Cu_T (15 °C)-2	17677572	85.5	61.0
2.4 μM Cu_T (15 °C)-1	18941216	83.8	59.2
2.4 μM Cu_T (15 °C)-2	12800486	83.3	57.5
0 μM Cu_T (19 °C)-1	18953728	88.5	57.8
0 μM Cu_T (19 °C)-2	14700212	80.7	57.4
2.4 μM Cu_T (19 °C)-1	17894912	84.0	60.0
2.4 μM Cu_T (19 °C)-2	15870576	79.9	57.0

5.3.3.1. Cu-induced gene regulation

Results of differential expression analysis are summarised in Figure 5.3. Venn diagrams were obtained with the online tool Venny 2.1 (http://bioinfogp.cnb.csic.es/tools/venny/). Copper treatment (2.4 μM Cu_T) at 15 °C resulted in 201 significantly regulated genes (Figure 5.3, purple circle left and right), of which 81 were up-regulated compared to control conditions (0 μM Cu_T at 15 °C) and 120 were down-regulated (*P*-adjusted < 0.05) (See appendices, Table S5.1.). Only one up-

regulated gene (Ec-14_002150), encoding for a hypothetical protein, and no down-regulated genes were shared between the Cu-only and temperature-only stress treatments. Conversely, 25 up-regulated genes and 15 down-regulated genes were shared between the Cu-only treatment (2.4 μM Cu_T at 15 °C) and the combined treatment (Table S5.1.).

5.3.3.2. Temperature induced gene regulation

The temperature-only treatment (0 μM Cu_T at 19 °C) resulted in the differential expression of 102 genes, 60 of which were up-regulated and 42 down-regulated (*P*-adjusted < 0.05; Figure 5.3, yellow circles) (Table S5.2.). Most of the up-regulated (35) and down-regulated (25) genes were shared with the combined treatment (2.4 μM Cu_T at 19 °C). Only 12 up- and 15 down-regulated genes were exclusively regulated by increased temperature (Table S5.2.).

5.3.3.3. Cu and temperature-induced gene regulation

Exposure to the combination of both increased Cu and temperature (2.4 μM Cu_T at 19 °C) resulted in the regulation of 349 genes, 259 were up-regulated and 90 down-regulated, compared to the control treatment (*P*-adjusted < 0.05) (Figure 5.3, green circles; Table S5.3). Eighteen genes were differentially expressed under all the treatments, 12 up-regulated and 2 down-regulated (See Figure 5.3, intersection of all treatments; Table 5.2. upper and middle part). Additionally, 4 genes (a copper transporter protein [Ec-13_001170], two trans-membrane ferric reductases [Ec-07_007480, Ec-18_002770] and a hypothetical protein [Ec-00_003170]) were down-regulated under Cu-only stress (2.4 μM Cu_T at 15 °C), up-regulated under temperature-only stress (0 μM Cu_T at 19 °C) and down-regulated by the combination of Cu and temperature (Table 5.2 lower part). Finally, in two additional genes (a putative carbohydrate-binding protein [Ec-00_007780] and an aminotransferase [Ec-25_002750]) their regulation swapped

between the Cu-only exposure (2.4 µM Cu_T at 15 °C) and the combined exposure to Cu and temperature (2.4 µM Cu_T at 19 °C). The former was down-regulated under the Cu-only treatment but up-regulated under the combined treatment while the latter showed the opposite expression pattern (Table S5.1. and S5.3.).

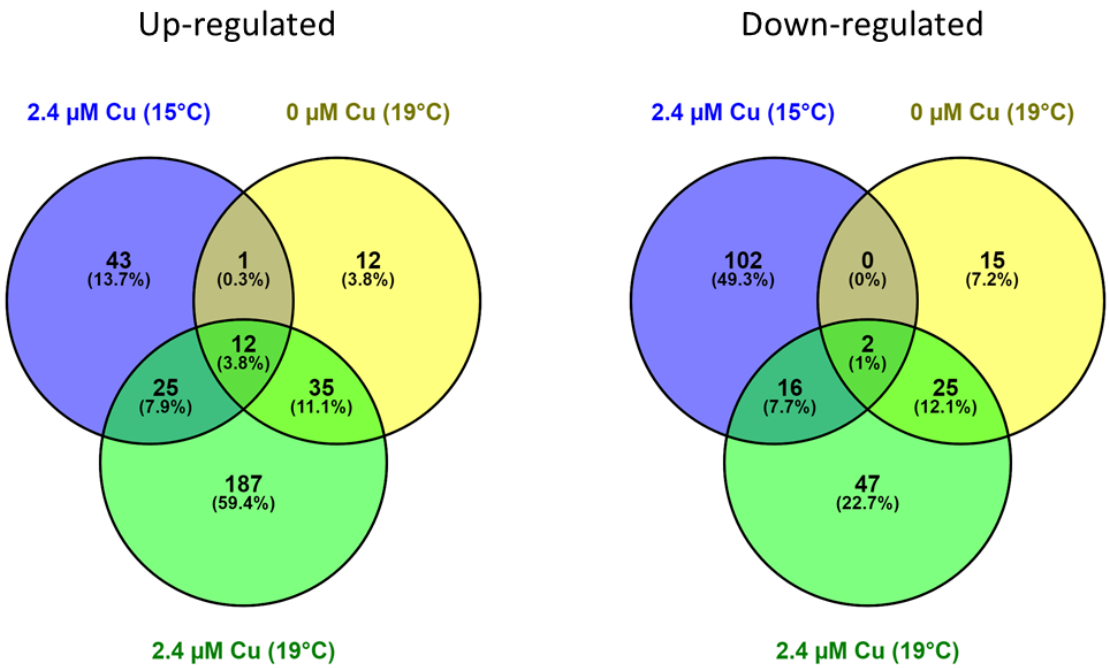

Figure 5.3. Venn diagrams showing number of over-expressed (left) and under-expressed (right) genes of *E. siliculosus* after 10 days of exposure to three treatments: 2.4 µM of Cu_T at 15 °C, 0 µM of Cu_T at 19 °C and 2.4 µM of Cu_T at 19 °C compared with control conditions (0 µM of Cu_T at 15 °C).

Table 5.2. Significantly (*P*-adjusted < 0.05) regulated genes under the three conditions of stress assessed: Cu-only (2.4 µM Cu_T), increased temperature-only (19 °C) and combination of both (2.4 µM Cu_T + 19 °C).

Gene ID	Annotation	Log 2 Fold Change		
		2.4 µM Cu_T	**19 °C**	**2.4 µM Cu_T + 19 °C**
Ec-25_000220	Manganese/iron superoxide dismutase	0.76	0.73	1.18
Ec-18_001740	Light harvesting complex protein	0.73	0.76	1.01
Ec-01_009740	Light harvesting complex protein	0.66	0.76	0.92
Ec-15_000985	Long non-coding RNA	1.17	1.25	1.87
Ec-20_003270	Hypothetical leucine rich repeat protein	0.84	0.80	1.11
Ec-07_006020	NUDIX hydrolase domain-like	0.78	0.71	0.96
Ec-12_008150	PKD/REJ-like protein	1.11	0.97	0.96
Ec-06_004500	Domain of unknown function DUF4149	0.64	0.94	1.11
Ec-00_000740	Hypothetical protein	0.99	1.16	1.53
Ec-24_001000	Expressed unknown protein	0.68	0.72	0.92
Ec-28_001370	Hypothetical protein	1.06	1.23	1.15
Ec-13_003370	Expressed unknown protein	1.39	1.43	1.67
Ec-06_000710	Light harvesting complex protein	-0.85	-1.25	-1.73
Ec-11_000370	SAM-dependent methyltransferases	-1.11	-0.87	-0.92
Ec-13_001170	Ctr copper transporter	-2.13	*0.83*	-2.30
Ec-07_007480	Ferric reductase, NAD binding	-4.83	*2.43*	-3.39
Ec-18_002770	Ferric reductase, NAD binding	-1.90	*1.72*	-1.90
Ec-00_003170	Hypothetical protein	-1.03	*1.51*	-1.45

5.3.3.3. GO enrichment analysis

The REVIGO visualization tool eliminated redundant GO terms from the list of enriched GO terms and produced semantic similarity-based scatterplots for the ontologies within the "Biological Process" domain (Figure 5.4.). Thirteen biological processes were significantly overrepresented in the Cu-only treatment (2.4 µM Cu_T at 15 °C) ($P < 0.05$).

Among those, the most represented processes were ‘transmembrane transport’ (GO:0055085), ‘transport’ (GO:0006810), ‘photosynthesis, light harvesting’ (GO:0009765) and ‘copper ion transmembrane transport’ (GO:0035434) (Figure 5.4 a). In the temperature-only treatment (0 µM Cu_T at 19 °C), nine processes were significantly over-represented ($P < 0.05$). The most represented processes were ‘photosynthesis, light harvesting’ (GO:0009765), ‘transmembrane transport’ (GO:0055085) and ‘nucleosome assembly’ (GO:0006334) (Figure 5.4 b). For the combined treatment (2.4 µM Cu_T at 19 °C), nineteen processes were significantly over-represented ($P < 0.05$). The most represented processes were ‘photosynthesis, light harvesting’ (GO:0009765), ‘translation’ (GO:0006412), ‘metabolic process’ (GO:0008152) and ‘transmembrane transport’ (GO:0055085) (Figure 5.4 c).

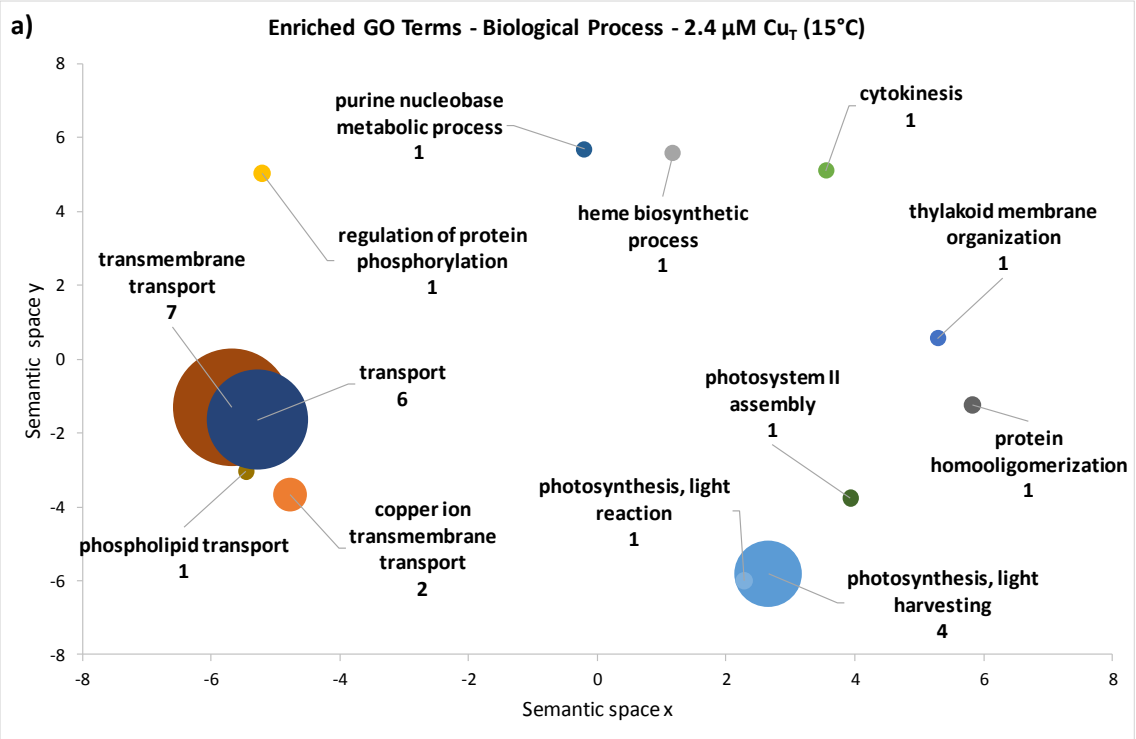

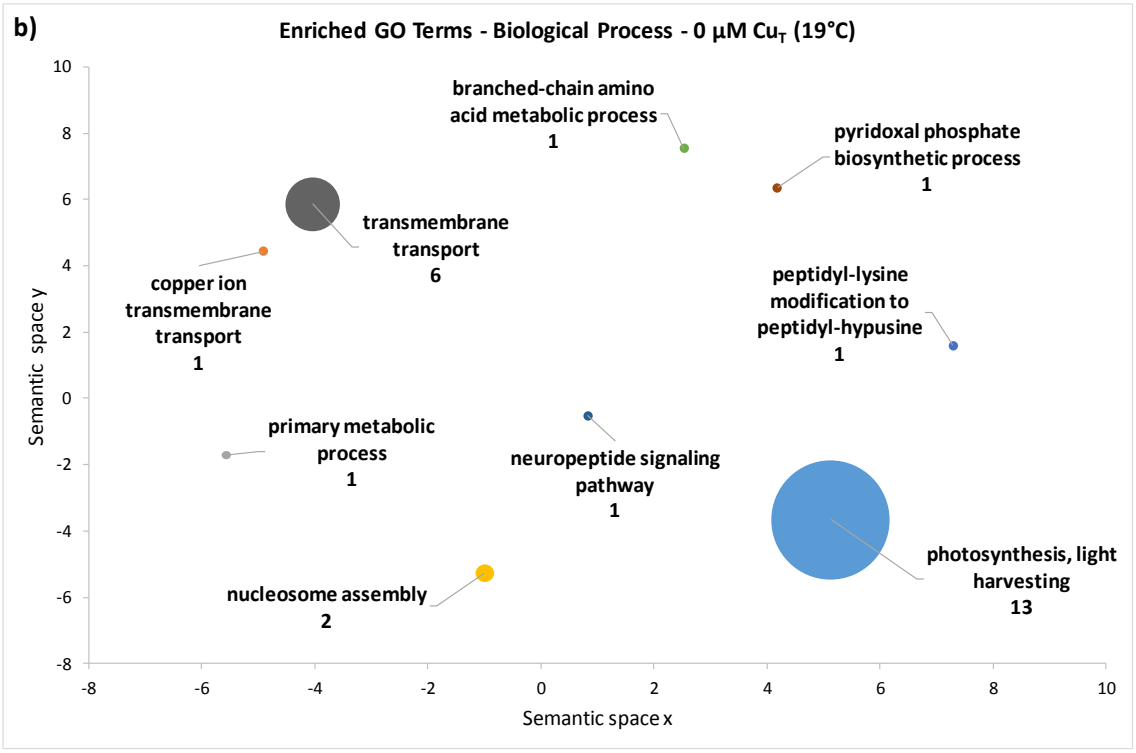

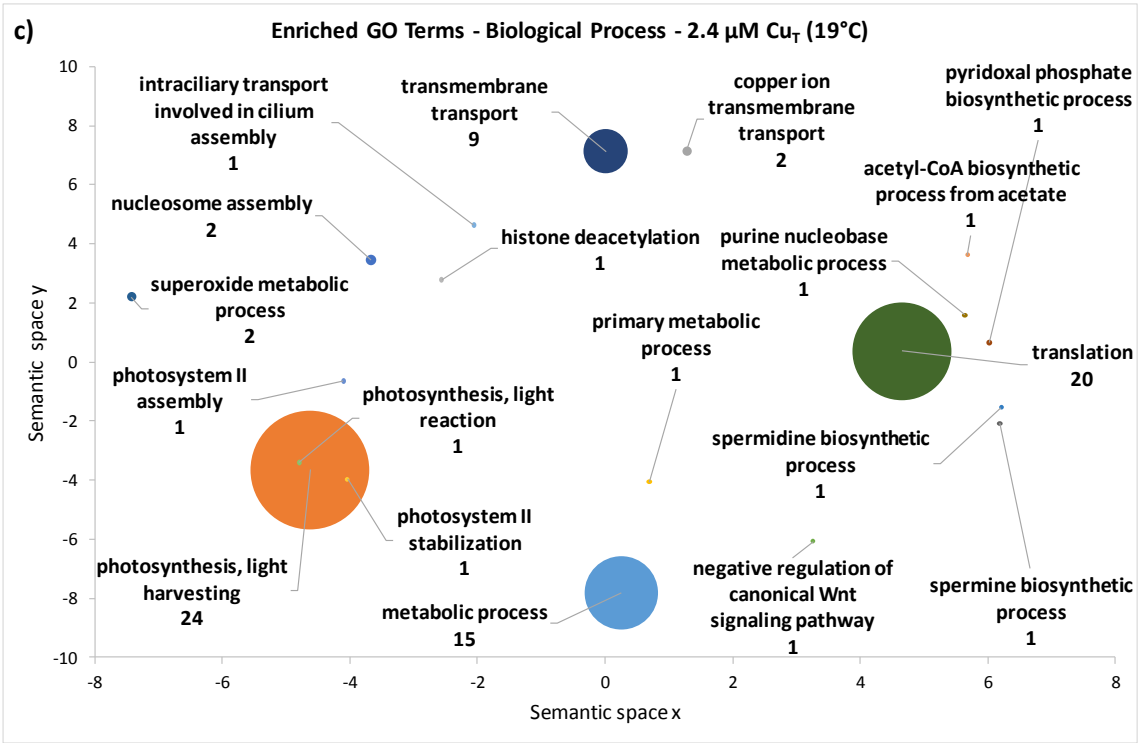

Figure 5.4. Semantic similarity scatterplot of the gene ontologies within 'Biological Process' in differentially expressed genes of *E. siliculosus* for treatments: a) 2.4 µM of Cu_T at 15 °C, b) 0 µM of Cu_T at 19 °C and c) 2.4 µM of Cu_T at 19 °C compared with control conditions (0 µM of Cu_T at 15 °C). Plots were obtained with the online tool REVIGO (http://revigo.irb.hr/) (Supek *et al.*, 2011).

Additionally, Figure 5.5. shows a comparison between the number of genes within the ontologies 'Cellular component' (a) 'Molecular Function' (b) and 'Biological process' (c) under exposure to the combined stressors. For 'Cellular component' the most represented terms were 'membrane' (GO:0016020), 'ribosome' (GO:0005840) and 'intracellular' (GO:0005622). For 'Molecular function' they were 'structural constituent of ribosome' (GO:0003735), 'copper ion transmembrane transporter activity' (GO:0005375) and 'superoxide dismutase activity' (GO:0004784) and for 'Biological process' the four terms described in the previous paragraph.

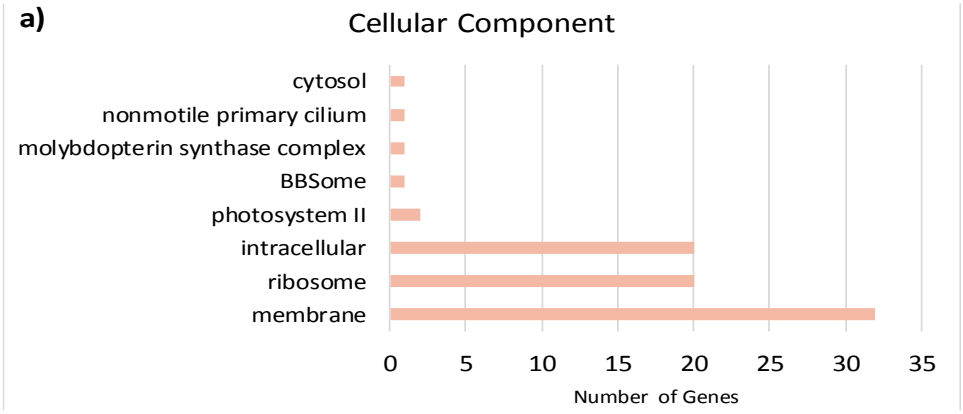

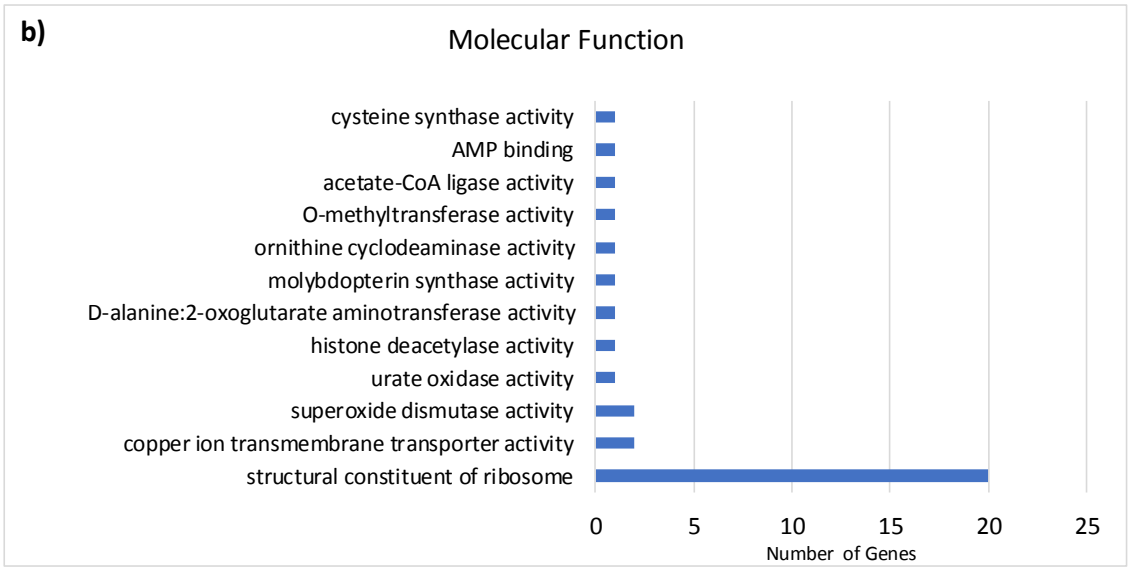

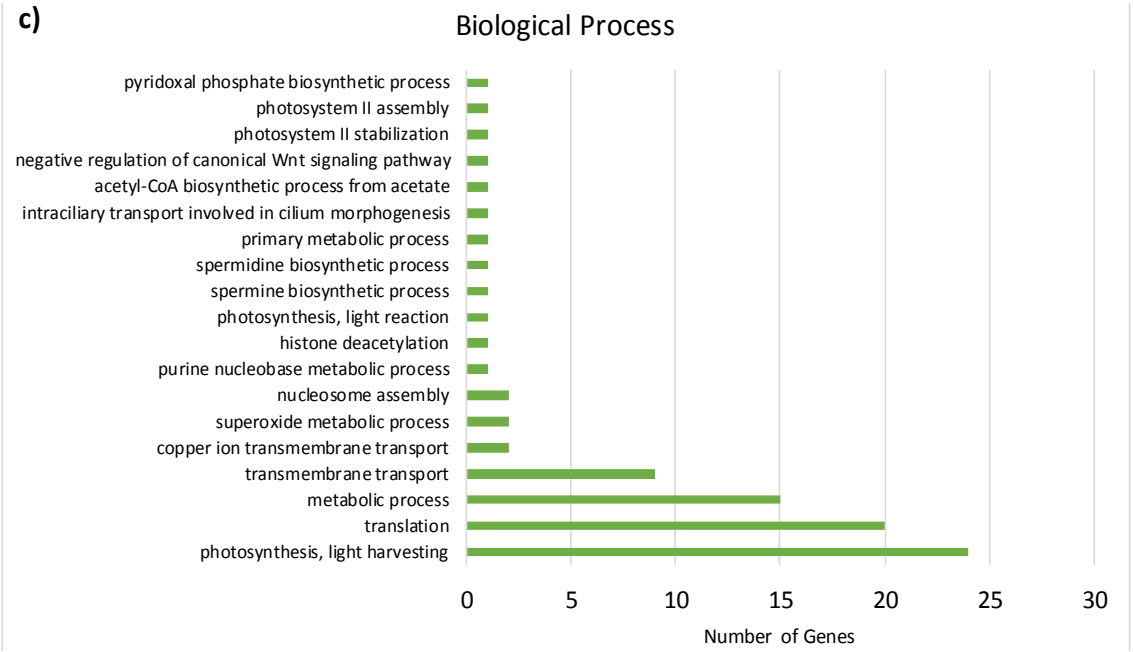

Figure 5.5. Gene Ontology (GO) analysis of *E. siliculosus* exposed to a combination of 2.4 µM of Cu_T and 19 °C. GO distribution of ontologies: Cellular component (A), molecular function (B) and biological process (C). Bars represent the number of differentially expressed genes in each category.

5.4. Discussion

The findings of this chapter have provided a deeper insight into the stresses mechanisms of copper and temperature and their interaction at the whole-organism, physiological and transcriptomic levels. In previous chapters of this thesis the complexity of interactions between stress factors was evidenced using traditional approaches such as physiological and biochemical tests. In the present chapter, the addition of a transcriptomic approach provides support for previous findings and also allows for the discovery of new elements involved in the responses to stress. In total, 516 genes were differentially expressed in all the experimental treatments in comparison with controls. Of these, only a few (12 up-regulated and 2 down-regulated) were shared between the Cu-only and temperature-only treatments, which indicates that responses to the two types of stress are very different. In contrast, the greatest number of regulated genes (349) occurred in samples exposed to the combined treatment. This highlights the importance of assessing combinations of stress factors in order to address the potential interactions that might occur under natural conditions in the face of ongoing global climate change (Harley *et al*., 2012; Todgham and Stillman, 2013; Koch *et al*., 2013; Ji *et al*., 2016).

5.4.1. Cu-only stress

At the physiological level, relative growth rates (RGR) were reduced in the Cu-only treatment compared to the control (Figure 5.1), as were the photosynthetic parameters F_v/F_m and α (Figure 5.2 a, b). These results provide further confirmation of the toxic effects of Cu on the photosynthetic apparatus in algae (Barón *et al*., 1995; Nielsen *et al*., 2003). The reductions in α and F_v/F_m are probably related to alterations in the light harvesting rather than electron transport chain, such as substitutions of the Mg^{2+} in the chlorophyll molecules bound to light harvesting complex II (LHCPII) (Küpper *et al*., 1996; Küpper *et al*., 1998; Küpper *et al*., 2002). This is also supported by

transcriptomic analysis, where 'light harvesting', 'photosynthesis light reaction' and 'photosystem II assembly' ontologies were overrepresented in the Cu-only treatment (Figure 5.4 a). It is known that the *E. siliculosus* genome contains at least 53 genes coding for chlorophyll-binding proteins (CBPs) (Dittami *et al.*, 2010). Several CBPs are considered stress-responsive. In the present study four putative genes for LHCPII proteins were up-regulated, of which two of are annotated as CBPs: Ec-18_001740 and Ec-01_009740; the latter was also up-regulated in the temperature-only and combined treatments. CBPs were also found to be up-regulated in previous microarray studies on *E. siliculosus* exposed to acute Cu stress (Ritter *et al.*, 2014), which confirms their importance as potential markers of acute and chronic Cu stress.

Other important ontology terms of over-represented genes under Cu-only stress were 'transmembrane transport', 'transport' and 'Cu ion transmembrane transport'. The first GO term included genes for a sugar/inositol transporter (Ec-04_003630); a voltage gated chloride channel (Ec-12_001240); a putative flippase (Ec-28_002170); a nitrate high affinity transporter (Ec-19_004150); and an inorganic phosphate transporter (Ec-24_001870), all of which were down-regulated. The 'transport' term included down-regulated genes for a mitochondrial carrier (Ec-05_005510); a xanthine/uracil/vitamin C permease (Ec-06_002490); an ABC membrane transporter (Ec-02_004150); and the up-regulated aquaporin-like (Ec-28_002600). For 'Cu ion transmembrane transport', two Cu transporters (Ec-13_001170 and Ec-13_001020) were down-regulated. All of the above is in agreement with the results of short-term Cu exposure studies, where also the down-regulation of genes related to N assimilation and other transporters related to lipid transport, such as member of the ATP-binding cassette (ABC) transporters family, was observed (Ritter *et al.*, 2014). ABC transporters are integral components of membranes and are able to bind ATP and use the energy to pump compounds across the membrane or to flip molecules from the inner to the outer leaflet of the membranes (Higgins, 1992;

Dean and Allikmets, 1995; Dean and Annilo, 2005). Besides downregulation of Cu transporters, the regulation of nutrients, lipid and sugars transporters indicates that Cu-exclusion mechanisms and primary metabolic processes might be acting together to compensate for the toxic effects of Cu on photosynthesis (Ritter *et al.*, 2014). However, chronic stress might exceed these strategies producing reductions in RGR.

5.4.2 Temperature-only stress

There were no significant reductions in RGR or most photosynthetic parameters under temperature-only stress. Only non-photochemical quenching (NPQ) was reduced which indicates regulation of the heat dissipation processes driven by pigments associated with the photosynthetic membranes. This was confirmed by the higher regulation of genes related to photosynthesis and light harvesting (See Table S5.2). This suggests that a 4 °C increase is not able to cause measurable reductions or increases in photosynthetic rates which might be correlated to the low production of ROS, as observed in chapter IV, and the lower amount of regulated genes (102). From studies in plants it has been proposed that the optimal thermal ranges for species is about 10 °C wide (Mahan *et al.*, 1995). However, in algae the optimal ranges might be dependent on the temperature adaptation history of species and populations. For example, Eggert *et al*. (2003) introduced the concept of 'performance breadth', which corresponds to the temperature ranges at which 80% and 20% of the maximal growth rate occurs. This is used to compare the optimal thermal ranges for marine algae, which has been observed to vary across populations and species. (Eggert and Wiencke, 2000; Eggert *et al*., 2006). Species with greater performance breadth are considered eurythermal, and species with a narrow performance breadth, stenothermal. Experiments on thermal tolerance concluded that *E. siliculosus* is a eurythermal species, but there was a correlation between the optimal ranges for growth and the prevailing temperatures in the site of collection of the isolates (Bolton, 1983).

This differential tolerance to temperature was attributed to genetic adaptation describing an ecocline. However, a recent study based on mitochondrial and nuclear molecular markers suggests that there are at least 15 different species within the so-called *Ectocarpus siliculosi* group, which are currently classified as *E. siliculosus* (Montecinos *et al.*, 2017). For example, the genome strain (Ec 32) was found to be different from *E. siliculosus* and from individuals sampled in the same biogeographic zone of strain Es524 (used in this study), which belonged either to *E. crouaniorum*, based on mitochondrial marker COI-5P, or to *Ectocarpus* 12, using the nuclear marker ITS1. However, more evidence and the development of new molecular markers could aid the unequivocal identification of this isolates with a cryptic morphology (Peters *et al*., 2010; Leliaert and De Clerck, 2017). This could confirm that the differences in optimal temperatures observed by Bolton (1983) were due to adaptations by different species of *Ectocarpus* to their natural temperature regimes. Thus, range of optimal temperatures for strain Es524 could be narrower than expected; however, further research is needed to solve this aspect.

Although the strain Es524 used in this study has long-term acclimation to 15 °C, it is possible that genetic adaptation allowed it to withstand a 4°C increase in temperature (Avia *et al.*, 2017). Mean sea surface temperature (SST) at the site of collection of Es524 was 18.3 °C during the summer months of 2016 and 14.1 °C for the winter months for the same year (see Section 2.1). Thus, despite the 15 °C temperature of the long-term culture conditions, 19 °C might not represent a sufficient challenge for Es524. This is supported by the fact that heat shock proteins (HSPs), which are characteristic of thermal stress responses (Larkindale *et al.*, 2005), were not regulated by temperature-only treatment. However, genes involved in iron uptake, such as three up-regulated ferric reductases (Ec-00_006340, Ec-00_011110, Ec-00_009420, Log2 fold change of 4.35, 2.68 and 2.58, respectively), and transporters such as N transporters (Ec-19_004130,

Ec-19_004170, Ec-19_004180) (Table S5.2), might be involved in the observed tolerance to 19 °C. It is interesting to note that the Ctr copper transporter Ec-13_001170 was down-regulated under the Cu-only treatment, but up-regulated under the temperature-only treatment (Table 5.2). This may be related to the up-regulation of Fe transporters, as it has been suggested that Cu assimilation is related to iron transport (Askwith *et al*., 1994; Blaby-Haas and Merchant, 2012). Thus, a combination of N and Fe transport regulation and a high turnover of light harvesting proteins could be involved in the tolerance mechanism to temperature acclimation.

5.4.3. Combined Cu and thermal stress

The combined exposure to an elevated Cu concentration and increased temperature induced a decrease in RGR but not in the photosynthetic rate (ETR_{max}) or quantum yield (F_v/F_m), as seen in the temperature-only treatment. In the same way, there was reduction in NPQ to a similar level as that in the temperature-only treatment. Thus, while Cu-stress apparently affects the light harvesting processes, and temperature-stress affects the excess energy dissipation process, in combination, the effects of temperature offset the toxic effects of Cu as no reductions in ETR_{max} and F_v/F_m were observed. Similar trends have been observed in other brown and red algae exposed to increases in temperature in combination with other stressors (Nielsen *et al*., 2014; Rautenberger *et al*., 2015). For example, the elevated temperature (from 6 to 22 °C) (Nielsen *et al*., 2014) improved the tolerance of PSII to Cu stress in *Fucus serratus* and (from 2 to 7 °C) to UV stress in *Himantothallus grandifolius* (Phaeophyceae) and *Iridaea cordata*, *Trematocarpus antarcticus*, and *Palmaria decipiens* (Rhodophyceae). Significantly, this mitigating effect occurs when the increase in temperature occurs within the species-specific range of thermal tolerance (van de Poll *et al*., 2002; Rautenberger and Bischof, 2006; Fredersdorf *et al*., 2009). Thus, it can be argued that in the present study the

increase in temperature was within the range of tolerance of Es524 (see previous section) and the activation of stress-specific genes, due to the mild increase in temperature, aided to compensate the effects of Cu stress on PSII. As observed in Figure 5.3, the number of up-regulated genes under the combined treatment surpassed the arithmetic sum of the up-regulated genes in the Cu-only and temperature-only treatments. In contrast, the number of down-regulated genes for the combined treatment was lower than the sum of the single-stress treatments. These results indicate that some pathways can interact synergistically under the combination of the stressors while others act antagonistically. These results are in accord with those presented in Chapter IV, where both synergistic and antagonistic interactions in different reactive oxygen metabolism (ROM) parameters were apparent. Results from other transcriptomic studies on interactions such as between temperature and light stress in *Saccharina latissima* from the Arctic, showed strong combined effects in the transcriptomic responses under increased temperature and high irradiance (Heinrich *et al.*, 2012). In this case, it is likely that *S. latissima* was exposed to a temperature regime beyond the natural range of tolerance, as supported by the observed activation of several heat shock proteins.

As for the single stress-treatments, photosynthesis and light harvesting-related genes were characteristic of the response to the combined treatment. In addition to the genes regulated by exposure to a single-stress, there were an additional 6 up- and 4 down-regulated genes under the combined treatment. One down-regulated gene (Ec-06_000550) that codes for putative stress-related chlorophyll binding proteins (CBPs), was previously found to up-regulate under Cu-stress in a microarray transcriptomic study on acute Cu-exposure (Ritter *et al.*, 2014). This indicates that responses to short-term exposure stress do not necessarily correspond to those under chronic exposure. Overall, the overrepresentation of photosynthesis-related genes may account for the above-discussed 'improvement' of the photosynthetic response. Of

particular interest is the up-regulation of 20 genes coding for structural components of the ribosome (Figure 5.5 a, b, c) (Table S5.3), which might imply a rapid turnover of proteins affected by high concentrations of reactive oxygen species (ROS). This is in contrast to previous short-term salinity and oxidative stress studies that showed that ribosomal genes were amongst the most stably expressed genes of the microarray (Dittami *et al.*, 2009). This highlights once more that differences between acute and chronic stress responses can arise because of dynamic regulation of the intracellular milieu (Okamoto and Colepicolo, 1998; Pinto *et al*., 2003). As shown in Chapter IV, there was a large accumulation of H_2O_2 in algae exposed to the combined treatment and this probably caused the inactivation and further degradation of proteins. Besides their toxic effects, ROS are also signalling molecules that are able to trigger cascades responses (Desikan *et al*., 2005; Agarwal and Zhu, 2005). Therefore, under chronic stress the up-regulation of transcription factors and chaperones would aid the repair of the damaged proteins (Feder and Hofmann, 1999; Wang *et al*., 2004). One heat shock factor (Ec-08_002570) and two heat shock proteins, HSP90 (Ec-18_001040) and HSP20 (Ec-21_001560), were up-regulated by the combined effect, confirming that protein repair and turnover mechanism are activated by the interaction of stressors. This further confirms that the combination of stressors may induce pathways not regulated by exposure to single environmental stressors.

5.4.4 Conclusions

The results obtained in the present study show that chronic exposure to sublethal levels of Cu and temperature induce responses at different levels of organisation that are different to those under acute stress. An increase in total Cu concentration (2.4 μM) caused a greater response than the increased temperature (19 °C) in the transcriptome. At all levels of organization investigated the impact of elevated temperature was less strong

than that of Cu. This is most likely due to the upper thermal tolerance limit of strain Es524 not being exceeded. The combined effect of Cu and temperature induced the greatest up-regulation of stress-related genes, such as HSPs and oxidative stress, but lower down-regulation when compared to Cu-only stress. It can be concluded that activation of some stress-responsive photosynthetic related genes by temperature compensated for the deleterious effect of Cu on PSII efficiency, as previously observed in other algae exposed to combination of stressors (van de Poll *et al*., 2002; Rautenberger and Bischof, 2006; Fredersdorf *et al*., 2009; Nielsen *et al*., 2014; Rautenberger *et al*., 2015). Future studies should aim to assess a wider range of temperatures in combination with Cu and other toxic metals over different periods of exposure. The results obtained here suggest that a bottom-up approach whereby responses at the transcriptomic level are assessed prior to analysing effects and responses at higher levels of organisation would be appropriate. With ongoing rapid development of new sequencing technologies, the use of Illumina and other platforms is encouraged in RNA-seq experiments, as no previous knowledge of the genome sequence is required.

Chapter VI

General Discussion

The aim of the work described in this thesis was to investigate the effects of a combination of anthropogenic Cu pollution and a naturally occurring stressor of marine macroalgae (seaweeds), increased seawater temperature. The impacts of the former affect seaweeds, and other marine organisms, on a local scale in coastal waters and estuaries adjacent to mining activities and industrial discharges (Gledhill *et al.*, 1997). The latter, while also occurring locally in for example, rock pools of the intertidal zone, occurs at a global scale due to events such as 'El Niño southern oscillation' (ENSO; Edgar *et al*., 2010). Events like ENSO can be exacerbated by global warming leading to the overall increase of ocean temperature (Laffoley & Baxter, 2016). This highlights the importance of studying the interactions between such stressors in the marine environment. Although the effects of metals and temperature on the biology of seaweeds have been studied independently, there is lack of knowledge about how they interact. In this study, the potential interactions between these two stress factors were investigated in controlled laboratory experiments using the filamentous seaweed, *Ectocarpus siliculosus* as a proxy for brown seaweeds, which are globally important primary producers and bioengineers of near-shore waters. The responses to chronic stress exposure were examined at different levels of biological organisation, from the whole organism to the molecular. Chapter III, reports the responses on the whole-organism, photosynthetic physiology and bio-accumulation of Cu ions. The results demonstrated that combinations of Cu and temperature interact in a complex manner. As Cu, and other abiotic stressors, are known to cause disturbances of the reactive oxygen metabolism (ROM) in seaweeds, in Chapter IV the effects of the combined stressors on the biochemical reactions and gene expression associated to ROM were investigated. The results confirmed the complexity of the interactions between stressors, but also demonstrated that temperature can mitigate, to some extent, Cu stress in various components of the cells' ROM, including gene expression. Finally, in Chapter V the whole-transcriptome response was studied by using

RNA-seq, which aided the identification of the processes that are differentially (or concomitantly) affected by the two individual stressors and their combination. In this last Chapter VI, the results obtained in each chapter and their implications for algal physiology will be discussed in an integrated view. Also, limitations encountered during the study and suggestions for future avenues of research will be covered.

In Chapter III, results obtained for relative growth rates (RGR) indicated that *E. siliculosus* strain Es524 is able to withstand high levels of Cu, independently of temperature. However, temperatures of 25 °C, which is out of the normal temperature range of the site from which the strain was isolated, impaired growth. However, according to warming models (IPCC, 2014; Laffoley & Baxter, 2016), an increase of 2-4 °C in global means in the next 80 years could cause several impacts in seaweed populations, as already observed in *Macrocystis pyrifera* during the ENSO event in 1997–1998 (Ladah *et al.*, 1999). This leaves open the question of which populations will be able to survive a long-term increase in ocean temperatures. Thus, more studies are necessary to understand the effects of long-term rise in temperature and the potential interactions with other local and global stressors not only on growth and survival but also at other levels of biological organisation. RGR were measured after 14 days of exposure to treatments to allow time for algal filaments to grow sufficiently to observe differences between treatments by the methods used. However, this might have resulted in discrepancies between growth and other parameters such as photosynthetic, pigment concentrations and Cu accumulation, which were measured after only 6 d of exposure. For this reason in Chapter V, the RGR and the other parameters were measured after the same time of exposure to stressors. An interesting difference arose from the observation of RGR at different times: after 10 days of exposure a reduction in RGR was observed at increased Cu concentrations whereas no differences where observed after 14 days. This suggests that there was acclimation to Cu exposure during chronic exposure to Cu, which to some

extent was corroborated by results in Chapter V. Also, these results highlight the necessity of developing new methods, such as live-image based combining the power of bioinformatics and high resolution imaging as reviewed in Sozzani *et al*. (2014), for assessing growth rates in a dynamic way.

The use of chlorophyll *a* measurements to assess photosynthetic performance is a well-known tool in ecophysiological studies. In the present study, it was demonstrated that the application of rapid light curves (RLC), using a MINI-PAM fluorimeter (WALZ) under controlled conditions, is a powerful technique for obtaining more detailed information about the status of photosystem II (PSII) compared to the classic maximum quantum yield (F_v/F_m) parameter often used in stress-studies. In fact, interactions between stress factors did not appear when evaluating only F_v/F_m, but were found when analysing the performance of PSII over a range of irradiances from the RLC. In general, the results in Chapter III indicated that the effects of Cu and temperature excess on the photosynthetic parameters were more accentuated at 15 °C. For example, the efficiency-related parameters F_v/F_m and α were reduced at 15 but not at 25 °C under elevated Cu treatments. In contrast, the maximum photosynthetic rates (estimated as ETR_{max}) increased under some Cu treatments at 15 °C after 6 days of exposure. This was partly confirmed by the results presented in Chapter V, where reductions in efficiency were also observed at 15 °C and 2.4 µM Cu after 10 days of exposure, but there were no difference observed in ETR_{max}. Those differences might be the result of different exposure times. It has been argued that cellular mechanisms acting under Cu exposure at 'optimal' temperatures (15 °C) might be different from mechanisms acting at supra-optimal temperatures (e.g. 25 and 19 °C). Even taking into account the fact that strain Es524 may be naturally adapted to both 25 and 19 °C during summer and low tides (Avia *et al.*, 2017), our results indicate that increases in temperature as small as 4 °C can interact with Cu excess and elicit a response in the photosynthetic physiology. We have suggested

interactions of Cu and temperature affect the light harvesting and heat dissipation processes. Thus, while Cu might affect the chlorophyll associated to PSII by replacing the central Mg in chlorophyll molecules (Küpper *et al.*, 2002), temperature may affect the stability of photosynthetic membranes and proteins associated with PSII (Los & Murata, 2004), altering the heat dissipation capacity.

In terms of metal accumulation, the results indicate that less total Cu was accumulated at 25 °C under the highest Cu treatment (3.2 µM). Also, the distribution of Cu (intracellular vs. cell wall-bound) differed between temperatures in the 1.6 µM Cu_T treatment. The percentage of intracellular Cu at 25 °C (50.11 ± 6.2) was significantly lower compared to 15 °C (81.42 ± 9.9). This suggest that detoxification mechanisms might be activated at lower Cu concentrations at elevated temperatures, whereas at a lower temperature the alga is able to tolerate a higher intracellular concentration of Cu. However, as the total accumulation was also reduced at 25 °C and high copper, this may indicate that temperature likely induced changes in speciation of Cu affecting its bioavailability. Both of the previous statements are in agreement with some of the results observed later in Chapter IV, where a combination of elevated Cu and temperature caused the largest production of phenolic compounds. Thus, the natural presence of organic ligands plus the enhanced release of polyphenols induced by temperature could alter the bioavailability of Cu in laboratory cultures. In nature, however, the effects of temperature in naturally occurring dissolved organic matter rather than the release of polyphenols would be more relevant (Byrne *et al*., 1988; Gledhill *et al*., 1999).

Due to the costs of the molecular analysis and a limited budget, in Chapter IV, the interactions between stressors were analysed using a simplified experimental 2^2 factorial design i.e. all combinations of two temperatures (15 and 19 °C) and two Cu concentrations (0 and 2.4 µM Cu_T). Also, the period of exposure was extended to 10 d to

allow for comparisons with previous chronic Cu exposure studies in *E. siliculosus* (Roncarati *et al*., 2015; Sáez *et al*., 2015a; Sáez *et al*., 2015b). The results demonstrated that increased Cu (2.4 μM Cu_T) and temperature (19 °C) can act synergistically for the production of H_2O_2 and thiobarbituric acid reactive substances (TBARS), the latter being an indicator of lipid peroxidation caused by reactive oxygen species (ROS). Despite the presence of high levels of ROS and TBARS under the combination of stressors, most of the parameters related to the antioxidant response did not increase or showed only a mild response compared to Cu-only stress responses. It is proposed that under the combination of stressors, Cu is responsible for the production of ROS while temperature is responsible for deactivation of antioxidant responses due to altered transcription and translation of genes involved, which caused enhanced ROS accumulation. For example, the results in expression of the superoxide dismutase (*SOD*) gene, illustrated this pattern, whereas the extractable activity of its gene product (i.e. the antioxidant enzyme SOD) did not. Additionally, it is known that ROS are able to deactivate enzymes when present at high concentrations (Casano *et al*., 1997; Asada, 1999) and act as signal transducers for the expression of certain genes (Desikan *et al.*, 2005), which might explain the response observed. However, it is known that there is more than one type of SOD in several compartment of the cell (Asada *et al*., 1975; Bakthavatchalu *et al*., 2012; Kuo *et al*., 2013), therefore the conclusions obtained with expression analysis of single genes are limited.

The concentrations of antioxidant molecules such as glutathione and intracellular phenolic compounds also showed antagonistic interactions under the combination of stressors. However, an interesting result was obtained when analysing the total production of phenolic compounds (i.e. total intracellular plus released into medium). The total production of phenolics was higher in individuals exposed to the combined stressors, but almost 50% was released into the growth medium. This might be related to an enhanced

metal detoxification strategy by releasing Cu chelated by polyphenols formed intracellularly (Gledhill *et al*., 1999; Schoenwaelder, 2002). This hypothesis is supported by Cu accumulation data from Chapter III, where a reduced intracellular accumulation was observed at higher temperatures and Cu concentrations. Alternatively, as phenolic compounds are also constituents of the cell wall (Connan & Stengel, 2011b), the increase in temperature might have caused an enhanced release by alterations of cell wall constituents (Torres *et al.*, 1991), as observed from the release data under temperature-only stress. The concentrations of the antioxidant ascorbate (ASC) and its oxidised form dehydroascorbate (DHA) increased only under Cu stress at both temperatures and no statistically significant interactions were observed. This could indicate that ASC concentrations could be used as a marker of Cu stress; however, more temperatures should be tested.

In Chapter V we looked at the whole transcriptomic responses in algae exposed to the same conditions as in Chapter IV and linked them to photosynthetic physiology and growth. This approach provided the opportunity to desegregate the responses observed in the previous chapters and led to the discovery of new strategies to deal with combined chronic metal and temperature stress. For instance, the high regulation of genes involved in light harvesting and photosynthesis confirmed the results observed using chlorophyll *a* fluorescence in Chapter III, which indicated that light harvesting was sensitive to Cu and temperature stress. Additionally, the overrepresentation of genes involved in transmembrane transport and metabolism under the combination of stressors are in agreement with the hypothesis proposed in Chapter IV, i.e. an increase in temperature may accelerate metabolic rates and also activate detoxification mechanisms, such as active transport of Cu-chelating molecules from internal storage an release into the growth medium. Finally, the regulation of chaperone proteins such as heat shock and ribosomal proteins, indicate a rapid turnover of proteins, which might be affected by high

intracellular ROS as observed by concentrations of H_2O_2 and TBARS in chapter IV. However, further research is needed in order to confirm such hypotheses. There is some correspondence between the results reported here and those obtained in a previous transcriptomic study, using microarrays, on *E. siliculosus* exposed to short-term (8 h) acute Cu stress (Ritter *et al.*, 2014). However, the responses to chronic Cu singly and combined with temperature stress at more environmentally relevant concentrations were less steep and provided insight of mechanisms that could be acting during acclimation processes.

The approach taken in this investigation was novel in its assessment of metal stress at different levels of organisation, making use of some of the new technologies available. The results have provided new insights into the stress responses of brown seaweeds to metal and temperature exposure, as interactions between these stressors are rarely studied. However, this type of study will become increasingly relevant to aid our understanding of the effects of ongoing climate change, and to improve our knowledge of natural processes. There were both antagonistic and synergistic interactions between temperature and Cu in the algal response when both stressors were applied simultaneously, whereas in nature the length of exposure to different stressors may vary (e.g. global warming combined with an acute pollution event). It has been suggested that exposure to one mild short stress could negate the adverse effects of a subsequent stress due to 'cross-adaptation' or 'cross-tolerance', in which the first factor induces defence mechanisms leading to increased resistance to the second factor. In contrast, the effect of a single stressor could lead to an enhanced susceptibility to a second factor of stress (cross-synergism or cross- susceptibility) leading to irreversible damage (Alexieva and Ivanov, 2003; Todgham and Stillman, 2013). Although we did not test the cross-adaptation and cross-susceptibility hypotheses directly, one could argue that applying increased temperature to a laboratory strain with a long term acclimation to constant 15 °C and

isolated from a Cu-polluted site could be considered a test of cross-adaptation or cross-tolerance. However, this deserves future attention in order to develop a predictive understanding of an organism's responses to multiple stressors. Additionally, the current availability of public repositories of bio-molecular data and the development of free bio-informatic statistical tools to analyse large quantities of biological data opens new avenues for future research. For example, studies analysing the whole metabolome and proteome by mass spectrometry (MS) coupled to liquid chromatography (LC) or gas chromatography (GC; Dunn *et al*., 2013), could greatly aid and complement the data generated by transcriptomics and thus our understanding of the biological systems acting in response to environmental perturbations or stimuli. Finally, while copper is one of the most well-studied metals in seaweed research, it rarely occurs in isolation. Therefore, when evaluating interactions between physical and chemical stressors more environmentally realistic (and complex) experimental designs, involving mixtures of toxic metals, and/or organic pollutants, should be considered.

The research presented in this thesis provides new insights on the responses of the economically important brown seaweeds to thermal and metal-induced stress. Those responses indicate that synergistic or antagonistic interactions occur at different levels of organisation between both factors of stress. The most important mechanisms involved are the regulation of photosynthetic physiology, reactive oxygen metabolism, and related gene expression. Antagonistic interactions occur in the photo-physiological response where Cu causes a reduction in efficiency at lower temperature compared to elevated temperature. Oxidative stress parameters show a synergism in the production of reactive oxygen and lipid peroxides, with higher concentrations of these compounds at elevated Cu and temperature. Accumulation of ascorbate and dehydroascorbate and the production of total phenolic compounds are the main biochemical response to such synergism. The expression of genes related to photosynthesis and particularly light harvesting proteins

are in agreement to the antagonistic response observed in physiological measurements. We hypothesise that elevated temperature facilitate a faster turnover of light harvesting proteins affected by Cu ions excess, which is reflected in higher efficiency of light harvesting at elevated temperature and a lower dissipation of light energy as heat. Finally, from gene expression data we conclude that transporter proteins have an important role in movilizing Cu ions outside the cell at high temperatures and this observation is supported by bioaccumulation data. The above information will aid to understand the potentially enhancing effect of global warming on the toxicity of metals for macroalgae in estuaries and coasts affected by pollution.

Appendices

Appendix 1.

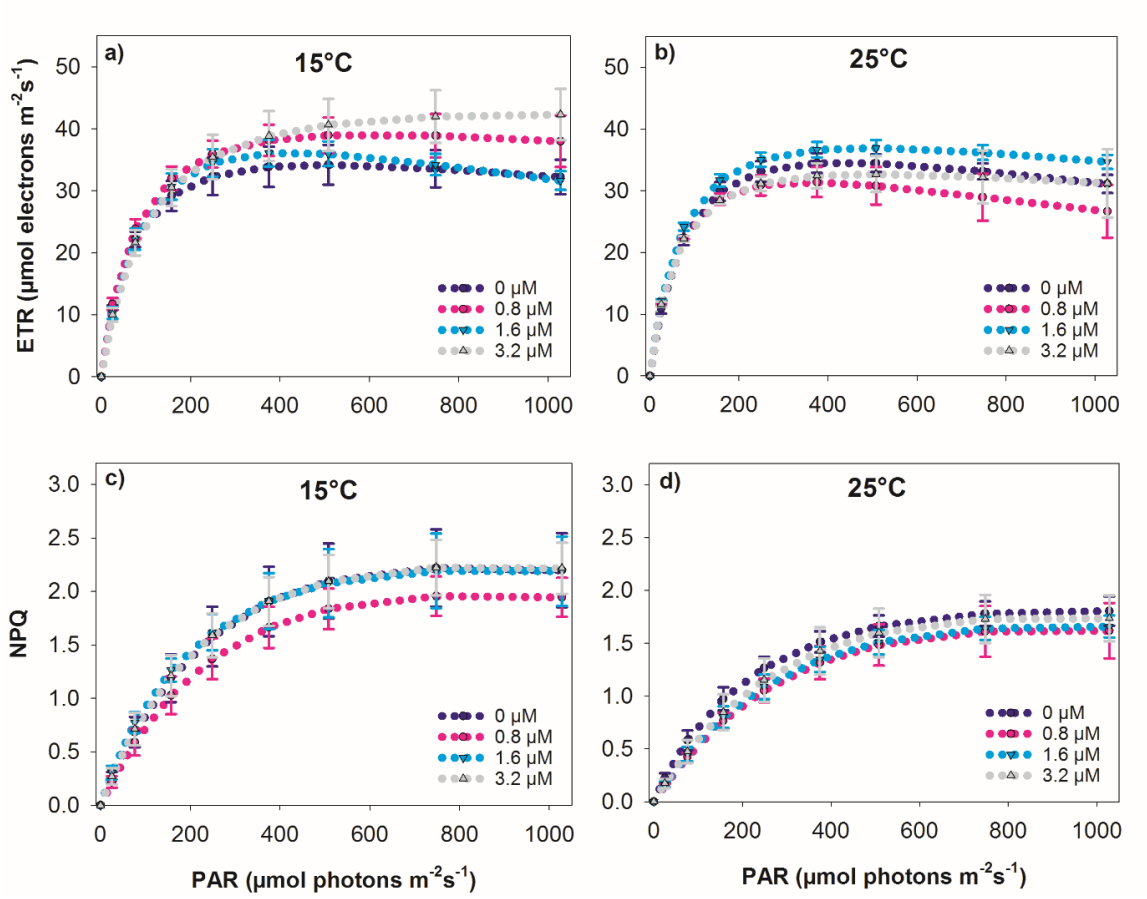

Figure S3.1. Rapid light curves (ETR or NPQ vs. irradiance) fitted according to Eilers and Peeters (1988). a) ETR at 15 °C, b) ETR at 25 °C, c) NPQ at 15 °C and d) NPQ at 25 °C. Error bars indicate ± 1 SD, $n = 3$.

Appendix 2.

Table S5.1. List of differentially expressed genes (DE) in *E. siliculosus* under Cu stress only. Positive Log_2 fold-change values indicate up-regulated genes and negative values down-regulated genes.

Gene Id	Description	log2 Fold Change	DE in other treatment	
Ec-13_001170	Ctr copper transporter	-2.13	Cu+19	19 only
Ec-13_001020	Ctr copper transporter	-3.14	Cu+19	
Ec-03_002320	Methyltransferase type 11	-2.53	Cu+19	
Ec-07_007480	Ferric reductase, NAD binding	-4.83	Cu+19	19 only
Ec-18_002770	Ferric reductase, NAD binding	-1.90	Cu+19	19 only
Ec-11_000370	SAM-dependent methyltransferases	-1.11	3 Conditions	
Ec-14_001470	K Homology domain	-2.87	Cu+19	
Ec-17_003230	expressed unknown protein	-1.07	Cu+19	
Ec-12_004100	Cyclic nucleotide-binding domain	-1.44		
Ec-27_000610	Tetratricopeptide-like helical domain	-0.91		
Ec-17_000180	expressed unknown protein	-1.05		
Ec-12_007610	hypothetical protein	-3.05		
Ec-06_000220	Mpv17/PMP22	-1.19		
Ec-27_005810	hypothetical protein	-1.17		
Ec-00_005790	Zinc finger, RING/FYVE/PHD-type	-1.00		
Ec-17_003760	CRAL-TRIO domain	-1.06		
Ec-06_003880	conserved unknown protein	-1.30		
Ec-06_004740	Hypothetical protein	-1.45		
Ec-17_003520	solanesyl diphosphate synthase-like protein	-0.76		
Ec-02_005140	Phox homologous domain	-1.21		
Ec-03_004150	expressed unknown protein	-1.11	Cu+19	
Ec-06_008970	expressed unknown protein	-1.35	Cu+19	
Ec-13_002900	fibronectin type III domain-containing protein	-1.62		
Ec-02_004150	ABC membrane transporter	-1.75		
Ec-11_000610	Glycosyltransferase AER61, uncharacterised	-0.93		
Ec-02_003670	Tetratricopeptide-like helical domain	-1.07		
Ec-02_004160	ABC transporters	-1.49		
Ec-24_002220	Regulatory factor, effector binding domain	-0.83		
Ec-00_001430	DEAD box helicase	-1.22		
Ec-28_002170	Flagellin assembly, membrane protein MviN	-1.15		

Ec-00_002940	AMP-dependent synthetase/ligase	-1.70		
Ec-09_003990	ENTH/VHS	-1.15		
Ec-19_003430	WW domain	-1.14		
Ec-09_001600	Ankyrin repeat-containing domain	-1.10		
Ec-19_004150	Nitrate high affinity transporter	-0.81	Cu+19	
Ec-22_001850	Armadillo-like helical	-1.04		
Ec-11_002540	Trehalose 6-phosphate synthase, family GT20 / Trehalose 6-phosphate phosphatase	-1.50		
Ec-12_003360	Microtubule-associated protein, MAP65/Ase1/PRC1	-1.39		
Ec-20_000740	Myosin head, motor domain	-0.80		
Ec-24_002550	Myosin light chain kinase (MLCK)	-1.12		
Ec-10_001410	Serine/threonine protein kinase	-1.16		
Ec-06_002470	Uricase	-0.87	Cu+19	
Ec-12_001240	Chloride channel, core	-1.07		
Ec-04_005780	Amine oxidase	-1.24		
Ec-09_002160	AAA+ ATPase domain	-0.83		
Ec-00_008060	Cathepsin-like proteinase	-0.69		
Ec-27_006330	c-myb-like transcription factor	-1.06		
Ec-03_002310	Hypothetical protein	-1.61	Cu+19	
Ec-06_009820	expressed unknown protein	-1.13		
Ec-10_003100	von Willebrand factor, type A	-0.92		
Ec-01_005360	Ferrochelatase-2, putative chloroplast precursor	-1.04		
Ec-10_003700	hypothetical protein	-0.83		
Ec-01_001630	Helicase-associated domain	-1.32		
Ec-13_001120	hypothetical protein	-1.34		
Ec-16_003450	GPA2, alpha subunit of a heterotrimeric G protein	-0.97		
Ec-20_002410	mitogen-activated protein kinase	-1.04		
Ec-23_002560	NAD-dependent epimerase/dehydratase, N-terminal domain	-0.79		
Ec-05_005510	Mitochondrial carrier domain	-0.74		
Ec-09_003660	Thioesterase superfamily	-1.18		
Ec-08_000840	PObg2, plastid Obg/CgtA-like GTPase 2	-1.38	Cu+19	
Ec-14_006520	Centromeric protein E, putative	-0.97		
Ec-05_001170	Protein phosphatase 2C (PP2C)-like domain	-0.93		
Ec-06_002490	Xanthine/uracil/vitamin C permease	-0.89		
Ec-05_002560	Cyclic nucleotide-binding-like	-0.91		
Ec-07_000980	expressed unknown protein	-1.84		
Ec-17_003880	conserved unknown protein	-1.09		

Ec-23_000950	Casein kinase (serine/threonine/tyrosine protein kinase)	-0.92		
Ec-28_002290	Serine-threonine/tyrosine-protein kinase catalytic domain	-0.91		
Ec-14_004360	P-loop containing nucleoside triphosphate hydrolase	-1.02		
Ec-01_004580	conserved unknown protein	-1.01		
Ec-26_001930	conserved unknown protein	-2.19		
Ec-26_002380	Homeodomain-like	-0.77		
Ec-23_002530	Autophagy-related protein 11	-0.86		
Ec-06_000710	Light harvesting complex protein	-0.85	3 Conditions	
Ec-27_002830	Ankyrin repeat-containing domain	-1.28		
Ec-01_001190	expressed unknown protein	-1.47		
Ec-13_002700	expressed unknown protein	-0.69		
Ec-20_003310	Mlo-related protein	-1.95		
Ec-04_003210	Acyltransferase 3	-0.71		
Ec-12_000590	CCT domain	-0.88		
Ec-21_000310	Ankyrin repeat-containing domain	-1.08		
Ec-18_004020	thioredoxin-like protein	-0.80		
Ec-26_002300	arsenite translocating ATPase like protein	-1.04		
Ec-06_004170	uroporphyrinogen-III C-methyltransferase, putative chloroplast precursor	-0.66	Cu+19	
Ec-00_003170	hypothetical protein	-1.03	Cu+19	19 only
Ec-24_001870	Similar to transporters, possibly for inorganic phosphate.	-1.01		
Ec-12_002640	Galactose-binding domain-like	-0.69		
Ec-06_003040	Cyclin, C-terminal domain	-0.64		
Ec-12_007270	expressed unknown protein	-0.67		
Ec-00_007780	Carbohydrate-binding WSC	-1.03	Cu+19	
Ec-03_003765	lncRNA	-1.64		
Ec-04_003630	Sugar/inositol transporter	-0.80		
Ec-04_003740	Glycoside hydrolase family 31	-0.71		
Ec-05_000930	Zinc finger, RING/FYVE/PHD-type	-2.34		
Ec-28_002800	conserved unknown protein	-1.33		
Ec-05_005200	expressed unknown protein	-0.92		
Ec-14_002300	Zn(2)-C6 fungal-type DNA-binding domain	-0.98		
Ec-15_002850	Heat shock protein 40 like protein/ DnaJ domain containing protein	-1.06		
Ec-23_001670	Helicase, C-terminal	-1.23		

Ec-27_006050	P-loop containing nucleoside triphosphate hydrolase	-1.27		
Ec-25_003160	P-type ATPase, subfamily IV	-1.44		
Ec-27_004960	protein of unknown function DUF399	-0.78		
Ec-08_003230	Tuf1, mitochondrial translation elongation factor EF-Tu	-0.71		
Ec-11_004850	Hypothetical leucine rich repeat protein	-0.88		
Ec-04_001840	conserved unknown protein	-0.79		
Ec-19_005180	hypothetical protein	-1.36		
Ec-21_002720	hypothetical protein	-3.00		
Ec-25_003210	DEAD box helicase DEAD/DEAH box helicase-like protein	-0.90		
Ec-06_007670	Cation-transporting P-type ATPase, N-terminal	-1.07		
Ec-05_002840	Potassium channel tetramerisation-type BTB domain	-0.78		
Ec-06_010790	Zn-dependent peptidase, Cym1 homolog	-0.76		
Ec-12_001740	expressed unknown protein	-0.74	Cu+19	
Ec-15_000060	Nucleotide-binding alpha-beta plait domain	-1.16		
Ec-27_006520	Photosystem II Psp29, biogenesis	-0.61		
Ec-03_002340	Pentatricopeptide repeat	-0.82		
Ec-17_002950	P-loop containing nucleoside triphosphate hydrolase	-0.74		
Ec-06_002630	Ankyrin repeat-containing domain	-1.25		
Ec-06_007470	NB-ARC	-0.75		
Ec-26_004480	Ubiquitin-conjugating enzyme E2	-0.87		
Ec-18_003040	expressed unknown protein	-0.80		
Ec-01_003020	expressed unknown protein	0.74		
Ec-25_000360	expressed unknown protein	1.54	Cu+19	
Ec-11_003300	expressed unknown protein	0.61	Cu+19	
Ec-21_005960	expressed unknown protein	0.96		
Ec-05_002200	WW domain	2.79		
Ec-27_001170	Endo-1,3-beta-glucanase N-terminal fragment, family GH16	0.73		
Ec-18_000270	conserved unknown protein	1.34		
Ec-04_006375	lncRNA	1.14		
Ec-22_003040	expressed unknown protein	0.88		
Ec-10_001490	Hypothetical protein	1.30	Cu+19	
Ec-07_000710	FAD-dependent pyridine nucleotide-disulphide oxidoreductase	0.71		

Ec-07_005530	expressed unknown protein	0.55	Cu+19	
Ec-01_007180	hypothetical protein	1.15		
Ec-07_001410	hypothetical protein	1.02		
Ec-07_002630	Notch domain	1.48		
Ec-08_003380	Hypothetical protein	1.00	Cu+19	
Ec-20_001230	Metallothionein	0.57	Cu+19	
Ec-03_000500	Carbohydrate-binding WSC, subgroup	1.61	Cu+19	
Ec-03_002980	Pectin lyase fold/virulence factor	0.69		
Ec-15_000430	Hypothetical protein	0.90		
Ec-03_005230	expressed unknown protein	0.56		
Ec-11_000420	PHM/PNGase F domain	2.27	Cu+19	
Ec-01_003000	Hypothetical protein	0.81		
Ec-06_004500	Domain of unknown function DUF4149	0.64	3 Conditions	
Ec-28_002600	Major intrinsic protein	0.99	Cu+19	
Ec-17_002080	Light harvesting complex protein	0.63		
Ec-27_002910	hypothetical protein	0.86		
Ec-04_006420	similar to 40S ribosomal protein S29	0.59	Cu+19	
Ec-02_003400	Light harvesting complex protein	0.67	Cu+19	
Ec-04_000450	TALE homeobox domain transcription factor	1.68	Cu+19	
Ec-05_006380	expressed unknown protein	0.82		
Ec-24_001530	DnaJ domain	0.80		
Ec-13_003370	expressed unknown protein	1.39	3 Conditions	
Ec-13_000880	expressed unknown protein	0.98	Cu+19	
Ec-26_001960	hypothetical protein	0.87		
Ec-06_009330	Fibronectin type III	0.72		
Ec-22_001570	Bicarbonate transporter, eukaryotic	0.75		
Ec-08_004400	WD40-repeat-containing domain	1.01		
Ec-21_005340	Ankyrin repeat-containing domain	1.15	Cu+19	
Ec-17_004020	expressed unknown protein	0.79		
Ec-05_000640	dynein heavy chain	0.71	Cu+19	
Ec-15_000480	UBA-like	0.60	Cu+19	
Ec-01_009740	Light harvesting complex protein	0.66	3 Conditions	
Ec-27_002790	Methyltransferase type 11	0.71		
Ec-00_011005	lncRNA	4.73		
Ec-01_010930	SPRY domain	0.77	Cu+19	
Ec-14_000700	expressed unknown protein	0.79		
Ec-21_004210	expressed unknown protein	0.75	Cu+19	
Ec-03_002760	cdk10/11, putative	1.17		
Ec-19_002690	expressed unknown protein	3.36		
Ec-25_001520	Pectin lyase fold/virulence factor	1.48		

Ec-26_006150	HPP family protein	0.73	Cu+19	
Ec-28_001370	Hypothetical protein	1.06	3 Conditions	
Ec-15_000985	lncRNA	1.17	3 Conditions	
Ec-13_003800	Hypothetical protein	0.90		
Ec-24_001000	expressed unknown protein	0.68	3 Conditions	
Ec-25_000220	Destroys Superoxide radical to produce hydrogen peroxide	0.76	3 Conditions	
Ec-14_002150	Hypothetical protein	0.89	19 only	
Ec-07_006020	NUDIX hydrolase domain-like	0.78	3 Conditions	
Ec-00_000740	Hypothetical protein	0.99	3 Conditions	
Ec-08_002830	Hypothetical protein	0.95		
Ec-20_003840	conserved unknown protein	1.13		
Ec-00_009510	expressed unknown protein	1.23		
Ec-00_010970	Hypothetical protein	0.98		
Ec-25_002750	Aminotransferase	0.88	Cu+19	
Ec-23_001870	WD40 repeat	1.77		
Ec-18_001740	Light harvesting complex protein	0.73	3 Conditions	
Ec-09_001490	Leucine rich repeat protein	1.33	Cu+19	
Ec-04_001370	imm downregulated 2	1.01		
Ec-20_003270	Hypothetical leucine rich repeat protein	0.84	3 Conditions	
Ec-17_002600	conserved unknown protein	1.25	Cu+19	
Ec-06_008230	Peptidase C2, calpain, large subunit, domain III	1.41	Cu+19	
Ec-19_000800	Hypothetical protein	0.80	Cu+19	
Ec-28_001310	Alpha-ketoglutarate-dependent dioxygenase AlkB-like	1.17		
Ec-09_004610	Ankyrin repeat-containing domain	3.13		
Ec-12_008150	PKD/REJ-like protein	1.11	3 Conditions	
Ec-13_003220	expressed unknown protein	1.15		
Ec-25_001580	hypothetical protein	2.04	Cu+19	
Ec-06_003380	Hypothetical protein	1.17		
Ec-22_001500	Carbohydrate-binding WSC	1.99	Cu+19	
Ec-08_005100	expressed unknown protein	3.56		

Table S5.2. List of differentially expressed genes (DE) in *E. siliculosus* under thermal stress only. Positive Log_2 fold-change values indicate up-regulated genes and negative values down-regulated genes.

Gene Id	Description	log2 Fold Change	DE in other treatment	
Ec-19_000740	conserved unknown protein	-2.12	Cu+19	
Ec-19_004140	Hypothetical protein	-3.11	Cu+19	
Ec-19_004130	Nitrate high affinity transporter	-2.15	Cu+19	
Ec-02_006190	expressed unknown protein	-1.26	Cu+19	
Ec-06_000710	Light harvesting complex protein	-1.24	3 Conditions	
Ec-26_005070	conserved unknown protein	-0.80	Cu+19	
Ec-06_004000	PAS domain	-1.21	Cu+19	
Ec-12_003080	conserved unknown protein	-1.00	Cu+19	
Ec-24_001600	CCT domain	-0.97		
Ec-12_005560	branched chain amino acid aminotransferase	-1.16	Cu+19	
Ec-13_002100	PBipA, plastid GTPase BipA/TypA	-0.96	Cu+19	
Ec-19_004170	Nitrate high affinity transporter	-1.42	Cu+19	
Ec-07_001970	conserved unknown protein	-0.92	Cu+19	
Ec-11_000370	SAM-dependent methyltransferases	-0.87	3 Conditions	
Ec-07_000700	Pectin lyase fold/virulence factor	-1.96	Cu+19	
Ec-05_006520	conserved unknown protein	-0.96		
Ec-19_004180	Nitrate high affinity transporter	-1.33	Cu+19	
Ec-23_001940	P-loop containing nucleoside triphosphate hydrolase	-1.18		
Ec-10_002450	Pyridoxal 5'-phosphate synthase	-0.65	Cu+19	
Ec-19_004730	hypothetical protein	-0.92		
Ec-06_000490	Light harvesting complex protein	-1.01	Cu+19	
Ec-06_000510	Chlorophyll A-B binding protein	-1.14	Cu+19	
Ec-08_003700	Peptidase M50	-1.92		
Ec-14_004380	DEAD box helicase	-1.50	Cu+19	
Ec-06_000470	Light harvesting complex protein	-1.03		
Ec-18_004560	Major facilitator superfamily domain	-0.88	Cu+19	
Ec-03_001980	hypothetical protein	-2.69	Cu+19	
Ec-27_004730	Domain of unknown function DUF4098	-0.65		
Ec-27_002000	Deoxyhypusine synthase	-0.87		
Ec-23_002100	High mobility group and SAP domain protein	-1.04	Cu+19	
Ec-28_003120	Light harvesting complex protein	-0.86	Cu+19	
Ec-18_003710	Major facilitator superfamily	-0.95		

Ec-06_000750	Light harvesting complex protein	-0.62	Cu+19	
Ec-01_003170	Hypothetical leucine rich repeat protein	-3.23		
Ec-07_001160	related to flotillin	-0.62	Cu+19	
Ec-01_006280	Beta-lactamase-like	-0.96		
Ec-27_004210	2Fe-2S ferredoxin-type domain	-1.01		
Ec-19_001380	expressed unknown protein	-1.31	Cu+19	
Ec-06_002400	Ankyrin repeat Transient receptor potential channel	-2.27		
Ec-26_005570	hypothetical protein	-0.88		
Ec-12_008200	L-fucokinase	-0.80		
Ec-06_000450	Light harvesting complex protein	-0.92	Cu+19	
Ec-13_001170	Ctr copper transporter	0.83	Cu only	Cu+19
Ec-07_007480	Ferric reductase, NAD binding	2.43	Cu only	Cu+19
Ec-18_002770	Ferric reductase, NAD binding	1.72	Cu only	Cu+19
Ec-06_004500	Domain of unknown function DUF4149	0.94	3 Conditions	
Ec-13_003370	expressed unknown protein	1.43	3 Conditions	
Ec-01_009740	Light harvesting complex protein	0.76	3 Conditions	
Ec-28_001370	Hypothetical protein	1.23	3 Conditions	
Ec-15_000985	lncRNA	1.25	3 Conditions	
Ec-24_001000	expressed unknown protein	0.72	3 Conditions	
Ec-25_000220	Destroys Superoxide radical to produce hydrogen peroxide	0.73	3 Conditions	
Ec-14_002150	Hypothetical protein	0.82	Cu only	
Ec-07_006020	NUDIX hydrolase domain-like	0.71	3 Conditions	
Ec-00_000740	Hypothetical protein	1.16	3 Conditions	
Ec-00_003170	hypothetical protein	1.51	Cu only	Cu+19
Ec-18_001740	Light harvesting complex protein	0.76	3 Conditions	
Ec-20_003270	Hypothetical leucine rich repeat protein	0.80	3 Conditions	
Ec-12_008150	PKD/REJ-like protein	0.97	3 Conditions	
Ec-15_001030	Light harvesting complex protein	0.88	Cu+19	
Ec-27_001370	conserved unknown protein	0.66	Cu+19	
Ec-27_003550	S-adenosyl-L-methionine-dependent methyltransferase	1.57	Cu+19	
Ec-17_002070	Light harvesting complex protein	0.62	Cu+19	
Ec-01_008960	Light harvesting complex protein	0.92	Cu+19	
Ec-13_001430	conserved unknown protein	0.71	Cu+19	
Ec-05_000320	expressed unknown protein	1.81	Cu+19	
Ec-12_008990	conserved unknown protein	0.78		
Ec-17_004130	ribosomal protein rpS22, plastidal	0.66	Cu+19	

Ec-10_003830	expressed unknown protein	1.06	Cu+19	
Ec-00_011110	Ferric reductase transmembrane component-like domain	2.68		
Ec-02_004790	hypothetical protein	0.77		
Ec-07_001300	Hypothetical leucine rich repeat protein	0.78	Cu+19	
Ec-20_001820	EF-hand domain pair	1.01	Cu+19	
Ec-12_001610	expressed unknown protein	0.85	Cu+19	
Ec-02_000550	hypothetical protein	0.90	Cu+19	
Ec-07_004930	Protein of unknown function DUF4281	1.05	Cu+19	
Ec-16_004460	AAA+ ATPase domain	0.90	Cu+19	
Ec-20_004070	expressed unknown protein	0.86	Cu+19	
Ec-00_001440	ATP-dependent Clp protease adaptor protein ClpS	0.79	Cu+19	
Ec-07_000770	Hypothetical protein	0.89	Cu+19	
Ec-26_005830	Histone H1	1.01	Cu+19	
Ec-11_004380	Ribosomal protein L7/L12, C-terminal/adaptor protein ClpS-like	0.68	Cu+19	
Ec-19_001040	Protein kinase-like domain	0.84	Cu+19	
Ec-15_003100	isochorismatase	0.83	Cu+19	
Ec-07_000520	Histone H2A	1.45	Cu+19	
Ec-00_009420	Ferric reductase, NAD binding	2.58		
Ec-01_010625	lncRNA	1.12	Cu+19	
Ec-13_000140	expressed unknown protein	0.67		
Ec-03_004400	hypothetical protein	0.98		
Ec-18_003120	Amino acid transporter, transmembrane	0.65	Cu+19	
Ec-22_001980	Alpha/Beta hydrolase fold	1.00	Cu+19	
Ec-12_002080	hypothetical protein	0.97		
Ec-17_001380	Light harvesting complex protein	0.69	Cu+19	
Ec-28_003780	Metacapase	1.40	Cu+19	
Ec-15_000280	oxt	1.03	Cu+19	
Ec-12_004990	Light harvesting complex protein	0.91	Cu+19	
Ec-26_006480	Histone H1	1.01	Cu+19	
Ec-00_006340	ferric reductase	4.35		
Ec-13_000270	expressed unknown protein	1.48	Cu+19	
Ec-05_003700	expressed unknown protein	1.17	Cu+19	
Ec-03_002070	hypothetical protein	2.18	Cu+19	
Ec-13_001890	Conserved hypothetical protein	0.79	Cu+19	

Table S5.3. List of differentially expressed genes (DE) in *E. siliculosus* under a combination of thermal and Cu stress. Positive Log_2 fold-change values indicate up-regulated genes and negative values down-regulated genes.

Gene Id	Description	log2 Fold Change	DE in other treatment	
Ec-13_001170	Ctr copper transporter	-2.30	Cu only	19 only
Ec-13_001020	Ctr copper transporter	-2.13	Cu only	
Ec-03_002320	Methyltransferase type 11	-1.95	Cu only	
Ec-07_007480	Ferric reductase, NAD binding	-3.39	Cu only	19 only
Ec-18_002770	Ferric reductase, NAD binding	-1.90	Cu only	19 only
Ec-11_000370	SAM-dependent methyltransferases	-0.92	3 Conditions	
Ec-14_001470	K Homology domain	-1.56	Cu only	
Ec-17_003230	expressed unknown protein	-0.88	Cu only	
Ec-03_004150	expressed unknown protein	-0.87	Cu only	
Ec-06_008970	expressed unknown protein	-1.07	Cu only	
Ec-19_004150	Nitrate high affinity transporter	-0.93	Cu only	
Ec-06_002470	Uricase	-0.73	Cu only	
Ec-03_002310	Hypothetical protein	-2.16	Cu only	
Ec-08_000840	PObg2, plastid Obg/CgtA-like GTPase 2	-1.43	Cu only	
Ec-06_000710	Light harvesting complex protein	-1.73	3 Conditions	
Ec-06_004170	uroporphyrinogen-III C-methyltransferase, putative chloroplast precursor	-0.75	Cu only	
Ec-00_003170	hypothetical protein	-1.45	Cu only	19 only
Ec-25_002750	Aminotransferase	-0.73	Cu only	
Ec-12_001740	expressed unknown protein	-0.77	Cu only	
Ec-19_004160	Nitrate high affinity transporter; pseudogene	-0.86		
Ec-19_004180	Nitrate high affinity transporter	-1.43	19 only	
Ec-08_005210	Ubiquitin-associated/translation elongation factor EF1B, N-terminal, eukaryote	-0.68		
Ec-26_001450	Zinc/iron permease	-1.64		
Ec-01_005650	Basic-leucine zipper and PAS domains	-1.53		
Ec-14_004380	DEAD box helicase	-1.45	Cu only	
Ec-21_003750	hypothetical protein	-0.80		
Ec-12_002050	Formylglycine-dependent sulfatase	-0.68		
Ec-07_001150	Flotillin	-0.80		
Ec-06_003280	Protein of unknown function DUF924	-2.53		
Ec-12_005560	branched chain amino acid aminotransferase	-1.29	Cu only	
Ec-22_002150	nucleolar complex associated 2 homolog	-1.39		
Ec-14_005360	expressed unknown protein	-0.71		

Ec-02_002750	EsV-1-7 domain protein	-0.89		
Ec-17_003860	DEAD box helicase	-1.06		
Ec-19_000740	conserved unknown protein	-1.57	19 only	
Ec-19_001380	expressed unknown protein	-1.17	19 only	
Ec-02_006190	expressed unknown protein	-1.05	19 only	
Ec-01_010650	hypothetical protein	-1.10		
Ec-13_002100	PBipA, plastid GTPase BipA/TypA	-0.93	19 only	
Ec-17_001300	RIO-like kinase	-0.66		
Ec-08_002960	LRR-GTPase of the ROCO family	-1.14		
Ec-14_001520	aldo/keto reductase family protein	-0.89		
Ec-08_004350	Proteasome, subunit alpha/beta	-0.88		
Ec-03_001980	hypothetical protein	-3.25	19 only	
Ec-27_000530	Pyruvate dehydrogenase E1 component alpha subunit, mitochondrial precursor (PDHE1-A)	-0.72		
Ec-19_004140	Hypothetical protein	-3.32	19 only	
Ec-10_004800	SH2 domain containing protein	-1.16		
Ec-21_004770	conserved unknown protein	-0.80		
Ec-16_002910	expressed unknown protein	-1.36		
Ec-23_002100	High mobility group and SAP domain protein	-0.98	19 only	
Ec-28_003120	Light harvesting complex protein	-0.97	19 only	
Ec-06_000470	Light harvesting complex protein	-1.08	19 only	
Ec-07_001970	conserved unknown protein	-0.96	19 only	
Ec-28_001400	Histone deacetylase	-0.81		
Ec-19_004130	Nitrate high affinity transporter	-2.27	19 only	
Ec-19_004170	Nitrate high affinity transporter	-1.44	19 only	
Ec-05_005600	Heat shock protein 70	-0.94		
Ec-16_004540	PAB-dependent poly(A)-specific ribonuclease subunit PAN2	-0.99		
Ec-14_001790	Serine/threonine protein kinase	-1.32		
Ec-06_000550	Light harvesting complex protein	-1.09		
Ec-06_000510	Chlorophyll A-B binding protein	-1.04	19 only	
Ec-26_004490	26S proteasome subunit like protein	-0.70		
Ec-12_003080	conserved unknown protein	-0.74	19 only	
Ec-06_004000	PAS domain	-1.16	19 only	
Ec-12_005050	expressed unknown protein	-0.86		
Ec-26_003060	Urea/Na+ high-affinity symporter	-0.52		
Ec-06_000750	Light harvesting complex protein	-1.02	19 only	
Ec-28_002950	Friend of PRMT1 duplication	-0.74		
Ec-06_001490	XPG-I domain	-1.73		
Ec-01_011040	Glutamate:glyoxylate aminotransferase	-1.00		

Ec-06_000460	Light harvesting complex protein	-0.82		
Ec-25_003130	Serine/threonine/dual specificity protein kinase, catalytic domain	-0.86		
Ec-06_000540	Chlorophyll A-B binding protein, plant	-1.25		
Ec-17_003620	Mitochondrial substrate/solute carrier	-0.73		
Ec-26_005070	conserved unknown protein	-1.10	19 only	
Ec-06_000490	Light harvesting complex protein	-1.32	19 only	
Ec-18_004550	Ornithine cyclodeaminase	-1.11		
Ec-25_000900	Casein kinase II, regulatory subunit	-0.69		
Ec-05_006350	Soluble NSF Attachment Protein (SNAP) Receptor (SNARE)	-1.04		
Ec-03_000330	Domain of unknown function DUF4440	-0.68		
Ec-10_002450	Pyridoxal 5'-phosphate synthase	-0.64	19 only	
Ec-18_004560	Major facilitator superfamily domain	-1.18	19 only	
Ec-27_002480	expressed unknown protein	-0.91		
Ec-06_000570	Light harvesting complex protein	-0.73		
Ec-14_000940	hypothetical protein	-0.79		
Ec-04_000060	Cyclophilin-like domain	-0.83		
Ec-06_000450	Light harvesting complex protein	-1.18	19 only	
Ec-07_001160	related to flotillin	-0.63	19 only	
Ec-16_002170	conserved unknown protein	-1.00		
Ec-20_001680	Protein of unknown function DUF2419	-0.93		
Ec-25_000360	expressed unknown protein	1.53	Cu only	
Ec-11_003300	expressed unknown protein	0.76	Cu only	
Ec-10_001490	Hypothetical protein	1.38	Cu only	
Ec-07_005530	expressed unknown protein	0.77	Cu only	
Ec-08_003380	Hypothetical protein	1.50	Cu only	
Ec-20_001230	Metallothionein	0.72	Cu only	
Ec-03_000500	Carbohydrate-binding WSC, subgroup	1.66	Cu only	
Ec-11_000420	PHM/PNGase F domain	2.18	Cu only	
Ec-06_004500	Domain of unknown function DUF4149	1.11	3 Conditions	
Ec-28_002600	Major intrinsic protein	1.10	Cu only	
Ec-04_006420	similar to 40S ribosomal protein S29	0.71	Cu only	
Ec-02_003400	Light harvesting complex protein	0.69	Cu only	
Ec-04_000450	TALE homeobox domain transcription factor	1.70	Cu only	
Ec-13_003370	expressed unknown protein	1.67	3 Conditions	
Ec-13_000880	expressed unknown protein	1.10	Cu only	
Ec-21_005340	Ankyrin repeat-containing domain	1.30	Cu only	
Ec-05_000640	dynein heavy chain	0.91	Cu only	

Ec-15_000480	UBA-like	0.82	Cu only	
Ec-01_009740	Light harvesting complex protein	0.92	3 Conditions	
Ec-01_010930	SPRY domain	0.85	Cu only	
Ec-21_004210	expressed unknown protein	0.70	Cu only	
Ec-26_006150	HPP family protein	0.74	Cu only	
Ec-28_001370	Hypothetical protein	1.15	3 Conditions	
Ec-15_000985	lncRNA	1.87	3 Conditions	
Ec-24_001000	expressed unknown protein	0.92	3 Conditions	
Ec-25_000220	Destroys Superoxide radical to produce hydrogen peroxide	1.18	3 Conditions	
Ec-07_006020	NUDIX hydrolase domain-like	0.96	3 Conditions	
Ec-00_000740	Hypothetical protein	1.53	3 Conditions	
Ec-00_007780	Carbohydrate-binding WSC	1.03	Cu only	
Ec-18_001740	Light harvesting complex protein	1.01	3 Conditions	
Ec-09_001490	Leucine rich repeat protein	1.71	Cu only	
Ec-20_003270	Hypothetical leucine rich repeat protein	1.11	3 Conditions	
Ec-17_002600	conserved unknown protein	1.44	Cu only	
Ec-06_008230	Peptidase C2, calpain, large subunit, domain III	1.50	Cu only	
Ec-19_000800	Hypothetical protein	0.63	Cu only	
Ec-12_008150	PKD/REJ-like protein	0.95	3 Conditions	
Ec-25_001580	hypothetical protein	1.85	Cu only	
Ec-22_001500	Carbohydrate-binding WSC	4.66	Cu only	
Ec-20_003900	Protochlorophyllide reductase, putative chloroplast precursor	0.89		
Ec-13_001040	hypothetical protein	1.36		
Ec-27_000810	Hypothetical protein	0.92		
Ec-08_003290	Light harvesting complex protein	0.86		
Ec-02_000430	Glutaredoxin	0.83		
Ec-25_003800	Light harvesting complex protein	0.71		
Ec-28_003750	S-adenosyl-L-methionine-dependent methyltransferase	1.08		
Ec-15_001030	Light harvesting complex protein	1.07	19 only	
Ec-02_004180	Uncharacterised protein family Cys-rich	1.31		
Ec-08_005750	Novel protein containing IQ calmodulin-binding motif	1.14		
Ec-27_001370	conserved unknown protein	0.86	19 only	
Ec-27_003550	S-adenosyl-L-methionine-dependent methyltransferase	2.09	19 only	
Ec-17_002070	Light harvesting complex protein	0.83	19 only	
Ec-11_005720	molybdopterin synthase	0.91		

Ec-02_005010	photosystem II 11 kDa protein	0.70		
Ec-16_003200	MORN motif	1.66		
Ec-09_001420	Hypothetical leucine rich repeat protein	1.75		
Ec-18_001730	Light harvesting complex protein	0.59		
Ec-07_003700	Beta-lactamase-like	0.78		
Ec-01_008960	Light harvesting complex protein	1.20	19 only	
Ec-14_003040	WD40/YVTN repeat-like-containing domain	0.68		
Ec-03_002210	Hypothetical leucine rich repeat protein	1.08		
Ec-28_000560	photosystem II 12 kDa extrinsic protein	0.61		
Ec-13_001430	conserved unknown protein	0.75	19 only	
Ec-00_011010	conserved unknown protein	1.21		
Ec-11_001780	conserved unknown protein	0.70		
Ec-12_007670	Armadillo-like helical	0.87		
Ec-05_000320	expressed unknown protein	1.68	19 only	
Ec-05_006280	Putative Metallothionein	0.85		
Ec-22_003120	Carbohydrate-binding WSC	1.44		
Ec-03_003130	Uncharacterised domain, di-copper centre	1.94		
Ec-09_001360	Kinesin motor domain protein	2.53		
Ec-09_000090	Hypothetical protein	1.63		
Ec-20_003820	conserved unknown protein	3.58		
Ec-17_004070	Ribosomal protein S30	0.57		
Ec-06_001890	Ribosomal protein L31e	0.59		
Ec-12_006020	expressed unknown protein	0.59		
Ec-17_004130	ribosomal protein rpS22, plastidal	0.74	19 only	
Ec-06_001970	hypothetical protein	1.56		
Ec-10_003830	expressed unknown protein	0.84	19 only	
Ec-27_007040	expressed unknown protein	1.06		
Ec-28_003810	Metacaspase	1.51		
Ec-11_001410	Triose-phosphate transporter domain	1.96		
Ec-18_000080	dihydrolipoamide acetyltransferase	0.57		
Ec-18_002270	alpha tubulin	0.63		
Ec-10_002900	Ribosomal protein L14b/L23e	0.51		
Ec-22_000400	similar to voltage-dependent calcium channel T-type alpha 1I subunit	1.09		
Ec-23_000590	expressed unknown protein	0.70		
Ec-18_002350	Phospholipid methyltransferase	0.77		
Ec-00_009430	Hypothetical protein	0.95		
Ec-15_001000	Light harvesting complex protein	1.05		
Ec-14_002020	expressed unknown protein	1.41		
Ec-14_006200	Isochorismatase-like	0.73		

Ec-07_001300	Hypothetical leucine rich repeat protein	0.67	19 only	
Ec-20_001820	EF-hand domain pair	1.12	19 only	
Ec-00_006310	Light harvesting complex protein	1.16		
Ec-19_003550	imm downregulated 17	0.72		
Ec-26_000690	conserved unknown protein	1.73		
Ec-00_008830	Cysteine synthase	0.72		
Ec-08_002570	Heat shock factor binding 1	0.68		
Ec-07_001760	conserved unknown protein	0.93		
Ec-12_001610	expressed unknown protein	1.03	19 only	
Ec-05_000630	Manganese/iron superoxide dismutase, C-terminal	0.81		
Ec-25_001570	Pectin lyase fold/virulence factor	0.60		
Ec-22_003190	Hypothetical protein	6.00		
Ec-25_001850	Mannuronan C-5-epimerase	0.98		
Ec-02_000550	hypothetical protein	1.18	19 only	
Ec-00_011420	ADP-ribosylation factor-like 2-binding protein, domain	2.67		
Ec-04_003100	conserved unknown protein	2.34		
Ec-06_008360	Ribosomal protein L5	0.56		
Ec-14_002010	Protein of unknown function DUF3110	1.54		
Ec-13_003330	expressed unknown protein	0.69		
Ec-08_001410	expressed unknown protein	0.85		
Ec-27_006510	Hypothetical protein	1.15		
Ec-17_000680	Ribosomal protein L27e	0.59		
Ec-24_003810	von Willebrand factor, type A	1.55		
Ec-27_002850	expressed unknown protein	2.90		
Ec-01_006720	Ribosomal protein S17	0.57		
Ec-19_003360	hypothetical protein	2.66		
Ec-11_004470	expressed unknown protein	0.94		
Ec-23_000020	mitogen-activated protein kinase	1.39		
Ec-07_004930	Protein of unknown function DUF4281	1.13	19 only	
Ec-10_000290	expressed unknown protein	0.78		
Ec-19_003980	Domain of unknown function DUF1995	0.76		
Ec-16_004460	AAA+ ATPase domain	1.06	19 only	
Ec-20_004070	expressed unknown protein	1.23	19 only	
Ec-08_000110	Carbohydrate-binding WSC, subgroup	6.07		
Ec-07_001470	Light harvesting complex protein	0.61		
Ec-02_006130	expressed unknown protein	1.47		
Ec-03_003300	Thioredoxin-like protein	0.60		
Ec-14_001610	conserved unknown protein	0.77		

Ec-26_003850	PDZ domain	0.83		
Ec-00_001440	ATP-dependent Clp protease adaptor protein ClpS	0.93	19 only	
Ec-07_000770	Hypothetical protein	0.78	19 only	
Ec-22_000290	40S ribosomal protein S4	0.52		
Ec-22_003160	WSC domain protein	4.79		
Ec-05_001620	conserved unknown protein	0.70		
Ec-01_009180	conserved carbohydrate binding protein	0.65		
Ec-22_002520	S-Adenosylmethionine decarboxylase	0.82		
Ec-28_001760	40S ribosomal protein S15	0.60		
Ec-19_000350	Hypothetical protein	1.12		
Ec-07_007580	hypothetical protein	0.65		
Ec-25_002570	40S ribosomal protein S12	0.48		
Ec-06_003350	expressed unknown protein	0.70		
Ec-24_004350	hypothetical protein	4.28		
Ec-01_002470	expressed unknown protein	2.56		
Ec-26_005830	Histone H1	1.05	19 only	
Ec-10_003480	Bulb-type lectin domain	0.70		
Ec-18_002220	alpha tubulin	0.55		
Ec-26_002130	Phosphoadenylyl-sulfate reductase (thioredoxin)	0.68		
Ec-27_005070	FAS1 domain	1.12		
Ec-21_000950	von Willebrand factor, type D domain	1.87		
Ec-11_004380	Ribosomal protein L7/L12, C-terminal/adaptor protein ClpS-like	0.72	19 only	
Ec-02_005390	Ribosomal protein L19/L19e domain	0.49		
Ec-25_001870	hypothetical protein	2.12		
Ec-17_003020	similar to ubiquitin specific protease 34	0.64		
Ec-10_002270	expressed unknown protein	1.61		
Ec-12_003210	plastidic ATP/ADP transporter	0.86		
Ec-19_001050	immunophilin	0.92		
Ec-13_000750	Thioredoxin domain	0.69		
Ec-06_011040	Kinesin light chain	3.38		
Ec-05_006630	Likely pseudogene	6.28		
Ec-00_008740	conserved unknown protein	3.99		
Ec-00_005880	hypothetical protein	1.63		
Ec-19_001040	Protein kinase-like domain	1.32	19 only	
Ec-15_003100	isochorismatase	0.94	19 only	
Ec-10_003790	Carbohydrate-binding WSC	2.46		
Ec-11_004820	Polyketide cyclase SnoaL-like domain	0.82		

Ec-03_004780	class-V aminotransferase	1.36		
Ec-19_005110	Triose phosphate/phosphate translocator, non-green plastid, chloroplast precursor (CTPT), C-terminal	1.24		
Ec-19_004240	Light harvesting complex protein	0.69		
Ec-15_000987	lncRNA	1.05		
Ec-16_004840	Ribosomal protein L38e	0.72		
Ec-07_000520	Histone H2A	1.60	19 only	
Ec-08_000100	von Willebrand factor, type D domain	2.57		
Ec-08_000710	putative FKBP-type peptidyl-prolyl cis-trans isomerase 2	0.83		
Ec-22_002060	Ribosomal protein L13e	0.51		
Ec-27_006390	conserved unknown protein	3.27		
Ec-11_003900	Sec20	1.12		
Ec-01_000660	Regulator of chromosome condensation 1/beta-lactamase-inhibitor protein II	1.21		
Ec-02_000560	hypothetical protein	1.01		
Ec-01_010625	lncRNA	1.19	19 only	
Ec-06_010720	2Fe-2S ferredoxin-type domain	0.67		
Ec-03_000520	Carbohydrate-binding WSC	2.39		
Ec-10_002620	30s ribosomal protein S13, C-terminal	0.52		
Ec-19_002440	40S ribosomal protein S17	0.50		
Ec-15_000205	lncRNA	6.15		
Ec-18_000060	Immunoglobulin E-set	0.68		
Ec-12_004390	Amidinotransferase	1.91		
Ec-23_002610	hypothetical protein	5.13		
Ec-18_001040	Heat shock protein 90	0.68		
Ec-15_002990	conserved unknown protein	0.98		
Ec-21_005170	Armadillo-type fold	4.38		
Ec-18_003120	Amino acid transporter, transmembrane	0.84	19 only	
Ec-05_006590	Carbohydrate-binding WSC	3.41		
Ec-03_003550	expressed unknown protein	0.70		
Ec-21_006210	Acetyl-coenzyme A synthetase	0.69		
Ec-22_001980	Alpha/Beta hydrolase fold	0.86	19 only	
Ec-00_007250	Carbohydrate-binding WSC, subgroup	0.60		
Ec-05_001780	Ribosomal protein L23	0.65		
Ec-24_003860	von Willebrand A domain containing protein	1.77		
Ec-17_000970	Carbohydrate-binding WSC, subgroup	0.89		
Ec-17_002100	60S ribosomal protein L35	0.53		
Ec-17_001380	Light harvesting complex protein	0.63	19 only	

Ec-28_003780	Metacaspase	1.66	19 only	
Ec-10_004190	beta(1,4)-N-acetylglucosaminyltransferase	0.79		
Ec-02_001470	60S ribosomal protein L6E	0.53		
Ec-15_000280	oxt	1.46	19 only	
Ec-15_003500	Six-bladed beta-propeller, TolB-like	1.41		
Ec-18_000660	Lipase, GDSL	2.92		
Ec-18_004390	expressed unknown protein	0.79		
Ec-11_003180	protein disulfide isomerase fusion protein	0.79		
Ec-27_006700	Mannuronan C-5-epimerase	1.11		
Ec-08_005760	Ribosomal protein L1, 2-layer alpha/beta-sandwich	0.49		
Ec-22_003210	hypothetical protein	5.11		
Ec-03_002270	hypothetical protein	4.41		
Ec-16_004860	Ribosomal protein S10, eukaryotic/archaeal	0.56		
Ec-11_000990	conserved unknown protein	0.70		
Ec-12_004990	Light harvesting complex protein	0.89	19 only	
Ec-19_003230	Acetyl-CoA carboxylase, partial	0.65		
Ec-00_010800	Mannuronan C-5-epimerase	0.55		
Ec-00_007790	Hypothetical protein	1.10		
Ec-15_000630	WSC-domain containing protein	0.97		
Ec-21_001560	HSP20-like chaperone	0.85		
Ec-26_001040	conserved secreted protein	2.62		
Ec-01_011860	Ribosomal protein L22e	0.58		
Ec-16_001460	60S ribosomal protein L12	0.69		
Ec-23_002620	hypothetical protein	5.34		
Ec-26_006480	Histone H1	1.02	19 only	
Ec-08_005220	sperm flagellar energy carrier protein	0.57		
Ec-12_006757	lncRNA	1.11		
Ec-24_004480	RGS domain	2.02		
Ec-15_000200	hypothetical protein	7.76		
Ec-13_000270	expressed unknown protein	2.08	19 only	
Ec-06_000690	2Fe-2S ferredoxin-type domain	0.67		
Ec-15_004870	contains SCP domain which is found in plant PR1 and cysteine-rich proteins	4.12		
Ec-10_001320	NAD(P)-binding domain	0.77		
Ec-08_003610	SAP domain	0.74		
Ec-12_004060	Bardet-Biedl syndrome 9, parathyroid hormone-responsive B1	3.28		
Ec-20_002340	Mitochondrial carrier protein, putative	1.12		
Ec-05_003700	expressed unknown protein	1.52	19 only	

Ec-22_000660	SANT/Myb domain	1.14		
Ec-13_002330	Pectin lyase fold	4.57		
Ec-22_001550	hypothetical protein	7.44		
Ec-05_003380	Catalase is an enzyme, present in all aerobic cells, that decomposes hydrogen peroxide to molecular	0.82		
Ec-03_002070	hypothetical protein	1.89	19 only	
Ec-09_002450	Beta-lactamase-like	0.89		
Ec-25_003490	Carbohydrate-binding WSC, subgroup	0.91		
Ec-13_001890	Conserved hypothetical protein	0.76	19 only	
Ec-11_003190	hypothetical protein	1.54		
Ec-21_000150	expressed unknown protein	1.63		
Ec-24_002150	cytochrome P450	3.00		
Ec-28_001940	hypothetical protein	4.07		
Ec-27_001490	expressed unknown protein	2.23		
Ec-27_005960	EF-hand domain pair	2.23		
Ec-22_003100	imm upregulated 8	1.29		
Ec-27_007030	expressed unknown protein	1.25		
Ec-01_003260	Glucose-methanol-choline oxidoreductase, C-terminal	0.91		
Ec-02_004700	asn/thr-rich large protein family protein	0.92		
Ec-21_003110	hypothetical protein	0.74		
Ec-23_004000	Chromo domain-like	2.60		

References

Agarwal M, Zhu J-K. **2005**. Integration of Abiotic Stress Signaling Pathways. In: Plant Abiotic Stress. Blackwell Publishing Ltd, 215–247.

Aksu Z. **2002**. Determination of the equilibrium, kinetic and thermodynamic parameters of the batch biosorption of nickel(II) ions onto *Chlorella vulgaris*. *Process Biochemistry* **38**: 89–99.

Al-Janabi B, Kruse I, Graiff A, Karsten U, Wahl M. **2016**. Genotypic variation influences tolerance to warming and acidification of early life-stage *Fucus vesiculosus* L. (Phaeophyceae) in a seasonally fluctuating environment. *Marine Biology* **163**: 14.

Alexieva V, Ivanov S. **2003**. Interaction between stresses. *Bulg. J. Plant Physiol*: 1–17.

Allakhverdiev SI, Kreslavski VD, Klimov V V, Los DA, Carpentier R, Mohanty P. **2008**. Heat stress: an overview of molecular responses in photosynthesis. *Photosynthesis Research* **98**: 541.

Alscher RG, Donahue JL, Cramer CL. **1997**. Reactive oxygen species and antioxidants: Relationships in green cells. *Physiologia Plantarum* **100**: 224–233.

Alscher RG, Erturk N, Heath L. **2002**. Role of superoxide dismutases (SODs) in controlling oxidative stress in plants. *J. Exp. Bot.* **53**: 1331–1341.

Altamirano M, Flores-Moya A, Figueroa FL. **2003**. Effects of UV radiation and temperature on growth of germlings of three species of Fucus (Phaeophyceae). *Aquatic Botany* **75**: 9–20.

Andersen GS, Pedersen MF, Nielsen SL, Harley C. **2013**. Temperature acclimation and heat tolerance of photosynthesis in Norwegian *Saccharina latissima* (Laminariales, Phaeophyceae). *Journal of Phycology* **49**: 689–700.

Andersson S, Kautsky L. **1996**. Copper effects on reproductive stages of Baltic Sea *Fucus vesiculosus*. *Marine Biology* **125**: 171–176.

Andrews S. (2010). FastQC: A quality control tool for high throughput sequence data.Available online at: http://www.bioinformatics.babraham.ac.uk/projects/fastqc

Apel K, Hirt H. **2004**. Reactive Oxygen Species: metabolism, oxidative stress, and signal transduction. *Annual Review of Plant Biology* **55**: 373–399.

Asada K. **1999**. The water-water cycle in chloroplasts: scavenging of active oxygens and dissipation of excess photons. *Annual Review of Plant Physiology and Plant Molecular Biology* **50**: 601–639.

Asada K, Takahashi M. **1987**. Production and scavenging of active oxygen in photosynthesis. In: Kyle DJ, Osmond CB, Arntzen CJ, eds. Photoinhibition. Amsterdam: Elsevier, 227–287.

Asada K, Yoshikawa K, Takahashi M, Maeda Y, Enmanji K. **1975**. Superoxide dismutases from a blue-green alga, *Plectonema boryanum*. *Journal of Biological Chemistry* **250**: 2801–2807.

Askwith C, Eide D, Van Ho A, Bernard PS, Li L, Davis-Kaplan S, Sipe DM, Kaplan J. **1994**. The FET3 gene of *S. cerevisiae* encodes a multicopper oxidase required for ferrous iron uptake. *Cell* **76**: 403–410.

Avia K, Coelho SM, Montecinos GJ, Cormier A, Lerck F, Mauger S, Faugeron S, Valero M, Cock JM, Boudry P. **2017**. High-density genetic map and identification of QTLs for responses to temperature and salinity stresses in the model brown alga *Ectocarpus*. *Scientific Reports* **7**: 43241.

Le Bail A, Billoud B, Maisonneuve C, Peters AF, Mark Cock J, Charrier B. **2008a**. Early development pattern of the brown alga *Ectocarpus siliculosus* (Ectocarpales, Phaeophyceae) sporophyte. *Journal of Phycology* **44**: 1269–1281.

Le Bail A, Dittami SM, de Franco P-O, Rousvoal S, Cock MJ, Tonon T, Charrier B. **2008b**. Normalisation genes for expression analyses in the brown alga model *Ectocarpus*

siliculosus. *BMC molecular biology* **9**: 75.

Bakthavatchalu V, Dey S, Xu Y, Noel T, Jungsuwadee P, Holley AK, Dhar SK, Batinic-Haberle I, St Clair DK. **2012**. Manganese superoxide dismutase is a mitochondrial fidelity protein that protects Polγ against UV-induced inactivation. *Oncogene* **31**: 2129–2139.

Barbier EB. **2012**. Progress and challenges in valuing coastal and marine ecosystem Services. *Review of Environmental Economics and Policy* **6**: 1–19.

Barón M, Arellano JB, Gorgé JL. **1995**. Copper and photosystem II: A controversial relationship. *Physiologia Plantarum* **94**: 174–180.

Beauchamp C, Fridovich I. **1971**. Superoxide dismutase: Improved assays and an assay applicable to acrylamide gels. *Analytical Biochemistry* **44**: 276–287.

Becker S, Graeve M, Bischof K. **2010**. Photosynthesis and lipid composition of the Antarctic endemic rhodophyte Palmaria decipiens: effects of changing light and temperature levels. *Polar Biology* **33**: 945–955.

Beer S, Björk M, Beardall J. **2014**. *Photosynthesis in the Marine Environment*. John Wiley & Sons, Ltd.

Beer S, Larsson C, Poryan O, Axelsson L. **2000**. Photosynthetic rates of *Ulva* (Chlorophyta) measured by pulse amplitude modulated (PAM) fluorometry. *European Journal of Phycology* **35**: 69–74.

Beer S, Vilenkin B, Weil A, Veste M, Susel L, Eshel A. **1998**. Measuring photosynthetic rates in seagrasses by pulse amplitude modulated (PAM) fluorometry. *Marine Ecology Progress Series* **174**: 293–300.

Benjamini Y, Hochberg Y. **1995**. Controlling the false discovery rate: a practical and powerful approach to multiple testing. *Journal of the Royal Statistical Society. Series B (Methodological)* **57**: 289–300.

Benzie IFF, Strain JJ. **1996**. The Ferric Reducing Ability of Plasma (FRAP) as a measure of "Antioxidant Power": The FRAP assay. *Analytical Biochemistry* **239**: 70–76.

Bermúdez YG, Rico ILR, Bermúdez OG, Guibal E. **2011**. Nickel biosorption using *Gracilaria caudata* and *Sargassum muticum*. *Chemical Engineering Journal* **166**: 122–131.

Bischoff-Bäsmann B, Bartsch I, Xia B, Wiencke C. **1997**. Temperature responses of macroalgae from the tropical island Hainan (P.R. China). *Phycological Research* **45**: 91–104.

Bischoff-Bäsmann B, Wiencke C. **1996**. Temperature requirement for growth and survival of Antarctic Rhodophyta. *Journal of Phycology* **32**: 525–535.

Blaby-Haas CE, Merchant SS. **2012**. The ins and outs of algal metal transport. *Biochimica et Biophysica Acta (BBA) - Molecular Cell Research* **1823**: 1531–1552.

Boivin M-EY, Massieux B, Breure AM, van den Ende FP, Greve GD, Rutgers M, Admiraal W. **2005**. Effects of copper and temperature on aquatic bacterial communities. *Aquatic Toxicology* **71**: 345–356.

Bold HC. **1985**. *Introduction to the algae : structure and reproduction* (MJ Wynne, Ed.). Englewood Cliffs, NJ: Prentice-Hall.

Bolton JJ. **1983**. Ecoclinal variation in *Ectocarpus siliculosu*s (Phaeophyceae) with respect to temperature growth optima and survival limits. *Marine Biology* **73**: 131–138.

Bonanno G, Orlando-Bonaca M. **2018**. Trace elements in Mediterranean seagrasses and macroalgae. A review. *Science of The Total Environment* **618**: 1152–1159.

Bors W, Michel C, Saran M. **1994**. Flavonoid antioxidants: rate constants for reactions with oxygen radicals. In: Enzymology BT-M in, ed. Oxygen Radicals in Biological Systems Part D. Academic Press, 420–429.

Bothwell JH, Marie D, Peters AF, Cock JM, Coelho SM. **2010**. Cell cycles and endocycles in the model brown seaweed, *Ectocarpus siliculosus*. *Plant signaling & behavior* **5**: 1473–1475.

Bradford MM. **1976**. A rapid and sensitive method for the quantitation of microgram quantities of protein utilizing the principle of protein-dye binding. *Analytical Biochemistry* **72**: 248–254.

Brock TD. **1967**. Life at high temperatures. Evolutionary, ecological, and biochemical significance of organism living in hot springs is discussed. *Science* **158**: 1012 - 1019.

Brock TD. **1985**. Life at High Temperatures. *Science* **230**: 132 - 138.

Brown MT, Newman JE. **2003**. Physiological responses of *Gracilariopsis longissima* (S.G. Gmelin) Steentoft, L.M. Irvine and Farnham (Rhodophyceae) to sub-lethal copper concentrations. *Aquatic Toxicology* **64**: 201–213.

Brown MT, Newman JE, Han T. **2012**. Inter-population comparisons of copper resistance and accumulation in the red seaweed, *Gracilariopsis longissima*. *Ecotoxicology* **21**: 591–600.

Bryan GW, Langston WJ. **1992**. Bioavailability, accumulation and effects of heavy metals in sediments with special reference to United Kingdom estuaries: a review. *Environmental Pollution* **76**: 89–131.

Bushnell B. 2014. BBMap: A fast, accurate, splice-aware aligner. Available online at: (http://jgi.doe.gov/data-and-tools/bbtools/

Byrne RH. **2002**. Inorganic speciation of dissolved elements in seawater: the influence of pH on concentration ratios. *Geochemical transactions* **3**: 11.

Byrne RH, Kump LR, Cantrell KJ. **1988**. The influence of temperature and pH on trace metal speciation in seawater. *Marine Chemistry* **25**: 163–181.

Cairns J, Heath AG, Parker BC. **1975**. The effects of temperature upon the toxicity of chemicals to aquatic organisms. *Hydrobiologia* **47**: 135–171.

Cairrão E, Pereira MJ, Pastorinho MR, Morgado F, Soares AMVM, Guilhermino L. **2007**. *Fucus* spp. as a mercury contamination bioindicator in costal areas (Northwestern Portugal). *Bulletin of Environmental Contamination and Toxicology* **79**: 388–395.

Campbell PGC, Errécalde O, Fortin C, Hiriart-Baer VP, Vigneault B. **2002**. Metal bioavailability to phytoplankton—applicability of the biotic ligand model. *Comparative Biochemistry and Physiology Part C: Toxicology & Pharmacology* **133**: 189–206.

Camus L, Davies PE, Spicer JI, Jones MB. **2004**. Temperature-dependent physiological response of *Carcinus maenas* exposed to copper. In: Marine Environmental Research. 781–785.

Cao D, Shi X, Li H, Xie P, Zhang H, Deng J, Liang Y. **2015**. Effects of lead on tolerance, bioaccumulation, and antioxidative defense system of green algae, *Cladophora*. *Ecotoxicology and Environmental Safety* **112**: 231–237.

Casano LM, Gómez LD, Lascano HR, González CA, Trippi VS. **1997**. Inactivation and degradation of CuZn-SOD by active oxygen species in wheat chloroplasts exposed to photooxidative Stress. *Plant and Cell Physiology* **38**: 433–440.

Celis-Plá PSM, Korbee N, Gómez-Garreta A, Figueroa FL. **2014a**. Seasonal photoacclimation patterns in the intertidal macroalga *Cystoseira tamariscifolia* (Ochrophyta). *Scientia Marina* **78**: 000–000.

Celis-Plá PSM, Martínez B, Korbee N, Hall-Spencer JM, Figueroa FL. **2017**. Ecophysiological responses to elevated CO_2 and temperature in *Cystoseira tamariscifolia* (Phaeophyceae). *Climatic Change* **142**: 67–81.

Celis-Plá PSM, Martínez B, Quintano E, García-Sánchez M, Pedersen A, Navarro

N, Copertino M, Mangaiyarkarasi N, Mariath R, Figueroa F, *et al.* 2014b. Short-term ecophysiological and biochemical responses of *Cystoseira tamariscifolia* and *Ellisolandia elongata* to environmental changes. *Aquatic Biology* **22**: 227–243.

Chakraborty S, Bhattacharya T, Singh G, Maity JP. **2014**. Benthic macroalgae as biological indicators of heavy metal pollution in the marine environments: A biomonitoring approach for pollution assessment. *Ecotoxicology and Environmental Safety* **100**: 61–68.

Chapman PM, Allen HE, Godtfredsen K, Z'Graggen MN. **1996**. Evaluation of bioaccumulation factors in regulating metals. *Environmental Science & Technology* **30**: 448–452.

Charrier B, Coelho SM, Le Bail A, Tonon T, Michel G, Potin P, Kloareg B, Boyen C, Peters AF, Cock JM. **2008**. Development and physiology of the brown alga *Ectocarpus siliculosus*: two centuries of research. *New Phytologist* **177**: 319–32.

Chesworth JC, Donkin ME, Brown MT. **2004**. The interactive effects of the antifouling herbicides Irgarol 1051 and Diuron on the seagrass *Zostera marina* (L.). *Aquatic Toxicology* **66**: 293–305.

Cho SH, Ji S-C, Hur SB, Bae J, Park I-S, Song Y-C. **2007**. Optimum temperature and salinity conditions for growth of green algae *Chlorella ellipsoidea* and *Nannochloris oculata*. *Fisheries Science* **73**: 1050–1056.

Choo K, Snoeijs P, Pedersén M. **2004**. Oxidative stress tolerance in the filamentous green algae *Cladophora glomerata* and *Enteromorpha ahlneriana*. *Journal of Experimental Marine Biology and Ecology* **298**: 111–123.

Christie H, Norderhaug K, Fredriksen S. **2009**. Macrophytes as habitat for fauna. *Marine Ecology Progress Series* **396**: 221–233.

Clark RB, Frid C, Attrill M. **1997**. *Marine Pollution*. Oxford University Press.

Clarke A, Morris GJ, Fonseca F, Murray BJ, Acton E, Price HC. **2013**. A low temperature limit for life on earth. *PLOS ONE* **8**: e66207.

Cobbett CS. **2000**. Phytochelatins and their roles in heavy metal detoxification. *Plant Physiology* **123**: 825 LP-832.

Cobbett C, Goldsbrough P. **2002**. Phytochelatins and Metallothioneins: roles in heavy metal detoxification and homeostasis. *Annual Review of Plant Biology* **53**: 159–182.

Cock JM, Sterck L, Rouzé P, Scornet D, Allen AE, Amoutzias G, Anthouard V, Artiguenave F, Aury J-M, Badger JH, *et al.* 2010. The *Ectocarpus* genome and the independent evolution of multicellularity in brown algae. *Nature* **465**: 617–621.

Coelho SM, Scornet D, Rousvoal S, Peters NT, Dartevelle L, Peters AF, Mark Cock J. **2012a**. *Ectocarpus*: A model organism for the brown algae. *Cold Spring Harbor Protocols* **7**: 193–198.

Coelho SM, Scornet D, Rousvoal S, Peters NT, Dartevelle L, Peters AF, Mark Cock J. **2012b**. Genetic crosses between *Ectocarpus* Strains. *Cold Spring Harbor Protocols* **7**: 262–265.

Coelho SM, Scornet D, Rousvoal S, Peters NT, Dartevelle L, Peters AF, Mark Cock J. **2012c**. How to cultivate *Ectocarpus*. *Cold Spring Harbor Protocols* **7**: 258–261.

Collén J, Davison I. **1999a**. Reactive oxygen metabolism in intertidal *Fucus* spp.(Phaeophyceae). *Journal of Phycology* **35**: 62–69.

Collén J, Davison I. **1999b**. Reactive oxygen production and damage in intertidal *Fucus* spp. (Phaeophyceae). *Journal of Phycology* **35**: 54–61.

Collén J, Davison I. **1999c**. Stress tolerance and reactive oxygen metabolism in the intertidal red seaweeds *Mastocarpus stellatus* and *Chondrus crispus*. *Plant, Cell & Environment* **22**: 1143–1151.

Collén J, Davison I. **2001**. Seasonality and thermal acclimation of reactive oxygen metabolism in. *Differences* **481**: 474–481.

Collén J, Guisle-Marsollier I, Léger JJ, Boyen C. **2007**. Response of the transcriptome of the intertidal red seaweed *Chondrus crispus* to controlled and natural stresses. *New Phytologist* **176**: 45–55.

Collén J, Pinto E, Pedersén M, Colepicolo P. **2003**. Induction of Oxidative Stress in the Red Macroalga *Gracilaria tenuistipitata* by Pollutant Metals. *Archives of Environmental Contamination & Toxicology* **45**: 337–342.

Connan S, Goulard F, Stiger V, Deslandes E, Ar Gall E. **2004**. Interspecific and temporal variation in phlorotannin levels in an assemblage of brown algae. *Botanica Marina* **47**: 410.

Connan S, Stengel DB. **2011a**. Impacts of ambient salinity and copper on brown algae: 1. Interactive effects on photosynthesis, growth, and copper accumulation. *Aquatic Toxicology* **104**: 94–107.

Connan S, Stengel DB. **2011b**. Impacts of ambient salinity and copper on brown algae: 2. Interactive effects on phenolic pool and assessment of metal binding capacity of phlorotannin. *Aquatic Toxicology* **104**: 1–13.

Connell DW. **1989**. Biomagnification by aquatic organisms — A proposal. *Chemosphere* **19**: 1573–1584.

Contreras-Porcia L, Dennett G, Gonzalez A, Vergara E, Medina C, Correa J a., Moenne A. **2011**. Identification of Copper-Induced Genes in the Marine Alga *Ulva compressa* (Chlorophyta). *Marine Biotechnology* **13**: 544–556.

Contreras L, Mella D, Moenne A, Correa J a. 2009. Differential responses to copper-induced oxidative stress in the marine macroalgae *Lessonia nigrescens* and *Scytosiphon lomentaria* (Phaeophyceae). *Aquatic Toxicology* **94**: 94–102.

Contreras L, Moenne A, Correa J a. 2005. Antioxidant responses in *Scytosiphon lomentaria* (Phaeophyceae) inhabiting copper-enriched coastal environments. *Journal of Phycology* **41**: 1184–1195.

Coquery M, Carvalho FP, Horvat M, Azemard S. **1997**. *Report on the World-wide Intercomparison Run IAEA-140/TM: Trace elements in Fucus sample IAEA/AL139; IAEA/MEL/64*. Monaco.

Correa JA, Castilla JC, Ramírez M, Varas M, Lagos N, Vergara S, Moenne A, Román D, Brown MT. **1999**. Copper, copper mine tailings and their effect on marine algae in Northern Chile. *Journal of Applied Phycology* **11**: 57–67.

Correa JA, González P, Sánchez P, Muñoz J, Orellana MC. **1996**. Copper-algae interactions: Inheritance or adaptation? *Environmental Monitoring and Assessment* **40**: 41–54.

Cosgrove J, Borowitzka MA. **2010**. Chlorophyll Fluorescence terminology: an introduction BT - Chlorophyll a fluorescence in aquatic sciences: methods and applications. In: Suggett DJ, Prášil O, Borowitzka MA, eds. Dordrecht: Springer Netherlands, 1–17.

Costa S, Crespo D, Henriques BMG, Pereira E, Duarte AC, Pardal MA. **2011**. Kinetics of mercury accumulation and its effects on *Ulva lactuca* growth rate at two salinities and exposure conditions. *Water, Air, and Soil Pollution* **217**: 689–699.

Costanza R, d'Arge R, de Groot R, Farber S, Grasso M, Hannon B, Limburg K, Naeem S, O'Neill R V., Paruelo J, *et al.* 1997. The value of the world's ecosystem services and natural capital. *Nature* **387**: 253–260.

Costanza R, de Groot R, Sutton P, van der Ploeg S, Anderson SJ, Kubiszewski I, Farber S, Turner RK. **2014**. Changes in the global value of ecosystem services. *Global Environmental Change* **26**: 152–158.

Croteau M-N, Luoma SN, Stewart AR. **2005**. Trophic transfer of metals along freshwater food webs: evidence of cadmium biomagnification in nature. *Limnology and Oceanography* **50**: 1511–1519.

Cruces E, Huovinen P, Gómez I. **2013**. Interactive effects of UV radiation and enhanced temperature on photosynthesis, phlorotannin induction and antioxidant activities of two sub-Antarctic brown algae. *Marine Biology* **160**: 1–13.

Darling ES, Côté IM. **2008**. Quantifying the evidence for ecological synergies. *Ecology Letters* **11**: 1278–1286.

Davis TA, Volesky B, Mucci A. **2003**. A review of the biochemistry of heavy metal biosorption by brown algae. *Water Research* **37**: 4311–4330.

Davison I. **1987**. Adaptation of photosynthesis in *Laminaria saccharina* (Phaeophyta) to changes in growth temperature. *Journal of Phycology* **23**: 273–283.

Davison I. **1991**. Environmental effects on algal photosynthesis: temperature. *Journal of Phycology* **27**: 2–8.

Davison I, Davison JO. **1987**. The effect of growth temperature on enzyme activities in the brown alga *Laminaria saccharina*. *British Phycological Journal* **22**: 77–87.

Davison I, Pearson GA. **1996**. Stress tolerance in intertidal seaweeds. *Journal of Phycology* **32**: 197–211.

Dean M, Allikmets R. **1995**. Evolution of ATP-binding cassette transporter genes. *Current Opinion in Genetics & Development* **5**: 779–785.

Dean M, Annilo T. **2005**. Evolution of the ATP-binding cassette (ABC) transporter superfamily in vertebrates. *Annual Review of Genomics and Human Genetics* **6**: 123–142.

Decho A, Luoma S. **1994**. Humic and fulvic acids: sink or source in the availability of metals to the marine bivalves *Macoma balthica* and *Potamocorbula amurensis*? *Marine*

Ecology Progress Series **108**: 133–145.

DeLorenzo ME, Fulton MH. **2012**. Comparative risk assessment of permethrin, chlorothalonil, and diuron to coastal aquatic species. *Marine Pollution Bulletin* **64**: 1291–1299.

Denman K, Hofmann E, Marchant H. **1996**. Marine biotic responses to environmental change and feedbacks to climate. In: Houghton JT, Meira Filho LG, Callander BA, Harris N, Kattenberg A, Maskell K, eds. Climate Change 1995 - The Science of Climate Change. Contribution of the Working Group I to the Second Assessment Report of the Intergovernmental Panel on Climate Change. Cambridge University Press.

Desikan R, Hancock J, Neill S. **2005**. Reactive Oxygen Species as signalling molecules. In: Antioxidants and Reactive Oxygen Species in Plants. Blackwell Publishing Ltd, 169–196.

Dietz K-J. **2005**. Plant thiol enzymes and thiol homestasis in relation to thiol-dependent redox regulation and oxidative stress. In: Antioxidants and Reactive Oxygen Species in Plants. Blackwell Publishing Ltd, 25–52.

Dittami SM, Gravot A, Renault D, Goulitquer S, Eggert A, Bouchereau A, Boyen C, Tonon T. **2011a**. Integrative analysis of metabolite and transcript abundance during the short-term response to saline and oxidative stress in the brown alga *Ectocarpus siliculosus*. *Plant, Cell & Environment* **34**: 629–642.

Dittami SM, Michel G, Collén J, Boyen C, Tonon T. **2010**. Chlorophyll-binding proteins revisited--a multigenic family of light-harvesting and stress proteins from a brown algal perspective. *BMC evolutionary biology* **10**: 365.

Dittami SM, Proux C, Rousvoal S, Peters AF, Cock JM, Coppée J-Y, Boyen C, Tonon T. **2011b**. Microarray estimation of genomic inter-strain variability in the genus *Ectocarpus* (Phaeophyceae). *BMC molecular biology* **12**: 2.

Dittami SM, Scornet D, Petit J-L, Ségurens B, Da Silva C, Corre E, Dondrup M, Glatting K-H, König R, Sterck L, *et al.* 2009. Global expression analysis of the brown alga *Ectocarpus siliculosus* (Phaeophyceae) reveals large-scale reprogramming of the transcriptome in response to abiotic stress. *Genome biology* **10**: R66.

Doemel WN, Brock TD. **1970**. The upper temperature limit of *Cyanidium caldarium*. *Archiv für Mikrobiologie* **72**: 326–332.

Doney SC. **2010**. The Growing Human Footprint on Coastal and Open-Ocean Biogeochemistry. *Science (New York, N.Y.)* **328**: 1512–1516.

Doney SC, Ruckelshaus M, Emmett Duffy J, Barry JP, Chan F, English C a., Galindo HM, Grebmeier JM, Hollowed AB, Knowlton N, *et al.* 2012. Climate Change Impacts on Marine Ecosystems. *Annual Review of Marine Science* **4**: 11–37.

Dring MJ. **1967**. Effects of daylength on growth and reproduction of the conchocelis-phase of *Porphyra Tenera*. *Journal of the Marine Biological Association of the United Kingdom* **47**: 501–510.

Dring MJ. **2005**. Stress resistance and disease resistance in seaweeds: the role of reactive oxygen metabolism. In: Research BT-A in B, ed. Incorporating Advances in Plant Pathology. Academic Press, 175–207.

Dummermuth AL, Karsten U, Fisch KM, König GM, Wiencke C. **2003**. Responses of marine macroalgae to hydrogen-peroxide stress. *Journal of Experimental Marine Biology and Ecology* **289**: 103–121.

Dunn WB, Erban A, Weber RJM, Creek DJ, Brown M, Breitling R, Hankemeier T, Goodacre R, Neumann S, Kopka J, *et al.* 2013. Mass appeal: metabolite identification in mass spectrometry-focused untargeted metabolomics. *Metabolomics* **9**: 44–66.

Edgar GJ, Banks SA, Brandt M, Bustamante RH, Chiriboga A, Earle SA, Garske LE, Glynn PW, Grove JS, Henderson S, *et al.* 2010. El Niño, grazers and fisheries

interact to greatly elevate extinction risk for Galapagos marine species. *Global Change Biology* **16**: 2876–2890.

Eggert A. **2012**. Seaweed Responses to Temperature BT - Seaweed Biology: Novel Insights into Ecophysiology, Ecology and Utilization. In: Wiencke C, Bischof K, eds. Berlin, Heidelberg: Springer Berlin Heidelberg, 47–66.

Eggert A, Burger EM, Breeman AM. **2003**. Ecotypic differentiation in thermal traits in the tropical to warm-temperate green macrophyte *Valonia utricularis*. *Botanica Marina* **46**: 69.

Eggert A, Visser RJW, Van Hasselt PR, Breeman AM. **2006**. Differences in acclimation potential of photosynthesis in seven isolates of the tropical to warm temperate macrophyte *Valonia utricularis* (Chlorophyta). *Phycologia* **45**: 546–556.

Eggert A, Wiencke C. **2000**. Adaptation and acclimation of growth and photosynthesis of five Antarctic red algae to low temperatures. *Polar Biology* **23**: 609–618.

Eilers PHC, Peeters JCH. **1988**. A model for the relationship between light intensity and the rate of photosynthesis in phytoplankton. *Ecological Modelling* **42**: 199–215.

Enríquez S, Borowitzka MA. **2010**. The use of the fluorescence signal in studies of seagrasses and macroalgae. In: Suggett DJ, Prášil O, Borowitzka MA, eds. Chlorophyll a Fluorescence in Aquatic Sciences: Methods and Applications. Dordrecht: Springer Netherlands, 187–208.

Falkowski PG, Raven JA. **2007**. *Aquatic Photosynthesis*. Princeton University Press.

Feder ME, Hofmann GE. **1999**. Heat-shock proteins, molecular chaperones, and the stress response: Evolutionary and Ecological Physiology. *Annual review of physiology* **61**: 243–282.

Feierabend J. **2005**. Catalases in plants: molecular and functional properties and role in stress defence. In: Antioxidants and Reactive Oxygen Species in Plants. Blackwell

Publishing Ltd, 101–140.

Fernandes JC, Henriques FS. **1991**. Biochemical, physiological, and structural effects of excess copper in plants. *The Botanical Review* **57**: 246–273.

Figueroa F, Conde-Álvarez R, Gómez I. **2003**. Relations between electron transport rates determined by pulse amplitude modulated chlorophyll fluorescence and oxygen evolution in macroalgae under different light conditions. *Photosynthesis Research* **75**: 259–275.

Figueroa FL, Domínguez-González B, Korbee N. **2014**. Vulnerability and acclimation to increased UVB radiation in three intertidal macroalgae of different morpho-functional groups. *Marine Environmental Research* **97**: 30–38.

Figueroa F, Israel A, Neori A, Martínez B, Malta E, Jr AP, Inken S, Marquardt R, Korbee N. **2009**. Effects of nutrient supply on photosynthesis and pigmentation in *Ulva lactuca* (Chlorophyta): responses to short-term stress. *Aquatic Biology* **7**: 173–183.

Folin O, Ciocalteu V. **1927**. On tyrosine and tryptophane determinations in proteins. *Journal of Biological Chemistry* **73**: 627–650.

Folt CL, Chen CY, Moore M V, Burnaford J. **1999**. Synergism and antagonism among multiple stressors. *Limnology and Oceanography* **44**: 864–877.

Forsberg A, Söderlund S, Frank A, Petersson LR, Pedersén M. **1988**. Studies on metal content in the brown seaweed, *Fucus vesiculosus*, from the Archipelago of Stockholm. *Environmental pollution (Barking, Essex : 1987)* **49**: 245–263.

Foyer CH, Gomez LD, van Heerden PDR. **2005**. Glutathione. In: Antioxidants and Reactive Oxygen Species in Plants. Blackwell Publishing Ltd, 1–24.

Foyer CH, Noctor G. **2011**. Ascorbate and Glutathione: the heart of the redox hub. *Plant Physiology* **155**: 2–18.

Fredersdorf J, Müller R, Becker S, Wiencke C, Bischof K. **2009**. Interactive effects of radiation, temperature and salinity on different life history stages of the Arctic kelp *Alaria esculenta* (Phaeophyceae). *Oecologia* **160**: 483–492.

Gaur JP, Rai LC. **2001**. Heavy metal tolerance in algae. In: Rai LC, Gaur JP, eds. Algal Adaptation to Environmental Stresses. New York: Springer, 363–388.

Genty B, Briantais J-M, Baker NR. **1989**. The relationship between the quantum yield of photosynthetic electron transport and quenching of chlorophyll fluorescence. *Biochimica et Biophysica Acta (BBA) - General Subjects* **990**: 87–92.

Gledhill M, Nimmo M, Hill SJ, Brown MT, Bryan K. **1999**. The release of copper-complexing ligands by the brown alga *Fucus vesiculosus* (Phaeophyceae) in response to increasing total copper levels. *Journal of Phycology* **35**: 501–509.

Gledhill M, Nimmo M, Stephen JH, Brown MT. **1997**. The toxicity of Copper (II) species to marine algae, with particular rference to macroalgae. *Journal of Phycology* **33**: 2–11.

Gómez I, Wulff A, Roleda MY, Huovinen P, Karsten U, Quartino ML, Dunton K, Wiencke C. **2009**. Light and temperature demands of marine benthic microalgae and seaweeds in polar regions. *Botanica Marina* **52**: 593.

Gonzalez a., Cabrera MDL a., Henriquez MJ, Contreras R a., Morales B, Moenne a. 2012. Cross talk among calcium, hydrogen peroxide, and nitric oxide and activation of gene expression involving calmodulins and calcium-dependent protein kinases in *Ulva compressa* exposed to copper excess. *Plant Physiology* **158**: 1451–1462.

Gonzalez A, Vera J, Castro J, Dennett G, Mellado M, Morales B, Correa J a., Moenne A. **2010**. Co-occurring increases of calcium and organellar reactive oxygen species determine differential activation of antioxidant and defense enzymes in *Ulva compressa* (Chlorophyta) exposed to copper excess. *Plant, Cell and Environment* **33**:

1627–1640.

Grace SC. **2005**. Phenolics as Antioxidants. In: Antioxidants and Reactive Oxygen Species in Plants. Blackwell Publishing Ltd, 141–168.

Graham MH. **2004**. Effects of local deforestation on the diversity and structure of southern california giant kelp forest food webs. *Ecosystems* **7**: 341–357.

Graiff A, Liesner D, Karsten U, Bartsch I. **2015**. Temperature tolerance of western Baltic Sea *Fucus vesiculosus* – growth, photosynthesis and survival. *Journal of Experimental Marine Biology and Ecology* **471**: 8–16.

Gray JS. **2002**. Biomagnification in marine systems: the perspective of an ecologist. *Marine Pollution Bulletin* **45**: 46–52.

Greco M, Sáez CA, Brown MT, Bitonti MB. **2014**. *A simple and effective method for high quality co-extraction of genomic DNA and total RNA from low biomass Ectocarpus siliculosus, the model brown alga*.

Grill E, Löffler S, Winnacker EL, Zenk MH. **1989**. Phytochelatins, the heavy-metal-binding peptides of plants, are synthesized from glutathione by a specific gamma-glutamylcysteine dipeptidyl transpeptidase (phytochelatin synthase). *Proceedings of the National Academy of Sciences of the United States of America* **86**: 6838.

de Groot R, Brander L, van der Ploeg S, Costanza R, Bernard F, Braat L, Christie M, Crossman N, Ghermandi A, Hein L, *et al.* 2012. Global estimates of the value of ecosystems and their services in monetary units. *Ecosystem Services* **1**: 50–61.

Gross JH. **2017**. Inorganic Mass Spectrometry BT - Mass Spectrometry: A Textbook. In: Gross JH, ed. Cham: Springer International Publishing, 889–925.

Grzymski J, Johnsen G, Sakshaug E. **1997**. The significance of intracellular self-shading on the bio optical properties of brown, red, and green macroalgae. *Journal of Phycology* **33**: 408–414.

Guo R, Ki J-S. **2012**. Differential transcription of heat shock protein 90 (HSP90) in the dinoflagellate *Prorocentrum minimum* by copper and endocrine-disrupting chemicals. *Ecotoxicology* **21**: 1448–1457.

Gutknecht J. **1981**. Inorganic mercury (Hg^{2+}) transport through lipid bilayer membranes. *The Journal of Membrane Biology* **61**: 61–66.

Hall A, Fielding AH, Butler M. **1979**. Mechanisms of copper tolerance in the marine fouling alga *Ectocarpus siliculosus* - Evidence for an exclusion mechanism. *Marine Biology* **54**: 195–199.

Halliwell B. **2006**. Reactive Species and Antioxidants. redox biology is a fundamental theme of aerobic life. *Plant Physiology* **141**: 312 LP-322.

Halpern BS, McLeod KL, Rosenberg AA, Crowder LB. **2008**. Managing for cumulative impacts in ecosystem-based management through ocean zoning. *Ocean & Coastal Management* **51**: 203–211.

Han T, Choi G-W. **2005**. A novel marine algal toxicity bioassay based on sporulation inhibition in the green macroalga *Ulva pertusa* (Chlorophyta). *Aquatic Toxicology* **75**: 202–212.

Harley CDG, Anderson KM, Demes KW, Jorve JP, Kordas RL, Coyle T a., Graham MH. **2012**. Effects of climate change on global seaweed communities. *Journal of Phycology* **48**: 1064–1078.

Harley CDG, Hughes a. R, Hultgren KM, Miner BG, Sorte CJB, Thornber CS, Rodriguez LF, Tomanek L, Williams SL. **2006**. The impacts of climate change in coastal marine systems. *Ecology Letters* **9**: 228–241.

Hassler CS, Slaveykova VI, Wilkinson KJ. **2004**. Discriminating between intra- and extracellular metals using chemical extractions. *Limnology and Oceanography: Methods* **2**: 237–247.

Haug A. **1961**. The affinity of some divalent metals to different types of alginates. *Acta Chemica Scandinavica* **15**: 1794–1795.

Heath RL, Packer L. **1968**. Photoperoxidation in isolated chloroplasts: I. Kinetics and stoichiometry of fatty acid peroxidation. *Archives of Biochemistry and Biophysics* **125**: 189–198.

Heesch S, Cho GY, Peters AF, Le Corguillé G, Falentin C, Boutet G, Coëdel S, Jubin C, Samson G, Corre E, *et al.* 2010. A sequence-tagged genetic map for the brown alga *Ectocarpus siliculosus* provides large-scale assembly of the genome sequence. *New Phytologist* **188**: 42–51.

Heinrich S, Valentin K, Frickenhaus S, John U, Wiencke C. **2012**. Transcriptomic analysis of acclimation to temperature and light stress in *Saccharina latissima* (Phaeophyceae). *PLOS ONE* **7**: e44342.

Henkel SK, Kawai H, Hofmann GE. **2009**. Interspecific and interhabitat variation in hsp70 gene expression in native and invasive kelp populations. *Marine Ecology Progress Series* **386**: 1–13.

Hertwig B, Streb P, Feierabend J. **1992**. Light dependence of catalase synthesis and degradation in leaves and the influence of interfering stress conditions. *Plant Physiology* **100**: 1547–1553.

Heugens EHW, Hendriks AJ, Dekker T, van Straalen NM, Admiraal W. **2001**. A review of the effects of multiple stressors on acquatic organisms and analysis of uncertainty factors for use in risk assessment. *Critical Reviews in Toxicology* **31**: 247–284.

Heumann H-G. **1987**. Effects of heavy metals on growth and ultrastructure of *Chara vulgaris*. *Protoplasma* **136**: 37–48.

Higgins CF. **1992**. ABC Transporters: from microorganisms to man. *Annual Review of*

Cell Biology **8**: 67–113.

Hill SJ (Ed.). **2006**. *Inductively coupled plasma spectrometry and its applications*. Oxford : Blackwell.

Hochachka PW, Somero GN. **2002**. *Biochemical Adaptation: mechanisms and process in physiological evolution*. New York: Oxford University Press.

Holmstrup M, Bindesbøl A-M, Oostingh GJ, Duschl A, Scheil V, Köhler H-R, Loureiro S, Soares AMVM, Ferreira ALG, Kienle C, *et al.* 2010. Interactions between effects of environmental chemicals and natural stressors: A review. *Science of The Total Environment* **408**: 3746–3762.

Hope AB, Aschberger PA. **1970**. Effects of temperature on membrane permeability to ions. *Australian Journal of Biological Sciences* **23**: 1047–1060.

Horta P a., Vieira-Pinto T, Martins CDL, Sissini MN, Ramlov F, Lhullier C, Scherner F, Sanches PF, Farias JN, Bastos E, *et al.* 2012. Evaluation of impacts of climate change and local stressors on the biotechnological potential of marine macroalgae - A brief theoretical discussion of likely scenarios. *Brazilian Journal of Pharmacognosy* **22**: 768–774.

Hosler JP, Yocum CF. **1987**. Regulation of cyclic photophosphorylation during ferredoxin-mediated electron transport: effect of DCMU and the NADPH/$NADP^+$ ratio. *Plant Physiology* **83**: 965–969.

Hudson RJM, Morel FMM. **1990**. lron transport in marine phytoplankton: Kinetics of cellular and medium coordination reactions. *Limnology and Oceanography* **35**: 1002–1020.

Hurd CL, Harrison PJ, Bichof K, Lobban C. **2014**. *Seaweed Ecology and Physiology*. Cambridge, UK: Cambridge University Press.

Hutchins LW. **1947**. The bases for temperature zonation in geographical distribution.

Ecological Monographs **17**: 325–335.

Inaba M, Suzuki I, Szalontai B, Kanesaki Y, Los DA, Hayashi H, Murata N. **2003**. Gene-engineered rigidification of membrane lipids enhances the cold inducibility of gene expression in *Synechocystis*. *Journal of Biological Chemistry* **278**: 12191–12198.

IPCC. **2014**. Climate Change 2014: Synthesis Report. Contribution of Working Groups I, II and III to the Fifth Assessment Report of the Intergovernmental Panel on Climate Change. [Core writing team, Pachauri RK, Meyer LA, (eds.)]. Geneva, Switzerland: IPCC, 151.

Ireland HE, Harding SJ, Bonwick GA, Jones M, Smith CJ, Williams JHH. **2004**. Evaluation of heat shock protein 70 as a biomarker of environmental stress in *Fucus serratus* and *Lemna minor*. *Biomarkers* **9**: 139–155.

Jackson M, Mantsch HH. **1991**. Beware of proteins in DMSO. *Biochimica et Biophysica Acta (BBA) - Protein Structure and Molecular Enzymology* **1078**: 231–235.

Jacobson PJ, Neves RJ, Cherry DS, Farris JL. **1997**. Sensitivity of glochidial stages of freshwater mussels (Bivalvia: Unionidae) to copper. *Environmental Toxicology & Chemistry* **16**: 2384–2392.

Jepson PD, Law RJ. **2016**. Marine Environment. Persistent pollutants, persistent threats. *Science (New York, N.Y.)* **352**: 1388.

Ji Y, Xu Z, Zou D, Gao K. **2016**. Ecophysiological responses of marine macroalgae to climate change factors. *Journal of Applied Phycology* **28**: 2953–2967.

Joshi MK, Mohanty P. **2004**. Chlorophyll a Fluorescence as a probe of heavy metal ion toxicity in plants. In: Papageorgiou GC, Govindjee, eds. Chlorophyll a Fluorescence: A signature of photosynthesis. Dordrecht, The Netherlands: Springer, 637–661.

Jueterbock A, Kollias S, Smolina I, Fernandes JMO, Coyer JA, Olsen JL, Hoarau G. **2014**. Thermal stress resistance of the brown alga *Fucus serratus* along the North-

Atlantic coast: Acclimatization potential to climate change. *Marine Genomics* **13**: 27–36.

Junglee S, Urban L, Sallanon H, Lopez-Lauri F. **2014**. Optimized Assay for Hydrogen Peroxide Determination in Plant Tissue Using Potassium Iodide. *American Journal of Analytical Chemistry* **5**: 730–736.

Kamala-Kannan S, Prabhu Dass Batvari B, Lee KJ, Kannan N, Krishnamoorthy R, Shanthi K, Jayaprakash M. **2008**. Assessment of heavy metals (Cd, Cr and Pb) in water, sediment and seaweed (*Ulva lactuca*) in the Pulicat Lake, South East India. *Chemosphere* **71**: 1233–40.

Kamiya M, Nishio T, Yokoyama A, Yatsuya K, Nishigaki T, Yoshikawa S, Ohki K. **2010**. Seasonal variation of phlorotannin in sargassacean species from the coast of the Sea of Japan. *Phycological Research* **58**: 53–61.

Kammenga JE, Arts MSJ, Oude-Breuil WJM. **1998**. HSP60 as a Potential Biomarker of Toxic Stress in the Nematode *Plectus acuminatus*. *Archives of Environmental Contamination and Toxicology* **34**: 253–258.

Kay J, Cryer A, Darke BM, Kille P, Lees WE, Norey CG, Stark JM. **1991**. Naturally occurring and recombinant metallothioneins: Structure, immunoreactivity and metal-binding functions. *International Journal of Biochemistry* **23**: 1–5.

Kehrer JP. **2000**. The Haber–Weiss reaction and mechanisms of toxicity. *Toxicology* **149**: 43–50.

Kempner ES. **1963**. Upper Temperature Limit of Life. *Science* **142**: 1318–1319.

Kimberly DA, Salice CJ. **2014**. Complex interactions between climate change and toxicants : evidence that temperature variability increases sensitivity to cadmium. : 809–817.

Klughammer C, Schreiber U. **2008**. Complementary PS II quantum yields calculated from simple fluorescence parameters measured by PAM fluorometry and the Saturation

Pulse method. *PAM application notes*: 27–35.

Knauert S, Knauer K. **2008**. The role of reactive oxygen species in copper toxicity to two freshwater green algae. *Journal of Phycology* **44**: 311–319.

Koch M, Bowes G, Ross C, Zhang X-H. **2013**. Climate change and ocean acidification effects on seagrasses and marine macroalgae. *Global Change Biology* **19**: 103–132.

Kübler J, Davison I. **1993**. High-temperature tolerance of photosynthesis in the red alga *Chondrus crispus*. *Marine Biology* **117**: 327–335.

Kübler J, Davison I, Yarish C. **1991**. Photosynthetic adaptation to temperature in the red algae *Lomentaria baileyana* and *Lomentaria orcadensis*. *British Phycological Journal* **26**: 9–19.

Kumar A, Castellano I, Patti FP, Delledonne M, Abdelgawad H, Beemster GTS, Asard H, Palumbo A, Buia MC. **2017**. Molecular response of *Sargassum vulgare* to acidification at volcanic CO_2 vents: insights from de novo transcriptomic analysis. *Molecular Ecology* **26**: 2276–2290.

Kuo WY, Huang CH, Liu AC, Cheng CP, Li SH, Chang WC, Weiss C, Azem A, Jinn TL. **2013**. Chaperonin 20 mediates iron superoxide dismutase (FeSOD) activity independent of its co-chaperonin role in *Arabidopsis* chloroplasts. *New Phytologist* **197**: 99–110.

Küpper H, Küpper F, Spiller M. **1996**. Environmental relevance of heavy metal-substituted chlorophylls using the example of water plants. *Journal of Experimental Botany* **47**: 259–266.

Küpper H, Küpper F, Spiller M. **1998**. In situ detection of heavy metal substituted chlorophylls in water plants. *Photosynthesis Research* **58**: 123–133.

Küpper H, Šetlík I, Spiller M, Küpper FC, Prášil O. **2002**. Heavy metal-induced inhibition of photosynthesis: Targets of in vivo heavy metal chlorophyll formation.

Journal of Phycology **38**: 429–441.

Ladah LB, Zertuche-González JA, Hernández-Carmona G. **1999**. Giant kelp (*Macrocystis pyrifera*, Phaeophyceae) recruitment near its southern limit in Baja California after mass disappearance during ENSO 1997–1998. *Journal of Phycology* **35**: 1106–1112.

Laffoley D, Baxter JM. **(editors) 2016**. Explaining Ocean Warming: Causes, scale, effects and consequences. Full report. Gland, Switzerland: IUCN. 456 pp.

Larkindale J, Mishkind M, Vierling E. **2005**. Plant Responses to High Temperature. In: Plant Abiotic Stress. Blackwell Publishing Ltd, 100–144.

Latowski D, Kuczyńska P, Strzałka K. **2011**. Xanthophyll cycle - a mechanism protecting plants against oxidative stress. *Redox Report* **16**: 78–90.

Lee RE. **2008**. *Phycology*. Cambridge: Cambridge University Press.

Leliaert F, De Clerck O. **2017**. Refining species boundaries in algae. *Journal of Phycology* **53**: 12–16.

Lewis S, Donkin ME, Depledge MH. **2001**. Hsp70 expression in *Enteromorpha intestinalis* (Chlorophyta) exposed to environmental stressors. *Aquatic Toxicology* **51**: 277–291.

Liao Y, Smyth GK, Shi W. 2014. featureCounts: an efficient general purpose program for assigning sequence reads to genomic features. *Bioinformatics* **30**: 923–930.

Liebeke M, Garcia-Perez I, Anderson CJ, Lawlor AJ, Bennett MH, Morris CA, Kille P, Svendsen C, Spurgeon DJ, Bundy JG. **2013**. Earthworms produce phytochelatins in response to arsenic. *PLoS ONE* **8**: e81271.

Lima RB, dos Santos TB, Vieira LGE, Ferrarese M de LL, Ferrarese-Filho O, Donatti L, Boeger MRT, Petkowicz CL de O. **2013**. Heat stress causes alterations in

the cell-wall polymers and anatomy of coffee leaves (Coffea arabica L.). *Carbohydrate Polymers* **93**: 135–143.

Liu F, Sun X, Wang W, Liang Z, Wang F. **2014a**. De novo transcriptome analysis-gained insights into physiological and metabolic characteristics of *Sargassum thunbergii* (Fucales, Phaeophyceae). *Journal of Applied Phycology* **26**: 1519–1526.

Liu F, Wang W, Sun X, Liang Z, Wang F. **2014b**. RNA-Seq revealed complex response to heat stress on transcriptomic level in *Saccharina japonica* (Laminariales, Phaeophyta). *Journal of Applied Phycology* **26**: 1585–1596.

Liu F, Wang W, Sun X, Liang Z, Wang F. **2015**. Conserved and novel heat stress-responsive microRNAs were identified by deep sequencing in *Saccharina japonica* (Laminariales, Phaeophyta). *Plant, Cell & Environment* **38**: 1357–1367.

Livak KJ, Schmittgen TD. **2001**. Analysis of relative gene expression data using real-time quantitative PCR and the $2^{-\Delta\Delta CT}$ Method. *Methods* **25**: 402–8.

Lobban CS, Harrison PJ. **1994**. *Seaweed ecology and physiology*. Cambridge University Press.

Lodenius M. **2016**. Factors affecting metal and radionuclide pollution in the Baltic sea. *European Journal of Environmental Sciences* **6**: 90-97.

Los DA, Murata N. **2004**. Membrane fluidity and its roles in the perception of environmental signals. *Biochimica et Biophysica Acta (BBA) - Biomembranes* **1666**: 142–157.

Love MI, Huber W, Anders S. **2014**. Moderated estimation of fold change and dispersion for RNA-seq data with DESeq2. *Genome Biology* **15**: 550.

Lüning K. **1984**. Temperature tolerance and biogeography of seaweeds: The marine algal flora of Helgoland (North Sea) as an example. *Helgoländer Meeresuntersuchungen* **38**: 305–317.

Machalek KM, Davison I, Falkowski PG. **1996**. Thermal acclimation and photoacclimation of photosynthesis in the brown alga *Laminaria saccharina*. *Plant, Cell & Environment* **19**: 1005–1016.

Mackenzie BR, Schiedek D. **2007**. Daily ocean monitoring since the 1860s shows record warming of northern European seas. *Global Change Biology* **13**: 1335–1347.

Mahan JR, McMichael BL, Wanjura DF. **1995**. Methods for reducing the adverse effects of temperature stress on plants: A review. *Environmental and Experimental Botany* **35**: 251–258.

Maheswari M, Joshi DK, Saha R, Nagarajan S, Gambhir PN. **1999**. Transverse relaxation time of leaf water protons and membrane injury in wheat (*Triticum aestivum* L.) in response to high temperature. *Annals of Botany* **84**: 741–745.

Major KM, Davison I. **1998**. Influence of temperature and light on growth and photosynthetic physiology of *Fucus evanescens* (Phaeophyta) embryos. *European Journal of Phycology* **33**: 129–138.

Merrifield ME, Chaseley J, Kille P, Stillman MJ. **2006**. Determination of the Cd/S cluster stoichiometry in *Fucus vesiculosus* Metallothionein. *Chemical Research in Toxicology* **19**: 365–375.

Merrifield ME, Ngu T, Stillman M. **2004**. Arsenic binding to *Fucus vesiculosus* metallothionein. *Biochem. Biophys. Res. Commun.* **324**: 127–132.

Miller WL, King DW, Lin J, Kester DR. **1995**. Photochemical redox cycling of iron in coastal seawater. *Marine Chemistry* **50**: 63–77.

Mittler R, Poulos TL. **2005**. Ascorbate Peroxidase. In: Antioxidants and Reactive Oxygen Species in Plants. Blackwell Publishing Ltd, 87–100.

Moenne A, González A, Sáez CA. **2016**. Mechanisms of metal tolerance in marine macroalgae, with emphasis on copper tolerance in Chlorophyta and Rhodophyta. *Aquatic*

Toxicology **176**: 30–37.

Montecinos AE, Couceiro L, Peters AF, Desrut A, Valero M, Guillemin M-L. **2017**. Species delimitation and phylogeographic analyses in the *Ectocarpus* subgroup siliculosi (Ectocarpales, Phaeophyceae). *Journal of Phycology* **53**: 17–31.

Morris CA, Nicolaus B, Sampson V, Harwood JL, Kille P. **1999**. Identification and characterization of a recombinant metallothionein protein from a marine alga, *Fucus vesiculosus*. *Biochemical Journal* **338**: 553.

Müller DG. **1964**. Life-cycle of *Ectocarpus siliculosus* from Naples, Italy. *Nature* **203**: 1402.

Nielsen HD, Brown MT, Brownlee C. **2003a**. Cellular responses of developing *Fucus serratus* embryos exposed to elevated concentrations of Cu^{2+}. *Plant, Cell and Environment* **26**: 1737–1747.

Nielsen HD, Brownlee C, Coelho SM, Brown MT. **2003b**. Inter-population differences in inherited copper tolerance involve photosynthetic adaptation and exclusion mechanisms in *Fucus serratus*. *New Phytologist* **160**: 157–165.

Nielsen HD, Nielsen SL. **2010**. Adaptation to high light irradiances enhances the photosynthetic Cu^{2+} resistance in Cu^{2+} tolerant and non-tolerant populations of the brown macroalgae *Fucus serratus*. *Marine Pollution Bulletin* **60**: 710–717.

Nielsen SL, Nielsen HD, Pedersen MF. **2014**. Juvenile life stages of the brown alga *Fucus serratus* L. are more sensitive to combined stress from high copper concentration and temperature than adults. *Marine Biology* **161**: 1895–1904.

Nikinmaa M. **2013**. Climate change and ocean acidification-Interactions with aquatic toxicology. *Aquatic Toxicology* **126**: 365–372.

Noctor G, Mhamdi A, Chaouch S, Han Y, Neukermans J, Marquez-Garcia B, Queval G, Foyer CH. **2012**. Glutathione in plants: An integrated overview. *Plant, Cell*

and Environment **35**: 454–484.

Nor YM. **1987**. Ecotoxicity of copper to aquatic biota: A review. *Environmental Research* **43**: 274–282.

Okamoto OK, Colepicolo P. **1998**. Response of superoxide dismutase to pollutant metal stress in the marine dinoflagellate *Gonyaulax polyedra*. *Comparative Biochemistry and Physiology Part C: Pharmacology, Toxicology and Endocrinology* **119**: 67–73.

Okamoto OK, Pinto E, Latorre LR, Bechara EJH, Colepicolo P. **2001**. Antioxidant modulation in response to metal-induced oxidative stress in algal chloroplasts. *Archives of Environmental Contamination and Toxicology* **40**: 18–24.

Olesik JW. **1991**. Elemental Analysis Using ICP-OES and ICP/MS. *Analytical Chemistry* **63**: 12A–21A.

Omae I. **2003**. General aspects of tin-free antifouling paints. *Chemical Reviews* **103**: 3431–3448.

Öncel I, Keleş Y, Üstün A. 2000. Interactive effects of temperature and heavy metal stress on the growth and some biochemical compounds in wheat seedlings. *Environmental Pollution* **107**: 315–320.

Van Oostdam J, Donaldson SG, Feeley M, Arnold D, Ayotte P, Bondy G, Chan L, Dewaily E, Furgal CM, Kuhnlein H, *et al.* 2005. Human health implications of environmental contaminants in Arctic Canada: A review. *The Science of the total environment* **351–352**: 165–246.

op den Camp RGL, Przybyla D, Ochsenbein C, Laloi C, Kim C, Danon A, Wagner D, Hideg É, Göbel C, Feussner I, *et al.* 2003. Rapid induction of distinct stress responses after the release of singlet oxygen in *Arabidopsis*. *The Plant Cell* **15**: 2320–2332.

OSPAR. **2010**. *Quality status report 2010*. London.

Oukarroum A, Perreault F, Popovic R. **2012**. Interactive effects of temperature and copper on photosystem II photochemistry in *Chlorella vulgaris*. *Journal of Photochemistry and Photobiology B: Biology* **110**: 9–14.

Padilla-Gamiño JL, Carpenter RC. **2007**. Seasonal acclimatization of *Asparagopsis taxiformis* (Rhodophyta) from different biogeographic regions. *Limnology and Oceanography* **52**: 833–842.

Patterson CC. **1965**. Contaminated and natural lead environments of man. *Archives of Environmental Health: An International Journal* **11**: 344–360.

Patterson C, Settle D, Glover B. **1976**. Analysis of lead in polluted coastal seawater. *Marine Chemistry* **4**: 305–319.

Pawlik-Skowrońska B, Pirszel J, Brown MT. **2007**. Concentrations of phytochelatins and glutathione found in natural assemblages of seaweeds depend on species and metal concentrations of the habitat. *Aquatic Toxicology* **83**: 190–199.

Pedersen A. **1984**. Studies on phenol content and heavy metal uptake in fucoids. In: Bird C, Ragan M, eds. Developments in Hydrobiology. Eleventh International Seaweed Symposium SE - 101. Springer Netherlands, 498–504.

Pedrielli P, Pedulli GF, Skibsted LH. **2001**. Antioxidant mechanism of flavonoids. solvent effect on rate constant for chain-breaking reaction of quercetin and epicatechin in autoxidation of methyl linoleate. *Journal of Agricultural and Food Chemistry* **49**: 3034–3040.

Perales-Vela HV, Peña-Castro JM, Cañizares-Villanueva RO. **2006**. Heavy metal detoxification in eukaryotic microalgae. *Chemosphere* **64**: 1–10.

Peters AF, Mann AD, Córdova C a., Brodie J, Correa J a., Schroeder DC, Cock JM. **2010a**. Genetic diversity of *Ectocarpus* (Ectocarpales, Phaeophyceae) in Peru and northern Chile, the area of origin of the genome-sequenced strain. *New Phytologist* **188**:

30–41.

Peters AF, Marie D, Scornet D, Kloareg B, Cock JM. **2004**. Proposal of *Ectocarpus siliculosus* (Ectocarpales, Phaeophyceae) as a model organism for brown algal genetics and genomics. *Journal of Phycology* **40**: 1079–1088.

Peters AF, Scornet D, Ratin M, Charrier B, Monnier A, Merrien Y, Corre E, Coelho SM, Cock JM. **2008**. Life-cycle-generation-specific developmental processes are modified in the immediate upright mutant of the brown alga *Ectocarpus siliculosus*. *Development* **135**: 1503–1512.

Peters AF, van Wijk SJ, Cho GY, Scornet D, Hanyuda T, Kawai H, Schroeder DC, Cock JM, Boo SM. **2010b**. Reinstatement of *Ectocarpus crouaniorum* Thuret in Le Jolis as a third common species of *Ectocarpus* (Ectocarpales, Phaeophyceae) in Western Europe, and its phenology at Roscoff, Brittany. *Phycological Research* **58**: 157–170.

Pfündel E. **2007**. *JUNIOR-PAM chlorophyll fluorometer operator's guide*. Heinz Walz GmbH.

Phillips DJH. **1977**. The use of biological indicator organisms to monitor trace metal pollution in marine and estuarine environments—a review. *Environmental Pollution (1970)* **13**: 281–317.

Pinto E, Sigaud-kutner TCS, Leitão MAS, Okamoto OK, Morse D, Colepicolo P. **2003**. Heavy metal-induced oxidative stress in algae. *Journal of Phycology* **39**: 1008–1018.

Pizarro a O, Hormazabal F S, Gonzalez C A, Yañez R E. **1994**. Variabilidad del viento, nivel del mar y temperatura en la costa norte de Chile. *Investigaciones marinas* **22**: 85–101.

van de Poll W, Eggert A, Buma A, Breeman A. **2002**. Temperature dependence of UV radiation effects in Arctic and temperate isolates of three red macrophytes. *European*

Journal of Phycology **37**: 59–68.

Popovic R, Dewez D, Juneau P. **2003**. Applications of chlorophyll fluorescence in ecotoxicology: heavy metals, herbicides, and air pollutants. In: DeEll JR, Toivonen PMA, eds. Practical Applications of Chlorophyll Fluorescence in Plant Biology. Dordrecht: Kluwer Academic Publishers, 151–184.

Prasad TK. **1996**. Mechanisms of chilling-induced oxidative stress injury and tolerance in developing maize seedlings: changes in antioxidant system, oxidation of proteins and lipids, and protease activities. *The Plant Journal* **10**: 1017–1026.

Prigent S, Collet G, Dittami SM, Delage L, de Corny FE, Dameron O, Eveillard D, Thiele S, Cambefort J, Boyen C, *et al.* 2014. The genome-scale metabolic network of *Ectocarpus siliculosus* (EctoGEM): a resource to study brown algal physiology and beyond. *The Plant Journal* **33**: n/a-n/a.

Provasoli L, Carlucci AF. **1974**. Vitamins and growth regulators. In: Stewart W, ed. Algal Physiology and Biochemistry. Los Angeles, California: Blackwell Publishing Ltd, 741–778.

Puig S, Thiele DJ. **2002**. Molecular mechanisms of copper uptake and distribution. *Current Opinion in Chemical Biology* **6**: 171–180.

Queval G, Noctor G. **2007**. A plate reader method for the measurement of NAD, NADP, glutathione, and ascorbate in tissue extracts: Application to redox profiling during *Arabidopsis* rosette development. *Analytical Biochemistry* **363**: 58–69.

Quinn PJ. **1988**. Effects of temperature on cell membranes. *Symposia of the Society for Experimental Biology* **42**: 237–258.

Ragan MA, Jensen A. **1978**. Quantitative studies on brown algal phenols. II. Seasonal variation in polyphenol content of *Ascophyllum nodosum* (L.) Le Jol. and *Fucus vesiculosus* (L.). *Journal of Experimental Marine Biology and Ecology* **34**: 245–258.

Ragan MA, Smidsrød O, Larsen B. **1979**. Chelation of divalent metal ions by brown algal polyphenols. *Marine Chemistry* **7**: 265–271.

Rai LC, Gaur JP, Kumar HD. **1981**. Phycology and heavy-metal pollution. *Biological Reviews* **56**: 99–151.

Rainbow PS. **1995**. Biomonitoring of heavy metal availability in the marine environment. *Marine Pollution Bulletin* **31**: 183–192.

Rainbow PS, Kriefman S, Smith BD, Luoma SN. **2011**. Have the bioavailabilities of trace metals to a suite of biomonitors changed over three decades in SW England estuaries historically affected by mining? *Science of the Total Environment* **409**: 1589–1602.

Rainbow PS, Luoma SN. **2011**. Metal toxicity, uptake and bioaccumulation in aquatic invertebrates-Modelling zinc in crustaceans. *Aquatic Toxicology* **105**: 455–465.

Ralph PJ, Gademann R. **2005**. Rapid light curves: A powerful tool to assess photosynthetic activity. *Aquatic Botany* **82**: 222–237.

Ratkevicius N, Correa JA, Moenne A. **2003**. Copper accumulation, synthesis of ascorbate and activation of ascorbate peroxidase in *Enteromorpha compressa* (L.) Grev. (Chlorophyta) from heavy metal-enriched environments in northern Chile. *Plant, Cell and Environment* **26**: 1599–1608.

Rauser WE. **1995**. Phytochelatins and related peptides (Structure, Biosynthesis, and Function). *Plant Physiology* **109**: 1141–1149.

Rautenberger R, Bischof K. **2006**. Impact of temperature on UV-susceptibility of two *Ulva* (Chlorophyta) species from Antarctic and Subantarctic regions. *Polar Biology* **29**: 988–996.

Rautenberger R, Huovinen P, Gómez I. **2015**. Effects of increased seawater temperature on UV tolerance of Antarctic marine macroalgae. *Marine Biology*.

Raven JA. **2013**. Iron acquisition and allocation in stramenopile algae. *Journal of Experimental Botany* **64**: 2119–2127.

Reed RH, Moffat L. **1983**. Copper toxicity and copper tolerance in Enteromorpha compressa (L.) Grev. *Journal of Experimental Marine Biology and Ecology* **69**: 85–103.

Rickert E, Wahl M, Link H, Richter H, Pohnert G. **2016**. Seasonal variations in surface metabolite composition of *Fucus vesiculosus* and *Fucus serratus* from the Baltic Sea. *PLOS ONE* **11**: e0168196.

Ridgway J, Breward N, Langston WJ, Lister R, Rees JG, Rowlatt SM. **2003**. Distinguishing between natural and anthropogenic sources of metals entering the Irish Sea. *Applied Geochemistry* **18**: 283–309.

Rijstenbil JW, Derksen JWM, Gerringa LJA, Poortvliet TCW, Sandee A, van den Berg M, van Drie J, Wijnholds JA. **1994**. Oxidative stress induced by copper: defense and damage in the marine planktonic diatom *Ditylum brightwellii*, grown in continuous cultures with high and low zinc levels. *Marine Biology* **119**: 583–590.

Ritter A, Dittami SM, Goulitquer S, Correa J a, Boyen C, Potin P, Tonon T. **2014**. Transcriptomic and metabolomic analysis of copper stress acclimation in *Ectocarpus siliculosus* highlights signaling and tolerance mechanisms in brown algae. *BMC plant biology* **14**: 116.

Ritter A, Ubertini M, Romac S, Gaillard F, Delage L, Mann A, Cock JM, Tonon T, Correa J a., Potin P. **2010**. Copper stress proteomics highlights local adaptation of two strains of the model brown alga *Ectocarpus siliculosus*. *Proteomics* **10**: 2074–2088.

Roncarati F, Sáez CA, Greco M, Gledhill M, Bitonti MB, Brown MT. **2015**. Response differences between *Ectocarpus siliculosus* populations to copper stress involve cellular exclusion and induction of the phytochelatin biosynthetic pathway. *Aquatic Toxicology* **159**: 167–175.

Rönnbäck P, Kautsky N, Pihl L, Troell M, Söderqvist T, Wennhage H. **2007**. Ecosystem goods and services from Swedish coastal habitats: identification, valuation, and implications of ecosystem shifts. *Ambio* **36**: 534–544.

Rosa IC, Pereira JL, Costa R, Gonçalves F, Prezant R. **2012**. Effects of upper-limit water temperatures on the dispersal of the asian clam *Corbicula fluminea*. *PLoS ONE* **7**: e46635.

Russell G. **1983**. Parallel growth patterns in algal epiphytes and *Laminaria* blades. *Marine Ecology Progress Series* **13**: 303–304.

Russell BD, Thompson J-AI, Falkenberg LJ, Connell SD. **2009**. Synergistic effects of climate change and local stressors: CO_2 and nutrient-driven change in subtidal rocky habitats. *Global Change Biology* **15**: 2153–2162.

Ryan S, McLoughlin P, O'Donovan O. **2012**. A comprehensive study of metal distribution in three main classes of seaweed. *Environmental Pollution* **167**: 171–177.

Sáez CA, González A, Contreras RA, Moody AJ, Moenne A, Brown MT. **2015a**. A novel field transplantation technique reveals intra-specific metal-induced oxidative responses in strains of *Ectocarpus siliculosus* with different pollution histories. *Environmental Pollution* **199**: 130–138.

Sáez CA, Pérez-Matus A, Lobos MG, Oliva D, Vásquez JA, Bravo M. **2012**. Environmental assessment in a shallow subtidal rocky habitat: approach coupling chemical and ecological tools. *Chemistry and Ecology* **28**: 1–15.

Sáez CA, Ramesh K, Greco M, Bitonti MB, Brown MT. **2015b**. Enzymatic antioxidant defences are transcriptionally regulated in Es524, a copper-tolerant strain of *Ectocarpus siliculosus* (Ectocarpales, Phaeophyceae). *Phycologia* **54**: 425–429.

Sáez CA, Roncarati F, Moenne A, Moody AJ, Brown MT. **2015c**. Copper-induced intra-specific oxidative damage and antioxidant responses in strains of the brown alga

Ectocarpus siliculosus with different pollution histories. *Aquatic Toxicology* **159**: 81–89.

Sakshaug E, Bricaud A, Dandonneau Y, Falkowski PG, Kiefer DA, Legendre L, Morel A, Parslow J, Takahashi M. **1997**. Parameters of photosynthesis: definitions, theory and interpretation of results. *Journal of Plankton Research* **19**: 1637–1670.

Schiedek D, Sundelin B, Readman JW, Macdonald RW. **2007**. Interactions between climate change and contaminants. *Marine Pollution Bulletin* **54**: 1845–1856.

Schlesinger MJ. **1990**. Heat shock proteins. *The Journal of biological chemistry* **265**: 12111.

Schoenwaelder MEA. **2002**. The occurrence and cellular significance of physodes in brown algae. *Phycologia* **41**: 125–139.

Schreiber U. **1986**. Detection of rapid induction kinetics with a new type of high-frequency modulated chlorophyll fluorometer. *Photosynthesis Research* **9**: 261–272.

Schreiber U. **2004**. Pulse-amplitude (PAM) fluorometry and saturation pulse method: an overview. In: Papageorgiou GC, Govindjee, eds. Chlorophyll fluorescence: A Signature of Photosynthesis. Advances in Photosynthesis and Respiration Series. Dordrecht, The Netherlands: Kluwer Academic Publishers, 279–319.

Schreiber U, Endo T, Mi H, Asada K. **1995**. Quenching analysis of chlorophyll fluorescence by the saturation mulse Method: particular aspects relating to the study of eukaryotic algae and Cyanobacteria. *Plant & cell physiology* **36**: 873–882.

Seely GR, Duncan MJ, Vidaver WE. **1972**. Preparative and analytical extraction of pigments from brown algae with dimethyl sulfoxide. *Marine Biology* **12**: 184–188.

Sharma RM, Azeez PA. **1988**. Accumulation of Copper and Cobalt by Blue-Green Algae at Different Termperatures. *International Journal of Environmental Analytical Chemistry* **32**: 87–95.

Shibata T, Hama Y, Miyasaki T, Ito M, Nakamura T. **2006**. Extracellular secretion of phenolic substances from living brown algae. *Journal of Applied Phycology* **18**: 787–794.

Shibata T, Miyasaki T, Miyake H, Tanaka R, Kawaguchi S. **2014**. The influence of phlorotannins and bromophenols on the feeding behavior of marine herbivorous gastropod *Turbo cornutus*. *American Journal of Plant Sciences* **5**: 387–392.

Sieburth JM. **1969**. Studies on algal substances in the sea. III. The production of extracellular organic matter by littoral marine algae. *Journal of Experimental Marine Biology and Ecology* **3**: 290–309.

Silberfeld T, Leigh JW, Verbruggen H, Cruaud C, de Reviers B, Rousseau F. **2010**. A multi-locus time-calibrated phylogeny of the brown algae (Heterokonta, Ochrophyta, Phaeophyceae): Investigating the evolutionary nature of the 'brown algal crown radiation'. *Molecular Phylogenetics and Evolution* **56**: 659–674.

Singh S, Mulchandani A, Chen W. **2008**. Highly selective and rapid arsenic removal by metabolically engineered *Escherichia coli* cells expressing *Fucus vesiculosus* metallothionein. *Appl. Environ. Microbiol.* **74**: 2924–2927.

Smirnoff N. **2005**. Ascorbate, Tocopherol and Carotenoids: Metabolism, Pathway Engineering and Functions. In: Antioxidants and Reactive Oxygen Species in Plants. Blackwell Publishing Ltd, 53–86.

Sokolova I, Lannig G. **2008**. Interactive effects of metal pollution and temperature on metabolism in aquatic ectotherms: implications of global climate change. *Climate Research* **37**: 181–201.

Somero GN. **2002**. Thermal Physiology and Vertical Zonation of Intertidal Animals: Optima, Limits, and Costs of Living. *Integrative and Comparative Biology* **42**: 780–789.

Somero GN. **2011**. The Physiology of Global Change: Linking Patterns to Mechanisms. *Annual Review of Marine Science* **4**: 39–61.

Sørensen JG, Kristensen TN, Loeschcke V. **2003**. The evolutionary and ecological role of heat shock proteins. *Ecology Letters* **6**: 1025–1037.

Sozzani R, Busch W, Spalding EP, Benfey PN. **2014**. Advanced imaging techniques for the study of plant growth and development. *Trends in plant science* **19**: 304–310.

Stengel DB, Dring MJ. **2000**. Copper and iron concentrations in *Ascophyllum nodosum* (Fucales, Phaeophyta) from different sites in ireland and after culture experiments in relation to thallus age and epiphytism. *Journal of Experimental Marine Biology and Ecology* **246**: 145–161.

Sterck L, Billiau K, Abeel T, Rouzé P, Van de Peer Y. **2012**. ORCAE: online resource for community annotation of eukaryotes. *Nature Methods* **9**: 1041.

Strömgren T. **1980**. The effect of dissolved copper on the increase in length of four species of intertidal fucoid algae. *Marine Environmental Research* **3**: 5–13.

Sugie K, Kuma K, Fujita S, Ikeda T. **2010**. Increase in Si:N drawdown ratio due to resting spore formation by spring bloom-forming diatoms under Fe- and N-limited conditions in the Oyashio region. *Journal of Experimental Marine Biology and Ecology* **382**: 108–116.

Sunda WG, Huntsman SA. **1998**. Processes regulating cellular metal accumulation and physiological effects: Phytoplankton as model systems. *Science of The Total Environment* **219**: 165–181.

Supek F, Bošnjak M, Škunca N, Šmuc T. **2011**. REVIGO summarizes and visualizes long lists of gene ontology terms. *PLOS ONE* **6**: e21800.

Swanson AK, Druehl LD. **2002**. Induction, exudation and the UV protective role of kelp phlorotannins. *Aquatic Botany* **73**: 241–253.

Takao S, Kumagai NH, Yamano H, Fujii M, Yamanaka Y. **2015**. Projecting the impacts of rising seawater temperatures on the distribution of seaweeds around Japan

under multiple climate change scenarios. *Ecology and Evolution* **5**: 213–223.

Teisseire H, Couderchet M, Vernet G. **1999**. Phytotoxicity of diuron alone and in combination with copper or folpet on duckweed (Lemna minor). *Environmental Pollution* **106**: 39–45.

Theophanides T. **1984**. Metals Ions in Biological Systems. *International Journal of Quantum Chemistry* **26**: 933–941.

Thomas WH, Holm-Hansen O, Seibert DLR, Azam F, Hodson R, Takahashi M. **1977**. Effects of copper on phytoplankton standing crop and productivity: controlled ecosystem pollution experiment. *Bulletin of Marine Science* **27**: 34–43.

Todgham AE, Stillman JH. **2013**. Physiological responses to shifts in multiple environmental stressors: Relevance in a changing world. *Integrative and Comparative Biology* **53**: 539–544.

tom Dieck (Bartsch) I. **1993**. Temperature tolerance and survival in darkness of kelp gametophytes (Laminariales, Phaeophyta) - Ecological and biogeographical implications. *Mar. Ecol.-Prog. Ser.* **100**: 253–264.

Torres M a., Barros MP, Campos SCG, Pinto E, Rajamani S, Sayre RT, Colepicolo P. **2008**. Biochemical biomarkers in algae and marine pollution: A review. *Ecotoxicology and Environmental Safety* **71**: 1–15.

Torres M, Niell FX, Algarra P. **1991**. Photosynthesis of *Gelidium sesquipedale*: effects of temperature and light on pigment concentration, C/N ratio and cell-wall polysaccharides. *Hydrobiologia* **221**: 77–82.

Tsai K-P. **2016**. Management of targ*et al*gae by using copper-based algaecides: effects of algal cell density and sensitivity to copper. *Water, Air & Soil Pollution* **227**: 1–11.

Uchida K, Kawakishi S. **1994**. Identification of oxidized histidine generated at the active site of Cu,Zn-superoxide dismutase exposed to H_2O_2. Selective generation of 2-oxo-

histidine at the histidine 118. *Journal of Biological Chemistry* **269**: 2405–2410.

Untergasser A, Cutcutache I, Koressaar T, Ye J, Faircloth BC, Remm M, Rozen SG. **2012**. Primer3—new capabilities and interfaces. *Nucleic Acids Research* **40**: e115–e115.

Vavilin D V, Polynov VA, Matorin DN, Venediktov PS. **1995**. Sublethal concentrations of copper stimulate photosystem ii photoinhibition in *Chlorella pyrenoidosa*. *Journal of Plant Physiology* **146**: 609–614.

Velikova V, Yordanov I, Edreva A. **2000**. Oxidative stress and some antioxidant systems in acid rain-treated bean plants: Protective role of exogenous polyamines. *Plant Science* **151**: 59–66.

Venegas M, Matsuhiro B, Edding M. **1993**. Alginate composition of lessonia trabeculata (phaeophyta: laminariales) growing in exposed and sheltered habitats. *Botanica Marina* **36**: 47.

Véron AJ, Church TM, Flegal AR. **1998**. Lead isotopes in the western north atlantic: transient tracers of pollutant lead inputs. *Environmental Research* **78**: 104–111.

Véron AJ, Church TM, Flegal AR, Patterson CC, Erel Y. **1993**. Response of lead cycling in the surface Sargasso Sea to changes in tropospheric input. *Journal of Geophysical Research: Oceans* **98**: 18269–18276.

Villares R, Carral E, Puente X, Carballeira A. **2005**. Metal levels in estuarine macrophytes: Differences among species. *Estuaries* **28**: 948–956.

Villegas MJ, Laudien J, Sielfeld W, Arntz WE. **2008**. *Macrocystis integrifolia* and *Lessonia trabeculata* (Laminariales; Phaeophyceae) kelp habitat structures and associated macrobenthic community off northern Chile. *Helgoland Marine Research* **62**: 33–43.

Visviki I, Rachlin JW. **1994**. Acute and chronic exposure of *Dunaliella salina* and *Chlamydomonas bullosa* to copper and cadmium: Effects on ultrastructure. *Archives of Environmental Contamination and Toxicology* **26**: 154–162.

Wahl M, Jormalainen V, Eriksson BK, Coyer JA, Molis M, Shubert H, Dethier M, Karez R, Kruse I, Lenz M, *et al.* 2011. Stress ecology in *Fucus*: abiotic, biotic and genetic interactions. *Advances in marine biology* **59**: 37.

Wang Z, Gerstein M, Snyder M. **2009**. RNA-Seq: a revolutionary tool for transcriptomics. *Nature reviews. Genetics* **10**: 57–63.

Wang W, Vinocur B, Shoseyov O, Altman A. **2004**. Role of plant heat-shock proteins and molecular chaperones in the abiotic stress response. *Trends in Plant Science* **9**: 244–252.

Wang M-J, Wang W-X. **2008**. Temperature-dependent sensitivity of a marine diatom to cadmium stress explained by subcelluar distribution and thiol synthesis. *Environmental Science & Technology* **42**: 8603–8608.

Wang W-J, Wang F-J, Sun X-T, Liu F-L, Liang Z-R. **2013**. Comparison of transcriptome under red and blue light culture of *Saccharina japonica* (Phaeophyceae). *Planta* **237**: 1123–1133.

Wernberg T, de Bettignies T, Joy BA, Finnegan PM. **2016**. Physiological responses of habitat-forming seaweeds to increasing temperatures. *Limnology and Oceanography* **61**: 2180–2190.

West J, Kraft G. **1996**. *Ectocarpus siliculosus* (Dillwyn) Lyngb. from Hopkins River Falls, Victoria—The first record of a freshwater brown alga in Australia. *Muelleria* **9**: 29–33.

White AJ, Critchley C. **1999**. Rapid light curves: A new fluorescence method to assess the state of the photosynthetic apparatus. *Photosynthesis Research* **59**: 63–72.

Wiencke C, I, Bartsch I, Bischoff B, Peters AF, Breeman AM. **1994**. Temperature requirements and biogeography of antarctic, arctic and amphiequatorial seaweeds. *Botanica Marina* **37**: 247.

Wu T-M, Hsu Y-T, Sung M-S, Hsu Y-T, Lee T-M. **2009**. Expression of genes involved in redox homeostasis and antioxidant defense in a marine macroalga *Ulva fasciata* by excess copper. *Aquatic Toxicology* **94**: 275–285.

Wu T-M, Lee T-M. **2008**. Regulation of activity and gene expression of antioxidant enzymes in *Ulva fasciata* Delile (Ulvales, Chlorophyta) in response to excess copper. *Phycologia* **47**: 346–360.

Yadav SK. **2010**. Heavy metals toxicity in plants: An overview on the role of glutathione and phytochelatins in heavy metal stress tolerance of plants. *South African Journal of Botany* **76**: 167–179.

Ye J, Coulouris G, Zaretskaya I, Cutcutache I, Rozen S, Madden TL. **2012**. Primer-BLAST: A tool to design target-specific primers for polymerase chain reaction. *BMC Bioinformatics* **13**: 134.

Yong YS, Yong WTL, Anton A. **2013**. Analysis of formulae for determination of seaweed growth rate. *Journal of Applied Phycology* **25**: 1831–1834.

Young MD, Wakefield MJ, Smyth GK, Oshlack A. **2010**. Gene ontology analysis for RNA-seq: accounting for selection bias. *Genome Biology* **11**: R14.

Yruela I. **2013**. Transition metals in plant photosynthesis. *Metallomics* **5**: 1090–1109.

Yu Z-W, Quinn PJ. **1998**. The modulation of membrane structure and stability by dimethyl sulphoxide (Review). *Molecular Membrane Biology* **15**: 59–68.